EFFECTS OF EPILEPSY-ASSOCIATED MUTATIONS ON $GABA_A$ RECEPTOR ASSEMBLY, TRAFFICKING, AND FUNCTION

By

Katharine Nicole Gurba

Dissertation

Submitted to the Faculty of the

Graduate School of Vanderbilt University

in Partial Fulfillment of the Requirements

for the Degree of

DOCTOR OF PHILOSOPHY

in

Neuroscience

August, 2013

Nashville, Tennessee

Approved:

Alfred George, M.D.

Todd Graham, Ph.D.

Martin J. Gallagher, M.D., Ph.D.

Robert L. Macdonald, M.D., Ph.D.

To Brad

and to my family,

for getting me here and getting me through.

The squirming facts exceed the squamous mind,
If one may say so. And yet relation appears,
A small relation expanding like the shade
Of a cloud on sand, a shape on the side of a hill.
...
This proves nothing. Just one more truth, one more
Element in the immense disorder of truths.
It is April as I write. The wind is blowing after days of constant rain.
All this, of course, will come to summer soon.
But suppose the disorder of truths should ever come
To an order, most Plantagenet, most fixed…
A great disorder is an order.

- Wallace Stevens, "Connoisseur of Chaos"

"It's the wanting to know that makes us matter. Otherwise, we're going out the way we came in."

- Tom Stoppard, *Arcadia*

"The doubter is a true man of science; he doubts only himself and his interpretations, but he believes in science."

- Claude Bernard

"Some of the channels close. The rest of the channels stay open until they close."

"Calling something an 'apparent Kd' is like calling a horse an apparent car because they both move."

"You are comparing apples to kumquats."

- Robert L. Macdonald

Now these points of data make a beautiful line
And we're out of beta, we're releasing on time
So I'm glad I got burned, think of all the things we've learned
For the people who are still alive

- GLaDOS

"I feel like a quote out of context."

- Ben Folds

ACKNOWLEDGEMENTS

It should be noted that several chapters in this dissertation have been or will be published as separate manuscripts. A manuscript modified from Chapter III is in preparation and will be submitted with the author list Katharine N. Gurba, Emmanuel J. Botzolakis, Andre H. Lagrange, Hua-Jun Feng, Aleksandar K. Stanic, Ningning Hu, and Robert L. Macdonald. The first two authors will be listed as having equal contributions. Chapter IV was published as reference 437 (Gurba et al., 2012). Chapter V was published as reference 480 (Hernandez et al., 2011). Co-authors on both papers included Ciria Hernandez and Ningning Hu. Chapter VI has been submitted for publication with author list Emily S. Todd, Katharine N. Gurba, Emmanuel J. Botzolakis, Aleksandar K. Stanic, and Robert L. Macdonald. Chapters V and VI were written in collaboration with the first authors.

First and foremost, I wish to thank my advisor, Dr. Robert Macdonald. Years ago, he was among those who interviewed me for Vanderbilt's MD/PhD program. I assume that he was instrumental in my being accepted to the program, and he certainly helped convince me that Vanderbilt was the right place for me. Over these years, I have come to realize that he could not have been more right. More importantly, however, Dr. Macdonald has provided an excellent training environment for an aspiring physician-scientist. He inhabits both roles more thoroughly than perhaps anyone else I have met, and he has hired many junior faculty members who are pursuing the same path. Together, they have provided excellent mentorship and inspiring career examples, and I can only hope to live up to their examples. Despite his inconceivably busy schedule, Dr. Macdonald manages to be available to discuss data on a regular basis. However, he also expects trainees to design their own experiments and organize their time and efforts appropriately, which has forced me to become (or, at least, begin to become) a scientific grownup. He is truly unusual in the amount of autonomy he grants to his trainees, and it took me too long to realize what a gift that is. My great regret from graduate school is that I did not fully

take advantage of the opportunity to dream big, test potentially crazy ideas, and succeed or fail independently. It will certainly be my goal to do so in the future. And finally, I also thank Dr. Macdonald for eating and sharing the occasional vegetarian sandwich.

Perhaps no one else helped me as much over the course of my graduate career as Dr. Emmanuel Botzolakis, who trained me during my rotation and my first year in the lab. He helped convince me to join this lab, in no small part because he is so enthusiastic (in retrospect, almost *too* enthusiastic) about every scientific endeavor. However, his enthusiasm was an excellent counterweight to my own inevitable cynicism, and the first half of this dissertation stems from projects that he began. As noted above, a modified version of Chapter III is in preparation and will be submitted as a co-first author publication by Manuel and myself; he conceived the original strategy and began the project (including conducting many experiments), while I performed and/or repeated all non-electrophysiological experiments, prepared the figures, and wrote the manuscript.

As Manuel was my scientific partner during my first years of graduate school, Dr. Ciria Hernandez has been so ever since. She is an excellent electrophysiologist with whom I have collaborated on many projects; with the exception of Chapters III and VI, all single-channel and macropatch recordings presented here are Ciria's work. As such, she saved me months of frustration at the rig and allowed us both to finish projects more efficiently. She will be working on several ongoing projects while I finish my last two years of medical school, and I hope that therefore we will have the opportunity to write several more papers together. As noted above, Chapter V was published as reference 380 (Hernandez et al., 2011).

Dr. Ningning Hu also saved me countless hours by preparing dozens of subunit constructs and managing an ever-growing antibody collection. She can bargain with sales representatives like no one I have ever seen and thus has given me access to tools that would have

been prohibitively expensive. Her warmth, continual eagerness to help, and delicious rice cakes have made my time in this lab much more enjoyable.

Our other research assistants, particularly Dr. Wangzhen Shen and Joseph Toplon, helped me in more ways than I can remember, but I particularly appreciate their patience and assistance with radiolabeling experiments. They were also remarkably patient with my absentmindedness about any non-scientific task and reminded me far too many times where various supplies should be kept.

Dr. Aurea Pimenta has greatly enriched the lab over the past year with her expertise. I thank her for continuing many of the flow cytometry projects, optimizing new techniques so that I could work on final experiments and this dissertation, and for suggesting new projects in which I could participate while in medical school.

Fellow graduate students past and present have also helped me immensely. Dr. Wen-yi Lo taught me how to produce immunoblots nearly as beautiful as her own and was an invaluable expert on glycosylation; Xuan Huang and Teniel Ramikie provided hours of late-night hilarity in the lab; and Dr. Mengnan Tian shared his invaluable molecular biology expertise.

Dr. Andre Lagrange and Dr. Martin Gallagher are two of the earlier-career physician-scientists hired by Dr. Macdonald. It has been inspirational to see them progress from K-award trainees to principal investigators, and I thank both of them for their advice and their perpetually open office doors. In particular, I thank Dr. Lagrange for his electrophysiology, participation in the project presented in Chapter III, and for occasionally sharing my cynicism; and I thank Dr. Gallagher for his expertise with all things biochemical and for serving on my thesis committee.

I would like to thank all members of my thesis committee – Dr. Alfred George, Dr. Todd Graham, Dr. Gallagher, and Dr. Macdonald – for their advice, their flexibility in scheduling (and re-scheduling), and for making my committee meetings relatively painless.

Laurel Jackson is a fellow graduate student who deserves particular mention for continuing my mutation projects, sharing my misery in the flow core, and helping with/performing monstrous experiments so I could wrap up projects in my final weeks. Most importantly, I would like to thank her for her friendship, her wonderful sense of humor, and her overall "big taste."

I thank Kelienne Verdier for additional assistance with DNA and antibodies, for maintaining my neuron cultures, for indulging my problematic affection for mice, for introducing me to so many new and interesting people, and for her friendship. In large part, Kelienne and Laurel have been responsible for my last year of graduate school being more enjoyable than the rest combined, and I will miss them tremendously when I return to medical school.

Dr. Jude McElroy has been a great friend since our first week at Vanderbilt so many years ago. He has patiently re-taught me genetics and statistics on a regular basis, spent hours listening to and expertly animating my PowerPoint presentations, and often turned a Greek alphabet soup of subunits into something vaguely intelligible to others. I am exceedingly grateful that he shares so many of my non-scientific interests and that he has introduced me to so much new art, music, and film. Our near-daily coffee/mental health breaks have helped me make it through graduate school and I will always remember them fondly.

Friends across the country have provided welcome weekend breaks, emotional support, and several delightfully punny suggestions for dissertation titles that cannot go unmentioned. My

favorites include: Go Go GABA Receptors; βig GABA, βig Taste; Yo GABA GABA; GABA-Dabba-Doo; and the forthright GABA is Good.

I would not have made it anywhere near this point in my life or career without the infinite love and support of my family – Carol, Dan, Chris, Tijana, and Helen Gurba – whom I love and miss with all my heart. I also thank them for not being too embarrassed to tell their friends that yes, I am STILL in school, and for their eagerness to forward any article about GABA.

Most of all, I thank my husband Brad Bakker, who is my best friend and the love of my life. Despite having had no science classes since AP Chemistry, he could probably give a comprehensive talk about GABA receptors by now because he has listened to every presentation and read every word that I have written. I thank him for resolving my weekly existential crises, for always believing in me, and for not minding that I will not have a real job until a decade later than him. I truly believe that he is the best spouse in the world, and that I am the luckiest.

TABLE OF CONTENTS

LIST OF FIGURES

Chapter I

Chapter II

Chapter III

Chapter VI

Chapter VII

LIST OF TABLES

LIST OF ABBREVIATIONS

AChBP	acetylcholine binding protein
ANOVA	analysis of variance
AP2	clathrin-adaptor protein 2
ATP	adenosine triphosphate
BIG2	brefeldin-A-inhibited GDP/GTP exchange factor 2
BiP	immunoglobulin heavy-chain-binding protein
BZD	benzodiazepine
CAE	childhood absence epilepsy
cDNA	complementary deoxyribonucleic acid
CHX	cycloheximide
CNS	central nervous system
DMEM	Dulbecco's Modified Eagle's Medium
DZP	diazepam
EC_{50}	effective concentration that yields half-maximal response
E_{Cl}	chloride equilibrium potential
eIPSC	evoked inhibitory post-synaptic current
ER	endoplasmic reticulum
FACS	fluorescence-activated cell sorting
FBS	fetal bovine serum
FI	fluorescence intensity
FRET	fluorescence resonance energy transfer
GABA	γ-aminobutyric acid
$GABA_A$	GABA receptor type A
$GABA_B$	GABA receptor type B

GABARAP	$GABA_A$ receptor-associated protein
GABA-T	GABA transaminase
GAD	glutamic acid decarboxylase
GAT	GABA transporter
GEFS+	generalized epilepsy with febrile seizures plus
GluCl	glutamate-gated chloride channel
GlyR	glycine receptor
GPCR	G-protein coupled receptor
GRIF1	$GABA_A$ receptor interacting factor 1 (aka, TRAK2)
GST	glutathione S-transferase
HA	hemagglutinin epitope
HEK	human embryonic kidney cell
HEPES	4-(2-hydroxyethyl)-1-piperazineethanesulfonic acid
IGE	idiopathic generalized epilepsy
I_{max}	peak current
IPSC	inhibitory post-synaptic current
JME	juvenile myoclonic epilepsy
KCC2	potassium-chloride co-transporter
kDa	kilodalton
LGIC	ligand-gated ion channel
mIPSC	miniature inhibitory post-synaptic current
mRNA	messenger ribonucleic acid
M1	first transmembrane domain
M2	second transmembrane domain
M3	third transmembrane domain

M4	fourth transmembrane domain
nAChR	nicotinic acetylcholine receptor
PB	pentobarbital
PBS	phosphate buffered saline
PG	penicillin G
PLIC1	protein linking integrin-associated protein to cytoskeleton-1
PKA	protein kinase A (cAMP-dependent protein kinase)
PKC	protein kinase C
PRIP	phospholipase-C-related catalytically inactive proteins
PTC	premature termination codon
Ro 15-4513	ethyl 8-azido-6-dihydro-5-methyl-6-oxo-4H-imidazo[1,5-a][1,4] benzodiazepine-3-carboxylate
RPE	repeated pulse enhancement
RPI	repeated pulse inhibition
RT-PCR	reverse transcription polymerase chain reaction
SEM	standard error of the mean
sIPSC	spontaneous inhibitory post-synaptic current
SMEI	severe myoclonic epilepsy of infancy (Dravet syndrome)
SNAT	sodium-coupled neutral amino acid transporter
SSA	succinic semialdehyde
SSADH	succinic semialdehyde dehydrogenase
TBPS	t-butylbicyclophosphorothionate
THDOC	tetrahydrodeoxycorticosterone
THIP	4,5,6,7-tetrahydroisoxazolo[5,4-c-]pyridin-3-ol
TM	transmembrane
VGAT	vesicular GABA transporter

WT	wild-type
$5\text{-}HT_3R$	5-hydroxytryptamine type 3 serotonin receptor

CHAPTER I

INTRODUCTION

GABAergic neurotransmission: ubiquitous, diverse, and essential

Approximately 30% of all cortical neurons release γ-aminobutyric acid (GABA), the predominant inhibitory neurotransmitter in the brain[1]. Unlike monoaminergic neurons, which signal primarily through specific projection pathways, GABAergic neurons are distributed throughout the brain and most signal via local rather than long-range circuits. These inhibitory "interneurons" are morphologically and functionally diverse; different populations express different neurochemical markers, exhibit different dendritic arborizations, fire at different rates, and form synapses with different regions of target cells. Although interneurons mediate the majority of inhibitory neurotransmission, long-range GABAergic projection neurons also exist. Both the local-circuit and long-range populations are essential for proper CNS function, as GABAergic signaling is necessary for processes ranging from neuronal migration to sensory perception to maintenance of sleep and wakefulness.

GABA metabolism and transport: GADs, GATs, and GABA-Ts

Biosynthesis of GABA occurs within GABAergic neurons themselves via a branch of the tricarboxylic acid (TCA) cycle called the GABA shunt. In this metabolic pathway, α-ketoglutarate is transaminated to yield glutamate, which then is decarboxylated by glutamic acid decarboxylase (GAD) to yield GABA. The latter constitutes the rate-limiting step of GABA biosynthesis and, notably, converts the most abundant excitatory neurotransmitter into the most abundant inhibitory neurotransmitter. Degradation of GABA is accomplished in astrocytes by GABA transaminase (GABA-T), which produces succinic semialdehyde. Finally, succinic

semialdehyde is metabolized by succinic semialdehyde dehydrogenase to succinate, which can re-enter the TCA cycle and close this metabolic loop.

Despite the simplicity of the GABA shunt, metabolism and transport of GABA is, unsurprisingly, a heavily regulated process that involves multiple enzymatic isoforms, cofactors, transporters, and cell types[2]. The rate-limiting enzyme, GAD, exists in two forms: GAD65 and GAD67, each encoded by a separate gene and named according to its molecular weight in kDa[3, 4]. Although these two enzymes catalyze identical reactions, their localization and regulatory properties (Table 1) suggest that they play very different roles in GABAergic neurotransmission. For instance, GAD67 is distributed throughout the cytoplasm of GABAergic neurons, exists predominantly as an active holoenzyme bound to its requisite cofactor pyridoxal phosphate, and synthesizes approximately 70% of all GABA present in the brain. In contrast, GAD65 is membrane-bound, localized to nerve terminals and synaptic vesicles, exists primarily as a dormant apoenzyme that can be activated rapidly after binding pyridoxal phosphate, and synthesizes approximately 30% of all GABA. Mice deficient in GAD67 suffer from severe cleft palate and die shortly after birth[5], whereas mice deficient in GAD65 exhibit only a few overt abnormalities, including increased anxiety and decreased seizure threshold[6-8]. Finally, GAD67 expression developmentally precedes that of GAD65[9]. Because of these divergent properties, it has been proposed that GAD67 maintains homeostatic levels of GABA and aids synaptogenesis, while GAD65 rapidly synthesizes GABA for neurotransmission and adaptation to changing metabolic states[10].

After neurotransmitter release, the concentration of GABA in the synaptic cleft is thought to reach 1.5-3 mM[11-13]. Clearance occurs via rapid reuptake by GABA transporters (GATs) located on plasma membranes of both presynaptic neurons and astrocytes. Four homologous GATs have been identified in humans: GAT-1, GAT-2, GAT-3, and BGT-1 (betaine/GABA transporter-1). Of these, GAT-1 and GAT-3 are highly expressed in cerebral cortex – GAT-1 is

Table 1: Characteristics of glutamic acid decarboxylase (GAD) isoforms

	GAD65	GAD67
Location	Terminals/vesicles	Whole cell
% GABA synthesized	30%	70%
Predominant form	Apoenzyme	Holoenzyme
KO phenotype	Anxiety Epilepsy	Cleft palate Perinatal lethal
Effect of expression in excitatory cells	Excitatory → inhibitory	No effect
Autoantibodies	Stiff-person syndrome	None
Effects of phosphorylation	Activates (PKCε/PP2A)	Inhibits (PKA/calcineurin)
Effects of palmitoylation	Targets to presynaptic	Not palmitoylated

primarily in presynaptic neuron terminals and GAT-3 primarily in perisynaptic regions of astrocytes[14]. These two isoforms have similar affinities for GABA, though it has been suggested that GAT-3 has a slightly lower K_m(GABA)[15]. GAT-2 and BGT-1 are expressed at lower levels, located in meninges and extrasynaptic locations, and display significantly lower affinities for GABA[16, 17]. Similar to many other neurotransmitter transporters, the GATs are twelve-transmembrane domain proteins that co-transport two sodium ions, one chloride ion, and one GABA molecule[18].

After neuronal reuptake, GABA is repackaged into synaptic vesicles by the vesicular GABA transporter (VGAT), which can transport glycine as well and thus is also known as the vesicular inhibitory amino acid transporter (VIAAT). This is a H^+/neurotransmitter antiporter; GABA is exchanged for protons flowing down the concentration gradient established by the vacuolar H^+/ATPase that acidifies vesicles[19]. In contrast, after astrocytic reuptake, GABA is catabolized and its metabolites re-enter the TCA cycle as described above. Ultimately, these metabolites return to neurons and replenish the supply of glutamate/GABA precursors, but the metabolites themselves do not represent the major transported molecules. Rather, α-ketoglutarate is converted to glutamate, which is amidated by glutamine synthetase to form glutamine. Two glutamine transporter complexes have been identified: confusingly, System N mediates efflux from astrocytes while System A mediates influx into neurons. Both complexes consist of

multiple sodium-coupled neutral amino acid transporters (SNATs). System N is a reversible Na^+/Gln symporter and H^+ antiporter comprising SNAT3 and SNAT5 (also known as SN1 and SN2, respectively), while System A is a unidirectional Na^+/Gln symporter only and comprises SNAT1, SNAT2, and SNAT4[20].

GABA, excitation, and inhibition: developmental changes in chloride reversal potential

As previously discussed, GABA serves as the predominant inhibitory neurotransmitter in adult brain; that is, binding of GABA to its receptors causes neuronal hyperpolarization. However, hyperpolarization occurs only due to prevailing chloride ion gradients. Specifically, ionotropic $GABA_A$ receptors (ligand-gated chloride channels) mediate hyperpolarization because the mature resting membrane potential is more negative than the chloride reversal potential. This, in turn, occurs because in mature neurons, $[Cl^-]_{out}$ is approximately twenty times greater than $[Cl^-]_{in}$.

Two different transporters are primarily responsible for maintaining the chloride gradient in neurons (Figure 1). NKCC1 is a Na^+-K^+-$2Cl^-$ co-transporter that is driven by sodium and potassium gradients and usually increases $[Cl^-]_{in}$, and KCC2 is the neuron-specific splice variant of the K^+-Cl^- co-transporter family that usually decreases $[Cl^-]_{in}$. Neuronal expression of NKCC1 peaks during late embryonic and early postnatal stages and subsequently declines through development; in adult mice, CNS expression of NKCC1 is largely restricted to glial cells[21]. Conversely, expression of KCC2 remains low or undetectable in most rat brain regions until reaching robust adult expression levels during the second postnatal week[22]. These changes in transporter expression levels correlate with the developmental switch in GABAergic neurotransmission from excitatory to inhibitory[21]. The mechanisms that alter expression of chloride transporters remain incompletely defined, though several trophic factors seem to contribute[23, 24] and, interestingly, GABA-mediated excitation itself may induce KCC2 upregulation[25]. After the "developmental switch" has occurred, chloride transporter expression

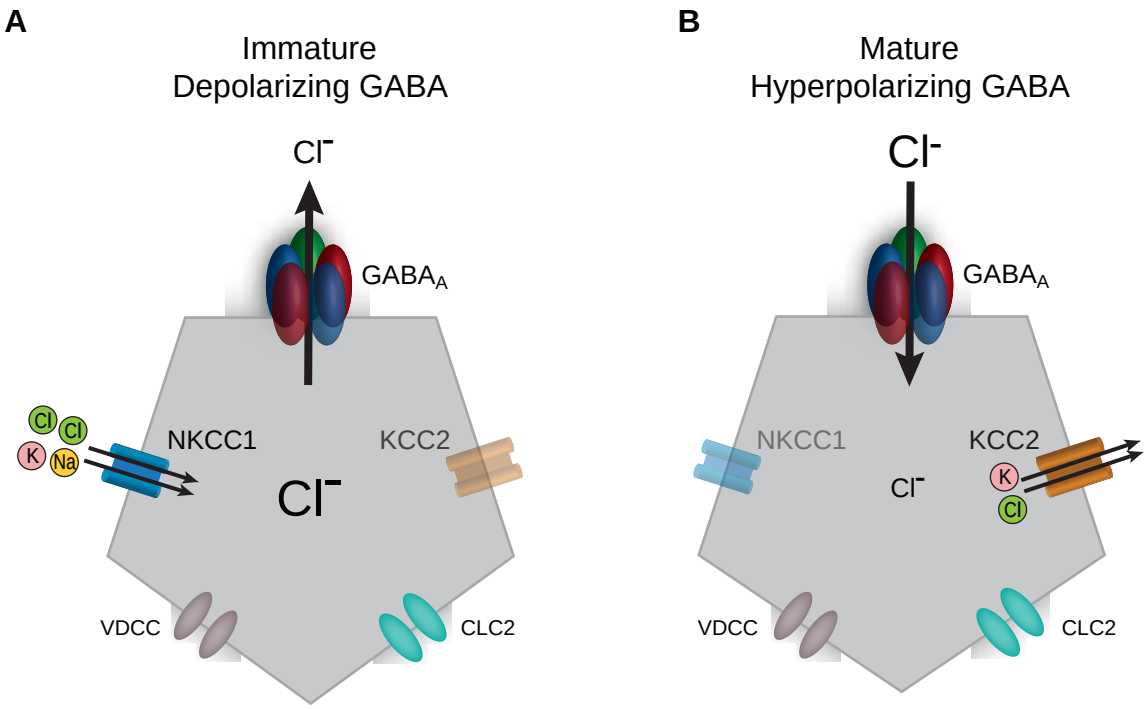

Figure 1. Developmental changes in chloride reversal potential.
A. The NKCC1 cotransporter is highly expressed in embryonic and postnatal neurons, where it co-imports one sodium, one potassium, and two chloride ions, thereby producing a high intracellular chloride concentration. When GABA binds to the $GABA_A$ receptor, chloride efflux occurs through the ion channel and the neuron becomes depolarized. **B.** Later in development (by the second postnatal week in rats), NKCC1 expression levels decrease and KCC2 cotransporter expression levels increase. Chloride and potassium are extruded from the neuron, leading to lower intracellular chloride concentrations. When GABA binds to the $GABA_A$ receptor, chloride influx occurs through the ion channel and the neuron becomes hyperpolarized. Other ion channels, such as the voltage-dependent calcium channel (VDCC) and chloride channels (CLC2) help to maintain these gradients.

(and, consequently, GABA-mediated inhibition) usually remains stable. However, abnormal NKCC1/KCC2 expression patterns and depolarizing GABAergic transmission have been observed in pathological conditions including epilepsy[26], neuropathic pain[27], ischemia[28], and schizophrenia[29].

Types of GABA receptors

Two classes of receptors mediate GABAergic signaling: ionotropic $GABA_A$ receptors and metabotropic $GABA_B$ receptors (Figure 2). $GABA_B$ receptors are class C guanine nucleotide-binding (G-protein) coupled receptors (GPCRs). Notably, this receptor class also includes metabotropic glutamate receptors[30]. $GABA_B$ receptors are obligate heterodimers comprising $GABA_{B1}$ subunits, which bind agonist, and $GABA_{B2}$ subunits, which bind and activate G-proteins. In addition to the seven transmembrane domains common to all GPCRs, each $GABA_B$ receptor subunit contains a large, two-lobed extracellular domain. GABA binds in a cleft between the two lobes and induces a conformational change in which the two lobes of the $GABA_{B1}$ subunit move closer together, which in turn allows a stronger intersubunit association between lobes two of the $GABA_{B1}$ and $GABA_{B2}$ subunits. It remains unclear what further conformational changes occur in $GABA_B$ receptor subunits during signal transduction, but it has been established that the three intracellular loops of $GABA_{B2}$ subunits are necessary for coupling to G-proteins. $GABA_B$ receptors specifically activate $G_{i/o}$-type heterotrimeric G-proteins; that is, they trigger GTP/GDP exchange at the $G\alpha_{i/o}$ subunit, which dissociates from the other two G-protein subunits and subsequently inhibits formation of cyclic AMP (cAMP), thereby evoking downstream signaling events[31]. However, it is the $G_{\beta\gamma}$ complex that ultimately affects neuronal inhibition by modulating the function of two different ion channels. First, the complex activates postsynaptic G protein-coupled inwardly-rectifying potassium channels (GIRKs), allowing potassium efflux and consequent hyperpolarization. Additionally, the $G_{\beta\gamma}$ complex inhibits both presynaptic and postsynaptic voltage-gated calcium (Ca_v) channels. Presynaptic Ca_v channel

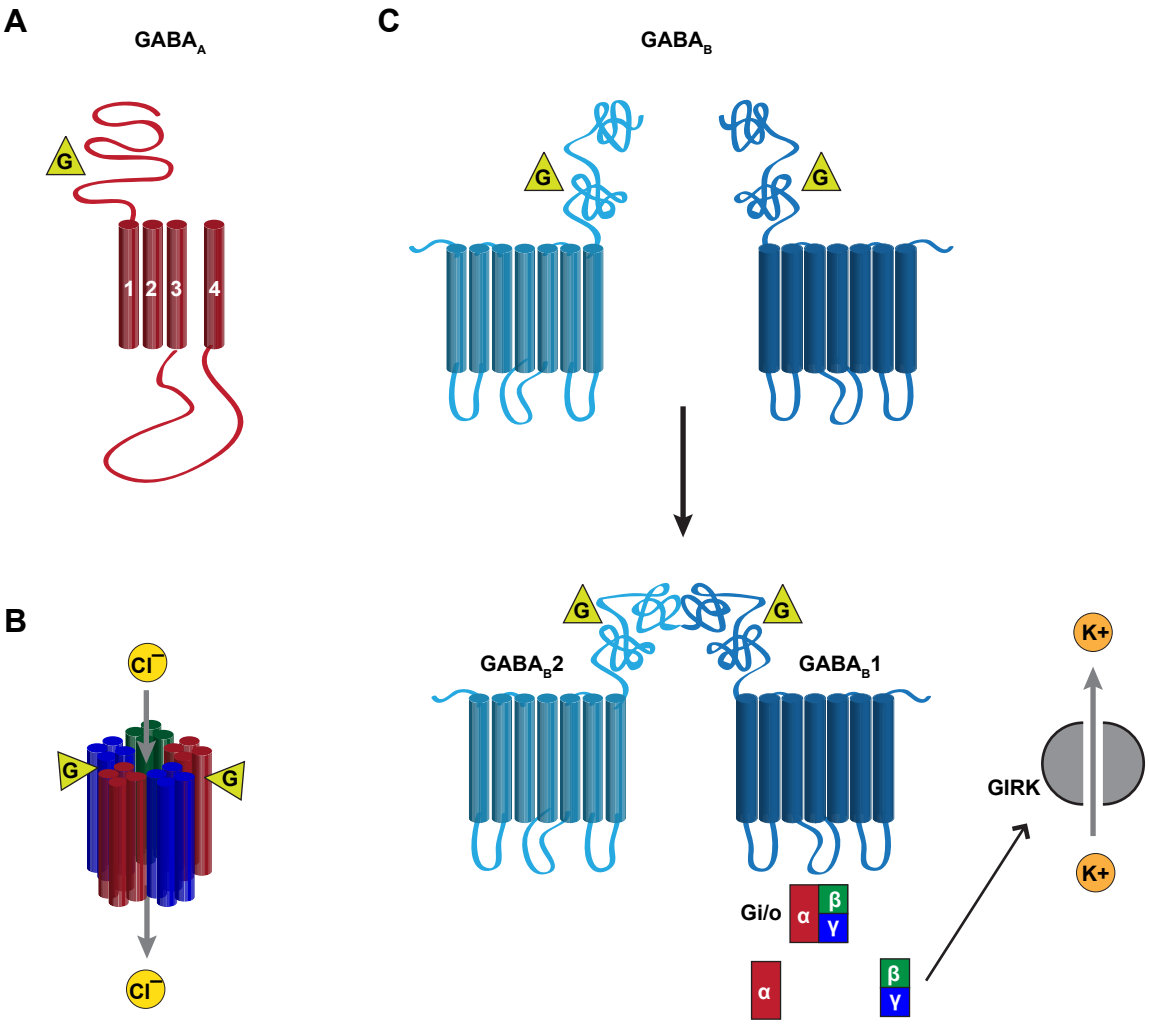

Figure 2. Schematic of GABA$_A$ and GABA$_B$ receptors.
A. Schematic of an individual GABA$_A$ receptor subunit, including an extracellular ligand-binding N-terminal domain, four transmembrane domains (numbered), and a large intracellular loop between the third and fourth transmembrane domains. **B.** Schematic of a heteropentameric GABA$_A$ receptor. (N-terminal domains and cytoplasmic loops have been omitted for clarity. When GABA (G, green triangle) binds to a pocket at the interface of two N-terminal domains, chloride (Cl, yellow circle) can pass through the ion pore. **C.** Schematic of two GABA$_B$ receptor subunits. Each is a traditional G-protein coupled receptor with seven transmembrane domains and three intracellular loops. When GABA (G, green triangle) binds to the N-terminal domain, the subunits dimerize and activate Gi/o-type G-proteins. The G(βγ) complex activates inwardly-rectifying potassium channels (GIRKs), causing potassium efflux and neuronal hyperpolarization.

inhibition prevents vesicle fusion and neurotransmitter release, while postsynaptic Ca_v channel inhibition impairs action potential generation[32]. Thus, $GABA_B$ receptors mediate three different forms of slow neuronal inhibition.

In contrast to $GABA_B$ receptors, $GABA_A$ receptors are chloride ion channels belonging to the Cys-loop receptor superfamily of pentameric ligand-gated ion channels (LGIC), which also includes nicotinic acetylcholine receptors (nAChRs), 5-hydroxytryptamine type 3 receptors (5-HT3Rs), and glycine receptors (GlyRs)[33]. $GABA_A$ receptor pentamers are assembled from an array of nineteen different subunit subtypes that confer diverse functional properties but contain common structural motifs. All $GABA_A$ receptor subunits comprise a large, N-terminal, extracellular ligand-binding domain; four α-helical transmembrane domains, one of which lines the ion pore; and, between the third and fourth transmembrane domains, a large intracellular loop that contains many motifs for post-translational modification and binding of accessory proteins. $GABA_A$ receptors will be the focus of this dissertation and, as such, will be discussed in greater depth in subsequent sections.

It is worth noting that, for many years, a subset of $GABA_A$ receptors was considered to be a separate class of "$GABA_C$ receptors". This classification was justified by the unusual pharmacology, physiology, and distribution of the subunits composing these receptors[34]. However, current consensus disfavors the use of $GABA_C$ and, accordingly, this dissertation will refer to all GABA-gated LGICs as $GABA_A$ receptors from this point forward.

Molecular biology of $GABA_A$ receptors

Among neurotransmitter receptors, $GABA_A$ receptors are remarkable for their diversity. In mammals, seven subunit families with nineteen subunit subtypes have been identified: α1-6, β1-3, γ1-3, δ, ε, θ, π, and ρ1-3 (Figure 3A). Amino acid sequence identity among subunits ranges from about 30-50% between families to about 60-80% within families (Tyndale, Olsen, and Tobin, 1995). Gene localization and phylogenetic tree analysis have indicated that this

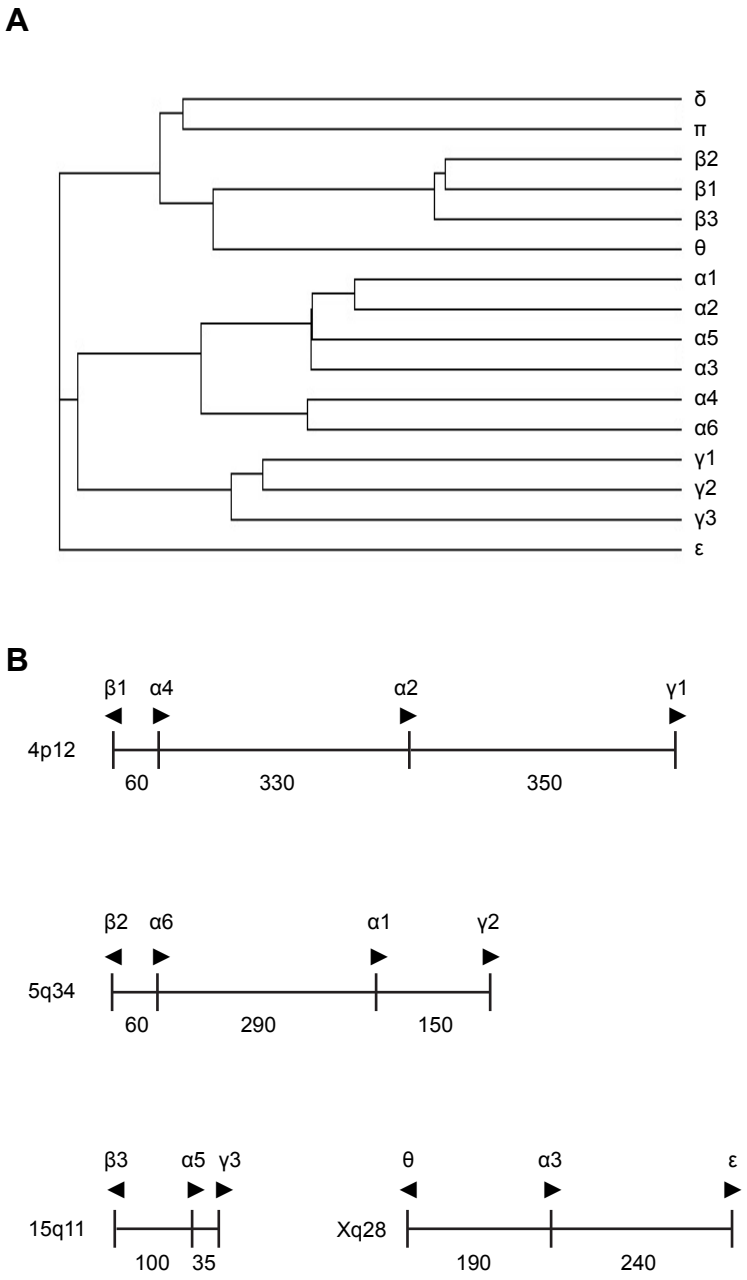

Figure 3. GABA$_A$ receptor subunit genes.

A. Dendrogram of GABA$_A$ receptor subunit genes. Lines are proportional to the divergence between each gene. Note that families are clustered, with the ε subunit being most similar to the γ subunit family and the θ subunit being most similar to the β subunit family. The δ and π subunit genes, which are not found in clusters, are most similar to one another (though still very divergent). **B.** Schematic of the chromosomal locations of the GABA$_A$ receptor gene clusters. Chromosomes are indicated to the left of each panel and arrowheads indicate the direction of transcription. Line length is proportional to the distance between genes, which is indicated (in kilobases) below the panels.

Table 2: Molecular biology of GABAA receptor subunits

Subunit	Gene	Chromosome			Splice variants	Exons	mRNA BP	AA	MW (kDa)
		Human	Mouse	Rat					
α1	GABRA1	5q34	11	10q21	1	9-11	4000-4376	456	51.8
α2	GABRA2	4p12	5	14p11	1	9-10	2426-2785	451	51.3
α3	GABRA3	Xq28	X	Xq37	1	10	2785	492	55.2
α4	GABRA4	4p12	5	14p11	1	9	11987	554	61.6
α5	GABRA5	15q11.2-12	7	1q22	1	11	2776-2910	462	52.1
α6	GABRA6	5q34	11	10q21	1	9	2519	453	51
β1	GABRB1	4p12	5	14p11	1	9	2226	474	54.2
β2	GABRB2	5q34	11	10q21	4	10 (11)	7295 (7409)	474 (512)	54.6 (59.1)
β3	GABRB3	15q13.2	7	1q22	4	7-9	5543-5783	473	54.1 (54.3)
γ1	GABRG1	4p12	5	14p11	1	9	6769	465	53.6
γ2	GABRG2	5q34	11	10q21	2	9 (10)	3933 (3957)	467 (475)	54.2 (55.2)
γ3	GABRG3	15q12	7	1q22	1		2031	467	54.3
δ	GABRD	1p36.3	4	5q36	1	9	1942	452	50.7
ε	GABRE	Xq28	X	Xq37	1	9	3167	506	57.9
θ	GABRQ	Xq28	X	Xq37	1	9	2000	632	72
π	GABRP	5q33-34	11	10q12	1	10	3310	440	50.6
ρ1	GABRR1	6q15	4	5q21	1	10	3161	479 (462)	55.8 (53.7)
ρ2	GABRR2	6q15	4	5q21	1	9	1631	490	56.8
ρ3	GABRR3	3q11.2	16	11q12	1	9 (10?)	1521	467	54.3

Abbreviations: BP, base pairs; AA, amino acids; MW, molecular weight

complexity largely derives from repeated duplication of an ancestral gene cluster[35]. Most $GABA_A$ receptor subunits exist in β-α-(α)-γ gene clusters of varying size, where the β subunit genes are transcribed in the opposite direction as the α and γ subunit genes (i.e., the β and α subunit transcriptional units are oriented head-to-head) (Figure 4B). In humans, the β1, α4, α2, and γ1 subunit genes are located on chromosome 4p12[36]; the β2, α6, α1, and γ2 subunit genes are located on chromosome 5q34[37]; and the β3, α5, and γ3 subunit genes are located on chromosome 15q11-13[38, 39]. Furthermore, the human Xq28 chromosome contains a θ-α3-ε cluster; both the gene orientation and phylogeny suggest that this represents another duplication of the ancestral cluster, with the rapidly-evolving θ and ε subunits replacing β and γ subunits, respectively[40, 41]. The remaining five subunit genes (δ, π, and ρ1-3) do not occur in comparable clusters. Like the β2, α6, α1, and γ2 subunit genes, the π subunit gene is located on the long arm of chromosome 5, but approximately 9 Mb telomeric to the γ2 subunit[42]. The δ subunit is located on chromosome 1p36[43]; the ρ3 subunit is located on chromosome 3q11-13, and the ρ1 and ρ2 subunits are located on chromosome 6q14-21[44]. The corresponding mouse and rat chromosomal locations are listed in Table 2.

Expression patterns of $GABA_A$ receptor subunits

Although $GABA_A$ receptors occur throughout the brain, receptor isoforms are likely to vary greatly because each subunit subtype has a unique temporal and spatial expression pattern. It must be noted, however, that it is the exception rather than the rule for brain regions to be entirely devoid of a given subunit subtype. Furthermore, by far the most comprehensive expression pattern studies have been conducted in rat brain, and expression patterns are similar but not identical among species. Consequently, the summary below serves as an overview of the most distinctive expression patterns rather than a complete list.

Temporal regulation of subunit expression

The α subunit subtypes appear to undergo similar changes in expression levels in developing rats[45-47], monkeys[48], and humans[49]. Generally, α1 subunit expression is undetectable in early embryonic stages and steadily increases until α1 subunits become the predominant α subunit subtype in adult brain. In contrast, α2-6 subunit expression levels peak at various points during prenatal and early postnatal life and decline thereafter, though expression of each subtype remains high in select regions of adult brain. Expression of α2 and α3 subunits is particularly strong in embryonic brain. Among β and γ subunits, β1, γ1, and γ3 subtype levels mostly decrease throughout development and are quite low in adult organisms. The β2 and γ2 subtypes display the opposite pattern; they continually increase and ultimately become the predominant subtypes of their respective families in most adult brain regions. The β3 subtype has more dynamic expression patterns; its expression increases during embryonic and early postnatal stages, then decreases overall but remains even higher than β2 subunit expression in certain areas. No δ subunit mRNA is present in early embryonic brain, and expression levels increase until adulthood. Although few systematic studies of ε and θ subunit temporal expression patterns have been conducted, it appears that the distribution of both subunits becomes more restricted over time (therefore, levels decrease overall), but in regions that retain ε and θ expression into adulthood, levels remain constant or increase from late embryonic stages onward[40]. Developmental changes in expression of π subunits have not been studied to date. Finally, ρ(1-3) subunit levels appear to increase during embryonic stages, peak within in the first two postnatal weeks, and then decline until adulthood[50, 51].

Spatial regulation of subunit expression

Once subunit levels stabilize in the adult organism, each displays a characteristic spatial distribution (though some changes do still occur throughout life[52]). Multiple studies have used techniques including *in situ* hybridization[45, 53, 54], quantitative PCR[51], and immunohistochemistry[47,

[55-57] to characterize these expression patterns at both regional and cellular levels in rat brain. Within the α subunit family, α1 subunits are the most abundant subtype. They are expressed at extremely high levels throughout most nuclei, cell types, and subcellular regions in cortex, hippocampus, basal ganglia, thalamus, hypothalamus, midbrain, cerebellum, brain stem, and cranial nerve nuclei. α2 subunits have a slightly more restricted but still widespread distribution; they have been detected throughout cortex, striatum, amygdala, hypothalamus, raphe nucleus, superior colliculus, and spinal cord, as well as in restricted regions/nuclei of thalamus, hippocampus, and cerebellum. α3 subunit expression patterns are very similar to those of α2 subunits, though they are somewhat more restricted. Presence of α3 subunits is particularly notable within lower cortical layers, basal ganglia, thalamic reticular nucleus (but not motor thalamus), anterior and lateral hypothalamus, midbrain, medulla, and cranial nerve nuclei. In most brain regions, α4 subunit levels are lower than those of all preceding α subunits; however, high levels are present in lower cortical layers, dentate gyrus, basal ganglia, and motor thalamus. Significant α5 subunit expression exists in olfactory bulb, lower cortical layers, hippocampus, and some midbrain and hypothalamic nuclei. Notably, subcellular localization of α5 subunits is almost exclusively extrasynaptic. Finally, α6 subunits are found exclusively within the cerebellar granule cell layer. Despite its low overall levels, β1 subunits are widely expressed through cortex, lateral septum, amygdala, thalamus, midbrain, medulla, and cranial nerve nuclei. Furthermore, particularly high β1 subunit expression levels are found in hippocampus, thalamic reticular nucleus, and hypothalamic supraoptic nucleus. β2 subunits are nearly ubiquitously expressed; notable exceptions include hippocampal granule cell layer, thalamic reticular nucleus, superior olive, and some cranial nerve nuclei. β3 subunits are also widely expressed, and regions with very high β3 subunit levels frequently have lower β2 subunit levels (though cerebellar granule cell and cortical layers contain high levels of both). As such, β3 subunit levels are high in thalamic reticular nucleus and throughout hippocampus and hypothalamus. γ1 subunits are sparsely expressed and found almost exclusively in globus pallidus, substantia nigra, central and

medial amygdaloid nuclei, and superior colliculus. In contrast, γ2 subunits are perhaps the most universally expressed subtype, as they have been detected in every brain region studied to date. Notably, different distributions have been reported for the short (γ2S) and long (γ2L) γ2 subunit splice variants, with γ2S subunits predominant in cerebral cortex, hippocampus, and olfactory bulb, and γ2L subunits predominant in medulla, inferior colliculus, and cerebellum[58]. In some ways, γ3 subunit expression patterns combine the characteristics of the other two γ subunits; γ3 subunit expression is widespread but sparse, with the highest levels reported in substantia nigra, hypothalamus, and raphe nucleus. The highest levels of δ subunits are found in cerebellar granule cells, dentate molecular layer, and throughout the thalamic nuclei. On a subcellular level, they are exclusively extrasynaptic. The ε and θ subunits have remarkably overlapping distributions with the exception of cortex, where ε but not θ subunits have been detected in early life only[40]. In adult animals, they have both been detected in substantia nigra pars compacta, medial and central thalamus, amygdala, and raphe nucleus. Additionally, levels of both ε and θ subunits are particularly high in locus coeruleus, hypothalamus, and monoaminergic neurons in general[59-61]. In brain, π subunits have been detected only at low levels in hippocampus, temporal cortex, and ventral pallidum[62, 63]. However, they are abundant in peripheral tissues including taste buds[64], lung[65], pancreas[66, 67], prostate[62], breast[68], and uterus[62]. Interestingly, changes in π subunit expression levels have been associated with cancers of many of those organs. For several years, ρ subunits were thought to be expressed almost exclusively in retina[69, 70]; indeed, ρ subunit-containing receptors were classified as "$GABA_C$ receptors" until recently, in part because of their isolated and sparse expression in brain. However, studies using quantitative RT-PCR as well as *in situ* hybridization have since detected all three ρ subunits in multiple brain regions. ρ2 subunits are the most abundant subtype and have been found in hippocampus (CA1), lateral geniculate nucleus, superior colliculus, basal ganglia, pituitary, substantia nigra pars compacta, visual cortex, and cerebellum[50, 71-74]. The ρ1 and ρ3 subunits are also expressed (albeit at lower

levels) primarily in hippocampus and superior colliculus. Clearly, a common theme among ρ subunits is their expression in areas related to visual signaling.

Finally, it should be noted that many chromosomally clustered subunits also display overlapping expression patterns. This fact has led researchers to propose that clustering facilitates coordinate expression, but little evidence exists to corroborate that theory. Indeed, very little is known to date about the elements regulating transcription of $GABA_A$ receptor genes[75]. Because selective subunit expression constitutes the first opportunity for neurons to control which of the myriad possible $GABA_A$ receptor isoforms will assemble, this area remains ripe for future study.

Biogenesis of $GABA_A$ receptors

The processes of synthesis, folding, oligomerization, and intracellular trafficking provide additional control over the distribution of $GABA_A$ receptor isoforms. As such, significant research effort has been expended to identify elements regulating receptor biogenesis. In addition to typical post-translational modifications, these elements include specific sequences and structural motifs within subunits that contribute to selective oligomerization as well as numerous associated proteins that escort isoforms along their intracellular journeys.

Transcription and translation

Human $GABA_A$ receptor subunit mRNAs contain 9-10 coding exons (9-13 total exons), and several subunits undergo alternative splicing. Notable examples in which both isoforms are functional and widely expressed include α1, α2, and α5 subunits, which have multiple 5'-UTRs; β3 subunits, which have alternative first exons and 5' UTRs that produce different signal and mature peptides; and β2 and γ2 subunits, which have "short" and "long" variants due to alternative splicing in the M3-M4 intracellular loop[76]. Additionally, α3 subunits undergo developmentally-regulated adenosine-to-inosine RNA editing[77, 78].

Endoplasmic reticulum: folding and oligomerization

All $GABA_A$ receptor subunits are predicted to contain signal peptides[79] and to be co-translationally inserted into the membrane of the endoplasmic reticulum (ER)[80], where they fold and oligomerize in a process that depends heavily upon ER-resident chaperones such as immunoglobulin heavy-chain binding protein (BiP) and calnexin[81]. As with other Cys-loop receptors, the process of subunit oligomerization occurs quickly but inefficiently; though oligomers may appear within five minutes, it is likely that 70% of subunits are degraded without ever being incorporated into a pentameric receptor. Furthermore, the full process of assembly and trafficking is quite slow, and receptors may not appear on the cell surface until several hours after transfection[80, 82].

The vast majority of neurons simultaneously express many subunit subtypes. Consequently, they presumably should have some sort of hierarchical yet flexible assembly mechanism that favors association between certain subunits and, ultimately, directs the incorporation of assembly intermediates (e.g. dimers, trimers) into full receptors. Some clues have been provided by knockout (KO) mouse studies; for instance, α6 subunit KO mice have reduced δ subunit expression, suggesting that these two subunits preferentially assemble. Multiple studies have identified amino acid sequences and individual residues that are important for specific subunit interactions[83, 84]. Such sequences have been found in α1[85-89], α6[85], β3[88-91], γ2[88, 92], and γ3[93] subunits, primarily in the large N-terminal domain, though there have been some reports of assembly sequences in the M3-M4 loop[94, 95] (Table 3 and Appendix 1). Interestingly, constructs lacking the transmembrane domains were also capable of oligomerization[96]. Although homology modeling based on nAChR[97] and acetylcholine binding protein (AChBP)[98] has provided some insight into the structural basis of these interactions (Figure 4), many sequences seem not to contact adjacent subunits; rather, they may simply facilitate oligomerization by encouraging proper protein folding. (Note that most sequences were identified using rodent subunits and numbered from the mature peptide. In the following section and in Table 3,

Table 3. Sequences and residues important for subunit oligomerization.

Subunit	Residues*	Interacts with	Comments
α1, α6	86-95 (esp. Q95)	β3	does not affect assembly with γ2
α1	108-128	γ2(130-143)	does not affect assembly w/ β3
α1	82-96	β3	sufficient for co-IP of β3 not sufficient for co-IP of α1 or γ2
α1	A136	β3, γ2	
β3	G196,K198,E204,R205	self? γ2?	necessary/sufficient for surf exp of β3 and β3γ2 not sufficient for spontaneous activity
β3	77-91	α1	removal: α1 IPs 30% of β3 and γ2 IPs similar % β3 (compared to co-IP of WT β3)
β3	101-114 (esp. 110-114)	α1	does not affect assembly w/ γ2 on (-) side of β3; interacts w/ (+) side of α1
γ2	130-143	α1	does not affect assembly w/ β3
γ2	122-131	α1, β3	
γ2	106-120	α1(mainly)	when α1β3γ2(mut) transfected and α1 IPed, 20% of γ2, 54% α1, and 65% β3 precipitated
γ3	86-100	α1, β3	γ3(86-94) binds slightly to α1
γ2	T164, P166	β3	predicted to be on (-) face (α1 interface), but only affects oligomerization with β3
ε	N229, K231, E233, K237 (homologous to β3 GKER)	α2? β3?	may affect whether 1 or 2 ε incorporated into α2β3ε

*All residue numbers include the signal peptide.

numbering has been adjusted to correspond to the immature human protein sequences used in Appendix 1.)

Within the α subunit family, assembly sequences have been identified in α1 and α6 subtypes. Mutating either of two invariant tryptophans, W97 and W116, prevented formation of the β2(-)/α1(+) interface, completion of the pentamer, and trafficking to the cell surface[85]. An α6 splice variant (α6S) lacking residues 76-86 (present in all other α subunits, including α6L, the most commonly expressed variant of α6) could not access the cell surface when co-transfected with β3 and γ2 subunits. This led to the discovery that α subunit residues 86-95, particularly Q95, were important for oligomerization of α1 and β3 subunits[86]. Two subsequent studies confirmed that overlapping sequences – 85-96 and 82-96 of the α1 subunit – were necessary for assembly of αβ receptors; moreover, one established that R66 apparently allows α1 subunits to discriminate among β subunits, because that residue was critical for formation of α1β2 but not α1β1 or α1β3 receptors[88, 89]. Regarding α1-γ2 oligomerization, residues 108-128 of the α1 subunit were found to interact directly with residues 130-143 of the γ2 subunit but not with β3 subunits[87, 92]. Finally, the α1(A136C) subunit mutation impaired α1 subunit assembly with both β3 and γ2 subunits[99].

Within the β subunit family, specific assembly sequences have been found only in the β3 subtype. Unlike most other $GABA_A$ receptor subunits, β3 subunits can reach the cell surface as homopentamers, and the residues G196, K198, E204, and R205 were found to be necessary and sufficient for β subunit homo-oligomerization and surface expression[90]. All other studies of β3 subunit assembly signals have focused upon the more common heteromeric receptors. Residues 77-91 of the β3 subunit formed one of the signals found to be important for heteromeric assembly; replacing this sequence with the homologous sequence from the ρ1 subunit strongly impaired association of the β3 and α1 subunits. In α1β3γ2 co-transfections, residues 76-89 of the β3 subunit, particularly residues 85-89, were similarly important for assembly with α1 but not with γ2 subunits. Radioligand binding studies and comparison with the AChBP structure indicated that these residues contribute to the β3(-)/α1(+) interface[91].

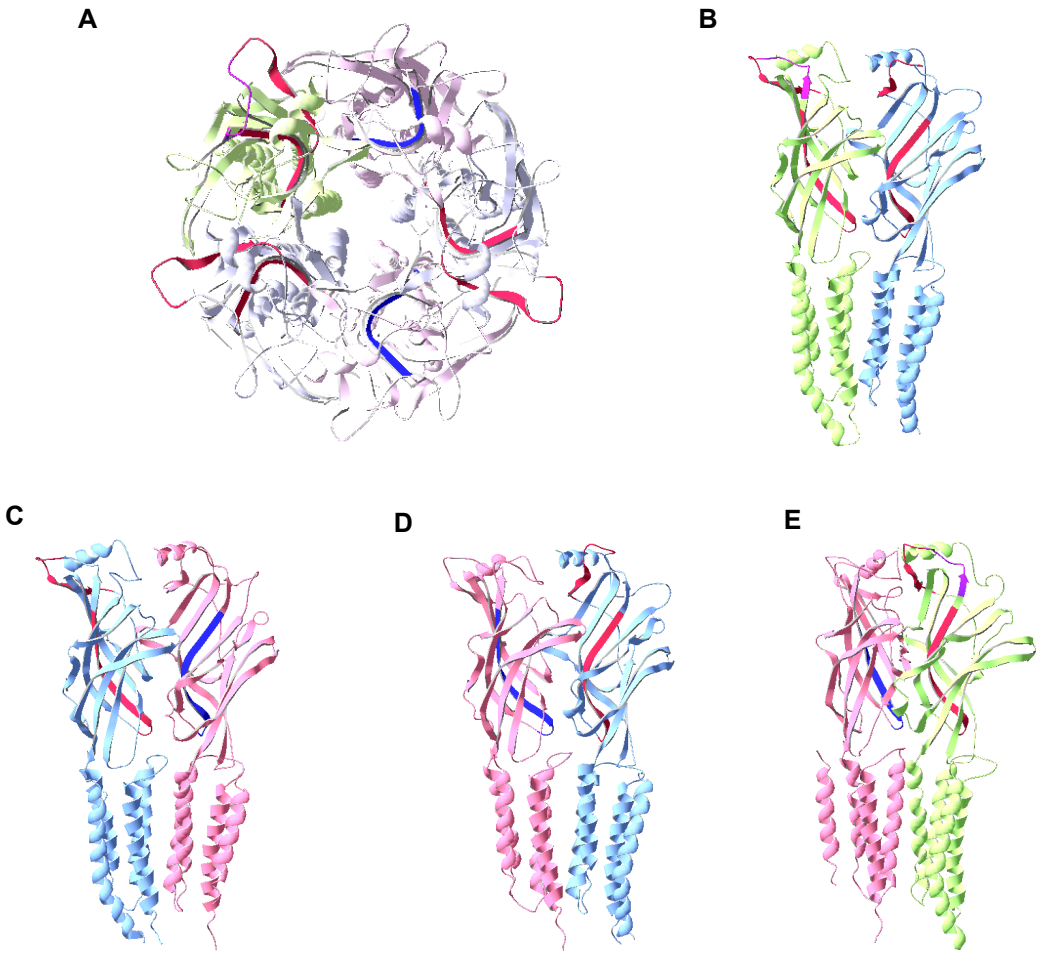

Figure 4. Identified assembly sequences in α, β, and γ GABA$_A$ receptor subunits.
A. Homology model of a ternary αβγ GABA$_A$ receptor isoform viewed from the extracellular N-terminal domain. Subunits were threaded in the order γ-β-α-β-α (anticlockwise in this view). α subunits are pink, β subunits are pale blue, and γ subunits are pale green. Sequences shown to interact with α subunits are colored red, sequences shown to interact with β subunits are dark blue, and sequences shown to interact with both α and β subunits are purple. Panels B-E are side views (from the membrane side) of this homology model. **B.** View of the γ-β subunit interface. **C.** View of the β-α subunit interface. **D.** View of the α-β subunit interface. **E.** View of the α-γ subunit interface.

Assembly sequences have also been studied in the γ subunit family. As previously mentioned, residues 130-143 of the γ2 subunit interacted directly with residues 108-128 of the α1 subunit, while residues 122-131 of the γ2 subunit interacted with the β3 subunit[87, 92]. Residues 106-120 of the γ2 subunit are also important for formation of the α1-γ2 interface; when added to an otherwise non-assembling α1 peptide, residues 106-120 of the γ2 subunit were sufficient to co-immunoprecipitate the α1 subunit but not the β3 subunit[88]. Several γ2 subunit point mutations have also been observed to affect assembly – mutating T164 and P166 interfered specifically with the formation of γ2-β3 intermediates[99], and the epilepsy-associated γ2 mutation R82Q was reported to impair binding to β2 subunits[100]. An assembly sequence has also been reported in the γ3 subunit; residues 86-100 of the γ3 subunit are sufficient to induce binding to both the α1 and β3 subunits[93].

It should be noted that many of these sequences lie in homologous regions. Indeed, the assembly sequences of α1 (82-96), β3 (77-91), and γ2 (106-120) subunits were originally investigated because they are homologous to the previously-identified γ3 subunit (86-100) sequence. Additionally, it has been suggested that residues on the ε subunit (N229, K231, E233, K237) that are homologous to the β3 subunit residues mediating homomeric assembly may influence whether one or two ε subunits are incorporated into α2β3ε receptors[101].

Despite this wealth of information pointing to mechanisms that promote selective oligomerization, to date there has been no direct demonstration of the order of $GABA_A$ receptor subunit assembly. The nAChR assembly intermediates were detected nearly two decades ago, and their order of oligomerization was subsequently determined using radiolabeled compounds known to bind only at specific subunit interfaces. However, when similar studies were attempted with $GABA_A$ receptors, only pentamers could be isolated from rat brain lysate or transfected fibroblasts cultured at 37C. When fibroblasts were instead cultured at 25˚C, dimers could be detected but no order of assembly could be determined[96]. This line of research has been largely abandoned in recent years and remains a potentially rich area for future study.

Exit from the endoplasmic reticulum and transport through the Golgi apparatus

Subunits that cannot form pentamers in the ER are shuttled to the proteasome and degraded, while successfully assembled receptors enter the secretory pathway. From this point forward, biogenesis depends heavily upon $GABA_A$ receptor-associated proteins, as illustrated in Figure 5 and summarized in Table 4. ER exit is facilitated by PLIC-1 and PLIC-2 (*p*roteins that *l*ink *i*ntegrin-associated protein with the *c*ytoskeleton), which contain a ubiquitin-like N-terminal domain and a ubiquitin-associated C-terminal domain[102]. The latter domain interacts with the intracellular loops of α and β subunits[103], inhibits the degradation of polyubiquitinated subunits[104], and thereby facilitates $GABA_A$ receptor surface expression. It has been established that PLICs increase surface expression without affecting endocytosis[104]; however, they were detected in Golgi, cisternae, and other intracellular vesicles of neurons[103], suggesting they may play additional roles in $GABA_A$ receptor trafficking.

Once in the Golgi apparatus, $GABA_A$ receptor subunits undergo many post-translational modifications facilitated by associated proteins. One of the most common Golgi modifications is palmitoylation, the formation of a reversible thioester linkage between a 16-carbon palmitic acid and a cysteine residue. Palmitoylation primarily serves to promote stable membrane attachment (and, potentially, targeting to lipid rafts), but it may also regulate trafficking, stability, and protein-protein interactions[105]. The majority of protein palmitoylation is accomplished by members of the DHHC (Asp-His-His-Cys) family of zinc-finger proteins[106]; to date, 25 members of this family have been identified in humans[107]. DHHC3, which is also known as GODZ (*Go*lgi-specific *D*HHC *Z*inc-finger protein), interacts with and palmitoylates cysteines located in the M3-M4 loop of γ1-3 subunits. The GODZ binding site has been mapped to residues 337-350 of the γ2 subunit, which are highly conserved within the γ subunit family[108]. Notably, this sequence contains four cysteine residues that could accept palmitate groups, though the specific palmitoylation site(s) have not been identified. When neuronal GODZ was eliminated using shRNA, mIPSC amplitude and frequency were reduced, as were the numbers of γ2 subunit

immunoreactive puncta. Moreover, neighboring GAT- and VIAAT-positive neurons tended not to form synapses with the transfected neurons[109]. Taken together, these data indicate that GODZ palmitoylates γ2 subunits in the Golgi apparatus and facilitates plasma membrane insertion of γ2 subunit-containing receptors.

Trans-Golgi network and beyond

The list of proteins that bind to $GABA_A$ receptors in secretory vesicles has grown immensely over the past decade. Arguably, the best-characterized of these is the aptly-named *GABA*$_A$ *r*eceptor-*a*ssociated *p*rotein (GABARAP). It is a 14 kDa ubiquitin-like protein belonging to the microtubule-associated protein family, which also includes three close GABARAP homologues called GABARAP-like proteins (GABARAPL1-3). All are widely expressed, but GABARAPL1 (also known as GEC1) levels are somewhat enriched in brain. These proteins are cytosolic, but they associate with intracellular lipid membranes through a C-terminal phospholipid[110].

The GABARAP crystal structure revealed an N-terminal microtubule-binding domain and two hydrophobic pockets that bind numerous proteins, including the cytoplasmic loop of $GABA_A$ receptor γ subunits[111-114]. In hippocampal neurons, native GABARAP immunofluorescence was seen throughout the soma and processes; however, it appeared to colocalize with γ2 subunits only in the Golgi apparatus and intracellular vesicles[115]. When GABARAP was overexpressed in the same system, γ2 subunit surface levels increased. Interestingly, when γ2 subunit cDNA was transfected in excess (i.e., α1:β2:γ2 at 1:1:10), GABARAP appeared to have no effect, suggesting that GABARAP might help determine receptor stoichiometry by promoting the formation of ternary α1β2γ2 receptors over binary α1β2 receptors[116]. The combination of GABARAP-γ2 intracellular colocalization and GABARAP's ability to bind microtubules suggests that GABARAP facilitates surface expression of γ2 subunit-

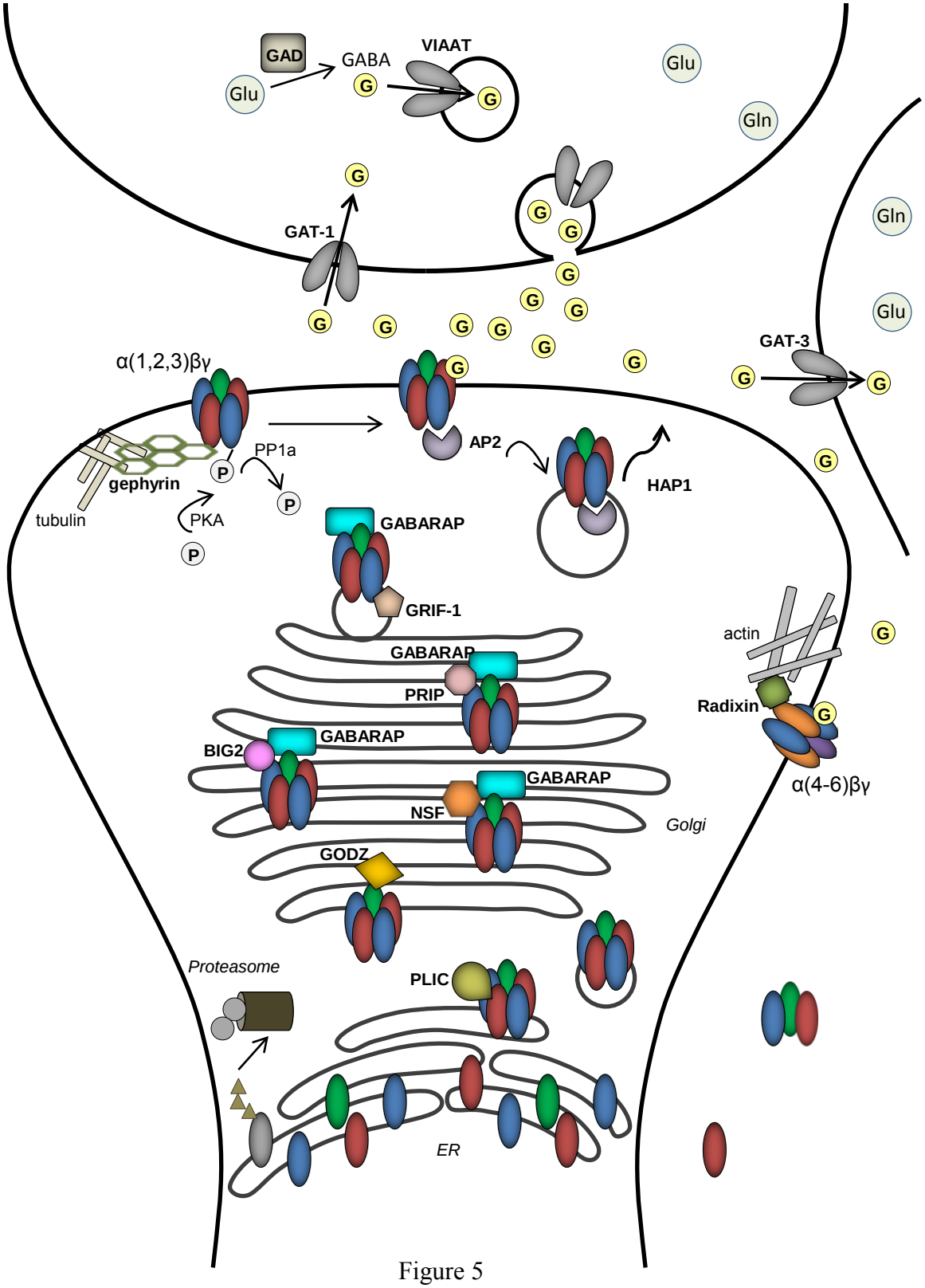
GAD
GABA
VIAAT
Glu
Gln
GAT-1
GAT-3
α(1,2,3)βγ
gephyrin
tubulin
PKA
PP1a
AP2
HAP1
GABARAP
GRIF-1
PRIP
BIG2
NSF
GODZ
actin
Radixin
α(4-6)βγ
Golgi
Proteasome
PLIC
ER

Figure 5

Figure 5. Schematic of a GABAergic synapse.
Presynaptic neuron (top), glial cell (right), and postsynaptic (bottom) neurons at a GABAergic synapse. GABA transport and $GABA_A$ receptor-associated proteins are illustrated. Note that the synaptic $GABA_A$ receptor represents isoforms including α(1,2,3,4,6)βγ and the extrasynaptic $GABA_A$ receptor represents isoforms including α5βγ and α(1,4,6)βδ.

ER = endoplasmic reticulum
PLIC = Proteins that Link Integrin-associated protein with the Cytoskeleton
GODZ = Golgi-specific DHHC Zinc-finger protein
GABARAP = $GABA_A$ Receptor-Associated Protein
NSF = N-ethylmaleimide-Sensitive Factor
PRIP = Phospholipase-C-Related catalytically Inactive Protein
PP1α = Protein Phosphatase 1α
BIG2 = Brefeldin-A-Inhibited GDP/GTP exchange factor 2
GRIF-1 = $GABA_A$ Receptor-Interacting Factor-1
AP2 = clathrin-Adaptor Protein 2
HAP1 = Huntingtin-Associated Protein 1
VIAAT = vesicular inhibitory amino acid transporter
GAD = Glutamic Acid Decarboxylase
GAT = GABA Transporter
Glu = glutamate
Gln = glutamine

Table 4: $GABA_A$ receptor-associated proteins

Protein	Full name	Interacts w/	Localization	Effect
AP2	adaptor protein (2)	**β1-3, γ1-3, δ** (*YXX*φ motif in β; basic patch motif (γ324-337; β401-412) in all)	clathrin-coated vesicles	endocytosis (recruits GABARs to clathrin-coated vesicles; phosphorylation inhibits AP2-GABAR binding)
GABARAP	$GABA_A$ receptor-associated protein	**γ1**, **γ2** (389-394)	intracellular membranes - *Golgi*, ER (somatodendritic, axonal)	clustering/links to microtubules binds clathrin heavy chain
Gephyrin		**γ2** **α1-3**	synapses	clustering/tubulin-binding
GRIP-1	GluR-interacting protein 1	**γ2**		synaptogenesis? regulation?
GRIF-1	GABAR-interacting factor-1	**β2** (348-361, 316-339)		forward trafficking (organelles/vesicles) kinesin-associated protein
GODZ	Golgi-specific DHHC Zn-finger protein	**γ1-3**, (γ2(415-428))	Golgi, cytoplasmic membrane	palmitoylation; surface expression of γ subunit-containing receptors
NSF	*N*-ethylmaleimide sensitive factor	**β1-3** (β1 395-415); GABARAP	just inside plasma membrane (processes, soma); some punctate intracellular	↓ surface levels *does not* ↑ endocytosis
Plic-1	Protein linking IAP and cytoskeleton (a.k.a. ubiquilin)	**α and β** (α1 346-355) via C-term UBA	clathrin-coated pits ER intracellular soma/processes	clathrin-coated vesicle trafficking ER stabilization
PRIP-1,2	PLC-related, catalytically inactive protein	**β1-3, γ2(weak)**; GABARAP	intracellular	↑trafficking of γ2-containing GABARs competes w/ γ2 for GABARAP binding site directly binds PP1/2A
Radixin	(note: an F-actin-binding ERM protein)	**α5** (342-357)	just inside plasma membrane	clustering (α5, extrasynaptic) membrane-cytoskeleton linkage
HAP-1	Huntingtin-associated protein	**β1-3**	intracellular soma, dendritic shafts	promotes recycling to membrane
BIG-2	Brefeldin-A-inhibited GDP/GTP exchange factor-2	**β1-3**	ER, TGN, dendrites, axon, synapse	promotes ER exit (HEK)

containing receptors by promoting exit from the Golgi apparatus and vesicular transport toward the plasma membrane.

Many of GABARAP's other binding partners suggest trafficking effects beyond simple microtubule association. For instance, GABARAP binds to *N*-ethylmaleimide-sensitive factor (NSF), which disaggregates SNARE proteins via ATP hydrolysis and is necessary for intracellular membrane fusion. NSF also binds to the cytoplasmic loop of β1-3 subunits and decreases $GABA_A$ receptor cell surface levels by approximately 20% in both transfected fibroblasts and cultured neurons, apparently by regulating receptor insertion rather than endocytosis[117]. Because the β subunit binding site (β3 residues 419-439) contains a phosphorylation site that can affect surface expression, it has been proposed that NSF could have different effects on $GABA_A$ receptor trafficking depending on whether it binds to GABARAP or β subunits themselves.

Similarly, *P*hospholipase-C-*R*elated catalytically *I*nactive *P*roteins (PRIP1, PRIP2) bind both to GABARAP and to the intracellular domain of $GABA_A$ receptor β and (weakly) γ2 subunits. It is unclear if PRIPs act as a bridging protein between GABARAP and β subunits, but they do compete with γ2 subunits for binding to GABARAP[118]. When the PRIP-β subunit association was disrupted by either a PRIP-binding peptide or PRIP gene deletion, surface expression of γ2 subunit-containing $GABA_A$ receptors declined[119]. Interestingly, there was a concomitant increase of α1 and β3 subunit surface levels in the PRIP-KO mice, suggesting that PRIPs may help determine receptor composition and/or stoichiometry[120]. PRIPs also inactivate *P*rotein *P*hosphatase *1α* (PP1α), which can dephosphorylate sites on β subunits that affect both function and internalization of $GABA_A$ receptors[121]. In summary, PRIP-1 and -2 have extremely complex effects on receptor trafficking and function and can act both through and independent of their association with GABARAP.

*B*refeldin-A-*I*nhibited *G*DP/GTP exchange factor *2* (BIG2) is another $GABA_A$ receptor-associated protein that is primarily localized to the Golgi apparatus. As its name suggests, BIG2

is a guanine nucleotide exchange factor (GEF) that catalyzes GDP/GTP exchange on the small G-protein *A*DP-*R*ibosylation *F*actor (ARF)[122, 123]. Activation of ARF by GDP/GTP exchange is required for membrane budding in the Golgi apparatus, which allows proteins to progress through the trans-Golgi network and the exocytotic pathway. In addition to its GEF functions, BIG2 binds with high affinity to the intracellular loops of β subunits. When this interaction was disrupted, $GABA_A$ receptors accumulated in the perinuclear ER, and when exogenous BIG2 was overexpressed, $GABA_A$ receptor surface expression increased[124]. Although the highest BIG2 levels were detected in the Golgi apparatus, $GABA_AR$/BIG2 colocalization also occurred in somatic and dendritic vesicles but not at synapses. Thus, it seems likely that BIG2 facilitates multiple steps in $GABA_A$ receptor forward trafficking.

Yet another protein that facilitates intracellular forward trafficking is *G*ABA_A *R*eceptor-*I*nteracting *F*actor-*1* (GRIF-1, also known as TRAK2), a kinesin-associated protein that binds to the β2 subunit cytoplasmic loop. GRIF-1 is soluble and thus widely distributed throughout the cytoplasm, and it colocalizes with β2 subunits in intracellular vesicles[125-127]. The exact mechanism by which GRIF-1 promotes $GABA_A$ receptor forward trafficking has not been determined, but its kinesin-binding abilities obviously suggest that it could facilitate vesicle movement along the cytoskeleton. Interestingly, mice lacking the closely-related gene TRAK1 displayed hypertonia and reduced $GABA_A$ receptor expression.

Plasma membrane targeting and maintenance

Studies have suggested that Akt-mediated phosphorylation of β3 subunits may promote *de novo* receptor surface delivery[128, 129] and that insertion is primarily extrasynaptic[130], but little else is known about factors regulating plasma membrane fusion of vesicles containing newly-synthesized $GABA_A$ receptors. However, it is clear that once $GABA_A$ receptors reach the plasma membrane, they can be localized to synaptic or extrasynaptic sites. In either case, the receptors often form clusters with the help of scaffolding proteins. Postsynaptic clustering is mediated by

gephyrin, a multi-domain scaffolding protein capable of oligomerizing with itself and with $GABA_A$ and glycine receptors[131]. Gephyrin likely assumes a hexagonal lattice structure, as its N-terminal domain forms trimers and its C-terminal domain forms dimers, and the lattice links to the cytoskeleton through a central tubulin-binding domain[132, 133]. However, the gephyrin-cytoskeleton interaction is likely much more complex, as gephyrin has been shown to interact with regulators of microfilament dynamics including profilin I and II[134]. Despite gephyrin's ubiquitous presence at inhibitory synapses[135], years of investigation failed to identify a direct interaction between gephyrin and native $GABA_A$ receptor subunits. The interaction site was long assumed to be in the γ2 subunit, as cultured neurons from γ2 subunit KO mice lacked postsynaptic $GABA_A$ receptor and gephyrin clusters[136, 137] and transfection of various γ2 subunit domains affected clustering[138]. However, recent studies have identified direct interactions between gephyrin and α1-3 subunits[139]. In any case, it is clear that gephyrin-mediated postsynaptic clustering of $GABA_A$ receptors is important but not absolutely required for normal inhibitory transmission and synapse development[138, 140].

Extrasynaptic $GABA_A$ receptors can also form clusters. Interestingly, most of these contained the relatively rare α5 subunit together with the usually-synaptic γ2 subunit, and clusters persisted in the absence of gephyrin[141-143]. A yeast two-hybrid (Y2H) screen using the intracellular loop of α5 subunits as bait identified the binding partner radixin, one member of the *Ez*rin-*R*adixin-*M*oesin (ERM) protein family known to crosslink actin and plasma membrane proteins[144]. In rat brain, α5 subunit-containing receptors and radixin colocalized in puncta, 90% of which were extrasynaptic. In contrast, radixin colocalized only slightly with gephyrin and/or VIAAT. When radixin levels were reduced in by antisense oligonucleotide injection, α5 (but not α1) subunit clusters nearly disappeared from cultured hippocampal neurons. Similarly, brain slices from radixin KO mice had greatly reduced α5 subunit clustering. Taken together, these data suggest that the majority of clustered extrasynaptic $GABA_A$ receptors contain α5 subunits and that clusters are maintained by radixin crosslinking with actin cytoskeleton.

Endocytosis and post-endocytic sorting

Most neuronal $GABA_A$ receptors are internalized via clathrin-mediated endocytosis, and the clathrin-*A*daptor *P*rotein *2* (AP2) plays a key role in targeting receptors to clathrin-coated pits[145]. AP2 is a tetramer comprising α, β2, σ2, and μ2 subunits; the latter binds to the intracellular loops of β1-3 and γ2 $GABA_A$ receptor subunits. Several AP2 binding motifs have been identified; various regions of μ2 subunits can bind basic, dileucine, or tyrosine-containing hydrophobic YXXφ sequences on target proteins[146]. Each of these motifs is important for AP2-mediated endocytosis of $GABA_A$ receptors. AP2 has been demonstrated to bind to β1-3(^{367}LL^{368}), β3(^{405}RRR^{407}), and γ2(^{414}YECL^{417}) subunit sequences[147-149]. In each case, phosphorylation of tyrosines within or serines near the binding motif impairs AP2-$GABA_A$ receptor association, thereby reducing receptor endocytosis and increasing inhibitory transmission. It should be noted that the role of phosphorylation in $GABA_A$ receptor expression, trafficking, and physiology is considerably more complex, but a comprehensive exploration of these effects would require a dedicated review.

After endocytosis, $GABA_A$ receptors can be recycled to the cell membrane or targeted for lysosomal degradation. *H*untingtin-*A*ssociated *P*rotein *1* (HAP1) plays a key role in this decision. HAP1, which bears polyglutamine repeats in Huntington disease, is a cytosolic protein that binds to *ki*nesin *f*amily motor protein *5* (KIF5), thereby linking other binding partners to the cytoskeleton and intracellular trafficking machinery[150]. With regard to $GABA_A$ receptors, HAP1 binds the intracellular loop of β subunits, inhibits lysosomal degradation, and promotes receptor recycling. In cultured neurons, HAP1 overexpression increased $GABA_A$ receptor surface expression and mIPSC amplitude[151]. Furthermore, the physiological importance of HAP1 was demonstrated by two recent studies. First, HAP1 is abundantly expressed in hypothalamus, and expression levels were recently shown to be directly correlated with food intake (i.e., decreasing HAP1 expression led to decreased feeding)[152]. Finally, the $GABA_A$ receptor/HAP1/KIF5/microtubule complex was disrupted in the HD mouse model.

Unsurprisingly, this led to reduced $GABA_A$ receptor surface expression and GABAergic neurotransmission, which might suggest a mechanism for neuronal excitotoxicity in Huntington disease[150].

Tertiary and quaternary structure of $GABA_A$ receptors

Thus far, we have discussed the major structural elements of $GABA_A$ receptors and their component subunits. The receptor comprises five subunits, each of which includes a large, extracellular N-terminal domain containing assembly signals; four transmembrane domains (M1-M4); and a large intracellular loop between the third and fourth transmembrane domains (M3-M4 loop) containing binding sites for many receptor-associated proteins. However, to understand the mechanisms of ligand binding and channel gating, it is necessary to provide a more detailed description of receptor structure.

To date, no $GABA_A$ receptors have been crystallized. Accordingly, homology models have used the structures of nAChRs[97, 153] and AChBP (homologous to the extracellular domain of the nAChR)[98] solved within the past decade. More recently, prokaryotic LGICs have also been crystallized[154-156]; however, all of these channels are cation-selective and accordingly were not ideal for modeling $GABA_A$ receptors, particularly in certain transmembrane domains[157, 158]. The first structure of an anionic Cys-loop receptor, the glutamate-gated chloride channel of *C. elegans* (GluCl) was reported in 2011[159]. All original homology models presented in this dissertation use the GluCl template, but prior studies obviously did not.

Major structural elements are common to all crystallized Cys-loop receptors (Figure 6). Each subunit is approximately 160Å long (extracellular, transmembrane, intracellular) and about 40Å wide. The extracellular N-terminal domain, which contains the binding sites for most ligands, comprises a distal α helix and ten β strands linked by loops. The β strands combine to form a β sandwich; strands 4, 7, 9, and 10 form an outer sheet while the rest form an inner sheet

facing the ion channel pore (see Appendix 1). These two sheets are linked by the eponymous Cys-loop and can pivot relative to one another during gating.

The aforementioned secondary and tertiary structure elements were found in all Cys-loop receptor crystal structures. However, the $GABA_A$ receptor N-terminal domain structure is also widely discussed in terms of "loops" A-F. These "loops" do not necessarily consist of the linkers between consecutive β-sheets; rather, they represent regions experimentally determined to be accessible to ligands. Most studies defining these loops used the *s*canning *c*ysteine *a*ccessibility *m*utagenesis method (SCAM), in which individual amino acids are systematically mutated to cysteine, exposed to sulfhydryl-reactive compounds, and then assessed for reagent binding and receptor function[160]. Clearly, this approach is limited by the possibility that the point mutations themselves may perturb receptor conformation; however, it provides a useful approximation in the absence of a crystal structure. Thus, loops A-F have been defined as illustrated in Table 5 and Appendix 1 of this dissertation. Briefly, in the primary structure, loops occur in the order D-A-E-B-F-C (see Table 5 for corresponding secondary structure elements). Loops A-C are located on the "principal" or "(+)" side of subunits, while loops D-F are located on the "complementary" or "(-)" side (Figure 6B). The interfaces between these motifs in different subunits constitute the binding sites for GABA, benzodiazepines, and their analogues, as discussed further in subsequent sections.

The four transmembrane (TM) domains are oriented such that M1 lies on the complementary side, M2 lines the ion pore, M3 lies on the principal side, and M4 lies on the outer side of the receptor facing the lipid membrane. The transmembrane helices (particularly M3 and M4) are rather loosely packed, leaving solvent-accessible cavities both within and between subunit transmembrane domains[158]; indeed, many modulators appear to bind within these cavities. Perhaps unsurprisingly, the pore-lining M2 domain is the most highly conserved region among $GABA_A$ receptor subunits. It contains major components of the ion selectivity filter and the channel gate, which in turn determine channel conductance. Once again, the solvent-accessible

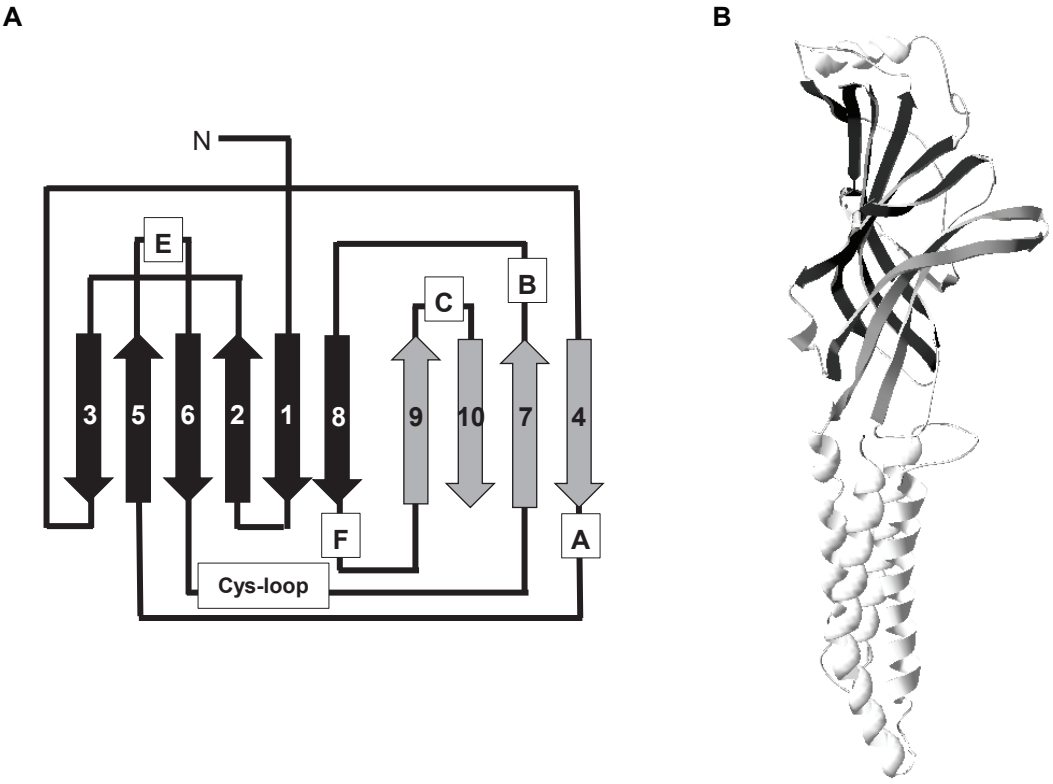

Figure 6. Secondary and tertiary structure of $GABA_A$ receptor subunit N-terminal domains.

A. Schematic of the β-strand composition of the $GABA_A$ receptor subunit N-terminal domain. Black arrows represent strands comprising the inner sheet and grey arrows represent strands comprising the outer sheet. "Loops" A-F are indicated, as is the Cys-loop (structurally, loop 7 between strands β-6 and β-7). The N-terminus is indicated at the top. **B.** Homology model of a $GABA_A$ receptor subunit. β-strands on the inner and outer sheets are colored as in Panel A.

residues of this region (i.e., those on the pore-lining face of the M2 helix) have been identified using SCAM. The N-terminal residues are mostly hydrophilic and are thought to interact with the hydration shell surrounding the chloride ions. While this function would be expected to improve conductance, it would not necessarily discriminate among hydrated ions and thus should not constitute the selectivity filter. Rather, it is likely that anion selectivity occurs approximately two-thirds of the way toward the cytoplasmic side of the channel; positively-charged sulfhydryl compounds can react with residues above this point[161, 162]. However, several other gate and filter locations have been proposed. First, the extracellular sides of both M1 and M2 contain highly conserved positively-charged residues that could compose a selective vestibule[163]. Second, a conserved leucine located approximately in the middle of the M2 domain is profoundly important for channel kinetics; it has also been suggested to line the narrowest point of the channel and thus constitute the gate. Finally, the intracellular M1-M2 linker has also been demonstrated to affect selectivity.

Table 5. Structural elements of $GABA_A$ receptor subunit interfaces.

Loop	Face	Approximate residues (β-α)	Structural elements (GluCl)
A	+	β2(21-25)	β-strand 4, loop 4
B	+	β2(79-85)	β-strand 7, loop 8
C	+	β2(24-31)	β-strand 9 & 10, loop 10
D	-	α1(86-96)	β-strand 2
E	-	α1(145-157)	β-strands 5 & 6, loop 6
F	-	α1(203-212)	β-strand 8, loop 9

Wherever the exact gating location may be, it clearly lies far from the ligand binding sites. Consequently, extensive efforts have been made to determine the transduction mechanism coupling ligand binding to channel gating. Current models suggest that GABA binding provokes

a constriction of the binding pocket (i.e., movement of loops A-F, especially loops C and F)[164, 165]. This causes a wave of conformational changes to propagate through the β-sandwich domain, which in turn allows conserved acidic residues in loop 2 (β subunits) and loop 7 (α and β subunits) to approach conserved basic residues in their respective M2-M3 linkers. Cross-linking studies suggest that the cascade concludes with a rotation of M2 that essentially twists the channel open[166, 167].

Physiology of $GABA_A$ receptor isoforms

The major elements of structure, binding, and gating are thought to be common to all $GABA_A$ receptor subunits. However, receptor isoforms exhibit widely divergent functional properties. Because most individual neurons express many subunits simultaneously, the physiological characteristics of individual isoforms can be studied most accurately by recording currents from fibroblasts (or other cells that do not express endogenous $GABA_A$ receptors) that have been transfected with specific subunit combinations. Under these conditions, it is possible to analyze both the "microscopic" (single-channel) and the "macroscopic" (population) behavior of individual receptor isoforms. Microscopic kinetic properties include channel conductance, open time, and closed time. Macroscopic kinetic properties include activation (channel opening in response to agonist), desensitization (decreased current in the continued presence of agonist), and deactivation (channel closure after removal of agonist). Each of these varies among $GABA_A$ receptor isoforms.

Unsurprisingly, perhaps the most widely studied isoform is α1βxγ2, which is thought to be the predominant isoform in whole brain. On a single-channel level, these receptors have a main conductance of approximately 26-30 pS, as well as several subconductance levels. Openings tend to occur in bursts and, based on the distribution of channel open times, the channel appears to enter at least three open states and at least five closed states (Figure 7A)[168]. Kinetic analysis has suggested that the receptor must pass through closed states rather than transitioning

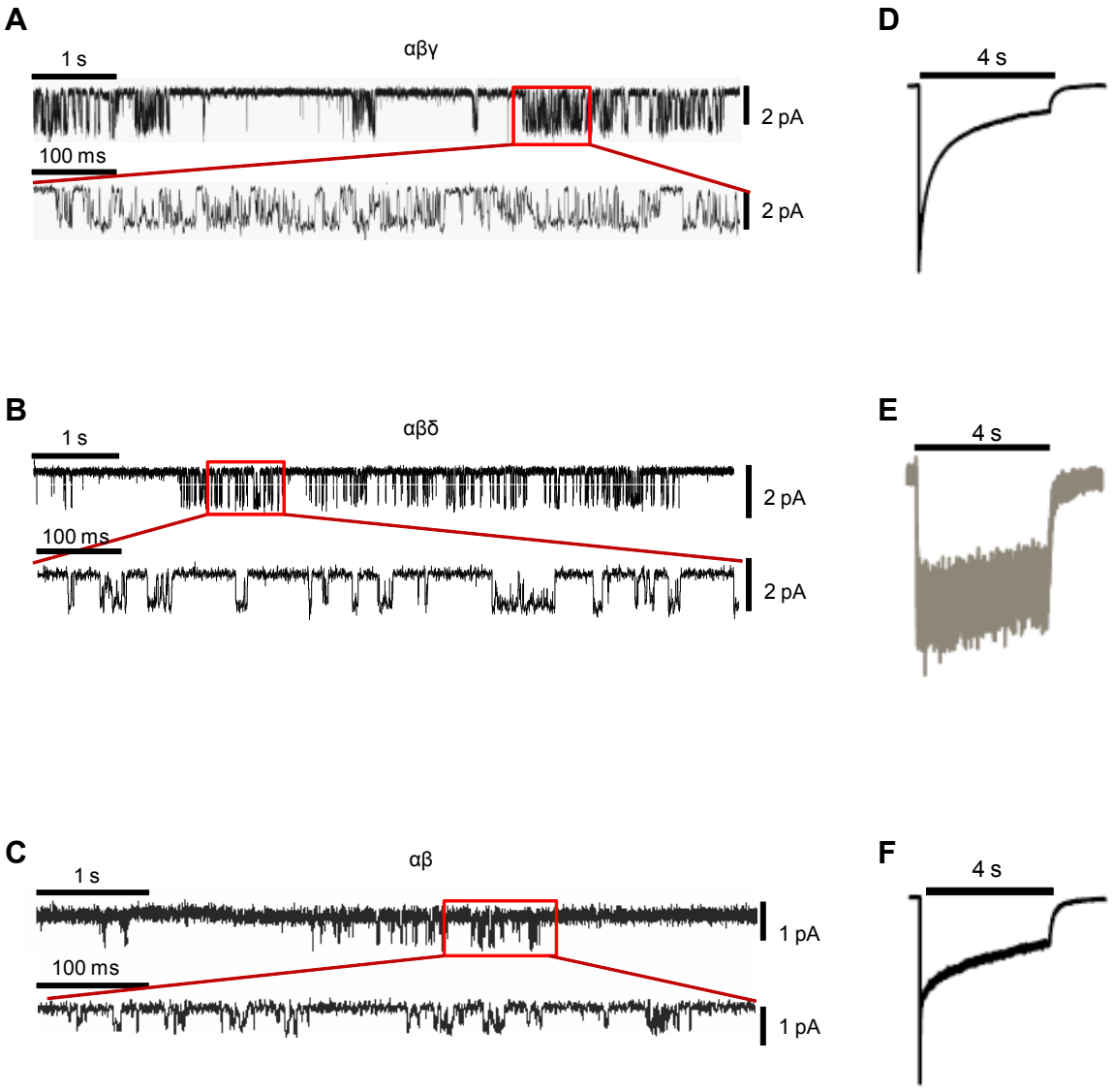

Figure 7. Representative single-channel and macropatch recordings from $GABA_A$ receptor isoforms.

Representative single-channel (**A-C**) and whole-cell (**D-F**) currents recorded from HEK293T cells expressing αβγ (A,D), αβδ (B,E), or αβ (C,F). Currents were evoked using 1 mM (saturating) GABA.

directly between open states; however, some interpretations differ. Macropatch or whole cell recordings reveal that α1βxγ2 receptors activate quickly, desensitize rapidly and extensively, and deactivate somewhat slowly (Figure 7B). When the time courses of desensitization and deactivation are fitted with a sum of exponential functions, it appears that α1βxγ2 receptors desensitize multiphasically and deactivate biphasically.

In contrast, α1βxδ receptors appear to have only two brief open states and several longer closed states (Figure 7C). Macroscopically, they activate more slowly, desensitize less extensively, and deactivate more quickly (Figure 7E). Notably, the peak current amplitude of α1βxδ receptors is approximately tenfold lower than that of α1βxγ2 receptors (Figure 7D).

As previously mentioned, $GABA_A$ receptors that contain only α and β subunits can be expressed and activated by GABA. These "binary" receptors constitute another major receptor category that has been systematically compared with "ternary" αβγ and αβδ receptors. Compared to α1βxγ2 receptors, α1βx receptors have a lower main conductance (~18 pS) and burst less often (Figure 7C). They activate more slowly, desensitize more extensively, and deactivate more quickly. Furthermore, their peak current amplitude is less than half as large (Figure 7F).

It is perhaps unsurprising that αβ, αβγ, and αβδ receptor isoforms have very different physiological characteristics. However, different subunit subtypes alter receptor kinetics as well; indeed, the wide array of $GABA_A$ receptor subunits might have evolved because they confer diverse physiological properties that facilitate fine-tuning of neuronal inhibition. Systematic comparisons of α(1-6)β3γ2 receptor currents have demonstrated that each isoform has a unique combination of GABA sensitivity, activation rate, desensitization rate and extent, deactivation rate, and recovery rate[169]. For instance, α6β3γ2 receptors were far more sensitive to GABA than any other isoform, while α3β3γ2 receptors were the slowest to activate[170].

Neuronal physiology: types of inhibitory transmission

There are two major types of GABAergic neurotransmission. "Phasic" inhibition describes the large, transient currents produced by synaptic receptors in response to the high concentrations of GABA periodically released by presynaptic vesicles. In contrast, "tonic" inhibition consists of smaller, more constant currents produced by extrasynaptic receptors in response to low concentrations of ambient GABA that escaped synaptic reuptake. Because receptor subunit composition is a major determinant of subcellular localization, phasic inhibition is mediated by synaptic γ subunit-containing receptors, while tonic inhibition is mediated mostly by extrasynaptic δ subunit-containing receptors. Each isoform is physiologically well adapted to its role. For instance, the synaptic γ subunit-containing receptors have a relatively low affinity for GABA, activate quickly, desensitize extensively, and deactivate slowly – all properties allowing them to respond to rapid changes in neurotransmitter release. In contrast, the extrasynaptic δ subunit-containing receptors have a relatively high affinity for GABA, activate slowly, and desensitize minimally, allowing them to respond to constant low levels of GABA. Although any individual phasic current produces more charge transfer than any individual tonic current, the sum of all tonic currents may provide the majority of inhibitory tone in the brain.

Pharmacology

GABA and analogues (muscimol, THIP, β-alanine)

The GABA binding site is located at the interface between the principal side of β subunits and the complementary side of α subunits. Because the proposed subunit arrangement of $GABA_A$ receptors is γ-β-α-β-α (anticlockwise as viewed from the synaptic cleft), each receptor contains two binding sites, which have been mapped using SCAM. Among the first identified residues were those defining loop D of the α1 subunit, including residues T88, D90, F92, R94, and S96. The alternating pattern of these residues suggested that at least part of "loop" D actually consisted of a β-sheet[171]. Other necessary α subunit residues included R147 in loop E[172] and residues from

P202-D219 in loop F[173]. Meanwhile, β subunit residues including R131 in loop C[174] and V117, D119, Y121, and Y123 in loop A[175] were found to be essential for GABA binding, thus defining the binding pocket as the intersubunit region between β and α subunit N-terminal domains.

Several other agonists act at the GABA binding site. These include the endogenous compounds β-alanine and taurine and the dissociative mushroom alkaloid muscimol. Partial agonists include the muscimol analogue tetrahydroisoxazolepyridinol (THIP; gaboxadol) and isoguvacine, while competitive antagonists include the plant alkaloid bicuculline and the GABA derivative gabazine. None of these compounds is currently approved for clinical use, but all are valuable experimental tools.

Benzodiazepines

No drugs have been so closely identified with $GABA_A$ receptors as the benzodiazepines; indeed, many years of literature refer to benzodiazepine-sensitive $GABA_A$ receptor isoforms as benzodiazepine receptors. Unsurprisingly, the benzodiazepine binding site and mechanism are particularly well defined. The binding pocket is located at the interface between the N-terminal domains of most α and γ subunits, in a position homologous to the GABA binding site at the β-α subunit interface. Receptors containing α4 or α6 subunits do not respond to benzodiazepines[176-178], and receptors containing γ1 or γ3 subunits are less sensitive than receptors containing γ2 subunits[179]. The basis for α subunit selectivity lies in the residue homologous to α1(H129), which is a histidine in benzodiazepine-sensitive α subunits (i.e., α1, α2, α3, and α5) and an arginine in benzodiazepine-insensitive α subunits (i.e., α4 and α6)[180].

H129 is located in loop A on the (+) side of sensitive α subunits, which is predicted to form the interface with γ subunits. Supporting this, mutating individual residues in the γ2 subunit loops D and E[181] or essentially any residue in loop F[182] impaired benzodiazepine binding. However, other studies have suggested that γ2 loop F residues do not directly participate in the binding site, but rather undergo a conformational change after benzodiazepine binding that helps

to transduce the signal[182]. Dissecting the signal transduction cascade has proved significantly more difficult than identifying the binding site, and residues throughout the γ2 subunit transmembrane domains and intracellular loop have been implicated as well[183, 184].

Table 6. Binding sites, specificity, and effects of major drug classes acting at $GABA_A$ receptors.

Compound	Residues	Region	Isoforms	Type	Effects	Citation
GABA	α1(T88, D90, F92, R94, S96, R147, P202-D219)	N-terminal	β-α interface	agonist		
benzodiazepines	α1(H140) γ2(F116, M169)	N-terminal	α(1-3,5)-γ interface	(+) allosteric	↑# of openings	185
barbiturates		M1-4	all	(+) allosteric	↑$GABA_A$ burst duration	185, 186
etomidate	β2(M286), β2(Y468)	M2-4	β2, β3	(+) allosteric	↑ GABA efficacy ↓IPSC charge transfer	187, 188
neurosteroids	α1(Q269,N435, Y438)	M1, M4	δ	(+) allosteric	↑ GABA efficacy prolong IPSCs ↑ open duration	187, 189-193
isoflurane	α1(L269, S297, A327)				↑ desensitized currents prolong IPSCs	194-196
picrotoxin	open-channel block	M2?	all	(-) allosteric	↓$GABA_A$ burst duration	186

Clinically-used benzodiazepines include diazepam, lorazepam, midazolam, and a number of other derivatives that differ primarily in metabolic half-life and time to onset of action. They produce a wide range of physiological effects, including sedation, anxiolysis, amnesia, and muscle relaxation; additionally, they increase seizure threshold. As such, they have been used to treat conditions such as insomnia, anxiety disorders, and epilepsy. Additionally, although benzodiazepines do not produce deep enough anesthesia for most surgical procedures, they are useful for preoperative sedation, induction of general anesthesia, and light anesthesia for minor but uncomfortable procedures such as endoscopies.

The discovery that α subunit residue H129 is essential for benzodiazepine binding has allowed investigators to determine which receptor isoforms mediate which of these effects by creating mice that contain the H129R mutation in α1, α2, α3, or α5 subunits and administering benzodiazepines. The resulting behavioral studies indicated that α1βγ receptors mediate sedation, anterograde amnesia, and anticonvulsant actions[197]; both α2βγ and α3βγ receptors mediate anxiolysis[198, 199], myorelaxation[184] and some spinal analgesia[200]; and α5βγ receptors mediate tolerance to sedation and possibly some amnestic effects[201, 202]. This specificity may be due to α subunit expression patterns; for instance, α1 subunits are expressed throughout the cortex, α2 subunits are highly expressed in limbic areas, and α2 and α3 subunits predominate in spinal cord. Because some benzodiazepine effects are therapeutic (anxiolysis, increased seizure threshold) and some are undesirable (sedation in non-anesthetic applications), there has been significant demand for subunit-specific drugs. One such drug is zolpidem, which acts predominantly at α1 subunits and thus is widely used to treat insomnia. Another, TPA-023, is a partial agonist for α2- and α3 subunit-containing receptors but an antagonist at α1 and α5 subunit-containing receptors; consequently, it is an effective anxiolytic and anticonvulsant but induces little sedation or dependence[203, 204].

Several benzodiazepine site antagonists and inverse agonists have been developed as well. One of these is flumazenil (Ro 15-1788), an antagonist that is used clinically to reverse symptoms of benzodiazepine overdose[205]. Inverse agonists include the β-carbolines (e.g., DMCM), which reduce chloride flux. Unsurprisingly, inverse agonists are anxiogenic and proconvulsant and therefore have no clinical application. However, they are useful research tools for investigators studying anxiety and epilepsy[206].

Barbiturates

For years, barbiturates were widely used to treat anxiety, insomnia, and epilepsy. Due to their low therapeutic index (LD_{50}/ED_{50}), they have largely been supplanted by other

anxiolytics/sedatives/anticonvulsants, but they are still occasionally used as anesthetic inducing agents. Interestingly, barbiturates have three distinct actions on $GABA_A$ receptors. At low concentrations (< 100 μM), they potentiate maximum GABA responses by increasing the duration of channel opening bursts[185]; at intermediate concentrations (approx. 100-1000 μM), they directly activate the receptor; and at higher concentrations (≥ 1 mM), they block the channel[207]. Although all $GABA_A$ receptor isoforms seem to respond to barbiturates, receptor subunit composition does affect barbiturate efficacy and potency. Both α and β subunit subtypes influence receptor responses, but α subunits appear to be more important. Potentiation occurred at similar barbiturate concentrations (EC_{50} 20-35 μM) for all α(x)β2γ2 receptors, but the degree of potentiation varied widely (α6 > α5 > α1 ≈ α2 ≈ α3). With regard to direct activation, subunit composition affected both efficacy and potency; barbiturate EC_{50} was approximately tenfold lower and maximum response was two- to fourfold greater for α6 subunit-containing receptors than for all other isoforms. Similarly, inhibition required higher barbiturate concentrations for α6 subunit-containing receptors than for other tested isoforms. The β subunit subtype affected barbiturate efficacy and potency only for direct activation and only when certain α subunits were coexpressed. All α6β(x)γ2 receptors had similar EC_{50} and maximum response values, but EC_{50} was higher and maximum response lower for α1β1γ2 receptors than for α1β2γ2 or α1β3γ2 receptors[207].

Theoretically, different binding sites are responsible for these different actions. To date, such sites have not been fully defined, but various studies have identified specific residues that are important for barbiturate activity. The α subunit-dependent differences in barbiturate efficacy seem to depend upon an α6 subunit residue in the extracellular N-terminal domain, T88[208], and barbiturates may directly activate α1 and α6 subunit-containing receptors with entirely different signal transduction pathways[209]. Barbiturates are very lipophilic compounds; consequently, most of the identified residues are located in the transmembrane domains of various subunits. Residues essential for barbiturate action have been identified in the first[174], second[175], and third[210]

transmembrane domains, and some of these were important for potentiation but not for direct activation[211].

Anesthetics

Given that short-acting barbiturates are used as inducing agents in anesthesia, it is perhaps unsurprising that many other anesthetics have similar actions at $GABA_A$ receptors. These include both volatile (isoflurane, sevoflurane) and intravenous (etomidate, propofol) agents. Like barbiturates, anesthetics potentiate GABAergic responses at low concentrations and directly activate receptors at higher concentrations. Furthermore, important residues but not full binding sites have been identified for most compounds.

Clinical anesthesia involves several components: sedation (decreased arousal), hypnosis (loss of consciousness), immobility, analgesia, and amnesia[212]. Different $GABA_A$ receptor isoforms located in different regions of the central nervous system are assumed be responsible for specific components. For instance, the considerable population of $GABA_A$ receptors present in spinal cord likely mediate immobility, while hippocampal receptors likely mediate amnesia. More specifically, particular subunits have been demonstrated to mediate particular actions of the intravenous agents etomidate and propofol. In heterologous systems, β2 or β3 subunit-containing receptors were both potentiated and directly activated by etomidate, but β1 subunit-containing receptors were poorly potentiated and could not be directly activated[213, 214]. The *Drosophila* $GABA_A$ receptor (*Rdl*) was similarly unresponsive to etomidate. The responsive subunits differ from the unresponsive subunits in a specific TM2 residue: the amino acid homologous to human β3 subunit residue N290, which is an asparagine in both β2 and β3 subunits, a serine in β1 subunits, and a methionine in the *Rdl* receptor. Mutagenesis studies confirmed that β3 subunit residue N290 was necessary and sufficient for etomidate responses. Subsequently, knockin (KI) mice with β2(N289S) or β3(N290S) subunit mutations were created, given etomidate, and subjected to behavioral tests. The β3(N290S) KI mice could still move in response to noxious

stimuli after etomidate administration, while the β2(N289S) KI mice recovered more quickly from light anesthesia[215]. Taken together, this suggested that β3 subunit-containing receptors are responsible for the immobilizing effects of etomidate, while β2 subunit-containing receptors are responsible for sedation, and both isoforms likely contribute to hypnosis.

Recently, photoaffinity labeling with a tritiated etomidate analogue was used to map the etomidate binding site. The ligand labeled residues in the first and third transmembrane domains of α and β subunits (M263 in α1 and M311in β3 subunits); both conserved within their respective subunit families)[216]. Another recent study found that the β3(N290S) subunit mutation reduced etomidate efficacy more than affinity[217]. Therefore, it seems likely that anesthetics bind to a pocket in the transmembrane domain (perhaps at the β(+)/α(-) interface), but they require the β subunit M2 asparagine for gating.

For several years, propofol and etomidate were thought to have identical binding sites. Recently, however, some residues important for binding of only one of these have been identified. Mutation of a conserved tyrosine in the β2 subunit M4 domain reduced $GABA_A$ receptor response to propofol but not etomidate[218]. The kinetics of IPSCs also seem to be differently affected by etomidate and propofol[188].

The volatile anesthetics (isoflurane and derivatives) also seem to bind to site(s) in the transmembrane domains, but likely in a distinct pocket. The α subunit may be more critical for volatile anesthetic binding, as essential residues have been identified in the first, second, and third transmembrane domains of α1 and α2 subunits[194]. At the channel level, volatile anesthetics appear to prolong IPSC decay, thereby increasing overall charge transfer[196].

In summary, most general anesthetics bind to pockets in the $GABA_A$ receptor transmembrane domains and either improve efficacy and potency of GABA-gated currents or, at higher concentrations, directly activate the receptor. In both cases, they increase overall inhibitory charge transfer, which could produce the various components of anesthesia by acting on receptors located in different parts of the CNS. Although many important residues have been

identified, neither precise binding sites nor gating mechanisms have been fully defined. Finally, it remains unclear how those mechanisms differ when anesthetics potentiate or directly activate receptors.

Neurosteroids

Most steroid hormones originate from peripheral organs such as the ovaries and adrenal glands and are capable of crossing the blood-brain barrier. Some neurons and glia express enzymes that synthesize steroids both *de novo* from cholesterol and from peripherally derived precursors; the products of both pathways are classified as neurosteroids. It has been known for years that cholesterol can cause CNS depression and that the synthetic steroid alphaxalone functions as an anesthetic. Eventually, it was demonstrated that alphaxalone could enhance GABA-evoked currents, and subsequent studies found that endogenous neurosteroids such as allopregnanolone and tetrahydro-deoxycorticosterone (THDOC) had similar effects. This could have very interesting physiological implications, as neurosteroid levels vary in response to the ovulatory cycle, pregnancy, and both acute and chronic stress.

Similar to barbiturates and other anesthetics, neurosteroids have dual actions on $GABA_A$ receptors. At low nanomolar concentrations, they potentiate GABA currents[219], and at higher nanomolar to micromolar concentrations they directly activate the receptor. Two distinct binding sites, identified using point mutagenesis and homology modeling, were proposed to mediate these effects. The potentiation binding site was localized to a hydrophobic pocket deep in the α subunit transmembrane domain, formed in part by α1 subunit residues Q269 (M1), N435 (M4), and Y438 (M4). In contrast, the direct activation binding site was localized to the interface between the β and α subunit transmembrane domains; α1 subunit residue T264 (M1 domain) and β2 subunit residue Y308 (M3 domain) contributed to the binding pocket[220].

Neurosteroids act on both synaptic and extrasynaptic $GABA_A$ receptors in many brain regions, but their efficacy and potency vary widely. They prolong mIPSCs mediated by synaptic

receptors, primarily by increasing the channel open duration[193]. Extrasynaptic (predominantly δ subunit-containing) receptors are particularly sensitive to neurosteroids[191], but this likely reflects the fact that GABA is a relatively low-efficacy partial agonist for δ subunit-containing receptors and neurosteroids shift activation to higher-efficacy gating patterns[192].

Ethanol

More mechanisms of action may have been proposed for ethanol than for any other drug. Potential targets include (but are not limited to) lipid rafts[221], NMDA receptors by way of Fyn kinase[222], purine receptors[223], opioid receptors[214], glycine receptors[224], and $GABA_A$ receptors[225]. Even ethanol's $GABA_A$ receptor-mediated effects are multifactorial; potentiation may occur due to altered subunit phosphorylation, increased neurosteroid production, enhanced presynaptic GABA release, or changes in subunit expression, trafficking and localization. Given these diverse effects, it is unsurprising that neither distinct binding sites nor subunit specificity for ethanol has been identified for $GABA_A$ receptors. However, ethanol efficacy and potency do seem to be greatest at extrasynaptic, δ subunit-containing receptors, where they enhance tonic inhibitory currents[226, 227].

Promiscuous pharmacology

Table 6 presents a summary of the major drugs found to act at $GABA_A$ receptor isoforms, their targets, and their functional effects. However, it is important to note that most drugs discussed above do not act solely at $GABA_A$ receptors. Both thiopental and pentobarbital inhibited nAChRs at clinically relevant concentrations[228]. Propofol potentiated glycine receptors[229] and inhibited both voltage-gated potassium channels[230] and L-type calcium channels[231], while isoflurane potentiated 5HT-3 and kainate receptors and inhibited AMPA and neuronal nicotinic acetylcholine receptors[212]. Most neurosteroid research has focused on $GABA_A$ receptors, but some action has been found at NMDA and nicotinic acetylcholine receptors[232].

Finally, as previously discussed, ethanol's targets are particularly broad. Therefore, it should not be assumed that all effects produced by these drugs are mediated by $GABA_A$ receptors.

Loss of $GABA_A$ receptor subunits: lessons from KO mice

Over the last 10-15 years, several $GABA_A$ receptor subunit KO mice have been created and studied. The α1-6, β2, β3, γ2, and δ subunits have all been individually eliminated, and the resulting phenotypes vary from mild behavioral abnormalities to pre- and perinatal lethality (summarized in Table 7).

One of the first (and most surprising) of these animals was the α1 subunit KO mouse. Approximately 60% of all adult rodent $GABA_A$ receptors may contain α1 subunits and, in agreement with this estimation, muscimol binding sites (i.e., all $GABA_A$ receptors with a β-α subunit interface) were reduced by 50% in α1 subunit KO mice. Nonetheless, these mice had few overt phenotypic abnormalities. They experienced increased perinatal mortality, but even this declined after a few generations. Interestingly, expression of α2 and α3 subunits increased and expression of β2/3 and γ2 subunits decreased over the same period[233]. Future studies found that α1 subunit KO mouse displayed decreased seizure threshold (but no spontaneous seizures), mild essential tremor, reduced response to synaptic or applied GABA (but no change in spontaneous IPSCs) and impaired dendritic spine maturation[234-236]. Considering the prevalence of α1 subunit-containing receptors, it is quite remarkable that α1 gene deletion produces so few harmful effects.

Mice lacking α2 subunits were created much more recently. These animals exhibited some increases in anxiety behavior and fear learning and, as expected, did not respond to the anxiolytic effects of benzodiazepines or barbiturates[237]. Other psychiatric disorders may be affected by α2 subunit-containing receptors as well; α2 subunit KO mice became immobile more quickly than wild-type mice when subjected to tail suspension or forced swim tests, both of which are tests used to assess depressive behaviors[238].

Table 7. Phenotypes of $GABA_A$ receptor subunit knockout mice.

Subunit	General	Subunit expression	Motor	Mood/ anxiety	Seizure/ EEG	Pharmacology	Refs
α1	↓ body weight ↓ dendritic spine maturation	↑ α2, α3 ↓ α6, β2, β3, γ2	mostly normal, tremor (handling)	↓ fear learning	↓ threshold no spontaneous		233-235
α2	grossly normal			↑ anxiety (CER) depressive behavior	no spontaneous	no anxiolysis by BZD/PB	237, 238
α3	grossly normal	none	↑ locomotor	↓ PPI for acoustic startle (sensorimotor gating defect)	no spontaneous resistant to evoked absence		239-242
α4	grossly normal	↓ δ (DG, CA1)		-		no gaboxadol response	243, 244
α5	better spatial memory	↑ eδ (hipp)		-	none	↓ EtOH reward	245-247
α6	grossly normal	↓ rδ (cb) ↑ K channel	impaired by BZD	-		↓ muscimol affinity	248-250
β2	grossly normal	↓ α1-6	↑ in unfamiliar areas	-	none		233
β3	~90% neonatal lethal cleft palate	↓ α2, α3	hyperactive motor impairment	↓ fear conditioning	clonic absence interictal spikes		251-254
γ2	lethal by P18 (hom)	↓ clustering	hyper-activity impaired reflexes abnormal gait	chronic anxiety (het, KD)	↓ single-channel conductance	no BZD response (hom) ~normal BZD (het, KD)	136, 255-258
δ	↓ fertility some prenatal death (hom)	↓ α4 (fore) ↑ γ2 (fore, cb, thal, str)				↓ γ2 (fore response ↓ neurosteroid effect ↓ EtOH consumption and withdrawal	191, 259-262

Abbreviations: DG, dentate gyrus; CER, conditioned emotional response; BZD, benzodiazepine; PB, pentobarbital; KD, knockdown; PPI, prepulse inhibition; EtOH, ethanol; het, heterozygous; hom, homozygous; fore, forebrain; cb, cerebellum; thal, thalamus; str, striatum.

Similarly, α3 subunit KO mice were created recently and exhibit phenotypes suggesting that α3 subunit-containing receptors may contribute to mood disorders. Schizophrenia generally involves sensorimotor gating defects and hyperdopaminergic neurotransmission, and α3 subunit KO mice recapitulate both phenotypes. Sensorimotor gating is commonly assessed by prepulse inhibition of acoustic startle reflex, in which an initial quiet sound typically reduces startling in response to a subsequent louder sound. The α3 subunit KO mice were startled to similar degrees with or without first hearing the quieter sound. Additionally, midbrain dopamine neurons displayed reductions in GABA-induced whole-cell current, resulting in hyperdopaminergic transmission that was rectified by D2 receptor antagonists.[239] Some evidence also indicates that α3 subunit KO mice may be less susceptible to depression, as they spent less time floating than wildtype mice in a forced swim test[240]. Because α3 subunit expression is high in thalamic reticular nucleus (nRT), which inhibits oscillations in the thalamocortical circuitry controlling sleep and arousal, the α3 subunit KO mice might be expected to lose nRT inhibition and consequently experience increased thalamocortical oscillations resulting in absence seizures or sleep disturbances. However, the mice displayed no significant abnormalities in sleep or waking EEGs, no apparent absence seizures, and normal thalamocortical oscillations in brain slices[241]. Further investigation revealed that α3 subunit KO mice experienced considerable compensatory responses that increased thalamic inhibitory neurotransmission and conferred resistance to oscillation and absence seizures[242].

Expression of α4 subunits is also high in thalamus, but in a pattern complementary to that of α3 subunits (i.e., in relay neurons of motor thalamus). As was the case for so many other $GABA_A$ receptor subunit KO mice, α4 subunit KO mice displayed no overt abnormalities. However, slice recording revealed an absence of thalamic tonic current, and the mice did not respond to the anesthetic effects of gaboxadol (THIP)[243]. Other areas of high α4 subunit expression include dentate gyrus and CA1, where they are frequently paired with δ subunits.

Unsurprisingly, α4 subunit KO mice display reduced δ subunit surface expression in hippocampal pyramidal cells, particularly in pubertal female mice[244].

Mice lacking α5 subunits display a particularly interesting phenotype. Receptors containing α5 subunits usually mediate the majority of tonic current in hippocampus, but some tonic current is preserved (albeit reduced) in α5 subunit KO mice due to upregulation of δ subunits. Phasic inhibition may or may not be affected; some studies found no change, while others observed a reduction in IPSC amplitude[245, 246]. What does seem clear, however, is that α5 subunit deletion enhances learning and memory, particularly spatial memory[245]. Furthermore, α5 KO mice were resistant to the rewarding effects of alcohol[247]. As such, there has been considerable effort to develop inverse agonists for α5 subunit-containing $GABA_A$ receptors.

The α6 subunits are expressed only in cerebellar granule cells, which contain only a few additional subunit subtypes (primarily α1, β2, β3, γ2, and δ). Global deletion of the α6 subunit caused loss of δ subunit protein and tonic current in granule cells[248]. However, in an excellent example of neuronal compensation, granule cell excitability was unaffected in α6 subunit KO mice due to a concomitant increase in "leak" current through K^+ channel TASK-1[248, 249]. In other respects, α6 subunit KO mice were mostly normal, but they did exhibit more motor impairment than wild-type mice after diazepam administration[250]. This also suggests complex interactions among receptor isoforms, because α6 subunit-containing receptors are insensitive to diazepam.

Within the β subunit family, the β2 and β3 subtype genes have been deleted. Considering that both subunits are widely expressed, deletion produced remarkably different effects. Mice lacking β2 subunits were created and studied at the same time as the α1 subunit KO mice and had a similar, unexpectedly normal phenotype[233]. Despite lacking 50% of all α subunits and muscimol binding sites, β2 KO mice had only slightly reduced GABA-evoked currents in cerebellar Purkinje neurons, normal rotarod performance, and increased locomotor activity.

In contrast, nearly 90% of β3 KO mice died pre- or perinatally. Some but not all of the increased mortality could be attributed to cleft palate, because only 60% of all KO animals had

cleft palate, and 30% of animals with normal palates also died within a few days of birth[251]. Furthermore, those that survived the perinatal period still had reduced longevity in addition to numerous other abnormalities, such as hyperactivity, incoordination, overt seizures, and interictal EEG abnormalities. The latter two symptoms worsened with age; at eight weeks, only intermittent slowing was apparent, but by 14 weeks the mice experienced both clonic and absence seizures as well as sharp interictal spikes[252]. Interestingly, despite reports that the β3 subunit gene is not imprinted, the phenotype of β3 heterozygous knockout mice depended on both the parental origin of β3 subunit deficiency and the gender of the heterozygote. EEG abnormalities were worse if the deficiency was of maternal origin, and β3 subunit levels were reduced less drastically in male mice with deficiency of paternal origin[253]. Given their various deficits, β3 heterozygous KO mice have been suggested as models for both Angelman syndrome[252] and autism spectrum disorders[254].

Deletion of γ2 subunits produces an equally severe phenotype. Despite normal morphology (including brain, intestinal tract, and peripheral organs known to express $GABA_A$ receptor subunits), all homozygotes died before P18. Most of these died within a few days of birth, and those that survived longer had progressive motor abnormalities including hyperactive limb movement, impaired righting reflexes, and gait abnormalities[255]. On the cellular level, γ2 subunit deletion reduced receptor clustering and shifted single-channel conductance to the lower level characteristic of αβ receptors[136, 256]. Interestingly, heterozygous KO mice lost only about 20% of their γ2 subunit protein, suggesting that γ2 subunits are normally expressed in excess[257]. However, global heterozygotes[257], adult/forebrain specific heterozygotes[258], and γ2 subunit knockdown mice[259] (which lost on average 65% of γ2 subunit protein) all displayed heightened anxiety. Because the lethality obviously makes γ2 subunit global homozygous KO mice impossible to study beyond the first 2-3 weeks of life, several other temporally and spatially selective KO lines have been generated. Mice that lost γ2 subunit expression in the third postnatal week also lost synaptic $GABA_A$ receptor clusters, indicating that the γ2 subunit is

essential for both formation and maintenance of clusters[137]. Deletion of γ2 subunits from gonadotropin-releasing hormone (GnRH) positive neurons had little effect[260], but deletion from parvalbumin (Pv) positive neurons caused progressive deficits in body weight, motor skills, pain sensitivity, anxiety, prepulse inhibition, and spatial learning, but no increase in mortality[261]. Taken together, these studies support the observation that γ2 subunit expression is widespread and essential, and that neither γ1 nor γ3 subunits can compensate for γ2 subunit loss.

Finally, δ subunit KO mice have also been created. Heterozygotes had slightly reduced litter sizes and homozygotes were born at slightly less than the expected Mendelian ratio, suggesting some prenatal death. Muscimol binding assays indicated that homozygotes lost nearly 50% of all $GABA_A$ receptors; however, the number of benzodiazepine binding sites actually increased in some brain regions (thalamus, striatum, and cerebellum) of δ KO mice, suggesting that γ2 subunit expression increased in compensation[191]. In agreement, future studies found γ2 subunit upregulation in most regions that typically express high levels of δ subunits. In contrast, those same regions had significantly decreased α4 subunit expression levels[262]. These changes in cellular expression were accompanied by increased rates of hippocampal mIPSC decay but no changes in mIPSC amplitude or frequency[263]. The δ subunit KO mice were less sensitive to behavioral effects of neuroactive steroids[191], gaboxadol[264], and ethanol[265], which contributed to the conclusion that δ subunit-containing isoforms mediate most responses to these drugs.

Heterogeneity in vivo: native $GABA_A$ receptor isoforms

Many of the studies mentioned thus far have been conducted in heterologous expression systems or in cultured neurons. Because of the great potential for $GABA_A$ receptor heterogeneity, it is necessary to use such systems to investigate properties of specific subunits (e.g., assembly sequences) and isoforms (e.g., kinetic and pharmacological properties). Unfortunately, these studies cannot answer a crucial question: what $GABA_A$ receptor isoforms actually exist in the brain? In an attempt to construct a standardized response to that question, the International Union

of Pharmacology recently established a list of potential native $GABA_A$ receptor isoforms[266] that were divided into three categories ("identified", "existence with high probability", and "tentative") based on multiple types of evidence. The authors also specified a logical strategy, summarized below, for determining whether or not a receptor isoform exists *in vivo*. First, the long list of potential isoforms can be narrowed based on subunit co-expression patterns, which can be ascertained by *in situ* hybridization and immunoreactivity. If subunits are indeed co-expressed in a specific cell type, evidence for direct association of those subunits should be sought, primarily through co-immunoprecipitation. Subunits that associate should be co-expressed in heterologous systems, where electrophysiology can be performed and characteristic kinetics and pharmacology can be assessed. These characteristic properties can then be sought in neurons. Finally, KO animals can be created and studied for the absence of characteristic physiology and pharmacology associated with isoforms containing the deleted subunit. The list of "identified" and "high probability" isoforms, along with their localization (regional and subcellular) and basic forms of inhibition (phasic or tonic), is presented in Table 8.

Isoforms that have been unequivocally identified

Each of the six α subunits has been co-immunoprecipitated from brain with β2/3 and γ2 subunits. Each subunit combination can be expressed in heterologous systems and responds differently to the array of benzodiazepine site ligands (e.g., flumazenil binds to receptors containing any α subunit, classic benzodiazepines bind only to receptors containing α1, α2, α3, or α5 subunits, and zolpidem binds with differing affinities to the benzodiazepine-sensitive receptors). These properties allow only tentative identification of α(2,3)βγ2 and α(4,6)βγ2 receptors; however, wild-type expression patterns and co-depletion in KO mice supports the existence of all four isoforms. Finally, the benzodiazepine-insensitive KI mice provide strong evidence that each benzodiazepine-sensitive isoform exists. Consequently, all αβγ2 isoforms are considered to have been identified *in vivo.* Four of the remaining identified isoforms contain δ

***Table 8. $GABA_A$ receptor isoforms likely to exist* in vivo.**

	Areas of high expression	Subcellular localization	Type of inhibition	Refs
Identified				
α1β2γ2	cerebral cortex (all layers) hippocampus (interneurons, principal cells) thalamus (relay nuclei) cerebellum (Purkinje and granule cells)	synaptic, extrasynaptic	phasic, tonic	233
α2βγ2	cerebral cortex (layers I-IV) hippocampus (pyramidal cells) striatum hypothalamus motor neurons	synaptic (most), extrasynaptic	phasic, tonic	198
α3βγ2	cerebral cortex (layers V-VI) hippocampus thalamus (nRT) cerebellum	synaptic (most), extrasynaptic	phasic, tonic	198
α4βγ2	hippocampus (granule cells) thalamus (relay nuclei)	synaptic, extrasynaptic	phasic, tonic	268
α4β2δ	thalamus (relay nuclei)	extrasynaptic	tonic	268, 269
α4β3δ	dentate gyrus (granule cells); thalamus	extrasynaptic	tonic	268
α5βγ2	hippocampus (pyramidal cells)	extrasynaptic – clustered (minor synaptic population)	tonic	270
α6βγ2	cerebellum (granule cells)	extrasynaptic	phasic	271, 272
α6β2δ	cerebellum (granule cells)	extrasynaptic	tonic	271-273
α6β3δ	cerebellum (granule cells)	extrasynaptic	tonic	271-273
ρ	retina (bipolar cells)	synaptic, extrasynaptic?	tonic?	274-276
Existence with high probability				
α1β3γ2	cortex? hippocampus?	synaptic?	phasic?	267, 277
α1βδ	hippocampus (interneurons)	extrasynaptic	tonic	278
α5β3γ2	hippocampus (pyramidal cells, granule cells)	extrasynaptic	tonic	279
αβ1γ/αβ1δ	cerebral cortex	?	?	280-282
αβ	hippocampus (pyramidal cells)	extrasynaptic	tonic	283, 284
α1α6βγ/ α1α6ββδ	cerebellum (granule cells)	synaptic/extrasynaptic	phasic	271, 273

subunits, which confer distinctive physiological and pharmacological properties (e.g., non-desensitizing currents and neurosteroid sensitivity). Demonstration of these properties *in vivo*[267], combined with co-localization, co-immunoprecipitation, and gene deletion studies[268], have allowed identification of the δ subunit-containing receptors listed in Table 8[269].

The last isoform that has been identified unequivocally *in vivo* comprises ρ subunits alone. These receptors were previously classified as $GABA_C$ receptors largely because they are sensitive to GABA but insensitive to both the $GABA_A$ receptor antagonist bicuculline and the $GABA_B$ receptor agonist baclofen. Currents with these pharmacological properties occur in cells that express ρ subunits (e.g., retinal bipolar cells), strongly suggesting that those cells express ρ subunit-containing pentamers. Evidence for both homomeric and heteromeric ρ isoforms has been reported[270, 271]; consequently, the subunit subtypes present in these receptors remain undefined.

Isoforms that exist with high probability

Finally, we will briefly discuss the evidence supporting the "existence with high probability" of certain key $GABA_A$ receptor isoforms listed in Table 8. Each of these isoforms assembles efficiently and has been studied extensively in heterologous systems[80, 168, 193, 272-276]; moreover, the subunits are co-expressed *in vivo*[45, 55, 57]. Most were not classified as "identified" simply because few animal studies have been conducted. First, although α1 and γ2 subunits seem to partner most frequently with the β2 subunit, expression patterns indicate that this cannot always be the case, because certain areas expressing α1 and γ2 subunits do not express β2 subunits[55]. In these areas, it is quite likely that α1β3γ2 receptors are formed, as indicated by various pharmacological properties[277]. Substantial evidence supports the existence of the α5β3γ2 isoform: the three subunits have been colocalized[55], α5 and β3 subunits were co-depleted in KO mice[266], α5 subunit-selective etomidate effects have been identified[278], and electrophysiology suggests that this isoform mediates tonic inhibition in the hippocampus[279]. In fact, α5β3γ2 receptors remain in the "high probability" category only because to date, α5 and β3 subunits have

not been co-immunoprecipitated[266]. Likewise, the widely-accepted α1βδ isoform clearly assembled in heterologous systems and responded to known modulators of δ subunit-containing receptors. One recent report claimed to identify this isoform in molecular layer interneurons of the hippocampus[280]. Finally, as previously mentioned, two different αβ isoforms have been identified in rat brain via sequential co-immunoprecipitation[281] and electrophysiology[282].

Pathology related to $GABA_A$ receptor dysfunction

Psychiatric disorders

$GABA_A$ receptor subunit gene loci have been associated with schizophrenia, bipolar disorder, and major depressive disorder[283-288], and as previously mentioned, several of the $GABA_A$ receptor subunit KO animals display behavioral phenotypes that are considered to model these conditions. In humans, reduced GABA levels have been found in CSF, plasma, and brain tissue of depressed patients. Furthermore, brains of suicide victims showed changes in $GABA_A$ receptor subunit mRNA levels; compared to controls, α1, α3, α4, and δ subunits were reduced, while α5, β3, and γ2 subunits were increased[289]. Studies of schizophrenic patients have sought evidence for GABAergic dysfunction throughout the GABA synthetic and signaling pathways[290]. Although results varied widely, reported findings in postmortem schizophrenic brain include increases in muscimol binding sites and decreases in GAD activity and expression, GABA concentration, and benzodiazepine sites[291]. Interestingly, a study of postmortem bipolar cortex found no changes in muscimol binding sites together with increases in benzodiazepine binding sites, suggesting that bipolar disorder and schizophrenia might alter $GABA_A$ receptor stoichiometry in opposite ways[292]. However, that is highly speculative, because nearly equal numbers of studies have and have not found linkage between $GABA_A$ receptor subunit loci and bipolar disorder. Perhaps the strongest connection was found recently, when two separate groups reported an association between several subunit genes and bipolar disorder with psychotic features[286, 293].

Autism

The search for a connection between $GABA_A$ receptors and autism spectrum disorders (ASDs)[294-299] began at the Angelman/Prader-Willi syndrome locus on the long arm of chromosome 15, where deletions, duplications, translocations, and inversions were found in autistic patients[300]. This region contains the β3-α5-γ3 subunit gene cluster, and ASD-associated polymorphisms have been identified in all three genes[296, 297, 301, 302]. Further studies found reductions in α5 subunit protein and benzodiazepine binding sites in autistic brain[298, 299] and linkage to other $GABA_A$ receptor subunit genes, including GABRA4, GABRA5, GABRB1, GABRR1, and GABRR2[303, 304].

Epilepsy

By definition, epileptic seizures result from abnormal excessive or synchronous neuronal activity. Two or more unprovoked seizures meet the diagnostic criteria for epilepsy, which is further classified as symptomatic (secondary to trauma, stroke or tumor) or idiopathic (primary). Most idiopathic epilepsies are likely genetic disorders; within the past two decades, numerous mutations have been identified in epileptic individuals and families. Considering that epilepsy is a disorder of hyperexcitability, it is perhaps unsurprising that most of these mutations were found in genes encoding ion channels, including several $GABA_A$ receptor subunits.

Epilepsy mutations and polymorphisms in $GABA_A$ receptor subunit genes

Epilepsy syndromes have been linked to mutations and variants in the GABRA1, GABRB3, GABRG2, and GABRD genes (Table 9). The syndromes vary widely in severity, ranging from the relatively benign childhood absence epilepsy to the catastrophic Dravet syndrome. Similarly, the mutations range from point mutations that alter channel kinetics to nonsense mutations that induce complete subunit degradation.

Four α1 subunit mutations have been reported. The first was found in a four-generation family with juvenile myoclonic epilepsy. The mutation, an alanine to aspartate mutation in the third transmembrane domain (A322D) was autosomal dominant and resulted in reduced whole-cell current amplitude[305]. Future studies found that mutant subunits were misfolded and mostly retained in the ER and degraded by proteasomes. Mutant subunits could oligomerize with wild-type subunits and thereby reduce surface expression of normal receptors as well. The few α1(A322D) subunits that were successfully incorporated into pentamers and trafficked to the cell surface produced receptors with abnormal current kinetics[306-308].

Two other α1 subunit mutations were found in French-Canadian families with varying epilepsy phenotypes. The D219N mutation, located in the ninth β-strand (outer sheet) region, caused partial ER retention of mutant subunits and consequently reduced receptor surface expression by approximately 50%. The remaining mutant surface receptors desensitized more slowly and deactivated more quickly than wild-type receptors. The other mutation, K353delins18X, caused aberrant translation of 18 amino acids from an intronic sequence, followed by a premature stop codon in the M3-M4 loop. The resulting protein lacked 103 amino acids present in wild-type subunits and could not traffic beyond the ER[309]. Finally, an α1 subunit mutation was found in a single patient with childhood absence epilepsy. A single base pair deletion produced a frameshift, translation of two abnormal amino acids, and a subsequent stop codon in the third transmembrane domain (S326fs328X). Similar to the A322D and K353delins18X mutant subunits, α1(S326fs328X) subunits did not reach the cell surface. Taken together, these three mutations suggest that the fourth transmembrane domain is essential for proper folding, oligomerization, and surface trafficking of α1 subunits.

Three separate point mutations in β3 subunits were recently found in families with childhood absence epilepsy. Two of these (P11S and S15F) were located in the signal peptide of one of the β3 subunit splice variants, while the other (G32R) was predicted to lie at the beginning of the N-terminal α helix. Interestingly, all three mutant subunits had abnormal increases in N-

glycosylation and decreased the current density of α1β3γ2 receptors[310]. Surface expression of β3(P11S) subunits was slightly reduced due to accelerated degradation of mutant subunits[296], but no explanation has been found for the increased *N*-glycosylation of either signal peptide mutant. On the other hand, the G32R mutation increased occupancy of an adjacent *N*-glycosylation site [296]. This increase appeared to result from introduction of a positive charge at residue 32, but glycosylation was not responsible for decreased current density. Rather, the G32R mutation disfavored incorporation of γ2 subunits and made α1β3γ2 receptors more likely to enter shorter open states[311].

The majority of epilepsy-associated $GABA_A$ receptor mutations have been found in γ2 subunits. Although dysfunctional GABAergic transmission was long suspected to contribute to epilepsy, no genetic evidence for $GABA_A$ receptor involvement existed until 2001, when a point mutation in the GABRG2 gene was found to segregate with GEFS+ in a multigenerational family[312]. The mutation, K328M, affected a charged residue in the M2-M3 linker, which participates in the binding-gating transduction pathway. Receptors containing γ2(K328M) subunits produced currents with smaller amplitudes and more rapid desensitization than wild-type receptors[313]. Shortly thereafter, another γ2 subunit mutation was found in a large family with various epilepsy phenotypes including childhood absence epilepsy and febrile seizures[314]. The mutation, R82Q, altered a residue in loop 1, which does not have a defined role in GABA binding or channel gating. There have been contradictory reports[313, 315] regarding the functional consequences of the R82Q mutation; however, there is a general consensus that most mutant subunits are retained in the ER, both pre- and post-oligomerization[316]. As a result, cells expressing γ2(R82Q) subunits have fewer surface receptors and many (but not all) of the remaining receptors contain only α and β subunits. Loop 1 is a highly conserved region on the principal side of subunits, and homology modeling predicts that γ2(R82) forms a salt bridge network with γ2(E217) and β2(R117) that is disrupted by the R82Q mutation[316]. Consequently, the mutation likely impairs oligomerization and causes conformational changes that propagate

Table 9. Epilepsy-associated mutations and polymorphisms in $GABA_A$ receptor subunits

Mutation	IGE	Type	Location	Protein	Current	Refs
α1(D219N)	IGE	point	β9	↓ surface expression		320
α1(A322D)	JME	point	M3	misfolding degradation	↓ amplitude	316-319
α1(S236fs328X)	CAE	frameshift/ nonsense	M3	NMD/ERAD		322
α1(K353delins18X)	IGE	insertion/ splice site	M3-M4 loop	no surface expression	no current	320
β3(P11S)	CAE	point	signal peptide	hyperglycosylation; degradation	↓ amplitude	321
β3(S15F)	CAE	point	signal peptide	hyperglycosylation	↓ amplitude	321
β3(G32R)	CAE	point	α1 helix γ-β interface	hyperglycosylation; altered assembly	↓ amplitude; shift to shorter open states	321, 323
γ2(Q40X)	DS	nonsense	N-terminus	degradation	↓ amplitude (αβ-like)	324
γ2(R82Q)	CAE/FS	point	loop 1 γ-β interface	ER retention; degradation	↓ amplitude	325-329
γ2(P83S)	IGE	point	loop 1 γ-β interface	no effect?	no effect?	320, 326
γ2(R177G)	FS	point	β6	impaired assembly	↓ amplitude	330
γ2(IVS6+2T→G)	CAE/FS	splice site/PTC	intron 6	ER retention/stress	↓ amplitude (αβ-like)	331, 332
γ2(K328M)	GEFS+	point	M2-M3 linker	none	↑ deactivation ↓ single-channel mean open time	326, 333
γ2(Q390X)	DS/GEFS+	nonsense	M3-M4 loop	ER retention ↓ receptor expression	↓ amplitude	334, 335
γ2(Q429X)	GEFS+	nonsense	M3-M4 loop	?	?	336
δ(E177A)	GEFS+	point	β7	?	↓ amplitude; ↓ single-channel mean open time	337, 338
δ(R220H)	GEFS+	point	β9	?	↓ amplitude; ↓ single-channel mean open time	337, 338

Abbreviations: IGE, idiopathic generalized epilepsy; JME, juvenile myoclonic epilepsy; CAE, childhood absence epilepsy; DS, Dravet syndrome (severe myoclonic epilepsy of infancy); FS, febrile seizures; GEFS+, generalized epilepsy with febrile seizures plus; NMD, nonsense-mediated decay; ER, endoplasmic reticulum; ERAD, endoplasmic reticulum-associated degradation

across both γ2 and β2 subunits and affect the distant GABA and benzodiazepine binding sites[317]. Of note, R82Q is the only $GABA_A$ receptor epilepsy-associated mutation for which a KI mouse has been created and studied. Heterozygous γ2(R82Q) KI mouse had a CAE-like phenotype; at approximately three weeks of age, they developed abnormal spike-and-wave discharges that coincided with behavioral arrest and could be treated with the anti-absence drug ethosuximide. Furthermore, the γ2(R82Q) subunit had reduced surface expression and oligomerized poorly with other $GABA_A$ receptor subunits in neurons cultured from the KI mice[318].

Truncation/nonsense mutations throughout the γ2 subunit sequence have also been found in epileptic families[319]. One such mutation, Q40X, actually truncated the transcript at the first residue of the mature peptide. Such a mutation would be expected to trigger nonsense-mediated decay, essentially producing a haploinsufficiency condition, but it is also possible that some of the signal peptide could escape decay and produce dominant negative effects. Another nonsense mutation associated with CAE and FS, IVS6+2TS6ne such mutation, Q40X, actually truncated the intron 6, producing a truncated protein that contained most of the γ2 subunit N-terminal domain with a novel 29-aa C-terminus. This tail was strongly hydrophobic and allowed the abnormal protein to be inserted into ER membranes, oligomerize with α and β subunits, and thereby escape degradation. However, most of the truncated proteins were retained in the ER. Consequently, most surface receptors were binary αβ receptors, which produce much less charge transfer than ternary αβγ receptors. Additionally, the truncated protein induced ER stress, which could prove to be a novel mechanism of epileptogenesis[320, 321]. Two other γ2 subunit truncation mutations, Q390X and Q429X, have been reported[322, 323]. Both were associated with GEFS+, were located in the last exon (and therefore should not trigger nonsense-mediated decay) and might produce proteins truncated in the M3-M4 intracellular loop. The γ2(Q351X) subunits oligomerized with α and β subunits but trapped them in the ER[324]. The other M3-M4 nonsense mutation, Q429X, would be expected to produce similar results, but this remains to be studied.

Finally, two epilepsy-associated variants, E177A and R220H, have been identified in δ subunits. Both were point mutations in outer-sheet β strands of the δ subunit N-terminal domain that were found in families with febrile seizures[325]. Furthermore, both mutations reduced the current amplitude of αβδ receptors by two separate mechanisms; receptor surface expression was reduced and the remaining mutant surface receptors had shorter open durations[326].

Rationale for experimental chapters: the immense disorder of truths

Assembly and trafficking of wild-type $GABA_A$ receptor isoforms

Despite the wealth of knowledge that has been accumulated regarding $GABA_A$ receptor assembly and trafficking, some very fundamental questions remain unanswered. First, although each subunit has a characteristic temporal and spatial expression pattern, most neurons express many $GABA_A$ receptor subunits at once. It is clear that pentamers do not assemble at random, because many subunit combinations produce unproductive oligomers *in vitro* and only a small subset of the mathematically possible receptor isoforms have been identified *in vivo*. Consequently, certain "rules" of assembly must exist to limit receptor heterogeneity. At present, these rules and their mechanisms remain poorly defined. For instance, it is not known if certain subunit pairs have stronger affinities for one another than others, or if the preferential oligomerization induced by such affinities could be overcome simply by subunit expression levels and mass action. Likewise, there have been no successful attempts to ascertain the order of subunit assembly. For the closely-related nicotinic acetylcholine receptors, this information has been known for nearly two decades. Finally, for years $GABA_A$ receptor stoichiometry and subunit arrangement have been assumed to be (γ/δ/ε)-β-α-β-α. However, remarkably little empirical evidence supports this assumption, and nearly all such evidence relies on concatenated subunit constructs that constrain subunit assembly. As such, the first part of this dissertation will address free assembly and trafficking of selected $GABA_A$ receptor subunits.

Characterization of epilepsy-associated mutations in $GABA_A$ receptor subunits

As previously discussed, numerous epilepsy-associated mutations have been identified in four different $GABA_A$ receptor subunits. Two have been introduced into KI or transgenic mice, some have been studied extensively in heterologous systems, and many have been characterized only perfunctorily. Furthermore, these mutations produce monogenic epilepsies, which affect approximately 2% of all idiopathic generalized epilepsy patients. A recent paper reported exome sequencing of all ion channel genes in a cohort of epileptic patients and non-epileptic controls[327] . The authors hoped to find patterns of ion channel variants (or "channotypes") that predict epilepsy risk, but no such patterns emerged. Cases and controls did not differ significantly in numbers of total variants, variants in established epilepsy genes, or rare variants predicted to be severe. Consequently, the authors concluded that the risk of hyperexcitability due to ion channel polymorphisms must depend heavily upon locations and levels of channel expression as well as compensatory mechanisms that occur during brain development. This conclusion is at once unsurprising and disappointing, as it confirms that neural networks are incredibly complex and that polygenic epilepsies are incredibly difficult to study. In fact, the results suggest a potentially insurmountable problem: networks can be studied only in animals, but it is impossible to make animals with all possible mutations. Furthermore, it is difficult even to predict which variants will be harmful and worth studying.

The second part of this dissertation takes a few small steps toward addressing this seemingly intractable problem. It is impossible to study all variants or even all channels; however, it may be possible to construct a framework that allows us to predict which variants in certain channels are likely to be deleterious. As such, the later chapters present thorough characterizations of some reported monogenic mutations, high-throughput screening of several previously unstudied variants, and homology mapping of both harmful and benign variants in an attempt to address "the immense disorder of truths".

CHAPTER II

ASSEMBLY, STOICHIOMETRY, AND SUBUNIT ARRANGEMENT OF α1β2 $GABA_A$ RECEPTORS: ANALYSIS BY FLOW CYTOMETRY

Abstract

$GABA_A$ receptors are heteropentameric ligand-gated chloride channels assembled from a large family of subunit subtypes (α1-6, β1-3, γ1-3, δ, ε, θ, π, and ρ1-3). However, subunits clearly do not assemble at random; rather, strict "rules" govern receptor formation, as only some of the myriad possible subunit combinations form pentamers that reach the cell surface. Both α and β subunit subtypes are required to form the GABA binding site, and it is commonly thought that all isoforms existing *in vivo* contain both subunits. Despite years of study, the stoichiometry of αβ receptors remains disputed. It has been reported that αβ isoform stoichiometry is exclusively 3α:2β, exclusively 2α:3β, or various mixtures thereof. The overwhelming majority of research has been conducted by evaluating the functionality of receptors formed by artificially tethered subunits, and these "concatemers" have well-established shortcomings.

Although it might seem that determining the precise stoichiometry of αβ $GABA_A$ receptor isoforms is an experimentally intriguing but physiologically irrelevant endeavor, stoichiometry was shown to alter agonist sensitivity of closely-related α4β2 nicotinic acetylcholine receptor isoforms. Here, we used techniques including flow cytometry and fluorescence resonance energy transfer (FRET) to assess the subunit composition and stoichiometry of $GABA_A$ receptors assembled from untethered α1 and β2 subunits. Both α1 and β2 subunits were required for efficient surface expression of either subunit, but surface expression was significantly higher for α1 than for β2 subunits. Indeed, the $\alpha1^{HA}/\beta2^{HA}$ subunit surface protein ratio was too high to be explained by even a homogeneous 3α:2β receptor

population. Additionally, all patterns of subunit adjacency (α1-α1, β2-β2, and α1-β2) were detected using FRET, and β2-β2 subunit FRET would not be expected in 3α:2β receptors. We conclude that α1β2 receptors expressed in cultured fibroblasts formed a heterogeneous population including receptors with both 3α:2β and 2α:3β stoichiometries, but "excess" α1 subunit surface protein suggested that α1 subunits might display unexpected patterns of oligomerization and assembly.

Introduction

$GABA_A$ receptors, the ligand-gated ion channels that mediate the vast majority of fast inhibitory signaling in the central nervous system, are heteropentamers assembled from a large array of subunit subtypes (α1-6, β1-3, γ1-3, δ, ε, π, θ, and ρ1-3). As a result of this subunit diversity, nearly half a million unique receptor isoforms could potentially exist. However, it has become abundantly clear that subunits do not associate indiscriminately and that many "rules" govern receptor assembly and trafficking[266]. Indeed, GABA binds only to β-α and ρ-ρ subunit interfaces, so it is debatable if any isoform lacking one of these interfaces should even be considered a $GABA_A$ receptor. Thus, the simplest GABA-gated isoforms that have been identified *in vivo* are "binary" αβ receptors and homopentameric ρ receptors[281, 282]. Of note, the latter display remarkably different subunit expression patterns and receptor pharmacology than other $GABA_A$ receptor isoforms; until recently, they were considered to be a separate class of "$GABA_C$ receptors" and have been studied far less extensively than traditional $GABA_A$ receptor isoforms.

Decades of research have focused upon determining the stoichiometry and subunit arrangement of isoforms that are apparently expressed in transfected cells and *in vivo*[84, 116, 328, 329] The majority of studies have addressed this question using "concatenated" or "tandem" subunit constructs, in which multiple subunit sequences are joined by artificial peptide linkers.

Traditionally, various combinations of concatemers and individual subunits are expressed in *Xenopus* oocytes or fibroblasts, electrophysiology is performed to determine what combinations yield functional receptors, and receptor composition and subunit arrangement are deduced from the resulting data.

Although concatenated subunits have been a valuable tool, the technique has well-documented drawbacks[330]. Chief among these is the possibility that the concatemers might not actually constrain stoichiometry at all. The linking elements could be cleaved, releasing free subunits to assemble at will; this may be a particular concern when non-N-terminal subunit sequences include the signal peptide. Alternatively, the concatemers may remain intact, but some subunits may be excluded or "loop out" from the receptor pentamer. In addition to the "false positive" conclusions that could be drawn from degraded or overly flexible concatemers, "false negative" conclusions are possible as well. For instance, a subunit combination might assemble successfully but fail to produce a current because concatenation interferes with conformational changes that occur during gating.

Both $GABA_A$ receptors and nicotinic acetylcholine receptors (nAChRs) are members of the Cys-loop ligand gated ion channel family. The α4β2 neuronal nicotinic acetylcholine receptor (nAChR) isoform has highlighted the potential importance of determining receptor stoichiometry. Initially, it was unclear whether the receptor contained three α and two β subunits or two α and three β subunits (3α:2β or 2α:3β receptor stoichiometries, respectively). It was subsequently discovered that oocytes transfected with α4 and β2 subunits had a biphasic concentration response curve, suggesting the presence of a heterogeneous receptor population[331]. Acetylcholine affinity was much higher when a 1:10 ratio rather than a 10:1 ratio of α4:β2 subunit cDNA was transfected; consequently, it was concluded that 2α:3β nAChR isoforms were more sensitive to nicotine than 3α:2β receptors. Interestingly, chronic nicotine administration increased expression of high-affinity 2α:3β isoforms, while transfection of subunits bearing an epilepsy-associated mutation increased expression of low-affinity 3α:2β isoforms[332, 333]. To date, no similar

phenomena have been reported for binary αβ $GABA_A$ receptor isoforms, but to our knowledge similar experiments have not been conducted. The apparent physiological importance of nAChR stoichiometry provides yet another reason to investigate $GABA_A$ receptor stoichiometry in greater detail.

Here, we used techniques including flow cytometry and fluorescence resonance energy transfer (FRET) to assess the subunit composition and stoichiometry $GABA_A$ receptors assembled from untethered α1 and β2 subunits. We confirmed that both α1 and β2 subunits were required for efficient surface expression of either subunit and using differential epitope-tagging we established that more α1 than β2 subunit protein was located on the cell surface. Particularly when protein was denatured, the ratio of $\alpha1^{HA}/\beta2^{HA}$ subunit surface protein was too large to be explained by a homogeneous 3α:2β receptor population. Moreover, all patterns of subunit adjacency (α1-α1, β2-β2, and α1-β2) were detected using FRET, and β2-β2 subunit FRET would not be expected in 3α:2β receptors. Therefore, it seems likely that α1β2 receptors expressed in cultured fibroblasts form a heterogeneous population including receptors with both 3α:2β and 2α:3β stoichiometries. Additionally, the "excess" α1 subunit surface protein suggested that α1 subunits might display unexpected patterns of oligomerization and assembly.

Materials and Methods

Cell culture and expression of recombinant $GABA_A$ receptors

Human $GABA_A$ receptor α1, β2, γ2L, and δ subunits were individually sub-cloned into the pcDNA3.1+ mammalian expression vector (Invitrogen, Grand Island, NY). Due to the lack of a highly specific, commercially available antibody targeting an extracellular domain on the γ2L and δ subunits, the HA (YPYDVPDYA) epitope was inserted between amino acids 4 and 5 of the mature peptide. This insertion site was selected for its minimal effect on receptor expression and function (REFS; Supplemental Figure X). The coding region of each vector was

sequenced by the Vanderbilt University Medical Center DNA Sequencing Facility and verified against published sequences.

HEK293T cells (American Type Culture Collection, Manassas, VA) were maintained at 37°C in humidified 5% CO_2 / 95% air using Dulbecco's Modified Eagle Medium (Invitrogen) supplemented with 10% fetal bovine serum (Invitrogen), 100 i.u./ml penicillin (Invitrogen), and 100 μg/ml streptomycin (Invitrogen). Cells were plated at a density of ~10^6 cells per 10 cm culture dish (Corning Glassworks, Corning, NY) and passaged every 2-4 days. For flow cytometry experiments, cells were plated at a density of $4x10^5$ cells per 6 cm culture dish (Corning Glassworks) and transfected ~24 hours later with the indicated amounts of subunit cDNA (see Results) using FuGene6 (Roche Diagnostics, Indianapolis, IN) per manufacturer protocol. In conditions where less than 3 μg of subunit cDNA was transfected, empty pcDNA3.1 vector was added such that a total of 3 μg of cDNA was used for each experimental condition (e.g., the "mock" transfection condition consisted of 3 μg of empty pcDNA 3.1 vector cDNA). For surface biotinylation and immunoblotting, cells were plated at a density of $1.2x10^6$ cells per 10 cm culture dish (Corning) and transfected with a total of 9 μg of cDNA

Flow Cytometry

Cells were harvested ~48 hours after transfection using 37°C trypsin/EDTA (Invitrogen) and placed immediately in 4°C FACS buffer composed of phosphate-buffered saline (PBS), 2% fetal bovine serum (FBS) (Invitrogen), and 0.05% sodium azide (VWR). Cells were then transferred to 96-well plates and washed twice in FACS buffer (i.e., pelleted by centrifugation at 450 x g, vortexed, and resuspended). For surface protein staining, cells were incubated in antibody-containing FACS buffer for 1 h at 4°C, washed in FACS buffer three times, and resuspended in 2% w/v paraformaldehyde (PFA) (Electron Microscopy Sciences). For total protein staining, samples were first fixed and permeabilized using Cytofix/Cytoperm (BD Biosciences) for 15 min. After washing twice with Permwash (BD Biosciences) to remove

residual fixative, cells were resuspended in antibody-containing Permwash for 1 h at 4°C. Following incubation with antibody, samples were washed four times with Permwash and twice with FACS buffer before resuspension in 2% paraformaldehyde. The anti-α1 antibody was obtained from Millipore (clone bd24), conjugated to the Alexa647 fluorophore using an Invitrogen kit, and used at 4 μg/ml for surface staining and 2 μg/ml for total protein staining. The anti-β2 antibody was obtained from Millipore (clone 62-3G1) and used at 8 μg/ml for surface staining and 4 μg/ml for total protein staining. Because anti-β2 antibody conjugation proved inefficient, an anti-IgG1-Alexa647 secondary antibody was used at a 1:500 dilution for most experiments. Because accurate FRET analysis requires directly conjugated antibodies, a different anti-β2 subunit antibody clone (bd17; same epitope as 62-3G1 but suspended in PBS alone) was obtained from Millipore, conjugated to Alexa555 or Alexa647 fluorophores as described above, and used at a 1:50 dilution for all FRET experiments. The anti-HA antibody (clone 16B12) was obtained from Covance as an Alexa647 conjugate and used at a 1:250 dilution for surface staining and a 1:500 dilution for total protein staining.

Samples were run on a LSR II flow cytometer (BD Biosciences). For each staining condition, 50,000 cells were analyzed. Nonviable cells were excluded from analysis based on forward- and side-scatter profiles, as determined from staining with 7-amino-actinomycin D (7-AAD) (Invitrogen). The Alexa555 fluorophore was excited using a 535 nm laser and detected with a 575/26 bandpass filter. The Alexa647 fluorophore was excited using a 635 nm laser and detected with a 675/20 bandpass filter. Data were acquired using FACSDiva (BD Biosciences) and analyzed off-line using FlowJo 7.1 (Treestar). To compare surface and total expression levels of $GABA_A$ receptor subunits, the mean fluorescence intensity of mock transfected cells was subtracted from the mean fluorescence intensity of each positively transfected condition. The remaining fluorescence was then normalized to that of a control condition, yielding a relative fluorescence intensity ("Relative FI"). Statistical significance was determined using Student's t-test or ANOVA, as appropriate. Data were expressed as mean ± SEM.

Surface biotinylation

Forty-eight hours after transfection, cells were washed twice with Dulbecco's phosphate-buffered saline (DPBS; PBS with 0.1 mM $CaCl_2$ and 1 mM $CaCl_2$) and then incubated for 40 minutes with 1 mg/ml NHS-SS-biotin (Pierce) diluted in DPBS. The biotinylation reaction was quenched by washing with 0.1 M glycine in DPBS, and plates were washed twice with DPBS before lysis with radioimmune precipitation assay buffer (RIPA buffer; 50 mM Tris-HCl pH 7.4, 1 % Triton-100, 250 mM NaCl, 5 mM EDTA) containing protease inhibitor cocktail (Sigma). Lysates were cleared by centrifugation at 16,000 x g for 15 minutes and equal protein amounts were incubated overnight with High-Capacity NeutrAvidin agarose resin (Pierce). The following day, the NeutrAvidin resin was washed four times with RIPA buffer before protein elution with Invitrogen sample buffer + 5 % β-mercaptoethanol (1 hr, room temperature). All steps prior to elution were performed on ice and/or at 4˚C.

Glycosidase digestion

Surface biotinylation was performed as described above, but biotinylated protein was simultaneously eluted from NeutrAvidin resin and denatured by incubation in 1x glycoprotein denaturing buffer (New England Biolabs) containing 50 mM dithiothreitol for 30 minutes at 50˚C. Eluates were divided into 15 µl aliquots and digested with 1 unit of peptide-N-glycosidase F (PNGase F) in manufacturer-supplied buffers (New England Biolabs) at 37˚C for 2 h.

Immunoblotting

SDS-PAGE electrophoresis was performed at 175 V for 2-3 hours, followed by transfer to a PVDF membrane (Li-Cor Biosciences, Lincoln, NE) at 100V for 1 hour. Membranes were blocked for one hour in Li-Cor blocking buffer and incubated overnight with antibodies dissolved in PBS with 0.1% Tween (PBST). Antibodies included mouse-anti HA (clone 16B12, Millipore, diluted 1:5000), rabbit polyclonal anti-β2 (Millipore, diluted 1:200), and anti –Na^+/K^+ ATPase α

chain as a loading control (Abcam, diluted 1: 10,000). Membranes were secondarily probed with a IRDye secondary antibodies (Li-Cor). Membranes were washed with PBST and imaged and quantified using a Li-Cor Odyssey infrared imaging system and software.

Results

Due to the possible defects previously discussed, all concatemers must be evaluated for potentially confounding malfunctions before they can be used to draw conclusions regarding receptor stoichiometry. Figure 1 presents the results of some of these control experiments. A very limited repertoire of concatemers is necessary to investigate the stoichiometry of binary αβ receptors, but even within that subset, considerable problems emerged. For instance, the β2-α1 subunit concatemer produced currents when transfected alone (Figure 1A). Obviously, no combination of dimers should form a pentameric receptor, so this is highly concerning. It is possible that similar transfection conditions (i.e., conditions that should not permit pentamer assembly) could result in aberrant forward trafficking of non-functional isoforms, so surface expression of concatenated subunits was also assessed using flow cytometry (discussed further below). Interestingly, the α1-β2 concatemer could be detected on the cell surface when transfected alone (Figure 1B, left panel). If it functions as intended, this concatemer should reach the cell surface when transfected with α1 subunits (if the receptor stoichiometry is 3α:2β) or with β2 subunits (if the stoichiometry is 2α:3β), but not when transfected alone. These conditions were tested using α1 and β2 subunits with hemagglutinin (HA) epitope tags engineered into the N-terminal domain; insertion of this tag disrupts the native epitope of the anti-α1 subunit antibody, so any α1 subunits detected by that antibody must derive from the concatemer. Surprisingly, surface expression of the α1-β2 subunit concatemer was not dramatically higher when it was transfected together with α1 (Figure 1B, middle panel) or β2 (Figure 1B, right panel) subunits than when it was transfected alone, suggesting that abnormal assembly of α1-β2

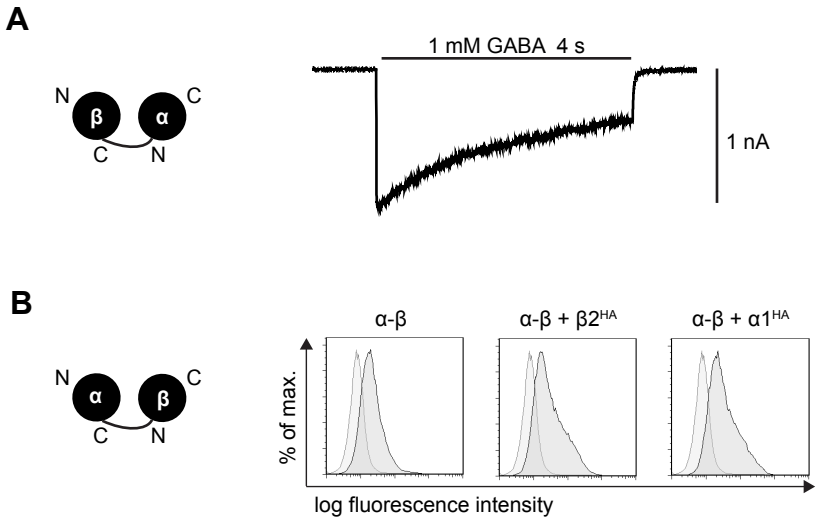

Figure 1. Concatenated subunit constructs may not effectively constrain receptor stoichiometry.

A. HEK293T cells were transfected with a $GABA_A$ receptor subunit concatemer in which a polyglutamine linker was used to connect the C-terminus of the β2 subunit to the N-terminus of the α1 subunit (left panel). Macroscopic currents were recorded from lifted cells (right panel). **B.** HEK293T cells were transfected with a $GABA_A$ receptor subunit concatemer in which a polyglutamine linker was used to connect the C-terminus of the α1 subunit to the N-terminus of the β2 subunit (left panel). Concatemers were transfected either alone (second panel) or in the presence of $\alpha1^{HA}$ (third panel) or $\beta2^{HA}$ (right panel), and surface expression of α1-β2 subunit concatemers was assessed using a fluorescently-tagged anti-α1 subunit antibody and flow cytometry. Representative flow cytometry histograms are presented; the abscissa indicates fluorescence intensity (FI; proportional to expression levels) in arbitrary units plotted on a logarithmic scale, and the ordinate indicates percentage of maximum cell count (% of max). Histograms for cells transfected with subunit combinations (dark gray) and cells transfected with blank vector (light gray) are overlaid.

concatenated subunits was a significant problem. Of note, identical concatemers (including linkers) have been used in previous studies, so these problems should not simply reflect improper construct design.

Flow cytometry indicated that both α1 and β2 subunits were required for surface expression and full total cellular expression levels in intact cells.

Given the apparent flaws of the α1/β2 subunit concatemers, studying assembly of α1β2 receptors with individual, untethered subunits became necessary. Using flow cytometry, the surface and total cellular protein expression of multiple subunits transfected in multiple combinations can be assessed efficiently and quantitatively. Flow cytometry also permits evaluation of protein expression in a relatively "natural" context; whereas immunoblotting requires cell lysis and often protein denaturation, flow cytometry allows selection of folded proteins expressed in intact cells. Thus, HEK293T cells were transfected with untethered α1, β2, or α1 and β2 subunit cDNA and surface and total cellular expression of both subunits were identified for each condition using fluorescently-conjugated, subunit-specific antibodies. Viable cells were selected based on a combination of forward scatter, side scatter, and viability stain profiles (data not shown); a consistent subset of cells excluded the viability stain 7-aminoactinomycin-D (7-AAD), indicating that their membranes were intact at the time of cell harvest. Subunit expression levels were quantified by determining the mean fluorescence intensity (FI) of this viable cell subset for each transfection condition; nonspecific staining was assessed by measuring the mean FI of cells transfected only with blank vector, and this background was subtracted from each experimental condition.

In agreement with previous reports[80, 81, 90], neither α1 subunits nor β2 subunits were expressed efficiently on the cell surface in the absence of the other subunit (Figure 2A, 2B). When α1 subunit cDNA was transfected alone, α1 subunit surface levels were only 2.9 ± 0.3 % of those seen when α1 and β2 subunit cDNAs were co-transfected, and when β2 subunit cDNA was

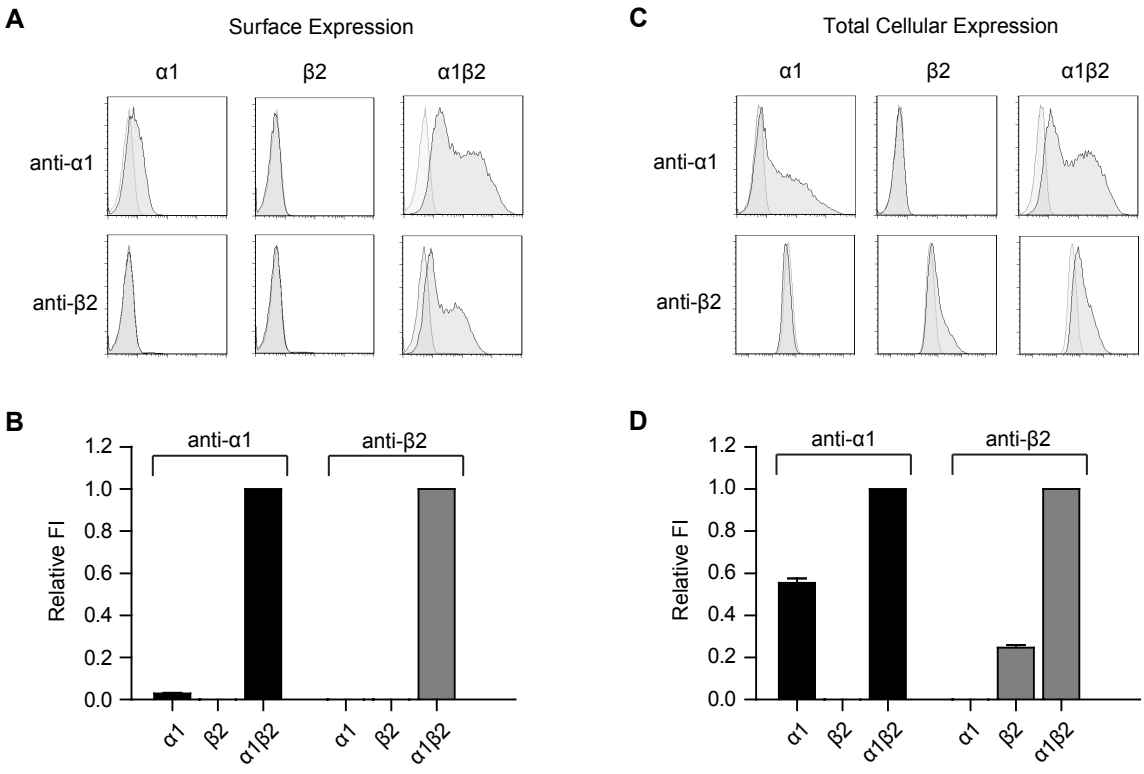

Figure 2. Flow cytometry indicated that surface expression and full total cellular expression of α1 and β2 subunits required co-transfection of α1 and β2 subunit cDNA. HEK293T cells were transfected with combinations of $GABA_A$ receptor subunit cDNAs (α1 alone, β2 alone, or both α1 and β2; 1 μg each) and surface and total cellular subunit expression was evaluated using flow cytometry. **A.** Representative flow cytometry histograms acquired from surface anti-α1 and anti-β2 antibodies are presented; the abscissa indicates fluorescence intensity (FI; proportional to expression levels) in arbitrary units plotted on a logarithmic scale, and the ordinate indicates percentage of maximum cell count (% of max). Histograms for cells transfected with subunit combinations (dark gray) and cells transfected with blank vector (light gray) are overlaid. **B.** The relative fluorescence intensity was quantified by subtracting the mean FI obtained from cells transfected with blank vector from the mean FI obtained from cells transfected with $GABA_A$ receptor subunits and normalizing the resulting net FI to that of the α1β2 transfection conditions. **C-D.** Total cellular detection of α1 and β2 subunits are presented as in panels A and B.

transfected alone, no β2 surface expression could be detected. Total cellular expression of α1 and β2 subunits (Figure 2C, 2D) was also significantly lower when subunits were transfected separately rather than together (α1 = 55.3 ± 2.2 % and β2 = 24.7 ± 1.2 % compared to respective α1β2 co-transfection levels). Importantly, these data also demonstrated that the antibodies were wholly subunit-specific; no α1 subunit signal was detected when only β2 subunit cDNA was transfected and vice versa.

Differential epitope tagging indicated that there were slightly more α1 than β2 subunits on the cell surface, but the exact ratio remained uncertain

These results demonstrated that flow cytometry is an efficient means of assessing subunit expression patterns, but did not provide insight into the stoichiometry or subunit arrangement of α1β2 receptors. To address receptor stoichiometry in the context of freely-assembled subunits, differential epitope tagging was employed. That is, HA epitope tags were inserted between the fourth and fifth amino acids of the mature α1 and β2 subunit peptides, an epitope-tagged subunit was co-expressed with a non-tagged subunit (i.e., $\alpha1^{HA}\beta2$ or $\alpha1\beta2^{HA}$), a fluorescently-conjugated anti-HA antibody was used to detect subunit expression levels with flow cytometry, and the fluorescence intensities of $\alpha1^{HA}$ and $\beta2^{HA}$ subunits were compared. It is, of course, possible that inserting the epitope tag could alter normal receptor assembly. However, it is commonly accepted that epitope tags can be inserted at this position in $GABA_A$ receptor subunit peptides without affecting receptor expression or function[81, 130, 334]. Nonetheless, potential byproducts of epitope tagging were assessed by comparing the levels of partnering subunits transfected with tagged or untagged subunits (i.e., β2 subunit expression levels were compared in $\alpha1^{HA}\beta2$ and α1β2 transfection conditions). The effects of FLAG and c-myc tags were tested as well, and the HA epitope tag was ultimately selected because it had the smallest effect on partnering subunit expression levels.

Therefore, relative HA fluorescence intensity was used to determine the relative amounts of α1 and β2 subunit protein produced from equimolar subunit cDNA co-transfection (Figure 3). This should indirectly indicate receptor stoichiometry; if all α1β2 receptors contained three α1 and two β2 subunits, the $\alpha1^{HA}/\beta2^{HA}$ ratio should be 1.5, and if all contained two α1 and three β2 subunits, the ratio should be 0.67. However, several circumstances could account for other ratios. First, it is important to remember that the antibody would detect any subunits expressed on the cell surface. Thus, the presence of any free $\alpha1^{HA}$ or $\beta2^{HA}$ subunits would skew the $\alpha1^{HA}/\beta2^{HA}$ ratio and make it unrepresentative of the components of pentameric receptors. As demonstrated in Figure 2, α1 and β2 subunits were negligibly expressed on the cell surface when only one subunit was transfected, so it seems unlikely that a substantial fraction of free or homomeric α1 or β2 subunits appears in the presence of partnering subunits. It is also possible that some (or all) α1β2 receptors have unexpected stoichiometries such as 4α:1β or 1α:4β. However, no study has concluded that such a stoichiometry occurs, and importantly neither of these isoforms could contain two GABA binding sites (β-α subunit interfaces). Nonetheless, these possibilities must be considered when drawing conclusions about stoichiometry from the results of differential epitope tagging.

First, one microgram each of α1 and β2 subunit cDNA was transfected per 6 cm plate of HEK293T cells (Figure 3A). In these experiments, α1 subunit ($\alpha1^{HA}\beta2$) expression levels were 124 ± 8.0 % of β2 subunit ($\alpha1\beta2^{HA}$) expression levels. In other words, the $\alpha1^{HA}/\beta2^{HA}$ ratio was 1.24 ± 0.08, suggesting that there was neither a homogeneous population of 3α:2β receptors or 2α:3β receptors. By looking at partnering subunit levels, however, it appeared that the HA tag might reduce subunit expression to a greater extent when inserted into β2 subunits rather than α1 subunits. As mentioned previously, subunit levels tended to be slightly lower when a tagged rather than non-tagged partnering subunit was co-expressed (e.g., α1 subunit levels were lower in the $\alpha1\beta2^{HA}$ condition than in the α1β2 condition). However, HA-tagging β2 subunits appeared to affect partnering α1 subunit levels more than HA-tagging α1 subunits affected partnering β2

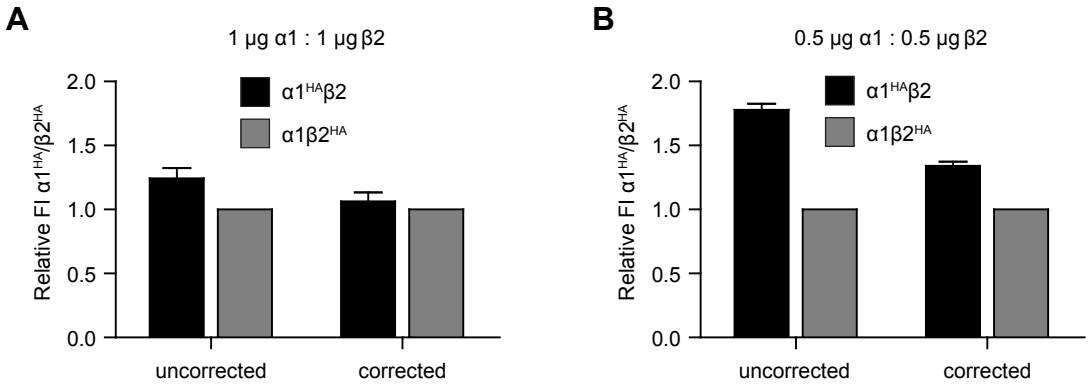

Figure 3. Differential epitope tagging indicated that α1β2 GABA$_A$ receptors could not have uniform stoichiometry.

A. HEK293T cells were transfected with 1 µg each of $\alpha1^{HA}$ and β2 (black bars) or α1 and $\beta2^{HA}$ (grey bars) subunit cDNA and the α1, β2, and HA FIs were determined using flow cytometry. Black bars represent relative levels of α1 subunits ($\alpha1^{HA}$) and grey bars represent relative levels of β2 subunits ($\beta2^{HA}$); $\beta2^{HA}$ levels were taken as a relative FI of 1.0 and $\alpha1^{HA}$ levels were normalized accordingly. The "corrected" values (right side) were adjusted to account for potential confounding effects of the HA tag. To correct $\alpha1^{HA}$ levels, β2 subunit levels were compared in $\alpha1^{HA}\beta2$ and α1β2 transfections. Any change in β2 subunit levels between the two conditions was taken as an effect of the HA tag, and $\alpha1^{HA}$ levels were adjusted proportionally. (Anti-α1 subunit antibodies could not be used to compare $\alpha1^{HA}$ and α1 subunit levels because the HA tag disrupted the native epitope.) Similarly, to correct $\beta2^{HA}$ levels, α1 subunit levels were compared in $\alpha1\beta2^{HA}$ and α1β2 transfections. **B.** Identical to Panel A except that 0.5 µg of each subunit cDNA was transfected.

subunit levels. If this partnering subunit decrease occurred because the HA tag reduced overall receptor expression, levels of the tagged subunit itself would be expected to decrease concomitantly. (Unfortunately, this theory could not be tested directly because the HA tag disrupts binding of the native α1 and β2 subunit antibodies suitable for flow cytometry; thus, levels of β2 and $\beta2^{HA}$ subunits could not be compared using an anti-β2 subunit antibody.) If the HA tag did decrease expression of both subunits similarly, then partnering subunit ratios could be used to correct for the adverse tag effects. When $\alpha1^{HA}$ and $\beta2^{HA}$ levels were adjusted accordingly, the $\alpha1^{HA}/\beta2^{HA}$ ratio decreased to 1.06 ± 0.07. Of course, it is debatable whether the "corrected" or "uncorrected" ratio is the best estimate of relative α1 and β2 subunit levels, but as such both methods are presented here.

There is another potential confounder in addition to the effects of the tag itself. Results could be inaccurate if transfected fibroblasts simply expressed so much protein that surplus subunits were forced into abnormal receptor isoforms. To address this possibility, the equimolar differential tagging experiments were repeated using only 0.5 μg each of α1 and β2 subunit cDNA (Figure 3B). Interestingly, in this context the $\alpha1^{HA}/\beta2^{HA}$ subunit protein ratio was greater (1.78 ± 0.05). After adjusting for tag effects as described previously, the ratio decreased to 1.34 ± 0.03, but still it was greater than the corrected ratio obtained using 1 μg of each subunit cDNA.

a1 subunits appeared to "drive" receptor surface expression, but receptor stoichiometry could not be forced by cDNA transfection ratios

Although the exact $\alpha1^{HA}/\beta2^{HA}$ subunit protein ratio varied depending on subunit cDNA levels and whether or not the raw levels were adjusted for HA tag effects, all conditions indicated that there was more α1 than β2 subunit protein on the cell surface. This, in turn, suggested that the majority of α1β2 receptors contained three α1 and two β2 subunits. To examine this possibility in more detail, titrations were conducted to see if the receptor stoichiometry is flexible; that is, whether or not the $\alpha1^{HA}/\beta2^{HA}$ subunit surface protein ratio could be altered by transfecting

different relative amounts of $\alpha1^{HA}$ and $\beta2^{HA}$ subunit cDNA (the technique used to deduce stoichiometry of α4β2 nAChRs). Comprehensive titrations were performed by transfecting each subunit cDNA at fivefold and twofold deficiencies and excess while the partnering subunit cDNA levels were held constant, then repeating the titrations with the opposite subunit tagged so that ratios could be determined for each transfection condition (Figure 4). For instance, Panel A presents the results of transfecting 0.5 μg of β2 subunit cDNA together with 0.1, 0.25, 0.5, 1, or 2.5 μg of α1 subunit cDNA when either the α1 subunit (black line) or β2 subunit (grey line) was HA-tagged. In Panel B, titrations were performed similarly, but α1 subunit cDNA was held constant at 0.5 μg while β2 subunit cDNA levels were varied. Interestingly, surface expression patterns differed depending on which subunit cDNA levels remained constant. When β2 subunit cDNA levels were held constant, surface levels of both α1 and β2 subunits were proportional to α1 subunit cDNA levels across the entire tested range; that is, both α1 and β2 subunit surface levels continued to increase even when α1 subunit cDNA was transfected at fivefold excess (2.5 μg α1 : 0.5 μg β2). In contrast, when α1 subunit cDNA was held constant, α1 and β2 subunit surface levels increased only up to the point of equimolar transfection (0.5 μg α1 : 0.5 μg β2). Subunit surface levels did not increase further when 1 μg of β2 subunit cDNA was transfected, and they decreased when 2.5 μg of β2 subunit cDNA were transfected.

The titrations also produced surprising $\alpha1^{HA}/\beta2^{HA}$ subunit protein ratios. If receptor stoichiometry were determined simply by relative subunit cDNA amounts, the $\alpha1^{HA}/\beta2^{HA}$ subunit protein ratio should be highest when there is a fivefold excess of α1 subunit cDNA (0.5 μg α1 : 0.1 μg β2 and 2.5 μg α1 : 0.5 μg β2 transfection conditions) and lowest when there is a fivefold excess of β2 subunit cDNA (0.5 μg α1 : 2.5 μg β2 and 0.1 μg α1 : 0.5 μg β2 transfection conditions). However, the $\alpha1^{HA}/\beta2^{HA}$ subunit protein ratio did not vary greatly; if anything, it trended toward higher values when β2 subunit cDNA was transfected in excess. This suggested that whatever the relative amount of α1 and β2 subunits might be, it was mostly independent of cDNA availability.

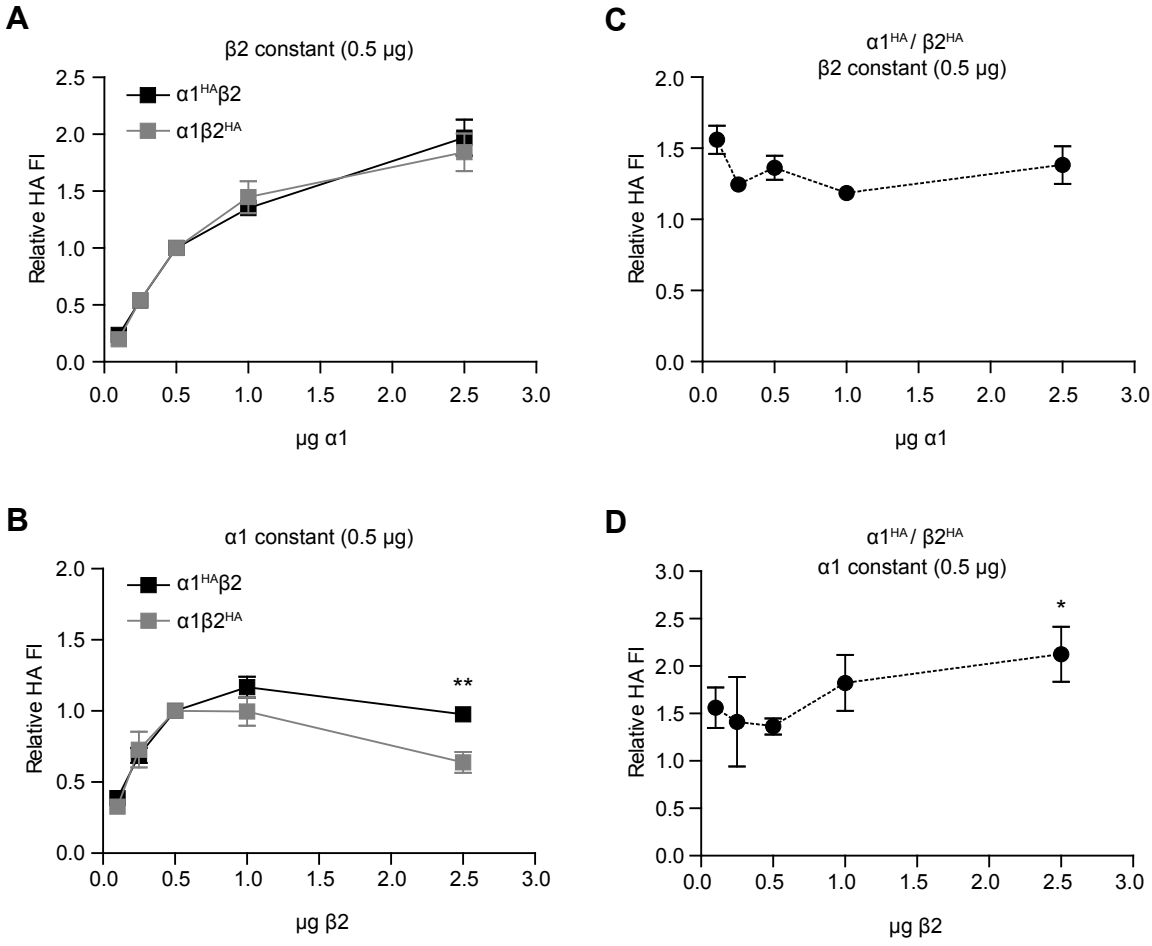

Figure 4. α1 and β2 subunits played different roles in receptor assembly and surface trafficking

A. HEK293T cells were transfected with 0.5 μg of α1 subunit cDNA and 0.1, 0.25, 0.5, 1.0, or 2.5 μg of β2 subunit cDNA. The black line represents transfections where the α1 subunit was epitope-tagged ($\alpha1^{HA}\beta2$) and the grey line represents transfections where the β2 subunit was epitope-tagged ($\alpha1\beta2^{HA}$). In each transfection condition, HA levels were measured using flow cytometry, quantified as described previously, and normalized to the levels obtained in the equimolar transfection condition (e.g., $\alpha1^{HA}\beta2$ levels are normalized to the HA fluorescence intensity obtained when 0.5 μg of $\alpha1^{HA}$ subunit and 0.5 μg of β2 subunit cDNAs were transfected). **B.** Identical to Panel A, but β2 subunit cDNA was held constant; i.e., HEK293T cells were transfected with 0.5 μg of β2 subunit cDNA and 0.1, 0.25, 0.5, 1.0, or 2.5 μg of α1 subunit cDNA. **C.** Transfections were identical to Panel A (β2 subunit cDNA held constant; α1 subunit cDNA levels indicated on the abscissa), but the $\alpha1^{HA}/\beta2^{HA}$ ratios are presented. **D.** Transfections were identical to Panel B (α1 subunit cDNA held constant; β2 subunit cDNA levels indicated on the abscissa), but the $\alpha1^{HA}/\beta2^{HA}$ ratios are presented.

Using surface biotinylation, $\alpha1^{HA}/\beta2^{HA}$ subunit protein ratios appeared to be even higher

While it seems preferable to study expression of proteins in their native conformations, there are scenarios in which denatured proteins might yield more accurate results. For instance, antibodies are approximately three times larger than $GABA_A$ receptor subunits (150 kDa vs. 50 kDa), so steric hindrance might prevent antibodies from binding to all subunits in a receptor and relative ratios could be skewed. Due to this possibility, some of the differential tagging experiments were repeated using HA antibody Fab fragments (50 kDa), but similar ratios were observed (data not shown). However, considering that $GABA_A$ receptor subunits and Fab fragments are approximately equal in size, steric hindrance might still occur. Moreover, even if antibody binding were not sterically hindered, protein folding could render some HA epitope tags inaccessible to antibodies and thereby alter the apparent ratios of α1 and β2 subunits.

To address these possibilities, differentially tagged subunit cDNA titrations were performed again, but the $\alpha1^{HA}/\beta2^{HA}$ subunit surface protein ratio was assessed using surface biotinylation, denaturing SDS-PAGE, and immunoblotting (Figure 5). Because denaturing conditions were used, neither steric hindrance nor epitope inaccessibility should pose an issue. Remarkably, the $\alpha1^{HA}/\beta2^{HA}$ subunit protein ratios obtained using surface biotinylation were even *higher* than those obtained using flow cytometry, ranging from approximately 2.5 to 5.5 (Figure 5A, 5B).

One more potentially confounding variable remained. As discussed, the HA epitope tag was inserted between the fourth and fifth amino acids of each mature subunit protein, and this insertion position has been shown not to affect receptor expression or function significantly. However, the seventh amino acid in the mature β2 subunit peptide (residue 32 including the signal peptide) is an N-linked glycosylation site that has been shown to be occupied by a glycan[335]. The homologous glycosylation site on α1 subunits occurs at residue 11 of the mature peptide. N-glycans can be relatively large, so it is possible that the β2 subunit glycan inhibited

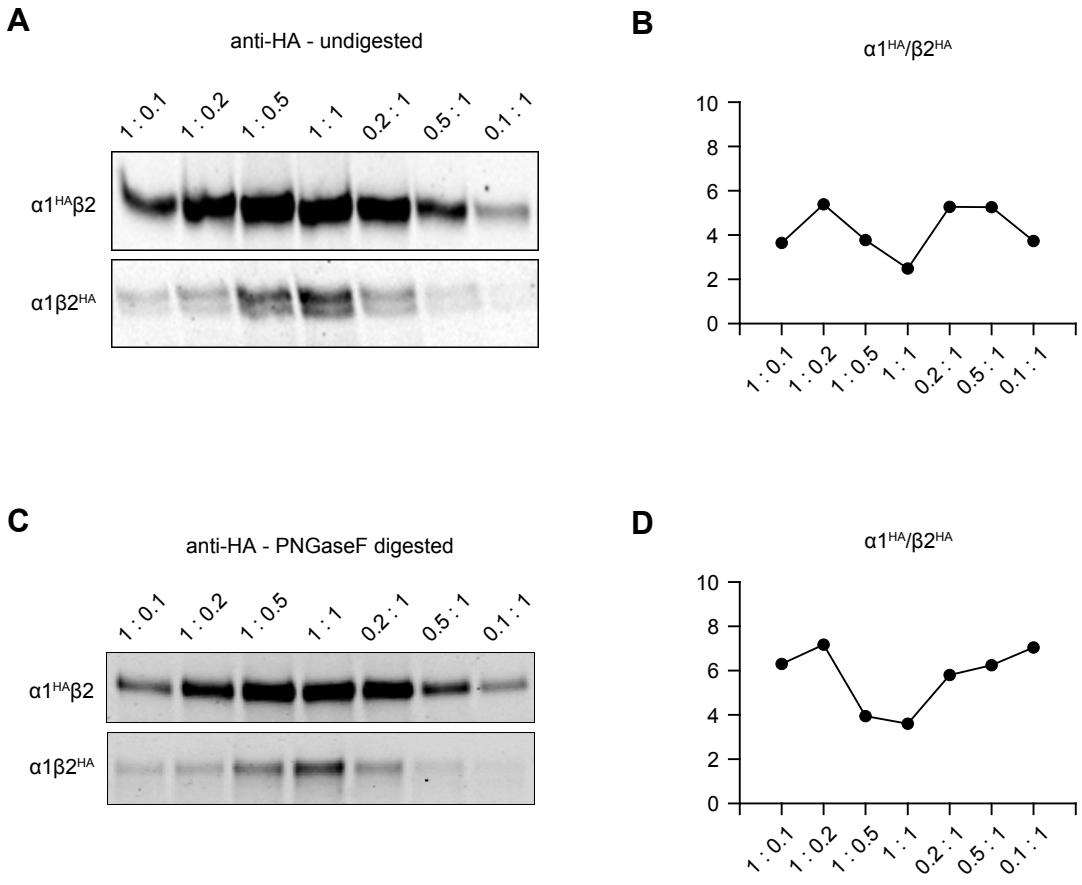

Figure 5. The $\alpha 1^{HA}/\beta 2^{HA}$ ratio obtained using denaturing SDS-PAGE and immunoblotting was substantially higher than the ratio obtained using flow cytometry.

A. HEK293T cells were transfected with the indicated amounts of $GABA_A$ receptor subunit cDNA (above gel). Surface protein was isolated using biotinylation, denaturing SDS-PAGE was performed, and Western blots were probed with anti-HA antibodies. In the top panel, α1 subunits were HA-tagged ($\alpha 1^{HA}\beta 2$); in the bottom panel, β2 subunits were HA-tagged ($\alpha 1\beta 2^{HA}$). **B.** Integrated intensity of protein bands in Panel A were quantified using Li-Cor Odyssey software, and the ratio of $\alpha 1^{HA}/\beta 2^{HA}$ was calculated and graphed. **C.** Identical to Panel A, but surface protein was deglycosylated with PNGaseF before SDS-PAGE. **D.** Bands in Panel C were quantified as described for Panel B.

HA antibody binding to the neighboring epitope tag (thereby underestimating β2 subunit levels) but that the α1 subunit glycan was distant enough from the epitope tag that HA antibody binding was not affected. As such, immunoblotting was repeated after removing all N-glycans with peptide-N-glycosidase F (PNGase F) (Figure 5C). Astonishingly, $\alpha1^{HA}/\beta2^{HA}$ ratios increased yet again, ranging from approximately 4.0 to approximately 7.5 depending on subunit cDNA levels (Figure 5D). Taken together, the results presented in Figures 3-5 suggest that differential epitope tagging might not be an ideal method for determining precise subunit ratios and receptor stoichiometry, but it seems very likely that equimolar amounts of α1 and β2 subunit cDNA yield more α1 than β2 subunit protein on the cell surface.

FRET indicated that the α1β2 receptor population could not have a uniform 3α:2β or 2α:3β subunit stoichiometry.

Even if differential epitope tagging could accurately determine receptor stoichiometry, it could not identify subunit arrangement. That is, even if the $\alpha1^{HA}/\beta2^{HA}$ ratio had been precisely 1.5, it would remain unclear if the subunits alternated (α1-β2-α1-β2-α1) or not (α1-α1-α1-β2-β2) – though, as discussed, the latter arrangement is unlikely because it contains only one GABA binding site. Conversely, assessing subunit arrangement could help determine receptor stoichiometry. If α1 and β2 subunits alternate, a uniform 3α:2β or 2β:3α population could be identified by the presence of specific subunit interfaces. Both populations would contain α1-β2 subunit interfaces, but 3α:2β receptors would not have β2-β2 subunit interfaces, while 2α:3β receptors would not have α1-α1 subunit interfaces.

Homology modeling predicts that the distal N-terminal (antibody-accessible) domains of adjacent $GABA_A$ receptor subunits are predicted to be separated by ~50 Å, while those of non-adjacent subunits are separated by ~80 Å. Therefore, adjacency of freely-assembled subunits must be assessed by a method that can differentiate those two distances. Fluorescence resonance energy transfer (FRET) is such a method, because energy transfer efficiency is inversely

proportional to the sixth power of the distance between donor and acceptor fluorophores [336]. Because fluorophores have a defined Forster radius (the distance at which FRET efficiency is 50% of maximum), careful selection of fluorophores should allow for exclusive monitoring of subunit adjacency. The Alexa555 and Alexa647 fluorophore pair employed here has a Forster radius of 51 Å (www.invitrogen.com), meaning that essentially no energy transfer should occur between the non-adjacent subunits that are 80 Å apart. In agreement with this, FRET did not occur between non-adjacent concatemer subunits (data not shown). More importantly, considering the potential defects of the concatemers, FRET did not occur between individual γ2L subunits when α1, β2, and γ2L subunit cDNAs were co-transfected (Chapter III).

To determine subunit adjacency using FRET and flow cytometry, cells transfected with HA-tagged α1 and β2 subunits were incubated with anti-HA and anti-α1 subunit antibodies conjugated to Alexa555 (donor) and/or Alexa647 (acceptor) fluorophores. To determine α1-α1 subunit adjacency, $\alpha1^{HA}$ and β2 subunit cDNAs were transfected; to determine β2-β2 subunit adjacency, α1 and $\beta2^{HA}$ subunit cDNAs were transfected, and to determine α1-β2 subunit adjacency, α1 and $\beta2^{HA}$ subunit cDNAs were transfected but stained with anti-HA-A555 and anti-α1-A647. Figure 6 presents results of these experiments together with necessary controls. FRET was identified by using a laser of the appropriate wavelength to excite the donor fluorophore (e.g., a 535 nm laser to excite Alexa555) and a filter that isolates emission from the acceptor fluorophore (e.g., a 675/20 nm bandpass filter to detect Alexa647 fluorescence). Ideally, the only fluorescence detected in the acceptor channel would be emitted from acceptor fluorophores that were excited by energy transfer. However, fluorophores have excitation and emission spectra that span a range of wavelengths. As such, some Alexa555 emission might "leak" into the 675/20 bandpass filter range, or alternatively some Alexa647 fluorophores might be excited by the 535 nm laser. Accurate assessment of protein adjacency with FRET requires that fluorescence detection channels be adjusted or "compensated" for this type of spectral leak.

Spectral compensation was performed by staining each sample with only HA-A555 (donor, top row) or only HA-A647 (acceptor, middle row) antibodies and plotting the resulting fluorescence intensity against the fluorescence detected in the FRET channel (the 535 nm laser coupled with the 675/20 bandpass filter). If only the donor or acceptor fluorophore was used and therefore FRET could not occur, there should be no correlation between these two fluorescence intensities. As shown in Figure 6, no correlation existed after spectral compensation was applied. The FRET threshold (horizontal line) was defined such that less than 1% of cells were positive when stained with HA-A555 or HA-A647 antibodies alone. When cells were stained with both HA-A555 and HA-A647 antibodies, strong FRET signals were detected between individual α1 subunits (left column), between individual β2 subunits (middle column), and between α1 and β2 subunits (right column). It should be noted that these results could be replicated using several different epitope tags, antibodies, and fluorophores; furthermore, several conditions were FRET-negative in experiments conducted using different subunit subtypes (Chapter III). As such, it seems unlikely that all possible FRET patterns were found simply because energy transfer occurred aberrantly between non-adjacent subunits. Thus, another piece of evidence indicated that α1β2 receptor stoichiometry was heterogeneous, comprising a mixture of 3α:2β and 2α:3β isoforms.

Discussion

The combination of flow cytometry and FRET provides an efficient, quantitative method for evaluating subunit requirements, assembly patterns, and subunit arrangement of $GABA_A$ receptor isoforms

Due to the large number of $GABA_A$ receptor subunit genes, neurons have the potential to produce a truly staggering variety of unique $GABA_A$ receptor isoforms. The receptor diversity is probably invaluable for fine-tuning neuronal physiology, but it also poses challenges for researchers. Because most neurons express a considerable subset of the available subunits,

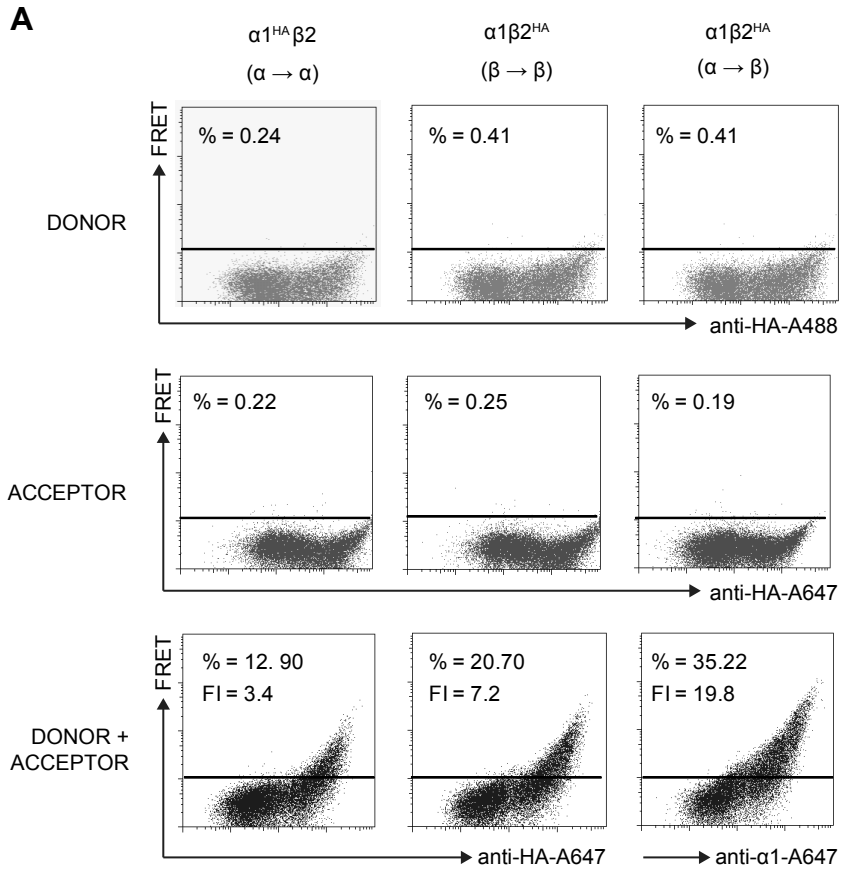

Figure 6. Flow cytometric analysis of $GABA_A$ receptor α1 and β2 subunit FRET also suggested that α1β2 receptors did not assemble with uniform stoichiometry.

HEK293T cells were transfected with 1 μg of α1 subunit cDNA and, 1 μg of β2 subunit cDNA. To determine subunit adjacency, each subunit was individually HA-tagged and cells were incubated with both anti-HA-Alexa555 and anti-HA-Alexa647 or anti-α1-Alexa647 before being subjected to flow cytometry. The left column presents α1-α1 subunit adjacency (α1 HA-tagged); the middle column presents β2-β2 subunit adjacency (β 2 HA-tagged); and the right column presents α1-β2 subunit adjacency. The x-axis indicates fluorescence intensity of the donor (Alexa555; top row) or acceptor (Alexa647; middle and bottom rows) fluorophore, while the y-axis indicates fluorescence intensity of the FRET channel (excitation of Alexa 555 and emission of Alexa647). The horizontal line represents the FRET threshold (see Methods) and the percentage of cells emitting above this threshold is indicated at the top of each dot plot.

recordings represent the aggregate currents produced by many different isoforms. Similarly, immunohistochemistry generally cannot identify receptor subunit composition or stoichiometry; colocalized subunits may be within the same receptor or simply in adjacent receptors. Resolution thresholds are continually improving, but atomic force or electron microscopy is still necessary to reliably assess subunit composition *in situ*. For this reason, a substantial portion of the $GABA_A$ receptor literature comprises evaluation of individual receptor isoforms expressed in fibroblasts. However, knowledge about the structure of receptors formed even in such a constrained system remains somewhat limited. The high-throughput techniques of flow cytometry and FRET have great potential to comprehensively evaluate the subunit composition and stoichiometry of $GABA_A$ receptor isoforms. Here, these techniques were used to study one of the simplest possible isoforms, α1β2. Although data quality, acquisition, and analysis were satisfactory and efficient, receptor assembly itself proved to be far more complicated than expected.

α1β2 receptor populations are unlikely to be homogeneous

We anticipated that relative subunit expression levels and subunit adjacency patterns would identify a 3α:2β or 2α:3β receptor stoichiometry. However, the $\alpha1^{HA}/\beta2^{HA}$ subunit level ratio was not consistent with either stoichiometry, and all possible subunit interfaces (α1-α1, β2-β2, and α1-β2) appeared to form. As such, it seems almost certain that the α1β2 receptor population was heterogeneous, even though it remained difficult to define its components.

When one microgram of each subunit cDNA was transfected and subunit expression levels were "corrected" for the potential effects of the epitope tags, there appeared to be approximately equal levels of α1 and β2 subunits on the cell surface (Figure 3). However, the correction was based on an indirect measure of epitope tag effects, and separate experiments using lower subunit cDNA levels (0.5 μg/subunit) yielded a higher $\alpha1^{HA}/\beta2^{HA}$ subunit level ratio. Using surface biotinylation, the ratio appeared to be higher still. Taken together, these data strongly suggested that α1 subunit surface levels were higher than β2 subunit surface levels.

However, the discrepancy clearly could not be explained wholly by a 3α:2β receptor population, because depending upon specific techniques and transfection conditions, $\alpha1^{HA}/\beta2^{HA}$ ratios ranged from around 1 to slightly less than 8. It therefore seemed that the cell surface contained a puzzling excess of α1 subunit protein.

To understand this phenomenon, it is necessary to consider how these "extra" α1 subunits were arranged – e.g., as monomers, homomultimers, or components of fully assembled pentameric receptors. Although it is possible that some α subunits were present as monomers, the strong α-α FRET patterns suggested that the majority of surface α subunits must be adjacent to at least one other α1 subunit. Furthermore, individual $GABA_A$ receptor subunits are thought to be retained in the endoplasmic reticulum (ER) and eventually degraded by ER-associated degradation (ERAD). The excess α1 subunits could be self-associated as homodimers, trimers, or tetramers, but nearly all α1 subunits were found in pentamers when α1 and β3 subunits were coexpressed [329]. Efficient α1 subunit homopentamerization and forward trafficking would be consistent with all of these observations. However, very few α1 subunits appeared to reach the cell surface in any arrangement when α1 subunit cDNA was transfected in isolation (Figure 2). Thus, if a large population of α1 homopentamers appeared when α1 subunit cDNA was co-transfected with β2 subunit cDNA, β2 subunits would have to somehow promote their formation.

This possibility seems counterintuitive – it is clear that GABA-gated α1β2 receptor isoforms assemble very efficiently when the subunits are co-expressed, so why should β2 subunit expression facilitate expression of presumably non-functional isoforms? A potential explanation includes basic subunit association properties together with experimental artifacts. First, the effects of β2 subunit overexpression on $\alpha1^{HA}/\beta2^{HA}$ levels must be considered. If α1β2 $GABA_A$ receptor assembly occurred in the same way as α4β2 nAChR assembly, surplus β2 subunit cDNA would promote formation of 2α:3β receptor isoforms. However, changing the relative amounts of α1 and β2 subunit cDNAs did not produce significant changes in the $\alpha1^{HA}/\beta2^{HA}$ ratio. Interestingly, though, there was a trend toward an *increased* $\alpha1^{HA}/\beta2^{HA}$ ratio when β2 subunit

cDNA was transfected in excess (Figure 4 C-D). This might occur if surplus β2 subunits form unproductive oligomers that are targeted for degradation, effectively causing a deficit of β2 subunits available for α1-β2 subunit heterooligomerization and promoting formation of 3α:2β heteropentamers.

This still cannot account for the fact that the $\alpha1^{HA}/\beta2^{HA}$ ratio was sometimes greater than 1.5, particularly when assessed via Western blotting. Given that two methods produced two mathematically inconsistent results, it seems likely that technical issues were responsible. The major difference between flow cytometry and immunoblotting is, of course, that the former evaluates folded proteins and the latter evaluates denatured proteins. Thus, it seems that the anti-α1 subunit antibody could access more epitopes in denatured than in folded proteins. As discussed, antibodies are much larger than $GABA_A$ receptor subunits, and it would probably be difficult for five antibodies to bind to a single pentamer. If so (and assuming that surface α1 subunit homomers were pentameric), the number of α1 subunits expressed on the cell surface when α1 subunit cDNA was transfected alone (Figure 2B) could be greatly underestimated. Robust formation of α1 subunit homopentamers could also explain why there seemed to be higher total cellular expression of α1 subunits compared to β2 subunits when both were co-expressed at equimolar amounts (Figure 2D); effectively, there would be more "room" available for α1 subunits because they could access all subcellular compartments regardless of whether they homo- or heterooligomerized. Finally, α1 subunit homopentamerization coupled with β2 homooligomer degradation would be consistent with the results presented in Figure 4A-B. That is, when α1 subunit cDNA was transfected in excess (Figure 4A, right side of graph), surplus α1 subunits formed homopentamers and were trafficked to the cell surface, but when β2 subunit cDNA was transfected in excess (Figure 4B, right side of graph), surplus β2 subunits produced unproductive lower-order homooligomers that were degraded.

There remains one interesting result that might not be explained by faulty detection of α1 subunit homopentamers: α1 subunit overexpression increased surface expression of β2 as well as

α1 subunits; i.e., α1 subunits seemed to "drive" overall expression levels. It is possible that any given amount of subunit cDNA produces far more β2 subunit protein than can be assembled and trafficked to the cell surface. However, it is also possible that in addition to forming pentameric receptors, α1 subunits can serve as chaperones. A recent study concluded that the short splice variant of γ2 subunits (γ2S) could externally modulate receptor function by binding to the outside of a pentameric receptor, essentially functioning as an accessory protein[337]. If α1 subunits assumed a similar role, the "accessory" α1 subunits could promote receptor assembly and forward trafficking, which would account for the fact that α1 (but not β2) subunit overexpression increases both α1 and β2 subunit surface trafficking. Presumably, receptors bearing "accessory" α1 subunits should sediment separately from simple pentameric receptors in gradient centrifugations, but this was not observed in previous experiments[329]. However, this could be reconciled with the accessory subunit theory if the interaction between the pentamer and the accessory subunits is relatively weak and was disrupted during the process of protein purification. That said, although it is an intriguing possibility, neither we nor the group reporting accessory γ2S subunits have presented direct evidence that individual $GABA_A$ receptor subunits bind to the outside of $GABA_A$ receptor pentamers even in heterologous expression systems. In future studies, it would be interesting to perform atomic force or electron microscopy to determine whether or not $GABA_A$ receptor subunits can assume the dual roles of receptor component and molecular chaperone.

CHAPTER III

$GABA_A$ RECEPTOR γ2L AND δ SUBUNITS ARE ASSEMBLED AND TRAFFICKED SIMILARLY BUT DEGRADED AT DIFFERENT RATES

Abstract

$GABA_A$ receptors are heteropentameric ligand-gated chloride channels assembled from a large family of homologous subunits (α1-6, β1-3, γ1-3, δ, ε, θ, and π). While the subunit stoichiometry and arrangement of αβγ receptor isoforms have been extensively investigated, relatively little is known about the assembly of receptor isoforms containing the δ subunit. Furthermore, there is still no consensus regarding how these receptors should be studied, as there is contradictory information about the technical requirements for forming homogeneous populations of αβγ or αβδ receptor isoforms in heterologous systems. We therefore used flow cytometry to compare the surface expression profiles of HEK293T cells transiently transfected with human α1β2γ2L and α1β2δ receptors. Similar to γ2L subunits, δ subunits were poorly expressed on the cell surface when transfected alone or in combination with either α1 or β2 subunits but were efficiently expressed when co-transfected with both α1 and β2 subunits. In addition, both γ2L and δ subunits appeared to be incorporated into ternary receptors at the expense of β2 subunits. However, far less δ subunit than γ2L subunit cDNA was required to eliminate functional signatures of α1β2 receptors and to produce comparable expression levels of all subunits; when 1 μg each of α1 and β2 subunit cDNAs were transfected, maximal receptor expression occurred with 1 μg of γ2L subunit cDNA but only 0.03 μg of δ subunit cDNA. The fact that both subunits were incorporated at the expense of β subunits suggested that α1β2γ2L and α1β2δ receptors might have identical arrangements, while the stark difference in efficiency suggests that they might not. To compare the arrangements of γ2L and δ subunits in ternary

receptors, we employed a flow cytometry-based FRET assay for subunit adjacency. Both α1β2γ2L and α1β2δ receptors yielded significant FRET signals between all possible combinations of non-identical subunits (i.e., α1-β2, α1-γ2L, α1-δ, β2-γ2L, and β2-δ), but only minimal FRET signals between identical subunits (i.e., α1-α1, β2-β2, γ2L-γ2L, or δ-δ), suggesting similar subunit arrangements of alternating α1, β2, and γ2L or δ subunits but failing to provide a reason for the different "potency" of γ2L and δ subunit cDNAs. Further investigation demonstrated that δ subunits degraded much more slowly than γ2L subunits and that this was not due to different subcellular distributions. We conclude that α1β2γ2L and α1β2δ receptors assemble similarly, but surprisingly low levels of γ2L and particularly δ subunit cDNAs are required to eliminate α1β2 receptor populations. Moreover, δ subunits are remarkably more stable than γ2L subunits, which might have important implications for adaptive neuronal physiology.

Introduction

$GABA_A$ receptors are ligand-gated ion channels that mediate the vast majority of fast inhibitory signaling in the central nervous system. They are assembled as heteropentamers from a large family of subunit subtypes (α1-6, β1-3, γ1-3, δ, ε, θ, π, and ρ1-3), and their subunit composition determines receptor kinetics, pharmacology, and subcellular localization. For example, αβγ receptors give rise to large amplitude, extensively desensitizing currents and tend to be concentrated in synapses, where they mediate "phasic" inhibition. In contrast, αβδ receptors give rise to small amplitude, minimally desensitizing currents and are predominantly found in peri- and extrasynaptic compartments, where they mediate "tonic" inhibition[168, 272, 338, 339].

There is a general consensus that αβγ $GABA_A$ receptor isoforms contain two α subunits, two β subunits, and one γ subunit, which are arranged γ-β-α-β-α (anticlockwise as viewed from the synaptic cleft)[328, 340]. It is also commonly assumed that the γ subunit is replaced by other subunits in other isoforms. For αβδ receptor isoforms, this conclusion was reached because in

most studies, γ and δ subunits were not colocalized in brain and functional receptors did not contain both γ and δ subunits in heterologous expression systems. The most direct evidence for the assumed stoichiometry and arrangement was provided by atomic force microscopy, which indicated that α4β3δ receptor isoforms do in fact assemble in the δ-β-α-β-α arrangement[341]. However, most studies of stoichiometry consist of functional characterization of receptors assembled from concatenated subunit constructs, and even these have reached contradictory conclusions[116, 328]. Furthermore, concatemeric constructs themselves can pose several technical problems. Expression levels are typically low, necessitating use of *Xenopus* oocytes that may express endogenous subunits; some dimeric or trimeric constructs have produced current when transfected alone; and the resulting receptors variably recapitulated the functional properties of freely-assembled receptors[116, 342]. Finally, it is possible that the constructs cannot even strictly constrain stoichiometry because individual subunits may "loop out" or linkers may be cleaved[330].

In short, there is a surprising dearth of conclusive data regarding the stoichiometry and arrangement of subunits in $GABA_A$ receptor isoforms, including those formed through heterologous expression. As such, we sought to examine certain simple questions. First, do HEK293T cells express endogenous subunits and if not, are the previously reported subunit combinations necessary for surface expression accurate? Is it possible to achieve a functionally homogeneous population of αβγ or αβδ receptor isoforms via heterologous expression? If so, how much γ2L or δ cDNA relative to α and β cDNA should be used? Finally, is there an efficient and direct method to determine the stoichiometry and/or subunit arrangement of freely-assembled receptors retaining their native conformation?

To address these questions, we expressed various combinations of $GABA_A$ receptor subunits in HEK293T cells and assessed surface and total cellular expression of all subunits using flow cytometry. We determined that our cell line contained no detectable endogenous $GABA_A$ receptor subunits, but there were clear rules for subunit surface trafficking. Surprisingly, δ subunit-containing receptors did prove difficult to express, but this appeared to result from

excessive rather than inadequate amounts of δ subunit cDNA; peak subunit expression levels were achieved with tenfold less δ than γ2L subunit cDNA. However, this phenomenon did not occur because γ2L and δ subunits were incorporated differently into receptor pentamers; rather, δ subunits were degraded at a markedly slower rate.

Materials and Methods

Cell culture and expression of recombinant $GABA_A$ receptors

Human $GABA_A$ receptor α1, β2, γ2L, and δ subunits were individually sub-cloned into the pcDNA3.1+ mammalian expression vector (Invitrogen, Grand Island, NY). Due to the lack of a highly specific, commercially available antibody targeting an extracellular domain on the γ2L and δ subunits, the HA (YPYDVPDYA) epitope was inserted between amino acids 4 and 5 of the mature peptide. This insertion site was selected for its minimal effect on receptor expression and function (see Chapter II). The coding region of each vector was sequenced by the Vanderbilt University Medical Center DNA Sequencing Facility and verified against published sequences.

HEK293T cells (American Type Culture Collection, Manassas, VA) were maintained at 37°C in humidified 5% CO_2 / 95% air using Dulbecco's Modified Eagle Medium (Invitrogen) supplemented with 10% fetal bovine serum (Invitrogen), 100 i.u./ml penicillin (Invitrogen), and 100 μg/ml streptomycin (Invitrogen). Cells were plated at a density of ~10^6 cells per 10 cm culture dish (Corning Glassworks, Corning, NY) and passaged every 2-4 days using trypsin-EDTA (Invitrogen). For flow cytometry and electrophysiology experiments, cells were plated at a density of $4x10^5$ cells per 6 cm culture dish (Corning Glassworks) and transfected ~24 hours later with equal amounts (1 μg/subunit) of subunit cDNA using FuGene6 (Roche Diagnostics, Indianapolis, IN) per manufacturer protocol. In conditions where less than 3 μg of subunit cDNA was transfected, empty pcDNA3.1 vector was added such that a total of 3 μg of cDNA was used

for each experimental condition (thus, the "mock" transfection condition consisted of 3 μg of empty pcDNA 3.1 vector cDNA). An additional 1 μg of pHook-1 cDNA (encoding the cell surface antibody sFv) was included for electrophysiology experiments so positively transfected cells could be selected ~24 hours later by immunomagnetic bead separation, as previously described[343]. Following selection, cells were re-plated at low density on collagen-coated 35 mm dishes for electrophysiological recording the following day.

Electrophysiology

Patch clamp recordings were performed at room temperature from excised outside-out membrane patches. Cells were maintained during recordings in a bath solution consisting of (in mM): 142 NaCl, 8 KCl, 6 $MgCl_2$, 1 $CaCl_2$, 10 glucose, and 10 HEPES (pH adjusted to 7.4; 325-330 mOsm). All chemicals used for solution preparation were purchased from Sigma-Aldrich (St. Louis, MO). Recording pipettes were pulled from thin-walled borosilicate capillary glass (Fisher, Pittsburgh, PA) on a Sutter P-2000 micropipette electrode puller (Sutter Instruments, San Rafael, CA) and fire polished with a microforge (Narishige, East Meadow, NY). When filled with a pipette solution consisting of (in mM) 153 KCl, 1 $MgCl_2$, 5 EGTA, 10 HEPES, and 2 MgATP (pH adjusted to 7.3; 300-310 mOsm) and submerged in the bath solution, this yielded open tip resistances of ~2 M Ω and a chloride equilibrium potential (E_{Cl}) of ~0 mV. Currents were recorded at a holding potential of -20 mV using an Axopatch 200B amplifier (Molecular Devices, Foster City, CA), low-pass filtered at 2 kHz using a 4-Pole Bessel filter, digitized at 10 kHz using the Digidata 1322A (Molecular Devices), and stored offline for analysis. GABA was prepared as a stock solution. Working solutions were made on the day of the experiment by diluting stock solutions with the bath solution.

Kinetic Analysis

Current kinetic properties were analyzed using Clampfit 9 (Molecular Devices). Currents greater than 6 nA were excluded from analysis to minimize the confounding impact of series resistance error. Rise time was defined as the time required for currents to increase from 10% to 90% of their peak. The time course of desensitization was fit with up to four exponential components. The time course of deactivation was fit using the Levenberg-Marquardt least squares method to the form $\sum a_n e^{(-t/\tau_n)} + C$, where t is time, *n* is the number of components, *a* is the relative amplitude, τ is the time constant, and C is the fraction of current remaining, with $\sum a_n = 1$. Additional components were accepted only if they significantly improved the fit, as determined by an F-test automatically performed by the analysis software on the sum of squared residuals. Deactivation was typically biphasic, though as many as four components could be resolved with larger amplitude currents. To facilitate comparison, the time course of deactivation was summarized as a weighted time constant in the form $\sum a_n \tau_n$ with $\sum a_n = 1$. Solution exchange time was defined as the time for an open-tip liquid-junction current to increase from 10% to 90% of its maximum value. Data were reported as mean ± SEM. One-way ANOVA followed by a Dunnet's multiple comparison test was used to compare results to the 1:1:0 and 1:1:1 μg transfection conditions, as indicated.

Flow Cytometry

Cells were harvested ~48 hours after transfection using 37°C trypsin/EDTA (Invitrogen) and placed immediately in 4°C FACS buffer composed of PBS (Mediatech), 2% fetal bovine serum (FBS) (Invitrogen), and 0.05% sodium azide (VWR). Cells were then transferred to 96-well plates, where they were washed twice in FACS buffer (i.e., pelleted by centrifugation at 450 x g, vortexed, and resuspended). For surface protein staining, cells were incubated in antibody-containing FACS buffer for 1 h at 4°C, washed in FACS buffer three times, and resuspended in

2% w/v paraformaldehyde (PFA) (Electron Microscopy Sciences). For total protein staining, samples were first fixed and permeabilized using Cytofix/Cytoperm (BD Biosciences) for 15 min. After washing twice with Permwash (BD Biosciences) to remove residual fixative, cells were resuspended in antibody-containing Permwash for 1 h at 4°C. Following incubation with antibody, samples were washed four times with Permwash and twice with FACS buffer before resuspension in 2% paraformaldehyde. The anti-α1 antibody was obtained from Millipore (clone bd24), conjugated to the Alexa647 fluorophore using an Invitrogen kit, and used at 4 μg/ml for surface staining and 2 μg/ml for total protein staining. The anti-β2 antibody was obtained from Millipore (clone 62-3G1) and used at 8 μg/ml for surface staining and 4 μg/ml for total protein staining. Because anti-β2 antibody conjugation proved inefficient, an anti-IgG1-Alexa647 secondary antibody was used at a 1:500 dilution for most experiments. Because accurate FRET analysis requires directly conjugated antibodies, a different anti-β2 subunit antibody clone (bd17; same epitope as 62-3G1 but suspended in PBS alone) was obtained from Millipore, conjugated to Alexa555 or Alexa647 fluorophores as described above, and used at a 1:50 dilution for all FRET experiments. The anti-HA antibody (clone 16B12) was obtained from Covance as an Alexa-647 conjugate and used at a 1:250 dilution for surface staining and a 1:500 dilution for total protein staining.

Samples were run on a LSR II flow cytometer (BD Biosciences). For each staining condition, 50,000 cells were analyzed. Nonviable cells were excluded from analysis based on forward- and side-scatter profiles, as determined from staining with 7-amino-actinomycin D (7-AAD) (Invitrogen). The Alexa-555 fluorophore was excited using a 535 nm laser and detected with a 575/26 bandpass filter. The Alexa-647 fluorophore was excited using a 635 nm laser and detected with a 675/20 bandpass filter. Data were acquired using FACSDiva (BD Biosciences) and analyzed off-line using FlowJo 7.1 (Treestar). To compare surface and total expression levels of $GABA_A$ receptor subunits, the mean fluorescence intensity of mock transfected cells was subtracted from the mean fluorescence intensity of each positively transfected condition.

The remaining fluorescence was then normalized to that of a control condition, yielding a relative fluorescence intensity ("Relative FI"). Statistical significance was determined using a one-sample t-test using a hypothetical mean of 1 (since data in each condition were normalized to wild-type expression). Data were expressed as mean ± SEM.

For protein degradation experiments, cells were plated at a density of $2x10^5$ cells per 3 cm culture dish and transfected as described above, but with a total of 1 μg of cDNA for each experimental condition. Approximately 48 hours after transfection, 100 μL of 0.1% cycloheximide (Sigma-Aldrich) was added to culture dishes, which were subsequently returned to the 37°C incubator for the times indicated in the figure legends. After incubation, cells were harvested, permeabilized, stained, and subjected to flow cytometry as previously described.

Radiolabeling, immunoprecipitation, and SDS-PAGE

HEK293T cells were plated and transfected with $\gamma 2L^{HA}$ or δ^{HA} subunit cDNA as described above. Two days after transfection, the culture medium was replaced with methionine-free medium for 30 minutes and then replaced with medium containing 150 μCi/mL ^{35}S-methionine, and cells were returned to the incubator. For synthesis studies, plates were removed after 5, 10, 15, or 20 minutes, immediately placed on ice, and washed with both non-radioactive media and PBS. Membranes were lysed using radioimmune precipitation assay buffer (RIPA buffer; 50 mM Tris-HCl pH 7.4, 1% Triton-100, 250 mM NaCl, 5 mM EDTA) containing protease inhibitor cocktail (Sigma) and insoluble components were removed by centrifugation at 15,000 x g for 20 minutes. $\gamma 2L^{HA}$ and δ^{HA} subunit proteins were incubated overnight with red anti-HA affinity gel (Sigma) and eluted using 125 μg/mL anti-HA peptide (Sigma). Proteins were separated using SDS-PAGE (10% Bis-Tris gel). The dried gel was exposed to a phosphor screen for two days and imaged using a Typhoon phosphorimager (Molecular Dynamics/GE Healthcare). The bands then were quantified using ImageJ. Degradation studies were performed

identically except that after addition of radioactive medium, cells were returned to 37C^{o} for 1, 2, 3, 4, or 6 hrs.

Results

$GABA_A$ receptor δ^{HA} subunits had markedly different patterns of surface and total cellular expression compared to $\gamma2L^{HA}$ subunits when co-transfected with $\alpha1$ and/or $\beta2$ subunits at equimolar ratios.

To determine the subunit requirements for receptor surface trafficking, we transfected HEK293T cells with all possible combinations of α1, β2, γ2L, and δ subunit cDNAs, detected subunit protein with fluorescently-conjugated antibodies and evaluated fluorescence levels using flow cytometry. Because no commercially-available antibodies raised against γ2 or δ subunits were suitable for flow cytometry, the HA epitope (YPYDVPDYA) was inserted between the fourth and fifth amino acids of γ2L and δ subunits and levels of these subunits were detected using an anti-HA antibody. In agreement with previous results[80], α1 (Figure 1A, 1D) and β2 (Figure 1B, 1E) subunits were trafficked efficiently to the cell surface only when both α1 and β2 subunit cDNA were coexpressed. Low levels of α1 subunit surface expression were present in all α1 subunit-containing transfection conditions when the β2 subunit was not transfected (α1 = 2.9 ± 0.3%, $\alpha1\gamma2L^{HA}$ = 5.2 ± 0.2%, and $\alpha1\delta^{HA}$ = 3.1 ± 0.5 of α1β2; n = 6), suggesting that small amounts of α1 subunits could be trafficked to the cell surface as monomers or homomultimers and that coexpressed $\gamma2L^{HA}$ or δ^{HA} subunits did not affect this process. The most unexpected results involved the $\alpha1\beta2\gamma2L^{HA}$ and $\alpha1\beta2\delta^{HA}$ transfection conditions. It is commonly thought that although αβγ and αβδ $GABA_A$ receptor isoforms differ greatly in their physiology and pharmacology[168], the receptors are nearly identical in structure[266]. Therefore, it was surprising that α1 subunit surface levels in the $\alpha1\beta2\gamma2L^{HA}$ expression condition were approximately 90% of those in the α1β2 expression condition (93.0 ± 4.0% of α1β2, n = 6), but α1 subunit surface levels

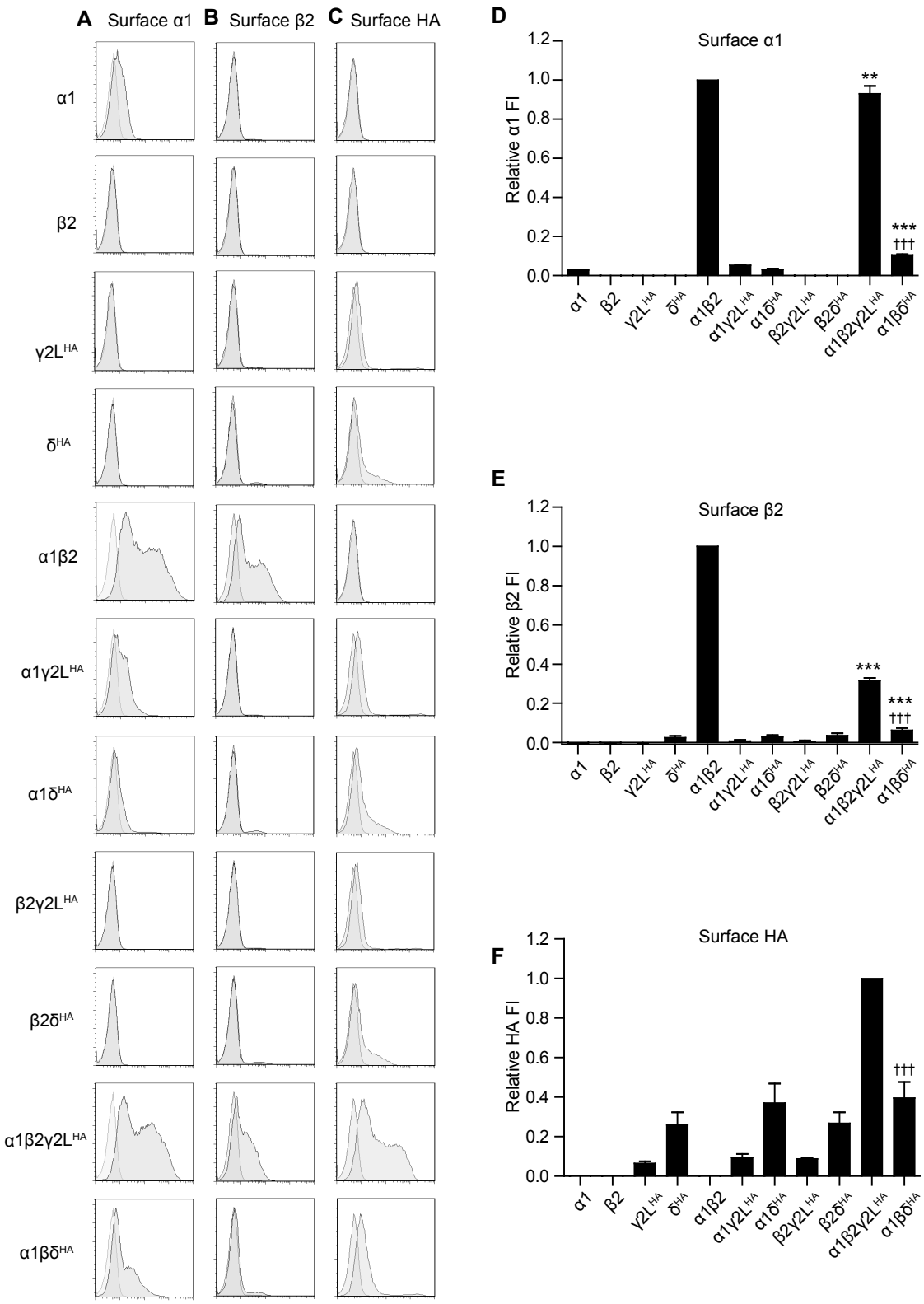
A Surface α1
B Surface β2
C Surface HA
α1
β2
γ2L^HA
δ^HA
α1β2
α1γ2L^HA
α1δ^HA
β2γ2L^HA
β2δ^HA
α1β2γ2L^HA
α1βδ^HA
D
Surface α1
Relative α1 FI
E
Surface β2
Relative β2 FI
F
Surface HA
Relative HA FI
α1
β2
γ2L^HA
δ^HA
α1β2
α1γ2L^HA
α1δ^HA
β2γ2L^HA
β2δ^HA
α1β2γ2L^HA
α1βδ^HA

Figure 1

Figure 1. $GABA_A$ receptor α1, β2, γ2L^{HA}, and δ^{HA} subunit surface expression was highly sensitive to the presence and identity of partnering subunits.

HEK293T cells were transfected with various combinations of $GABA_A$ receptor subunit cDNAs and surface expression was evaluated using subunit-specific antibodies and flow cytometry. **A-C.** Representative flow cytometry histograms from cells transfected with the indicated combination of subunit cDNAs (left) and incubated with antibodies raised against α1 **(A)** or β 2/3 **(B)** $GABA_A$ receptor subunits or the HA epitope tag **(C)**. The abscissa indicates fluorescence intensity (FI) in arbitrary units plotted on a logarithmic scale, and the ordinate indicates percentage of maximum cell count (% of max). Histograms for cells transfected with subunit combinations (dark gray) and cells transfected with blank vector (light gray) are overlaid. **D-F.** Quantifications of fluorescence intensities from cells transfected with the indicated combination of subunit cDNAs and incubated with antibodies raised against α1 **(D)** or β2/3 **(E)** $GABA_A$ receptor subunits or the HA epitope tag **(F)**. Mean fluorescence intensities from cells transfected with blank vector alone were subtracted from mean fluorescence intensities of all other expression conditions. All mock-subtracted fluorescence intensities were normalized to the mock-subtracted fluorescence intensity of the α1β2γ2L^{HA} expression condition.

in the $\alpha1\beta2\delta^{HA}$ expression condition were only approximately 10% of those in the $\alpha1\beta2$ expression condition (10.6 ± 0.4% of $\alpha1\beta2$, n = 6).

The β2 subunit surface expression patterns also suggested that $\alpha1\beta2\gamma2L^{HA}$ and $\alpha1\beta2\delta^{HA}$ isoforms might assemble differently (Figure 1B, 1E). Once again, addition of δ^{HA} subunits decreased surface levels of partnering subunits more than addition of $\gamma2L^{HA}$ subunits. Specifically, β2 subunit surface levels in the $\alpha1\beta2\gamma2L^{HA}$ expression condition were approximately 30% of those in the in the $\alpha1\beta2$ expression condition (31.6 ± 1.3% of $\alpha1\beta2$, n = 5), but β2 subunit surface levels in the $\alpha1\beta2\delta^{HA}$ expression condition were only approximately 5% of those in the in the $\alpha1\beta2$ expression condition (6.2 ± 1.3% of $\alpha1\beta2$, n = 5). It was also noteworthy that incorporation of either $\gamma2L^{HA}$ or δ^{HA} subunits reduced β2 subunit surface expression far more than they reduced α1 subunit surface expression.

Finally, we examined $\gamma2L^{HA}$ and δ^{HA} subunit surface levels using fluorescently-tagged anti-HA antibodies (Figure 1C, 1F). Consistent with previous studies[81, 344], we found that unless they were coexpressed with both α1 and β2 subunits, $\gamma2L^{HA}$ subunits reached the cell surface only at low levels ($\gamma2L^{HA}$ = 6.5 ± 0.9%, $\alpha1\gamma2L^{HA}$ = 9.6 ± 1.6%, and $\beta2\gamma2L^{HA}$ = 8.9 ± 0.7 of $\alpha1\beta2\gamma2L^{HA}$; n = 6). In contrast, δ^{HA} subunits reached the cell surface quite efficiently without regard to cotransfected subunits. Surprisingly, surface HA levels did not differ significantly among δ^{HA} (26.1 ± 6.3%), $\alpha1\delta^{HA}$ (37.0 ± 9.8%), $\beta2\delta^{HA}$ (26.7 ± 5.6%) and $\alpha1\beta2\delta^{HA}$ (39.8 ± 8.1%) transfection conditions (all compared to $\alpha1\beta2\gamma2L^{HA}$; n = 6).

The results presented in Figure 1 demonstrated that, when equimolar amounts of α1, β2, and $\gamma2L^{HA}$ or δ^{HA} subunits were expressed in fibroblasts, surface expression levels of all subunits were greatly suppressed by δ^{HA} subunits. To determine if this reflected impairment of surface trafficking or of subunit expression, total cellular expression levels were assessed by repeating the previous experiments after cell permeabilization (Figure 2). In general, the patterns of total cellular subunit expression resembled those of surface subunit expression but were less pronounced. For instance, α1 subunit expression levels were approximately 80% when $\gamma2L^{HA}$

subunits were included ($\alpha1\beta2\gamma2L^{HA}$ = 81.3 ± 4.1% of α1β2; $p < 0.01$) but were approximately 25% when δ^{HA} subunits were included ($\alpha1\beta2\delta^{HA}$ = 24.5 ± 1.0% of α1β2; $p < 0.001$ compared to both α1β2 and $\alpha1\beta2\gamma2L^{HA}$). Furthermore, when α1 subunits were transfected in the absence of β2 subunits, the α1 subunits were expressed but at markedly lower levels (α1 = 55.3 ± 2.2%, $\alpha1\gamma2L^{HA}$ = 50.0 ± 2.1%, and $\alpha1\delta^{HA}$ = 20.6 ± 1.1% of α1β2; n = 6). Total cellular expression of β2 subunits also recapitulated less drastically the patterns seen in surface expression. When $\gamma2L^{HA}$ subunits were included, β2 subunit expression decreased by almost half ($\alpha1\beta2\gamma2L^{HA}$ = 60.5 ± 3.9% of α1β2; $p < 0.001$), but when δ^{HA} subunits were included, β2 subunit expression was only approximately 10% ($\alpha1\beta2\delta^{HA}$ = 11.6 ± 3.1% of α1β2; $p < 0.001$ compared to both α1β2 and $\alpha1\beta2\gamma2L^{HA}$). In contrast to surface expression patterns, β2 subunits were expressed at low levels in the absence of α1 subunits (β2 = 24.7 ± 1.2%, $\beta2\gamma2L^{HA}$ = 24.0 ± 5.9%, and $\beta2\delta^{HA}$ = 9.0 ± 5.1% of α1β2; n = 5).

Unlike α1 and β2 subunits, the total cellular expression patterns of $\gamma2L^{HA}$ and δ^{HA} subunits were quite different from their surface expression patterns. First, when $\gamma2L^{HA}$ subunits were expressed alone or with either α1 or β2 subunits, $\gamma2L^{HA}$ levels were only about 50% compared to levels seen in the $\alpha1\beta2\gamma2L^{HA}$ condition ($\gamma2L^{HA}$ = 46.2 ± 1.4%, $\alpha1\gamma2L^{HA}$ = 59.6 ± 1.0%, $\beta2\ \gamma2L^{HA}$ = 59.6 ± 1.8% of $\alpha1\beta2\gamma2L^{HA}$, n = 5). Second, total cellular δ^{HA} levels were equal to or higher than $\gamma2L^{HA}$ levels in all expression conditions. On the cell surface, δ^{HA} subunits were expressed at similar levels regardless of coexpressed subunits, and all were less than 50% of $\gamma2L^{HA}$ levels present in the $\alpha1\beta2\gamma2L^{HA}$ condition. Total cellular δ^{HA} levels were also similar in all δ subunit-containing expression conditions, but they were not significantly different from $\gamma2L^{HA}$ levels in the $\alpha1\beta2\gamma2L^{HA}$ condition (δ^{HA} = 96.9 ± 5.6%, $\alpha1\delta^{HA}$ 89.5 ± 5.0%, $\beta2\delta^{HA}$ = 91.2 ± 12.6%, and $\alpha1\beta2\delta^{HA}$ = 83.7 ± 10.6% of $\alpha1\beta2\gamma2L^{HA}$; n = 6).

In summary, α1, β2, and $\gamma2L^{HA}$ subunits all required both α1 and β2 subunits for efficient surface expression and for maximal total cellular expression, but δ^{HA} subunits could reach the cell surface alone or with any combination of coexpressed subunits. Compared to $\gamma2L^{HA}$ subunits,

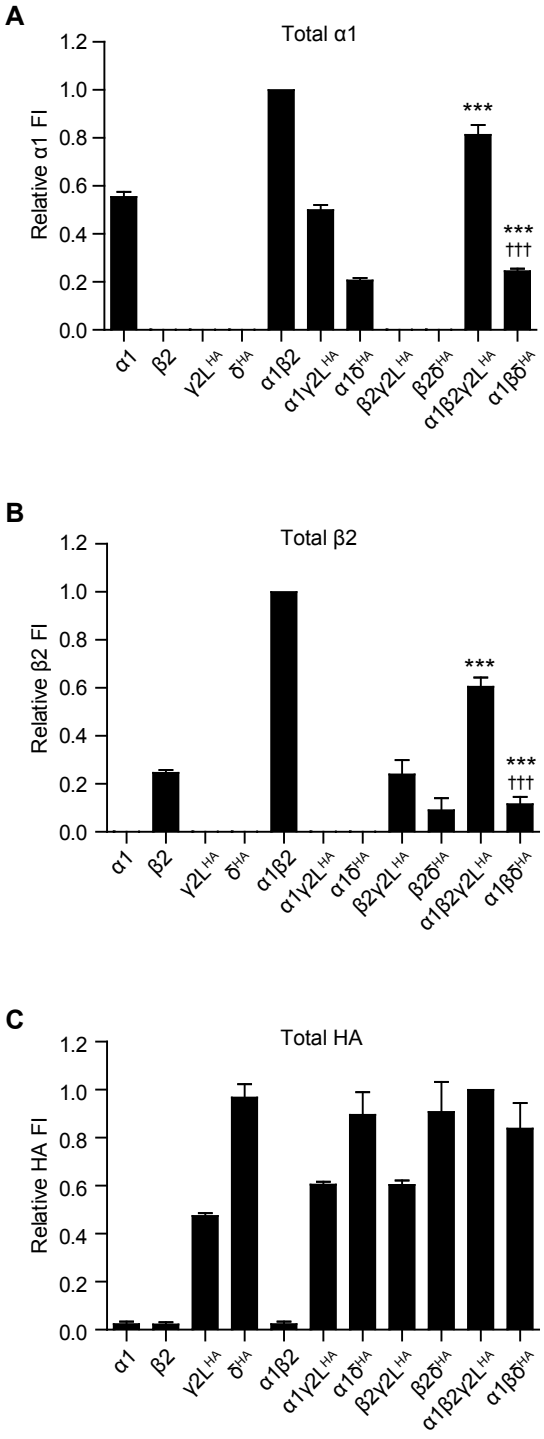

Figure 2. $GABA_A$ receptor α1, β2, $γ2L^{HA}$, and $δ^{HA}$ subunit total cellular expression was highly sensitive to the presence and identity of partnering subunits.

HEK293T cells were transfected with various combinations of $GABA_A$ receptor subunit cDNAs and total cellular subunit expression was evaluated after permeabilization using flow cytometry. **A-C.** Fluorescence intensities were quantified from cells transfected with the indicated combination of subunit cDNAs and incubated with antibodies raised against α1 **(A)** or β 2/3 **(B)** $GABA_A$ receptor subunits or the HA epitope tag **(C)**. Mean fluorescence intensities from cells transfected with blank vector alone were subtracted from mean fluorescence intensities of all other expression conditions. All mock-subtracted fluorescence intensities were normalized to the mock-subtracted fluorescence intensity of the $α1β2γ2L^{HA}$ expression condition.

δ^{HA} subunits strongly reduced surface expression of all subunits and more moderately reduced total cellular expression of α1 and β2 subunits. Despite these effects, total cellular expression of δ^{HA} subunits was robust; in other words, ample amounts of δ^{HA} subunits were produced, but they seemed to impede surface trafficking of all subunits. Taken together, the expression levels of all four subunits could indicate that more δ subunits than γ subunits were incorporated into a receptor pentamer (i.e., α and β subunit levels were lower in the $\alpha1\beta2\delta^{HA}$ condition than in the $\alpha1\beta2\gamma2L^{HA}$ condition because δ subunits were more likely than γ subunits to displace α1 and β2 subunits), which would in turn mean that δ subunit-containing and γ subunit-containing receptors assemble quite differently. On the other hand, coexpression of either $\gamma2L^{HA}$ or δ^{HA} subunits reduced expression of β2 subunits more than α1 subunits, which could indicate that both γ and δ subunits are usually incorporated into pentamers at the expense of β subunits. Thus, some properties suggested that γ subunit-containing and δ subunit-containing receptors assembled similarly, while others suggested that the receptors assembled differently.

$GABA_A$ receptor δ^{HA} subunits had nearly identical patterns of surface expression compared to $\gamma2L^{HA}$ subunits when co-transfected with α1 and β2 subunits at ten-fold lower levels.

When subunits were transfected at equimolar ratios, the differences between $\gamma2L^{HA}$ and δ^{HA} levels were particularly striking. For years, there has been a continuing debate in the $GABA_A$ receptor literature regarding what subunit cDNA ratios should be used in recombinant receptor studies[276, 345, 346]. We began with equimolar ratios because this should reflect the relative gene dosage in organisms; α1, β2, γ2, and δ $GABA_A$ receptor subunit genes are autosomal and none has been shown to be imprinted. However, it is possible that γ and δ subunits incorporate into pentamers with different affinities and therefore require different transfection ratios. To investigate this possibility, one microgram each of α1 and β2 subunit cDNA was transfected together with 0.001 – 10 μg of $\gamma2L^{HA}$ or δ^{HA} cDNA.

Increasing amounts of either $\gamma 2L^{HA}$ or δ^{HA} subunit cDNAs appeared to produce similar patterns of subunit expression, but far less δ^{HA} subunit cDNA was required to produce comparable levels of subunit protein. For instance, α1 subunit surface levels remained stable when low levels of either $\gamma 2L^{HA}$ or δ^{HA} subunit cDNA was transfected (Figure 3A). When ≥ 1 μg of $\gamma 2L^{HA}$ subunit cDNA was transfected, α1 subunit levels progressively decreased (Figure 3A, black line). However, only ≥ 0.1 μg of δ^{HA} subunit cDNA was required to produce a similar decrease (Figure 3A, grey line). Interestingly, it proved impossible to test subunit expression with higher δ^{HA} subunit levels due to widespread cell death when more than one microgram of δ^{HA} cDNA was transfected.

Surface expression levels of β2 subunits responded somewhat differently to increasing amounts of $\gamma 2L^{HA}$ or δ^{HA} cDNA. There was no significant change in α1 subunit surface levels across a range of low levels of $\gamma 2L^{HA}$ or δ^{HA} subunit cDNA, but β2 subunit levels did not exhibit a similar "plateau" phase. Rather, all tested amounts of $\gamma 2L^{HA}$ or δ^{HA} subunit cDNA caused concentration-dependent decreases in β2 subunit surface levels. Similar to α1 subunit patterns, however, β2 subunit levels were equal when approximately tenfold less δ^{HA} than $\gamma 2L^{HA}$ subunit cDNA was transfected. Finally, $\gamma 2L^{HA}$ and δ^{HA} subunit surface levels also had similar patterns but were different in subunit cDNA "potency." For both subunits, surface levels increased over a range of cDNA levels, peaked, and then decreased. However, peak subunit surface expression occurred with 0.03 μg of δ^{HA} cDNA and 1 μg of $\gamma 2L^{HA}$ cDNA. Notably, these were also similar to the $\gamma 2L^{HA}/\delta^{HA}$ cDNA amounts at which α1 subunit protein levels began to decline.

As seen with equimolar subunit expression (Figure 2), total cellular subunit expression patterns over a range of $\gamma 2L^{HA}$ and δ^{HA} subunit cDNA levels were similar to surface expression patterns, though total cellular levels did not decrease quite as drastically as surface levels at the highest amounts of $\gamma 2L^{HA}$ or δ^{HA} cDNA. Levels of α1 subunits declined when more than 1 μg of $\gamma 2L^{HA}$ subunit cDNA or 0.03 μg of δ^{HA} subunit cDNA was transfected, and levels of β2 subunits declined continuously, particularly when more than 0.01 μg of either $\gamma 2L^{HA}$ or δ^{HA} subunit cDNA

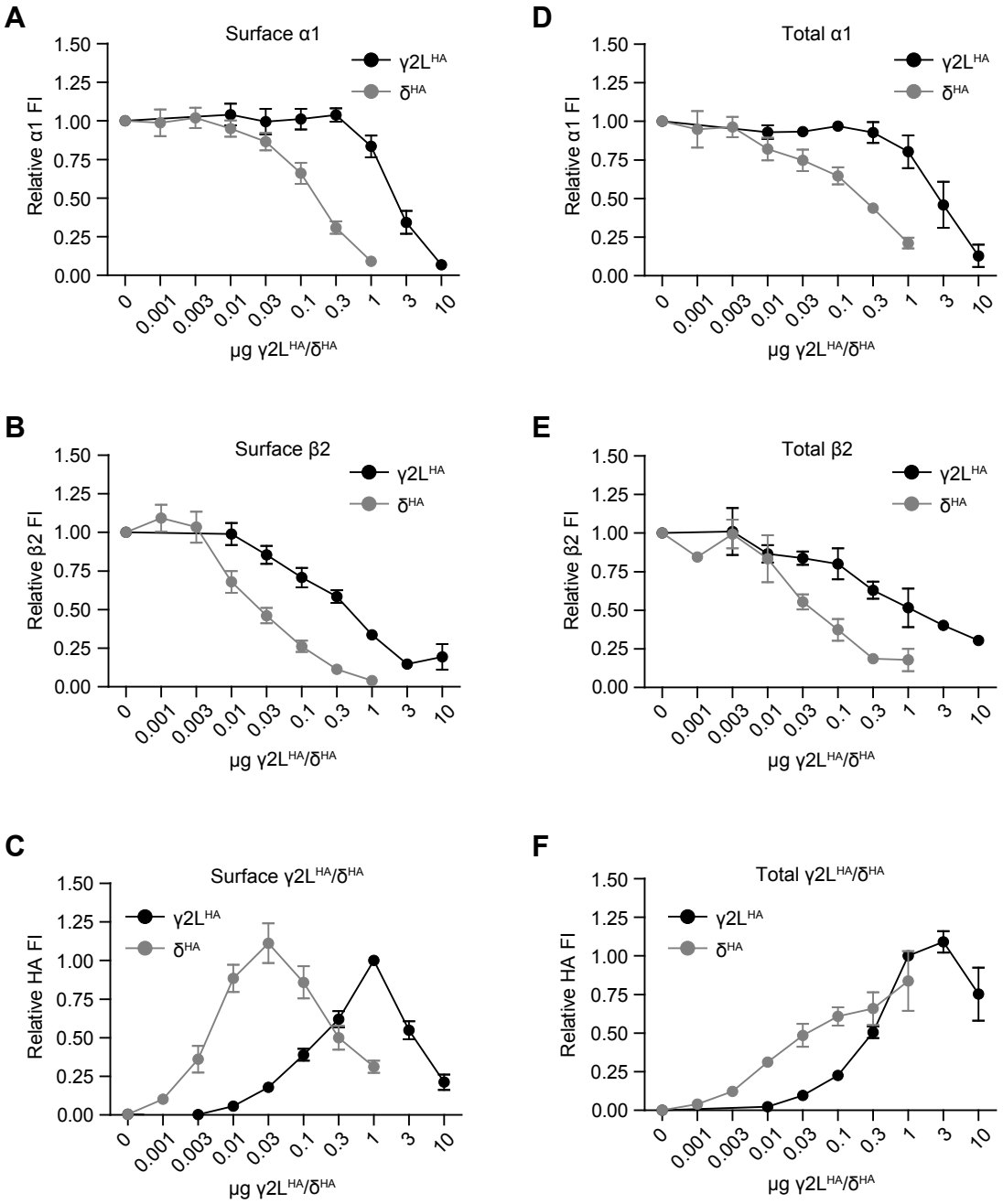
A
Surface α1
Relative α1 FI
γ2L^HA
δ^HA
μg γ2L^HA/δ^HA
D
Total α1
B
Surface β2
Relative β2 FI
E
Total β2
C
Surface γ2L^HA/δ^HA
Relative HA FI
F
Total γ2L^HA/δ^HA
0
0.001
0.003
0.01
0.03
0.1
0.3
1
3
10

Figure 3

Figure 3. $GABA_A$ receptor α1, β2, γ2L^{HA}, and δ^{HA} subunits had similar surface expression levels and patterns but required markedly different amounts of γ2L^{HA} or δ^{HA} cDNA.

Flow cytometry was used to evaluate surface expression of $GABA_A$ receptor subunits in HEK293T cells transfected with α1, β2, and varying amounts of γ2L^{HA} or δ^{HA} subunit cDNAs. **A-C.** Surface expression levels of α1 **(A)**, β2 **(B)**, and γ2L^{HA} **(C)** subunits were evaluated in cells transfected with 1 μg α1 subunit cDNA, 1 μg β2 subunit cDNA, and 0.01–10 μg γ2L^{HA} subunit cDNA. Mean fluorescence intensities from cells transfected with blank vector alone were subtracted from mean fluorescence intensities of all other expression conditions. All mock-subtracted fluorescence intensities were normalized to the mock-subtracted fluorescence intensity of the 1 μg α1 : 1 μg β2 : 1 μg γ2L^{HA} expression condition. **D-F.** Surface expression levels of α1 **(D)**, β2 **(E)**, and γ2L^{HA} **(F)** subunits were evaluated in cells transfected with 1 μg α 1 subunit cDNA, 1 μg β2 subunit cDNA, and 0.001–1 μg δ^{HA} subunit cDNA. Mean fluorescence intensities from cells transfected with blank vector alone were subtracted from mean fluorescence intensities of all other expression conditions. All mock-subtracted fluorescence intensities were normalized to the mock-subtracted fluorescence intensity of the 1 μg α1 : 1 μg β2 : 0.1 μg δ^{HA} expression condition.

was transfected. Interestingly, the total cellular expression patterns of $\gamma 2L^{HA}$ and δ^{HA} subunits themselves were somewhat different from their surface expression patterns. Here, $\gamma 2L^{HA}$ subunit levels peaked when 3 μg rather than 1 μg of cDNA was transfected, and levels declined from that peak by about 25% rather than 80% when 10 μg of cDNA was transfected. Whereas δ^{HA} subunit surface levels peaked when 0.03 μg of cDNA was transfected and declined by about 75% when 1 μg of cDNA was transfected, δ^{HA} total cellular levels increased over the entire range of cDNA amounts.

These results suggest the following conclusions. First, the fact that there was a range of $\gamma 2L^{HA}/\delta^{HA}$ subunit cDNA amounts that produced no change in α1 subunit levels, a decrease in β2 subunit levels, and an increase in $\gamma 2L^{HA}/\delta^{HA}$ subunit levels implies that both γ2L and δ subunits preferentially replaced β2 subunits in surface receptors. Because (1) neither α1 nor β2 subunits reached the cell surface at substantial levels when transfected alone (Figure 1), (2) $GABA_A$ receptors are pentameric[347], and (3) each receptor has two GABA binding sites, both located at β-α interfaces[348], these patterns of subunit surface expression suggest that binary α1β2 receptors contain two α and three β subunits, and that γ and δ subunits replace one of the β subunits in ternary αβγ or αβδ receptors. Second, surface levels of all subunits declined after $\gamma 2L^{HA}/\delta^{HA}$ subunit levels peak, and α1 and β2 subunit levels in particular were low at the highest tested amounts of $\gamma 2L^{HA}/\delta^{HA}$ subunit cDNA. At these high levels of $\gamma 2L^{HA}$ and δ^{HA} subunit cDNA (> 1 μg $\gamma 2L^{HA}$ and > 0.3 μg δ^{HA}), there was also considerable cell death. Comparable levels of cell death were not seen in plates of cells treated with equal levels of transfection reagent alone or with transfection reagent plus blank pcDNA vector. Taken together, these observations indicate that high levels of $GABA_A$ receptor subunit cDNA could impair both receptor trafficking and necessary cellular functions. Further investigation will be required to identify the mechanism(s) responsible for these observations. It will be interesting to determine if, for instance, large amounts of $GABA_A$ receptor subunits might exceed assembly capacity, thus causing ER retention, ER stress, and eventually apoptosis. Finally, far less δ^{HA} than $\gamma 2L^{HA}$ cDNA was required to

produce similar patterns and expression levels of all subunits. Once again, this complicates the relatively simple question of whether or not γ subunit-containing and δ subunit-containing receptors assemble similarly or not. The fact that both are incorporated at the expense of β subunits suggests that they do, while the stark difference in efficiency suggests that they may not.

Low levels of both γ2L and δ subunits could eliminate the functional signature of α1β2 receptors, but isoform populations may not become homogeneous.

Frequently, the goal of heterologous expression studies involves identifying and characterizing properties of a particular receptor isoform (e.g., α1β2γ2). Kinetic analysis, in particular, will be most accurate if the receptor population is homogeneous. Thus, most disagreement regarding proper transfection ratios of subunit-encoding nucleic acids focuses on achieving homogeneity. Because αβ receptors are expressed quite efficiently (Figure 1), some groups consider it necessary to transfect γ (or δ/ε/θ) subunit-encoding amino acids in excess (e.g. 1:1:10 μg of α:β:γ cRNA)[345, 346] to achieve a homogeneous ternary receptor population. In contrast, other groups have found that the functional signature of α1β2 receptors (e.g., small single channel conductance, small current amplitude, slow current rise time, extensive fast desensitization, and slow deactivation) can be eliminated with equimolar cotransfection of the γ2 subunit[168, 276]. Finally, the subunit expression titrations presented here (Figure 3) suggest that significantly lower levels of δ subunits, in particular, would eliminate the α1β2 receptor population.

To test the hypothesis that low levels of γ2/δ subunit cDNA could eliminate the functional signatures of α1β2 receptors, HEK293T cells were transfected with 1 μg each of α1 and β2 subunit cDNA together with 0.01 – 10 μg of γ2 or δ subunit cDNA (for all conditions, both γ2 splice variants were compared; no significant differences were found, and data from the γ2S variant are presented here). GABA was applied for 4 seconds and whole-cell currents were recorded and analyzed for peak amplitude and macroscopic kinetic properties including rise time,

extent of desensitization, and time of deactivation (Figure 4). It should be noted that all experiments were conducted with the electrophysiologist blinded to transfection conditions, but this proved impossible for cells transfected with the highest tested levels of γ2 (10 μg) or δ (1 μg) cDNA due to widespread cell death and abnormal morphology. Furthermore, the effects of > 1 μg of δ subunit cDNA could not be tested due to nearly universal death and poor membrane integrity of surviving cells.

For the most part, very low levels of γ2 subunit cDNA did produce significant changes in macroscopic current properties. In these experiments, cells transfected with only α1 and β2 subunit cDNAs had peak current amplitudes of 814 ± 266 pA (n = 14) (Figure 4B). Surprisingly, adding only 0.01 μg of γ2 subunit cDNA significantly increased peak current amplitude to 3510 ± 682 pA (n = 17, $p < 0.05$). Higher γ2 subunit cDNA levels yielded similar increases in current amplitudes; all γ2 subunit cDNA amounts from 0.01 – 3 μg produced currents that were significantly larger than α1β2 currents. The largest current occurred in the 1:1:0.3 μg transfection condition, which produced a peak current amplitude of 5866 ± 761 pA (n = 14, $p < 0.001$ compared to α1β2). However, none of these amplitudes was significantly different from that seen in the 1:1:1 μg transfection condition, despite the fact that $\gamma 2L^{HA}$ subunit surface levels in the 1:1:0.1 μg transfection condition were only about 15% of those in the 1:1:1 μg transfection condition. Interestingly, there was a trend toward decreasing amplitude with high γ2 subunit cDNA amounts. For the 1:1:10 μg transfection condition, peak current amplitude was only 2870 ± 480 pA (n = 21), which was 40% lower than the peak current amplitude seen in the 1:1:1 μg transfection condition (4530 ± 483 pA, n=25). Despite this striking trend, peak current amplitudes of the 1:1:10 condition did not differ significantly from the peak current amplitude of any other experimental condition. Nonetheless, these data suggest that high levels of γ2 subunit cDNA might promote formation of an unusual receptor population.

It is somewhat understandable that a small αβγ receptor population could greatly increase current amplitude compared to a homogeneous αβ receptor population; due to various

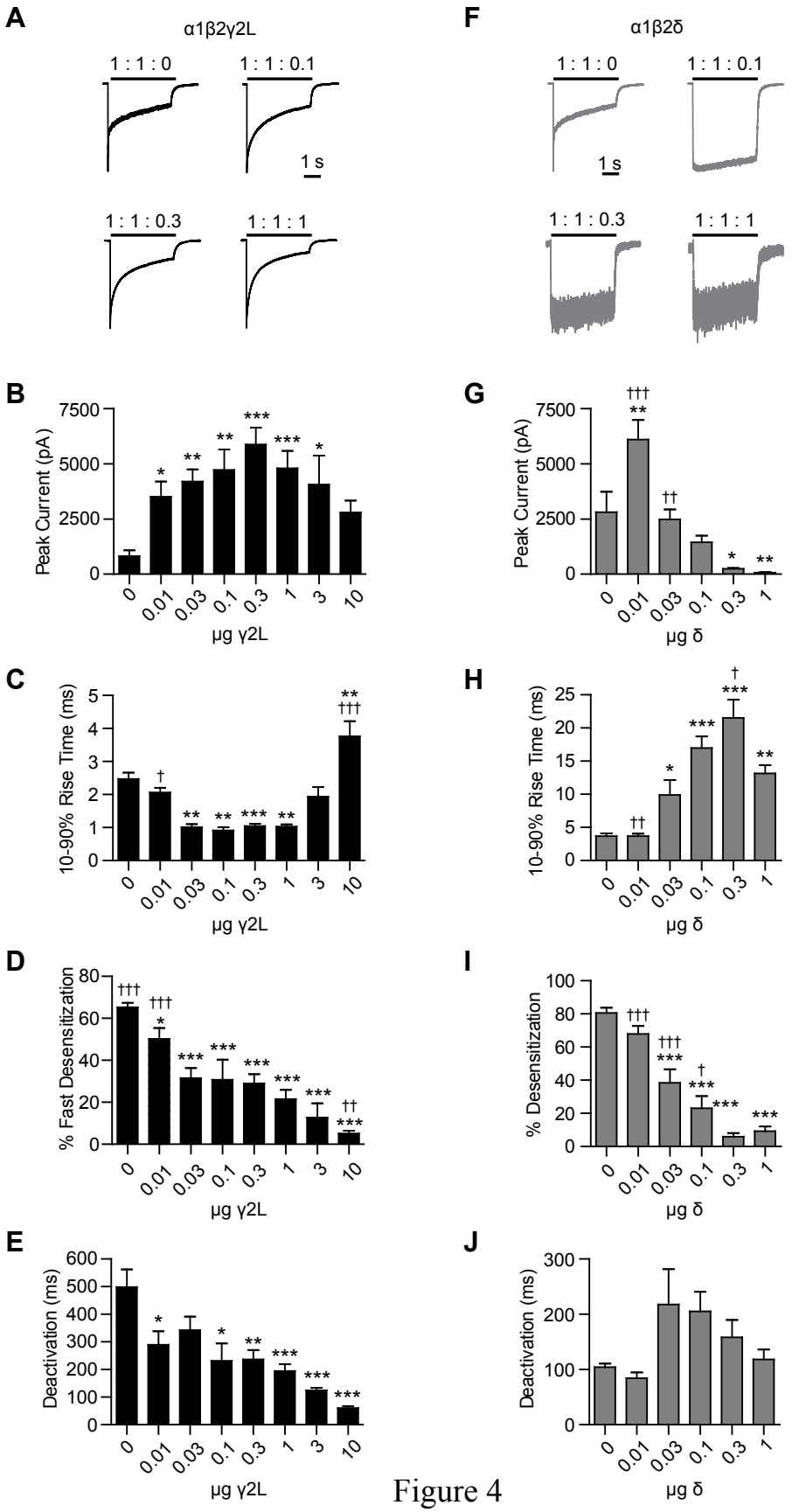
A
α1β2γ2L
1 : 1 : 0
1 : 1 : 0.1
1 s
1 : 1 : 0.3
1 : 1 : 1
F
α1β2δ
1 : 1 : 0
1 : 1 : 0.1
1 s
1 : 1 : 0.3
1 : 1 : 1
B
Peak Current (pA)
7500
5000
2500
0
0
0.01
0.03
0.1
0.3
1
3
10
µg γ2L
G
Peak Current (pA)
7500
5000
2500
0
0
0.01
0.03
0.1
0.3
1
µg δ
C
10-90% Rise Time (ms)
5
4
3
2
1
0
µg γ2L
H
10-90% Rise Time (ms)
25
20
15
10
5
0
µg δ
D
% Fast Desensitization
80
60
40
20
0
µg γ2L
I
% Desensitization
100
80
60
40
20
0
µg δ
E
Deactivation (ms)
600
500
400
300
200
100
0
µg γ2L
J
Deactivation (ms)
300
200
100
0
µg δ

Figure 4

Figure 4. GABA-evoked currents recorded from cells coexpressing α1, β2, and low levels of γ 2 and δ subunit cDNA had kinetic properties different from those of cells expressing only α1 and β2 subunits.

GABA (1 mM; 4s) was applied to HEK293T cells transfected with 1 μg α1, 1 μg β2, and varying amounts of γ2L **(A-E)** or δ **(F-J)** subunit cDNA. Whole-cell currents were recorded and analyzed to determine peak current amplitude **(B, G)**; 10-90% rise time **(C, H)**; percent fast desensitization **(D)** or overall desensitization (I) over 4 s from peak amplitude; and weighted time constant of deactivation **(E, J)**. Representative currents from a subset of transfection conditions are presented in panels A and F.

microscopic kinetic properties, αβγ receptors yield about seven times the charge transfer of αβ receptors. Consequently, if adding 0.01 μg of $\gamma 2L^{HA}$ subunit cDNA converted 15% of surface α1β2 receptors into α1β2γ2L receptors, current amplitude would be expected to increase by approximately 90%. It is possible, however, that macroscopic kinetic properties of αβ receptors would not be obscured. Thus, currents obtained from each of these transfection conditions were analyzed for rise time, percent desensitization, and weighted deactivation times constants.

These macroscopic current kinetic properties further supported the hypothesis that low levels of γ2 cDNA were sufficient to eliminate or greatly reduce the αβ receptor population. The average 10-90% rise time (Figure 4C) of α1β2 receptor currents was 2.47 ± 0.19 ms (n = 14). This remained similar for the 1:1:0.01 μg transfection condition (2.23 ± 0.15 ms, n = 13), but decreased significantly for the 1:1:0.03 μg transfection condition (1.00 ± 0.10 ms, n = 9, $p < 0.01$). Rise times were similar (approximately 1 ms) when 0.03 – 1 μg of γ2 subunit cDNA was transfected, but trended upward when γ2 cDNA was used in excess. At 1:1:3 μg, the 10-90% rise time was 1.79 ± 0.31 ms (n = 5), nearly slightly slower than that of the 1:1:1 μg transfection condition (1.48 ± 0.13 ms, n = 15), though this difference did not reach significance. However, the 1:1:10 μg transfection condition yielded rise times dramatically longer than any other condition (3.48 ± 0.47 ms, n = 18; $p < 0.05$ compared to 1:1:0 and $p < 0.001$ compared to 1:1:1), again suggesting that abnormal isoforms might assemble when high levels of γ2 subunit cDNA are used.

According to most reports, αβ and αβγ receptor isoforms both desensitize extensively, but αβ isoforms desensitize more rapidly. To determine if a shift from α1β2 to α1β2γ2 receptor populations could be detected by changes in desensitization kinetics, 1 mM GABA was applied for 4 s to transfected cells and the desensitization time course of resulting currents was fitted with up to four exponential components (i.e., time constants; τ). The percent of all desensitization contributed by the two shorter components (τ1 and τ2) was summed and defined as fast desensitization (Figure 4D). For α1β2 receptors, 65% of all desensitization was contributed by τ1

and τ2, and this fraction dropped significantly when 0.01 μg of γ2 subunit cDNA was coexpressed (50 ± 5%, $p < 0.05$). Only 0.03 μg of γ2 subunit cDNA was necessary to reduce fast desensitization to levels statistically indistinguishable from those produced by 1 μg of γ2 subunit cDNA (32 ± 5% and 23 ± 5%, respectively). Interestingly, 10 μg of γ2 subunit cDNA reduced fast desensitization further, to a level that was significantly lower than 1 μg (5 ± 1%, $p < 0.01$). Thus, similar to the results for current rise time, the percentage of fast desensitization indicated that low levels of γ2 subunit cDNA were sufficient to produce kinetic properties different from those of α1β2 receptors, but high levels of γ2 subunit cDNA changed kinetic properties again, suggesting that a different receptor population may exist when γ2 subunit cDNA is transfected above equimolar amounts.

The weighted time constant of deactivation (Figure 4E) also changed dramatically in response to the amount of γ2L subunit cDNA that was transfected (see Methods for calculation details). Specifically, when more γ2L subunit cDNA was transfected, currents deactivated more rapidly (i.e., the deactivation time constant decreased). For instance, the 1:1:0 μg transfection condition produced currents with a deactivation time constant of 498 ± 64 ms, while the 1:1:1 μg transfection condition produced currents with a deactivation time constant of 163 ± 27 ms and the 1:1:10 μg transfection condition produced currents with a deactivation time constant of 68 ± 8 ms. In contrast to the patterns seen with current amplitude or rise time, deactivation accelerated rather steadily throughout the tested range of γ2L subunit cDNA levels, suggesting that the receptor population might not become homogeneous even when γ2L subunit cDNA is used in considerable excess. In general, however, the macroscopic current properties of α1β2γ2L receptors seemed to indicate that low γ2L subunit levels could obscure the functional properties of α1β2 receptors, but receptor subunit composition might change again at very high γ2L subunit levels.

Results from δ subunit titrations (Figure 4F-J) were similar but slightly more complex. GABA was applied for 4 s to HEK293T cells transfected with 1 μg each of α1 and β2 subunit

cDNA and 0 – 1 μg of δ subunit cDNA, and the resulting currents were analyzed for peak current amplitude (Figure 4G), 10-90% rise time (Figure 4H), percent desensitization (Figure 4I), and time constant of deactivation (Figure 4J). In these experiments, cells expressing only α1 and β2 subunits produced currents with peak amplitudes of 2811 ± 921 pA (n = 7). When 0.01 μg of δ subunit cDNA was included, peak current amplitudes increased significantly to 6099 ± 880 pA (n = 6, $p < 0.01$ compared to 1:1:0 μg condition), but when 0.03 μg of δ subunit cDNA was included, peak current amplitude was only 2477 ± 453 pA (n = 8) – nearly indistinguishable from the 1:1:0 μg condition. When still more δ subunit cDNA was included, peak current amplitudes continued to decline, and equimolar transfection yielded peak current amplitudes of only 68.8 ± 24.1 pA (n = 6, $p < 0.01$ compared to 1:1:0 μg condition). Theoretically, these small currents could have been produced by abnormal receptor isoforms that assembled due to high δ subunit levels, but it seems more likely that the small current amplitudes reflected the remarkably low subunit surface levels that were observed when 1 μg each of α1, β2, and δ subunit cDNA were transfected (Figures 1 and 3). Given that the 1:1:0.3 and 1:1:1 μg α1β2δ currents were so small, all subsequent kinetic analysis should be interpreted with caution. Additionally, it should be noted that similarly low subunit surface levels were present in cells transfected with 1:1:10 α1β2γ2, but current amplitudes remained relatively high (2800 ± 528 pA). This discrepancy likely occurred because αβγ receptors produce larger currents than αβδ receptors, allowing current amplitude to compensate partially for the sharp decrease in surface levels.

As δ subunit cDNA levels increased, 10-90% rise times became significantly slower. When only α1 and β2 subunits were transfected, currents had an average rise time of 3.7 ± 0.4 ms (n = 7), but when 0.03 μg of δ subunit cDNA was included, average rise time slowed to 9.9 ± 2.2 ms (n = 8, $p < 0.05$ compared to 1:1:0 transfection condition). The slowest rise times were observed in the 1:1:0.3 transfection condition, in which average rise time was 21.5 ± 2.7 ms (n = 5, $p < 0.001$ compared to 1:1:0 transfection condition). Interestingly, this was also significantly slower ($p < 0.05$) than average rise time in the 1:1:1 transfection condition (13.1 ± 1.2 ms, n = 6),

again suggesting that high transfection levels might not produce a homogeneous receptor population.

It is commonly accepted that αβ receptor currents desensitize far more extensively than αβδ receptor currents [168]. In agreement, higher levels of δ subunit cDNA generally were correlated with lower desensitization percentage; in the 1:1:0 μg transfection condition, currents desensitized by 80.5 ± 3.2% (n = 7), while in the 1:1:1 μg transfection condition, currents desensitized by only 9.2 ± 3.0% (n = 6). In all conditions other than 1:1:0.01 μg, desensitization percentage was significantly different than that of the 1:1:0 μg condition ($p < 0.001$). However, all conditions other than 1:1:0.3 μg also desensitized differently than the 1:1:1 μg condition. Taken together, these data suggested that 0.03 μg of δ subunit cDNA was sufficient to greatly reduce current desensitization (i.e., to reduce the α1β2 receptor population), but that ≥ 0.3 μg of δ subunit cDNA might be necessary to achieve homogeneity. However, as previously stated, the exceptionally small amplitude of the currents recorded from the 1:1:0.3 μg and 1:1:1 μg transfection conditions could render these observations suspect.

Finally, the time course of channel deactivation was fitted for all transfection conditions and weighted deactivation time constants were calculated. In previous studies, α1β3 and α1β3δ receptors deactivated at similar rates[168], so it was perhaps unsurprising that there were no significant differences in deactivation time constants among all transfection conditions. There was a trend toward slower deactivation when ≥ 0.03 μg of δ subunit cDNA was transfected (217.5 ± 64.2 ms, n = 8) compared to α1 and β2 subunits alone (104 ± 6.8 ms, n = 6), but substantial variability obscured any significance.

Taken together, the electrophysiological data obtained from cells transfected with 1 μg α1 and β2 subunit cDNA and 0 – 1 μg of δ subunit cDNA did not indicate a point at which a homogeneous α1β2δ receptor population appeared. However, all kinetic parameters were significantly different from those of α1β2 receptors when only 0.03 μg of δ subunit cDNA was cotransfected with α1 and β2 subunits. Furthermore, higher levels of δ subunit cDNA produced

such small currents (likely due to extremely low subunit surface levels) that kinetics were difficult to interpret; thus, the continual changes in kinetic parameters might not indicate that increasing δ subunit levels continually changed receptor stoichiometry. Consequently, these data support but do not confirm the hypothesis that low levels of δ subunit cDNA are sufficient to eliminate α1β2 receptor populations.

Low γ2 subunit cDNA levels were sufficient to produce pharmacological signatures of αβγ receptor isoforms.

αβ and αβγ receptor isoforms can be distinguished pharmacologically in two different ways. First, αβ, but not αβγ, receptor currents are strongly inhibited by Zn^{++} [349]. In contrast, αβ receptors are insensitive to diazepam (DZP), which binds to the interface between α and γ subunits and thereby enhances αβγ receptor GABA-evoked currents[182, 255]. (Of note, αβδ receptors are partially Zn^{++}-sensitive and entirely DZP-insensitive, so these techniques are not useful for differentiating αβ and αβδ receptors.) To determine how much γ2 subunit cDNA was necessary to produce a Zn^{++}-insensitive receptor population, peak current amplitude in response to GABA (1 mM, 4 s) was recorded (I_{max}(GABA)), Zn^{++} (10 μM) was pre-applied for 10 seconds, and peak current amplitude was recorded again while GABA and Zn^{++} were co-applied (I_{max}(GABA+Zn^{++})). Zn^{++} inhibition was quantified by dividing I_{max}(GABA+Zn^{++}) by I_{max}(GABA) (Figure 5A). As expected, cells transfected with only α1 and β2 subunits produced currents that were inhibited strongly by Zn^{++} co-application (peak current amplitude was 19 ± 1% of those evoked by GABA alone.) When 0.01 or 0.03 μg of γ2 subunit cDNA was included, peak current amplitude was partially Zn^{++} sensitive (32 ± 13 and 84 ± 9% of I_{max}(GABA), respectively; $p < 0.001$ compared to αβ). Surprisingly, when ≥ 0.1 μg of γ2 subunit cDNA was included, peak current amplitude was maximally Zn^{++} insensitive, again suggesting that low γ2 subunit levels are sufficient to produce currents that functionally resemble α1β2γ2 receptor currents.

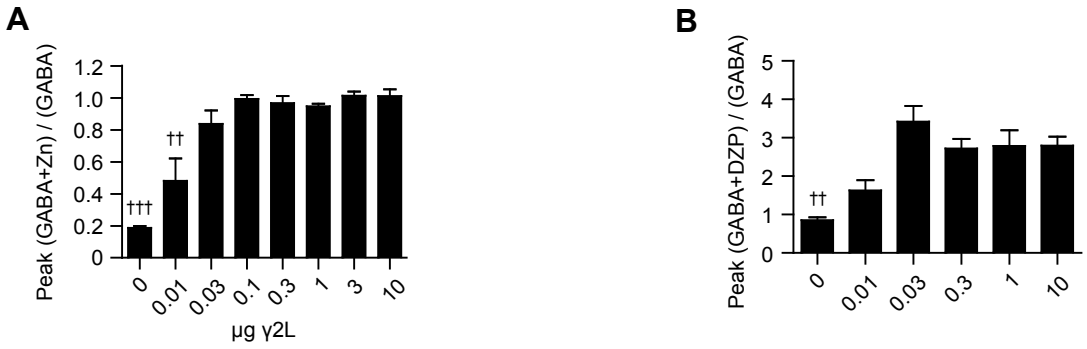

Figure 5: Low levels of γ2 subunit cDNA were sufficient to produce Zn++-insensitive and DZP-sensitive currents.

A. HEK293T cells transfected with 1 µg α1, 1 µg β2, and varying amounts of γ2L subunit cDNA were pre-treated (10 s) with Zn++ (10 µM) and currents were recorded during a 4 s co-application of GABA (1 mM) and Zn++ (10 µM). Zn++ resistance was calculated by dividing the peak current amplitude in response to GABA + Zn++ by the peak current amplitude in response to GABA alone. **B.** Currents were recorded from HEK293T cells transfected with 1 µg α1, 1 µg β2, and varying amounts of γ2L subunit cDNA during a 4 s co-application of GABA (~EC20) and DZP (1 µM). DZP enhancement was calculated by dividing the peak current amplitude in response to GABA + DZP by the peak current amplitude in response to GABA alone.

As mentioned previously, αβγ receptors are inhibited by Zn^{++} but enhanced by DZP. To determine how much γ2 subunit cDNA was necessary to produce a DZP sensitive receptor population, the percent enhancement of ~EC_{20} GABA-evoked peak current amplitude by 1 μM DZP was evaluated. Even 0.01 μg of γ2 subunit cDNA permitted substantial DZP potentiation of peak current amplitude (134 ± 13% of control current), and 0.03 μg was sufficient to produce potentiation (204 ± 18%) indistinguishable from 1 μg (260 ± 26%) or 10 μg (257 ± 56%). In summary, both of the pharmacological methods that most reliably differentiate αβ and αβγ receptors indicated that remarkably low levels of γ2 subunit cDNA are necessary to produce α1β2γ2 receptors.

$GABA_A$ receptor δ^{HA} subunits had nearly identical patterns of subunit adjacency compared to $\gamma2L^{HA}$ subunits when transfected at ten-fold lower levels.

The data presented thus far revealed several interesting differences between γ2L and δ subunits. First, the presence of both α1 and β2 subunits was required for surface expression of α1, β2, or $\gamma2L^{HA}$ subunits, but δ^{HA} subunits reached the surface without regard to coexpressed subunits. Second, equimolar transfection of α1, β2, and $\gamma2L^{HA}$ subunits produced far higher surface levels of all subunits than equimolar transfection of α1, β2, and δ^{HA} subunits, but both $\gamma2L^{HA}$ and δ^{HA} subunits seemed to be expressed and trafficked at the expense of β2 subunits. When increasing amounts of either $\gamma2L^{HA}$ or δ^{HA} subunit cDNAs were cotransfected with 1 μg each of α1 and β2 subunit cDNAs, maximal surface expression of all subunits occurred with 1 μg of $\gamma2L^{HA}$ but only 0.03 μg of δ^{HA} subunit cDNA. Beyond this point, α1 subunit levels began decreasing sharply, while β2 subunit levels began decreasing with even the smallest amount of $\gamma2L^{HA}$ or δ^{HA} subunit cDNA that was transfected. Finally, patch clamp recording suggested that low levels of $\gamma2L^{HA}$ or δ^{HA} subunit cDNA could eliminate the physiological signatures of α1β2 receptor isoforms (i.e., produce αβγ/αβδ receptor populations), but very high levels of $\gamma2L^{HA}$ or

δ^{HA} cDNA might produce receptors with yet another, different stoichiometry, particularly for $\alpha1\beta2\gamma2L^{HA}$ receptors.

As previously mentioned, it is commonly thought that γ and δ subunits are essentially interchangeable in receptor assembly; i.e., that receptor stoichiometry and arrangement are γ/δ-β-α-β-α, anticlockwise as viewed from the synaptic cleft[350]. However, more recent studies using have suggested that δ subunit-containing receptors may assemble in multiple different ways[351]. Both conclusions have been drawn mostly from functional characterization of receptors assembled from concatenated subunits, which artificially constrain subunit arrangement. One goal of the present study was to determine if these two isoforms assemble similarly or differently when native subunits are used. As discussed in Chapter II, patterns of subunit adjacency could help answer this question.

Fluorescence resonance energy transfer (FRET) is an established methodology for monitoring protein-protein interactions[336]. In contrast to conventional biochemical techniques (e.g., co-immunoprecipitation), FRET can be used to monitor proteins in their native conformations and to identify direct protein interactions. Although FRET can be measured by spectrofluorimetry and microscopy, flow cytometry offers several advantages over these techniques. Unlike spectrofluorimetry, measurements can be performed in individual cells, and importantly, donor emission can easily be distinguished from sensitized emission of the acceptor. While microscopy allows the subcellular localization of protein interactions to be evaluated, the technique is less sensitive, analysis is labor intensive and poorly quantitative, and selecting regions of interest is highly subjective. Flow cytometry, in contrast, allows for rapid, quantitative, and unbiased analysis of FRET in large cell populations, and permits the simultaneous analysis of other cellular properties (e.g., viability).

Based on homology modeling to nAChRs, $GABA_A$ receptors are thought to assemble into pseudo-symmetrical pentamers[158]. As a result, each subunit is predicted to have two "adjacent" subunits and two "non-adjacent" subunits. The amino termini (where our subunit- and epitope-

specific antibodies bind) of adjacent subunits are separated by ~50 Å, while those of non-adjacent subunits are separated by ~80 Å. Since FRET efficiency is inversely proportional to the sixth-power of distance[336], careful selection of fluorophores should allow for exclusive monitoring of subunit adjacency. For example, the Alexa-555 and Alexa-647 fluorophore pair has a Forster radius (the distance at which FRET efficiency is 50% of maximum) of 51 Å (www.invitrogen.com), meaning that non-adjacent subunits should contribute minimally to the FRET signal.

To determine if identical subunits were adjacent in α1β2, α1β2γ2L, or α1β2δ receptors, one subunit was HA-tagged at a time (e.g., $\alpha1^{HA}\beta2$), and the resulting receptors were stained with the HA-A555 / HA-647 antibody mixture. For α1β2 receptors (top row), FRET was observed between individual α1 subunits (Figure 6, left column) and individual β2 subunits (Figure 6, middle column). Addition of 1 μg of the γ2L subunit (Figure 6, middle row) or 0.1 μg of the δ subunit (Figure 6, bottom row) produced essentially identical FRET patterns. In both cases, subunit addition greatly reduced FRET between individual α1 subunits and essentially eliminated FRET between individual β2 subunits. Consistent with incorporation of γ2L/δ subunits into the pentamer, FRET was also detected between α1 and γ2L/δ subunits and between β2 and γ2L/δ subunits). FRET was not detected, however, between individual γ2L or δ subunits, suggesting either that a single γ2L or δ subunit was incorporated into each pentamer or, alternatively, that two γ2L or δ subunits were incorporated but separated by either an α1 or β2 subunit. Considering the presumed stoichiometry of ternary $GABA_A$ receptors (2α:2β:1γ/δ), these results supported previous conclusions that the majority of α1β2γ2L/δ receptors were composed of alternating α1, β2, and γ2L/δ subunits. If true, then the only possible arrangements around the pentamer would be γ/δ-α-β-α-β or γ/δ-β-α-β-α (clockwise when viewed from the synaptic cleft). The FRET patterns also suggest that α1β2 receptors have a similar arrangement, with the γ2L/δ subunit position being occupied by either α1 or β2 subunits.

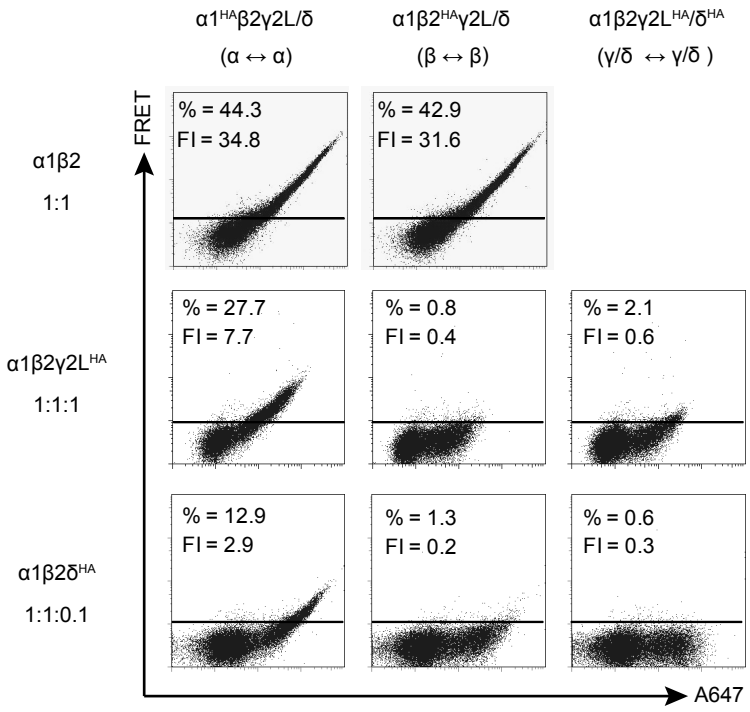

Figure 6. Flow cytometric analysis of GABAA receptor γ2L^{HA} or δ^{HA} subunit FRET with partnering α1 and β2 subunits when transfected at "expression-equivalent" levels suggested that γ2L^{HA} and δ^{HA} subunits assembled in similar patterns.

HEK293T cells were transfected with 1 μg of α1 subunit cDNA, 1 μg of β2 subunit cDNA, and either blank pcDNA vector or the amount of γ2L^{HA} or δ^{HA} subunit cDNA that achieved maximal expression (Figure 3). The α1 and β2 subunit cDNAs were cotransfected with 1 μg pcDNA vector (top row), 1 μg γ2L^{HA} subunit cDNA (middle row), or 0.1 δ^{HA} cDNA + 0.9 μg pcDNA vector (bottom row). To determine subunit adjacency, each subunit was individually HA-tagged and cells were incubated with both anti-HA-Alexa555 and anti-HA-Alexa647 before being subjected to flow cytometry. The left column presents α1-α1 subunit adjacency (α1 HA-tagged); the middle column presents β2-β2 subunit adjacency (β2 HA-tagged); and the right column presents γ2L-γ2L or δ-δ subunit adjacency. For all dot plots, the x-axis indicates fluorescence intensity of the acceptor fluorophore (Alexa 647), while the y-axis indicates fluorescence intensity of the FRET channel (excitation of Alexa 555 and emission of Alexa 647). The horizontal line indicates the FRET threshold (see Methods) and the percentage of cells emitting above this threshold is listed at the top of each dot plot.

The ten-fold difference in $GABA_A$ receptor $\gamma2L^{HA}$ and δ^{HA} subunit total cellular expression persisted in the absence of partnering subunits.

The phenomenon observed in Fig. 3 (peak subunit protein expression at tenfold lower levels of δ compared to γ2L subunit cDNA) could result from different levels of subunit synthesis/degradation or from more efficient incorporation of δ subunits into $GABA_A$ receptors. However, the FRET studies suggested that $\gamma2L^{HA}$ and δ^{HA} subunits incorporated similarly into pentamers. Therefore, subunit mRNA and protein levels were evaluated in HEK293T cells transfected with varying concentrations of $\gamma2L^{HA}$ or δ^{HA} subunit cDNA alone (i.e., without α1 and β2 subunits). Because α1 and β2 subunits were necessary for full surface expression of $\gamma2L^{HA}$ and δ^{HA} subunits, these experiments should determine if the greater efficiency of δ^{HA} subunit expression was an artifact of receptor assembly or due to some intrinsic difference between the subunits themselves. To test the hypothesis that the difference between $\gamma2L^{HA}$ and δ^{HA} expression levels was a result of more efficient transcription, real-time PCR was performed on cells transfected with the same range of subunit cDNA used in the single-subunit protein studies. Transcript levels were determined by normalized difference in cycle number fold increase. As cDNA levels increased, mRNA levels for $\gamma2L^{HA}$ and δ^{HA} subunits increased similarly and proportionally (Figure 6A), indicating that equivalent amounts of $\gamma2L^{HA}$ and δ^{HA} cDNA did not produce different amounts of protein because of differences in transcription efficiency.

Next, HEK293T cells were transfected with 0.001 μg to 1 μg of $\gamma2L^{HA}$ or δ^{HA} subunit cDNA and total cellular levels of $\gamma2L^{HA}$ and δ^{HA} subunit protein were assessed using flow cytometry. Total cellular expression of δ^{HA} subunits (solid grey line) was significantly higher than that of $\gamma2L^{HA}$ subunits (solid black line) when less than 1 μg of subunit cDNA was transfected (Figure 6B); for instance, levels of δ^{HA} subunit protein levels present when 0.03 μg of δ^{HA} cDNA was transfected were nearly identical to levels of $\gamma2L^{HA}$ subunit protein when 0.3 μg of $\gamma2L^{HA}$ cDNA was transfected. Thus, the ten-fold difference in $\gamma2L^{HA}$ and δ^{HA} subunit expression levels (Figure 3) persisted in the absence of partnering subunits, suggesting that δ^{HA}

subunit cDNA was not more "potent" due to more efficient receptor assembly; rather, δ^{HA} and $\gamma2L^{HA}$ subunits might differ in efficiency of subunit production and/or degradation.

Heterologous expression is useful for basic biochemical studies because many possible confounding variables can be controlled or eliminated. However, this depends upon the design of the nucleic acid construct. For instance, if the $\gamma2L^{HA}$ coding sequence and untranslated regions were significantly longer than those of the δ^{HA} subunit, then equimolar amounts of plasmid DNA might not represent equimolar amounts of subunit cDNA. Full sequencing confirmed that the $\gamma2L^{HA}$ and δ^{HA} subunit inserts (translated and untranslated sequences) were approximately the same length; however, the sequences of their immediate 5' untranslated regions differed slightly. This could be problematic, because the three base pairs preceding and two base pairs following a start codon constitute the Kozak sequence, which contributes to the efficiency of translation initiation. Specifically, ribosome binding is strongly enhanced by the presence of purines at the -3 and +4 positions with respect to the start codon[352]. In our cDNA constructs, the Kozak sequence of $\gamma2L^{HA}$ subunit cDNA was TCC(AUG)A, while the corresponding sequence in δ^{HA} subunit cDNA was GCC(AUG)G; consequently, the δ^{HA} subunit would be predicted to be translated more efficiently than the $\gamma2L^{HA}$ subunit. To rule out the possibility that the previous observations were due to this difference in cDNA sequence, the Kozak sequences were swapped. That is, plasmids were engineered such that the $\gamma2L^{HA}$ construct contained the Kozak sequence GCC(AUG)G and the δ^{HA} construct contained the Kozak sequence TCC(AUG)G ($\gamma2L(T\text{-}3G)^{HA}$ and $\delta(G\text{-}3T)^{HA}$, respectively).

The single-subunit titration experiments were repeated using the $\gamma2L(T\text{-}3G)^{HA}$ and $\delta(G\text{-}3T)^{HA}$ constructs. Surprisingly, the Kozak sequence mutations had little effect on subunit expression levels; there was no significant difference between $\gamma2L^{HA}$ (Figure 7, solid black line) and $\gamma2L(T\text{-}3G)^{HA}$ (Figure 7, dotted black line) or between δ^{HA} (Figure 7, solid grey line) and $\delta(G\text{-}3T)^{HA}$ (Figure 7, dotted grey line) subunit levels at any tested amount of subunit cDNA. Therefore, it seemed that the ten-fold difference in $GABA_A$ receptor $\gamma2L^{HA}$ and δ^{HA} subunit

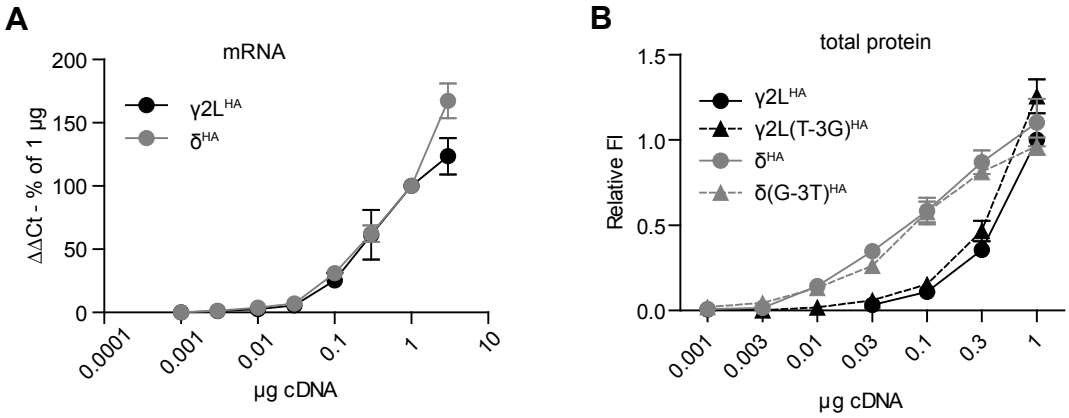

Figure 7. The ten-fold difference in total cellular expression of γ2L^{HA} and δ^{HA} subunit protein persisted in the absence of partnering subunits and was not due to different rates of transcription or translation.

A. RNA was extracted from HEK293T cells transfected with 0.001-3 µg of γ2L^{HA} (black line) or δ^{HA} (grey line) cDNA and relative mRNA levels of each subunit were determined by real-time PCR. The x-axis indicates the amount of subunit cDNA transfected, and the y-axis indicates the ΔΔCt for subunit RNA normalized to the value for 1 µg cDNA. All mRNA levels were normalized to housekeeping genes. **B.** Flow cytometry was used to detect total cellular levels of γ2L^{HA} (solid black line) and δ^{HA} (solid grey line) subunits when 0.001 – 3 µg of subunit cDNA was transfected in the absence of partnering α1 and β2 subunits. To determine if translation initiation due to Kozak sequences could affect subunit expression levels, the experiments were repeated after the Kozak sequences were swapped (γ2L(T-3G)^{HA}, dashed black line; δ(G-3T)^{HA}, dashed grey line). All mock-subtracted fluorescence intensities were normalized to that of cells transfected with 1 µg of γ2L^{HA} subunit cDNA.

expression did not result from differences in subunit synthesis at either the stage of transcription or translation initiation.

The ten-fold difference in $GABA_A$ receptor $\gamma2L^{HA}$ and δ^{HA} subunit expression could not be explained fully by different rates of synthesis or by degradation of newly-synthesized subunits.

Because receptor assembly, transcription efficiency, and translation initiation were not responsible for the disparity in $\gamma2L^{HA}$ and δ^{HA} subunit protein levels, it stood to reason that something further along the biogenic pathway could explain that difference. Although *initiation* of protein synthesis did not seem to differ between the two subunits, it is possible that the subsequent *rate* of protein synthesis differed significantly and thus was responsible for the higher levels of δ subunit protein. To assess the rate of protein synthesis, HEK293T cells transfected with 1 μg of either $\gamma2L^{HA}$ or δ^{HA} subunit cDNA were incubated for 0-20 min in media containing 150 μCi/mL ^{35}S-methionine (Figure 8A). At 5 min intervals, radiolabeled $GABA_A$ receptor subunit protein was precipitated by incubation with anti-HA beads. After elution, protein was subjected to SDS-PAGE and exposed to a phosphor screen. Integrated band density for each time point was calculated and normalized to the integrated band density of $\gamma2L^{HA}$ subunits that were radiolabeled for 20 min (Figure 8B). Surprisingly, it appeared that despite being engineered into identical plasmids and thus being regulated by identical promoters, δ^{HA} subunits were synthesized at a slightly faster rate than $\gamma2L^{HA}$ subunits. When levels at each time point were directly compared, δ^{HA} subunit levels were significantly greater than $\gamma2L^{HA}$ subunit levels at the 5, 10, and 15 min time points ($p < 0.01$ for all). In contrast, when the synthesis curves were fitted using a mixed procedure model produced in consultation with the Vanderbilt University Department of Biostatistics, the estimated difference in the synthesis curve slopes was not significantly different ($p = 0.099$). Although somewhat difficult to interpret, these data suggested that different rates of synthesis could contribute to the disparity in subunit levels, but other factors such as subunit degradation likely contribute as well.

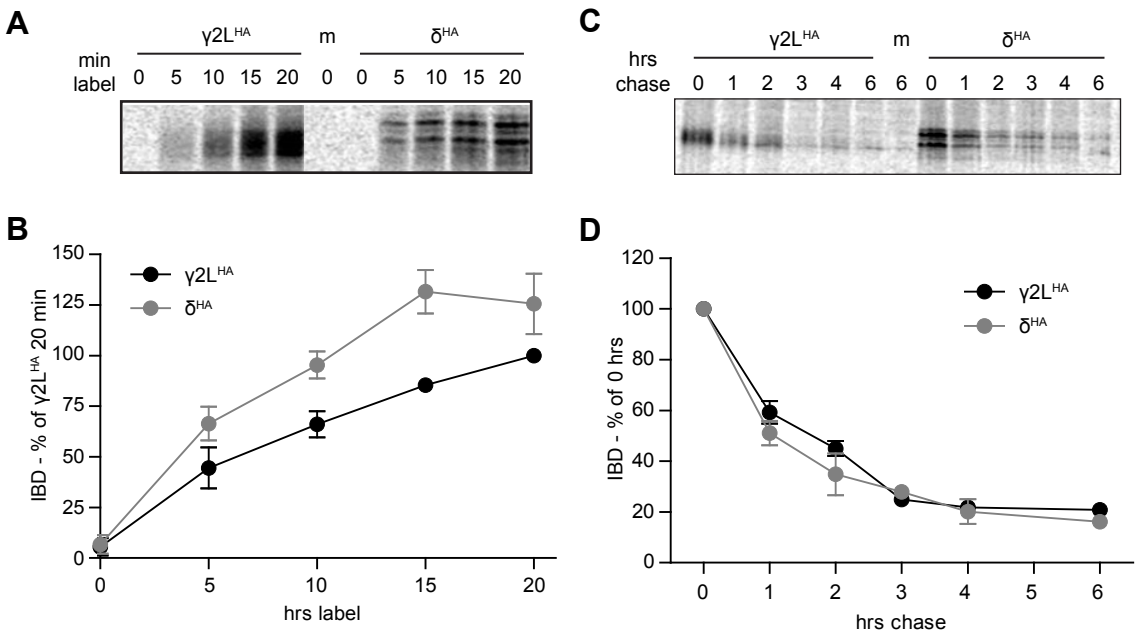

Figure 8. GABA$_A$ receptor γ2L^{HA} and δ^{HA} subunits were synthesized at similar rates, and newly-synthesized γ2L^{HA} and δ^{HA} subunits were degraded at similar rates.

Metabolic labeling was used to assess the synthesis and degradation rates of γ2L^{HA} and δ^{HA} subunits. **A.** HEK293T cells expressing equivalent amounts of γ2L^{HA} or δ^{HA} subunits were cultured for 0 – 20 min in media containing 35S-methionine. Subunit protein was isolated from cell lysates by immunoprecipitation and separated by SDS-PAGE. The upper panel presents a representative gel exposure, and the lower panel presents a quantification of band intensity (IDV) averaged from four separate experiments. Band intensities are normalized to that of the 20 min incubation condition. **B.** HEK293T cells expressing equivalent amounts of γ2L^{HA} or δ^{HA} subunits were cultured for 20 min in media containing 35S-methionine. To assess degradation rates of this newly-synthesized protein population, radioactive media was subsequently replaced by regular media and cells were returned to incubators for 0 – 6 hours. Subunit protein was isolated from cell lysates by immunoprecipitation and separated by SDS-PAGE. The upper panel presents a representative gel exposure, and the lower panel presents a quantification of band intensity (IDV) averaged from four separate experiments. Band intensities are normalized to that of the 0 min chase condition.

Radiolabeling was also used to determine the degradation rates of $\gamma 2L^{HA}$ and δ^{HA} subunits. HEK293T cells transfected with 1 μg of either $\gamma 2L^{HA}$ or δ^{HA} subunit cDNA were incubated for 20 min in radioactive media. Subsequently, the radioactive medium was replaced with normal culture medium, and cells were returned to the incubator. After 0, 1, 2, 3, 4, or 6 hours, $\gamma 2L^{HA}$ and δ^{HA} subunit proteins were extracted, immunoprecipitated, and processed as described above (Figure 8C). Integrated band density for each subunit was calculated and normalized to the 0 hr time point. Both subunits had a half-life of approximately 1.5 hrs and decayed with essentially identical time courses (Figure 8D). It should be noted that a similar decay course has been reported for γ2S subunits[353]. Thus, it seemed that different rates of degradation were not responsible for the differing levels of $\gamma 2L^{HA}$ and δ^{HA} subunits.

$\gamma 2L^{HA}$ and δ^{HA} subunits at steady state had markedly different rates of degradation.

To this point, it was evident that approximately tenfold less δ^{HA} than $\gamma 2L^{HA}$ subunit cDNA was required to produce equivalent amounts of protein two days after transfection and that no biogenic step was obviously responsible for the disparity. However, it is important to note that pulse-chase studies measure degradation only of protein that was synthesized during the 20-minute labeling period. This should represent only a fraction of all subunits, whereas flow cytometry measures total cellular protein. It is possible that the $\gamma 2L^{HA}$ and δ^{HA} subunit populations that were not radiolabeled could degrade differently. To determine if the entire cellular populations of $\gamma 2L^{HA}$ and δ^{HA} subunits were degraded at different rates, HEK293T cells were transfected with $\gamma 2L^{HA}$ and δ^{HA} subunit cDNA and cultured as in previous experiments, but protein synthesis was inhibited by adding 100 μg/mL cycloheximide (CHX) to the culture medium two days after transfection. Cells were cultured in the presence of CHX for 0-6 hrs before being harvested, permeabilized, incubated with antibodies, and subjected to flow cytometry. Thus, the degradation rates of the total cellular subunit populations were assessed over a 6 hour time period.

In contrast to the results obtained using radiolabeling, $\gamma 2L^{HA}$ subunits degraded significantly more quickly than δ^{HA} subunits (Figure 9A). During the first hour of treatment, both subunits decayed similarly; after one hour, $\gamma 2L^{HA}$ subunit levels (solid black line) had decreased to 77.2 ± 4.4% of 0 hr levels, while δ^{HA} subunit levels (solid grey line) had decreased to 81.9 ± 4.8% of 0 hr levels. After this point, however, degradation time courses diverged. Surprisingly, δ^{HA} subunit levels remained stable at approximately 80% of 0 hr levels (6 hrs CHX: 86.0 ± 7.1%). In contrast, after three hours of CHX treatment, $\gamma 2L^{HA}$ subunit levels were approximately half (53.8 ± 2.3%) of 0 hr levels, and they remained similar through the rest of the 6 hr treatment period (6 hrs: 49.1 ± 3.5% of 0 hr levels). However, it is important to note that $\gamma 2L^{HA}$ and δ^{HA} subunits had somewhat different cellular distributions when transfected alone. In the absence of α1 and β2 subunits, $\gamma 2L^{HA}$ subunits were mostly retained intracellularly, but many δ^{HA} subunits were trafficked to the cell surface. A substantial fraction of intracellular protein is destined for proteasomal degradation, so the different degradation rates of $\gamma 2L^{HA}$ and δ^{HA} subunits might simply reflect their different cellular distributions. If so, $\gamma 2L^{HA}$ and δ^{HA} subunits should degrade at similar rates when expressed together with α1 and β2 subunits, which enable surface trafficking of all subunits. Interestingly, coexpression of α1 and β2 subunits did not affect degradation rates of either $\gamma 2L^{HA}$ or δ^{HA} subunits. The $\gamma 2L^{HA}$ subunit population (dashed black line) had decreased by nearly half after 3 hrs of CHX application ($\gamma 2L^{HA}$ = 53.8 ± 2.3% of 0 hr; $\alpha 1\beta 2\gamma 2L^{HA}$ = 60.8 ± 9.9% of 0 hr) and then remained similar until the 6 hr time point ($\gamma 2L^{HA}$ = 49.1 ± 3.5% of 0 hr; $\alpha 1\beta 2\gamma 2L^{HA}$ = 47.7 ± 5.3% of 0 hr). Likewise, δ^{HA} levels decreased by around 20% within the first hour of treatment (1 hr: δ^{HA} = 81.9 ± 4.8% of 0 hr; $\alpha 1\beta 2\delta^{HA}$ = 85.8 ± 12.0% of 0 hr) and then remained stable until the 6 hr time point (δ^{HA} = 86.0 ± 7.1% of 0 hr; $\alpha 1\beta 2\delta^{HA}$ = 79.8 ± 10.7% of 0 hr). Thus, it seems that the different degradation rates of $\gamma 2L^{HA}$ and δ^{HA} subunits are intrinsic to the proteins themselves rather than a consequence of different subcellular distributions.

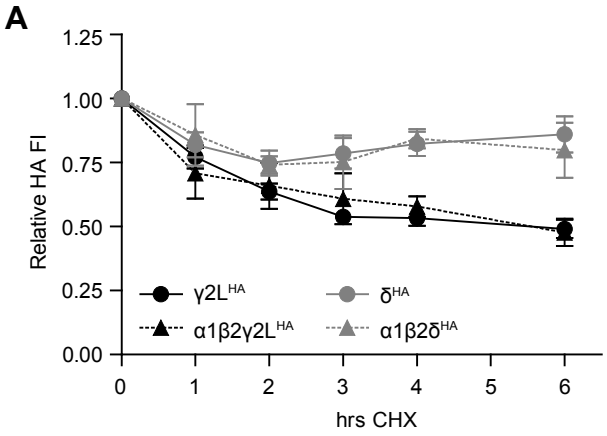

Figure 9. $GABA_A$ receptor $\gamma 2L^{HA}$ and δ^{HA} subunits had markedly different rates of degradation.

To assess degradation rates of the entire pool of $GABA_A$ receptor subunits, HEK293T cells expressing $\gamma 2L^{HA}$ or δ^{HA} subunits were incubated for 0 – 6 hours in the presence of 300 μM cycloheximide (CHX), harvested, incubated with anti-HA-Alexa647 antibody, and subjected to flow cytometry. Mock-subtracted mean fluorescence intensities from each time point were normalized to that of the same subunit at the 0 hr time point.

Discussion

The combination of flow cytometry and FRET provides an efficient, quantitative method for evaluating subunit requirements, assembly patterns, and subunit arrangement of $GABA_A$ receptor isoforms

Among ion channels, $GABA_A$ receptors are remarkable for their complexity. The nineteen subunits, many of which are coexpressed in individual neurons, could produce hundreds or thousands of unique isoforms, and most isoforms that have been studied to date display characteristic physiological and pharmacological properties. Thus, the potential functional diversity of neuronal $GABA_A$ receptors presents a fascinating and frustrating problem for researchers. To narrow the scope of the problem and to characterize individual isoforms, $GABA_A$ receptor subunits are frequently expressed in heterologous systems, but even this approach requires enormous amounts of work and has reached contradictory conclusions. Concatenated subunits provide the greatest control over assembly, but they are difficult to express, linkers must be optimized, and many concatemers may be cleaved or incorporate only partly into receptors. Traditional biochemical approaches are untenable for determining which of all possible isoforms are assembled and trafficked; furthermore, co-immunoprecipitation does not prove direct association between subunits. Similarly, it is highly inefficient to transfect hundreds of possible subunit combinations (many of which might not even reach the cell surface) and perform full physiological characterizations. Here, we showed that flow cytometry allows high-throughput, quantitative characterization of subunit expression resulting from many transfection combinations. When combined with FRET, this approach also provides insight into direct subunit adjacency and thereby helps to determine receptor stoichiometry and subunit arrangement. Even when used to evaluate the most commonly expressed and widely studied subunit combinations, these techniques revealed novel properties of $GABA_A$ receptor subunits and isoforms.

Specific subunit combinations were necessary for full expression and surface trafficking of α1, β2, and γ2L^{HA} subunits

In agreement with numerous prior studies, our results indicated that both α1 and β2 subunits were necessary for efficient surface trafficking of α1, β2, and γ2 subunits[80, 81, 89]. All three subunits were expressed without regard to subunit combination, but their total cellular expression levels were greatest when both α1 and β2 subunits were transfected. Interestingly, substantial amounts of δ subunits were expressed on the cell surface when transfected alone or with only α1 or only β2 subunits. Previously, among $GABA_A$ receptor subunits, only β1, β3, γ2S, and ρ1-3 subunits have been reported to be trafficked independently to the cell surface, ostensibly as homopentamers[90, 337, 344, 354, 355]. However, the most surprising result involved the relative subunit expression levels produced by equimolar amounts of α1, β2, and either γ2L^{HA} and δ^{HA} subunit cDNA. Although there have been previous reports that δ subunits were difficult to express, these focused on the δ subunit alone. In our experiments, α1 and β2 subunit levels were also drastically lower when coexpressed with δ^{HA} rather than γ2L^{HA} subunits, suggesting that δ subunit expression difficulties might derive from something other than insufficient δ subunit protein.

Both γ2L^{HA} and δ^{HA} subunits appeared to be incorporated into receptors at the expense of β2 subunits, but receptor stoichiometry remained ambiguous

Although γ2L^{HA} and δ^{HA} subunit expression produced markedly different subunit expression levels, similar patterns emerged. Specifically, addition of either γ2L^{HA} or δ^{HA} subunit cDNA caused a greater reduction in β2 subunit expression than in α1 subunit expression. A simple explanation for this phenomenon would be that α1β2 receptor stoichiometry is 2α:3β, and that γ2L^{HA} or δ^{HA} subunits replace the third β2 subunit. However, that interpretation contradicts the FRET patterns presented in Figure 5. When no γ2L^{HA} or δ^{HA} subunit cDNA was transfected, FRET occurred between individual α1 subunits and individual β2 subunits, as well as between α1 and β2 subunits. If FRET cannot occur either across one pentamer or between two pentamers

(possibilities that we excluded using concatenated subunits that allowed two or one epitope(s) per receptor, respectively), and receptors contain two GABA-binding β-α subunit interfaces (overwhelmingly supported by the literature), the only possible receptor population that could produce the α1β2 FRET patterns would be a mixed population of 3α:2β (α-α subunit FRET) and 2α:3 β receptors (β-β subunit FRET). This, in turn, would imply that most of the 3α:2β receptors were not affected by maximal γ2L^{HA} and δ^{HA} subunit expression, which produced only a ~10% decrease in α1 subunit surface expression. However, FRET patterns once again contradict this explanation, because FRET between individual α1 subunits decreased substantially with maximal γ2L^{HA} and δ^{HA} subunit expression.

It is also possible that FRET occurred between α1 subunits that were not incorporated into standard pentameric receptors. Unlike β2 subunits, α1 subunits appeared on the cell surface when transfected alone, potentially in homooligomers that could produce FRET. However, individual α1 subunit surface expression levels were very low (~5% of α1β2 levels). Thus, unless coexpression of partnering subunits substantially increased the α1 homooligomer population, it is quantitatively unlikely that such a population could explain the relatively stable α1 subunit expression levels. Alternatively, extra α1 subunits could be attached to α1β2/α1β2γ2L/α1β2δ receptor isoforms. A recent study proposed that γ2S subunits can modulate $GABA_A$ receptor function as an "accessory subunit" that is attached to but not incorporated within the pentamer [337]. To date, this interpretation has not been supported by microscopy, and further investigation would be necessary to determine if α1 subunits can play a similar role.

Remarkably low amounts of δ^{HA} subunit cDNA yielded peak subunit expression levels

As previously mentioned, several groups have reported difficulties expressing δ subunits[356, 357] and some have attempted to overcome that technical problem by transfecting δ subunit RNA in tenfold excess compared to α and β subunit RNAs[358]. Our γ2L^{HA}/δ^{HA} subunit titrations indicate that this approach is both unnecessary and counterproductive, because peak δ

subunit expression occurred with only 0.03 μg of δ^{HA} subunit cDNA. Equimolar expression of α1, β2, and δ^{HA} subunits produced extremely small currents that might not be suitable for kinetic analysis and, troublingly, induced cell death. Taken together, these results suggest that heterologous studies of δ subunit-containing receptors should perhaps use δ subunit cDNA at a tenfold lower rather than higher level compared to α and β subunit cDNAs. Of course, this raises the concern that αβ receptors might remain and contaminate the αβδ receptor population, but our titrations demonstrated that cells transfected with 1:1:0 or 1:1:0.1 μg (α1:β2:δ) produce currents with significantly different kinetic properties (particularly rise time and percent desensitization).

Receptor homogeneity: eliminating αβ isoforms may not be the problem

Numerous studies have been conducted under the assumption that it is impossible to obtain a homogeneous αβγ receptor population unless γ subunit cDNA is transfected in excess. Our results indicate that although $\gamma2L^{HA}$ subunit cDNA was not as "potent" as δ^{HA} subunit cDNA (and thus should not be used at similarly low levels), equimolar expression of α1, β2, and γ2L subunits should be sufficient to achieve a structurally and functionally homogeneous αβγ receptor population. Equimolar α1β2γ2L transfection yielded peak γ2L subunit expression levels as well as currents that were kinetically and pharmacologically distinct from α1β2 receptor currents. Interestingly, even though 0.1 μg of $\gamma2L^{HA}$ subunit cDNA produced relatively low $\gamma2L^{HA}$ subunit surface expression levels (39.0 ± 10.3% of 1 μg $\gamma2L^{HA}$; n = 7), the associated currents exhibited peak current amplitudes, percent fast desensitization, Zn^{++} resistance, and diazepam sensitivity that were statistically indistinguishable from those produced by equimolar expression. This likely occurred because αβγ receptors effect far greater charge transfer than αβ receptors, essentially obscuring their functional signatures. Although we do not think that a homogeneous population of α1β2γ2L receptors existed when 0.1 μg of γ2 subunit cDNA was transfected, the fact that α1β2 receptor properties were obscured even at such low γ2 subunit levels again suggests that γ2 subunits need not be expressed at tenfold molar excess.

As with δ subunits, overexpression of γ2L subunits might be deleterious as well as unnecessary. In both cases, the highest cDNA levels actually produced lower protein levels and induced cell death, suggesting that excess γ2L/δ subunit protein might divert even assembled receptors to the proteasome, perhaps due to ER stress. Indeed, it would be interesting to determine if ER-resident proteins (e.g., calnexin) or early apoptotic markers are upregulated in response to high γ2L/δ subunit cDNA levels. However, our electrophysiological data indicated that there might be yet another problem associated with excess γ2L subunit transfection. As discussed, the characteristic α1β2 receptor physiology and pharmacology disappeared with remarkably low γ2 subunit cDNA levels. However, several properties changed again when γ2 subunit cDNA was transfected in molar excess. Notably, 1:1:10 transfection produced currents with remarkably slower rise times, less fast desensitization, and more rapid deactivation than 1:1:1 transfection currents. Interestingly, the lower fraction of fast desensitization seen in 1:1:10 transfection might explain previous reports of α1β2γ2 receptor currents that desensitized minimally during 400 ms GABA application[315].

We propose that in both of these cases, currents might have been recorded from receptors containing two γ2 subunits. Although a major goal of this study was to study freely-assembled receptors, this theory would be strengthened substantially if functional double-γ receptors could be obtained from tandem constructs. Currents were recorded from cells expressing β2-α1-γ2 tandems together with α1 and γ2 monomers and from cells expressing α1-γ2 tandems together with β2 monomers. If the tandem constructs function properly, no "canonical" $GABA_A$ receptor isoform ([α/β/γ]-β-α-β-α) could be assembled in either condition. Rather, any pentamer must contain at least two γ2 subunits. Several other γ2 subunit-containing tandem/monomer combinations capable of producing receptors with two γ subunits were also tested (Table 1). Currents were produced by all combinations that could yield double-γ receptors with two non-adjacent γ subunits, but no currents were produced by combinations that could yield only double-γ receptors with adjacent γ subunits. Finally, formation of double-γ2 subunit receptors with

minimal fast desensitization when γ2 subunits were expressed at molar excess could explain discrepancies between α1βγ2 currents reported by us[313, 359] and by other groups[315]. At equimolar transfection ratios, we have consistently obtained α1βγ2 receptor currents that desensitize approximately 70% over 400 ms[313], while groups using γ2 subunit overexpression have reported currents that desensitized only about 35% over 500 ms[315]. It has been argued that the discrepancy occurred because equimolar expression produces a mixture of αβ and αβγ receptors, but we demonstrated here that equimolar expression produced currents that were physiologically and pharmacologically distinct from α1β2 receptor currents. In contrast, the putative double-γ2 subunit receptors desensitized very slowly, similar to results reported by other groups. For this reason as well, we suggest that "canonical" 2α : 2β : 1γ receptors be studied with equimolar subunit transfection.

δ^{HA} subunits were markedly more stable than γ2L^{HA} subunits

The disparities between γ2L^{HA} and δ^{HA} subunit protein levels and degradation rates constitute perhaps the most surprising results reported here. Notably, these disparities occurred when γ2L^{HA}/δ^{HA} subunits were expressed either singly or in a receptor context, indicating that they were intrinsic to the subunits themselves but also could be extended to the assembled receptors. Substantial further investigation will be required to determine the basis for differences in γ2L^{HA} and δ^{HA} subunit degradation rates. Given that γ2L and δ subunits have only about 34% sequence identity, it is possible that a signal sequence or structural motif in γ2L or δ subunits could bind to accessory proteins that enhance degradation or stability, respectively. Chimeric γ2/δ subunit cDNA constructs have been constructed[360] and might be useful for addressing this possibility.

It remains to be seen whether or not the differences in γ2L and δ subunit degradation occur in neurons as well as heterologous systems. It is technically challenging but possible to conduct CHX degradation experiments in brain slices; this requires incubating very consistently

healthy brain slices in artificial cerebrospinal fluid with CHX for multiple hours and is beyond the scope of this paper. Admittedly, such experiments might not recapitulate the data presented in the current study, but our data did indicate that the difference in degradation rates was an intrinsic property of the γ2L and δ subunit proteins. Thus, it stands to reason that if the difference does not persist in neurons, some regulatory protein must block γ2L subunit degradation signals. As such, it would be interesting to assess subunit degradation rates in tissue from animals lacking various γ2L/δ subunit binding partners. The implications of different degradation rates *in vivo* would still remain unclear, but it is tempting to speculate that they could serve as valuable regulatory mechanisms reflecting the different subcellular localization of γ2 and δ subunits. As discussed, γ2 subunit-containing receptors are primarily postsynaptic and mediate fast phasic current, while δ subunit-containing receptors are exclusively extrasynaptic and mediate persistent tonic current. Postsynaptic receptors must adapt more quickly to changes in neuronal physiology, so more rapid degradation of γ2 subunit-containing receptors could be advantageous.

CHAPTER IV

THE *GABRB3* MUTATION, G32R, ASSOCIATED WITH CHILDHOOD ABSENCE EPILEPSY, ALTERS α1β3γ2L $GABA_A$ RECEPTOR EXPRESSION AND CHANNEL GATING.

Abstract

A $GABA_A$ receptor β3 subunit mutation, G32R, has been associated with childhood absence epilepsy. We evaluated the possibility that this mutation, which is located adjacent to the most N-terminal of three β3 subunit *N*-glycosylation sites, might reduce GABAergic inhibition by increasing glycosylation of β3 subunits. The mutation had three major effects on $GABA_A$ receptors. First, coexpression of β3(G32R) subunits with α1 or α3 and γ2L subunits in HEK293T cells reduced surface expression of γ2L subunits and increased surface expression of β3 subunits, suggesting a partial shift from ternary αβ3γ2L receptors to binary αβ3 and homomeric β3 receptors. Second, β3(G32R) subunits were more likely than β3 subunits to be *N*-glycosylated at N33, but increases in glycosylation were not responsible for changes in subunit surface expression. Rather, both phenomena could be attributed to the presence of a basic residue at position 32. Finally, α1β3(G32R)γ2L receptors had significantly reduced macroscopic current density. This reduction could not be explained fully by changes in subunit expression levels (because γ2L levels decreased only slightly) or glycosylation (because reduction persisted in the absence of glycosylation at N33). Single channel recording revealed that α1β3(G32R)γ2L receptors had impaired gating with shorter mean open time. Homology modeling indicated that the mutation altered salt bridges at subunit interfaces, including regions important for subunit oligomerization. Our results suggest both a mechanism for mutation-induced hyperexcitability and a novel role for the β3 subunit N-terminal α-helix in receptor assembly and gating.

Introduction

Childhood absence epilepsy (CAE) is characterized by frequent absence seizures, during which patients manifest brief losses of consciousness and generalized, synchronous 3 Hz spike-and-wave discharges on EEG. The seizures typically begin at age 3-8 years, continue through adolescence, last 3-10 seconds, and occur up to 200 times per day. CAE is highly genetic, and 16-45% of patients have a positive family history[361]. Mutations, polymorphisms, and variants associated with CAE have been identified in several genes encoding ion channels, including T-type calcium[362-365], chloride[366], and $GABA_A$ receptor[320, 324, 367] channels.

$GABA_A$ receptors are pentameric, ligand-gated chloride channels that mediate the majority of fast inhibitory neurotransmission in the brain. They assemble from an array of 19 homologous subunits from eight subunit families: α1-6, β1-3, γ1-3, δ, ε, π, θ and ρ1-3[266]. The predominant receptor isoforms *in vivo* likely contain two α, two β, and one γ or δ subunit (Figure 1)[328, 329, 340]; however, some subunits (notably β3 subunits) may assemble less discriminately, forming homopentamers as well as heteropentamers[90].

Three separate CAE-associated mutations were recently identified in $GABA_A$ receptor β3 subunits: *GABRB3(P11S), GABRB3(S15F)* and *GABRB3(G32R)*[310]. Mutant subunit-containing receptors exhibited reduced current density. Moreover, the mutant proteins all appeared to be "hyperglycosylated", because they migrated at higher molecular masses than wildtype β3 subunits unless digested with an enzyme that removed all *N*-glycans. The investigators consequently hypothesized that hyperglycosylation might be responsible for the reduced current density, which might in turn lead to neuronal hyperexcitability and, ultimately, to the abnormal EEG patterns of absence seizures.

Approximately half of all eukaryotic proteins carry *N*-linked glycans[368]. The process of *N*-linked glycosylation begins in the ER lumen, where standard "core" glycans are attached to the side chain nitrogen of asparagines located in the glycosylation consensus sequon, Asn-Xaa-

Ser/Thr (Xaa ≠ Pro)[369, 370]. Sequons containing threonine residues have higher glycan occupancy than sequons containing serine residues[371]. *N*-linked glycosylation serves several functions in biogenesis of multimeric proteins. First, addition of glycans facilitates monomer folding and multimer assembly, thus preventing aggregation and degradation of newly synthesized subunits[372, 373]. Furthermore, glycan conjugation may favor assembly of certain subunits, thereby determining subunit stoichiometry[374]. Finally, *N*-linked glycosylation can affect functional properties of ion channels once they reach the cell surface[375]. Perhaps unsurprisingly, most congenital disorders of glycosylation cause severe pathology, often with significant neurological involvement[376]. However, these disorders generally impair rather than enhance glycan attachment and processing. In this study, we evaluated the possibility that the β3(G32R) subunit mutation, which is located adjacent to the first of three β3 subunit *N*-glycosylation sites (Figure 1), might reduce GABAergic inhibition by aberrantly increasing glycosylation.

Experimental Procedures

Molecular biology

Complementary DNAs (cDNAs) encoding individual human $GABA_A$ receptor subunits (α1, NM_000806.5; α3, NM_000808.3; β3 variant 2, NM_021912.4**;** and γ2L, NM_000816.3) were cloned into the pcDNA3.1(+) vector. The hemagglutinin (HA) epitope tag (YPYDVPDYA) was inserted between amino acids 4 and 5 of the mature γ2L subunit protein. Point mutations were introduced using the QuikChange Site-Directed Mutagenesis Kit (Stratagene). All constructs were sequenced by the Vanderbilt DNA core facility prior to use. Note that all amino acids are numbered according to the immature peptide sequence.

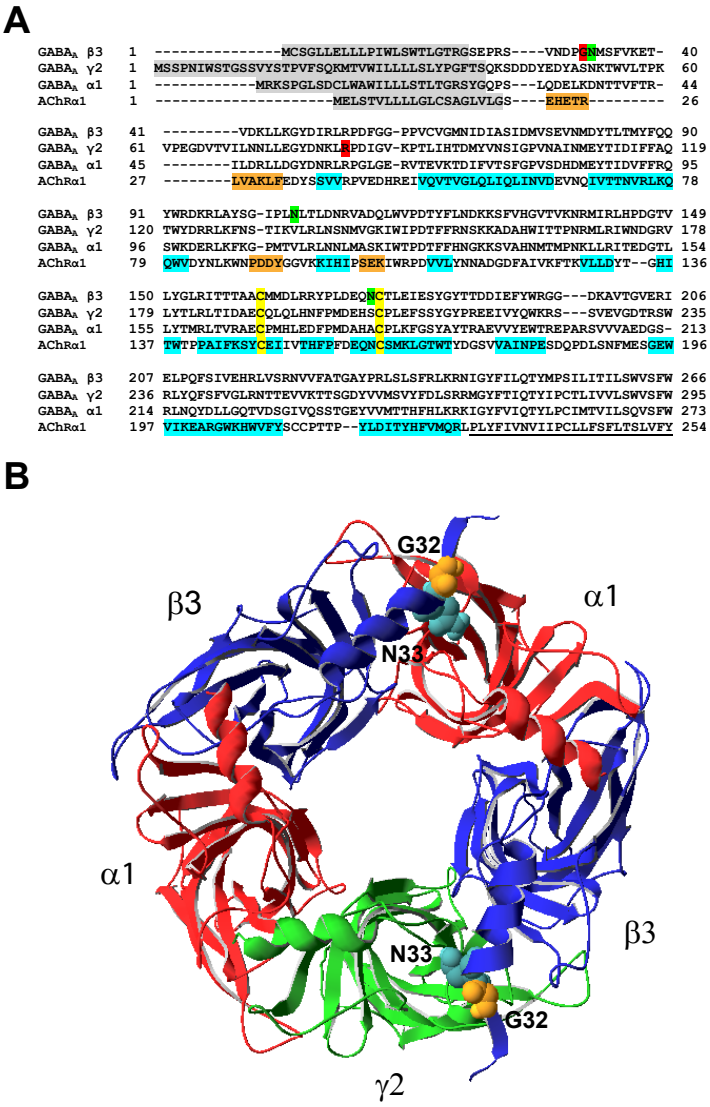

Figure 1. The G32R mutation was predicted to be adjacent to the first of three putative glycosylation sites in β3 subunits and to lie at subunit interfaces in assembled GABA$_A$ receptors.

A. The sequences of human α1, β3, and γ2L GABAA receptor subunits were aligned with the sequence of the human nicotinic acetylcholine receptor α1 subunit (AChRα1). In the AChRα1 sequence, α-helices are highlighted in orange, β-sheets are highlighted in blue, and the first transmembrane domain is underlined. In the GABA$_A$ receptor β3 subunit sequence, putative N-glycosylation sites are highlighted in green. In all sequences, signal peptides are highlighted in gray and the cysteines forming the Cys-loop are highlighted in yellow. Sites of epilepsy-associated mutations in GABA$_A$ receptor subunits (β3(G32R) and γ2(R43Q)) are highlighted in red. **B.** A model of the α1β3γ2L GABAA receptor, as viewed from the synaptic cleft, is presented. The nicotinic acetylcholine receptor α1 subunit crystal structure (2qc1) was used to generate homology models of individual GABAA receptor subunits, which were threaded onto the *Lymnaea stagnalis* acetylcholine binding protein crystal structure in the order γ2L-β3-α1-β3-α1. The α1, β3, and γ2L subunits are colored red, blue, and green, respectively. Glycine 32 and asparagine 33 are presented as orange and cyan space-filling models, respectively.

Cell culture and transfection

HEK293T cell culture methods have been described previously [335]. For immunoblotting, 1.2 x 10^6 cells were plated onto 100-mm diameter culture dishes; for flow cytometry, 4 x 10^5 cells were plated onto 60-mm diameter culture dishes; and for electrophysiology, 1 x 10^5 cells were plated onto 30-mm diameter culture dishes.

Twenty-four hours after plating, cells were transfected with $GABA_A$ receptor subunit cDNAs using 3 μl FuGENE 6 (Roche) per 1 μg subunit cDNA. For immunoblotting, 3 μg of each subunit cDNA was transfected (i.e., 9 μg cDNA altogether); for other experiments, cDNA amounts were scaled proportionally to the number of cells plated. For "wildtype" or "homozygous" subunit expression flow cytometry experiments, 60-mm culture dishes were transfected with 1 μg each α1 (or α3) and $\gamma2L^{HA}$ subunit cDNAs and 1.0 μg of β3 or β3(G32R) subunit cDNAs, respectively. For "heterozygous" expression flow cytometry experiments, 60-mm culture dishes were transfected with 1 μg each α1 (or α3) and $\gamma2L^{HA}$ subunit cDNAs and 0.5 μg each β3 and β3(G32R) subunit cDNAs. The terms "wildtype", "heterozygous" and "homozygous" are used as a shorthand designation for the subunit expression conditions and are not meant to imply any genetic condition.

Surface biotinylation

Biotinylation protocols have been described previously [335]. Briefly, culture plates were washed, incubated with 1 mg/ml NHS-SS-biotin (Pierce) diluted in Dulbecco's PBS (DPBS) and lysed with radioimmune precipitation assay buffer (RIPA buffer; 50 mM Tris-HCl pH 7.4, 0.1 % Triton X-100, 250 mM NaCl, 5 mM EDTA) containing protease inhibitor cocktail (Sigma). Lysates were cleared by centrifugation at 16,000 x g for 15 minutes and subsequently incubated overnight with High-Capacity NeutrAvidin agarose resin (Pierce). After overnight incubation, protein was eluted and subjected to immunoblotting.

Immunoblotting

Proteins in sample buffer were separated on 4-12 % Bis-Tris NuPAGE gels (Invitrogen) and transferred to Odyssey PVDF membranes (Li-Cor). A monoclonal antibody raised against intracellular residues 370-433 of the $GABA_A$ receptor β3 subunit (4 μg/ml, clone N87/25, UC Davis/NIH NeuroMab Facility) was used to detect β3 subunit protein, and anti-Na^+/K^+ ATPase antibody (0.2 μg/ml, clone 464.6, ab7671, Abcam) was used as a loading control. Anti-mouse IRdye conjugated secondary antibodies (Li-Cor) were used in all cases. Membranes were scanned using the Li-Cor Odyssey system and integrated intensities of bands were determined using Odyssey software.

Glycosidase digestion

Biotinylated protein was simultaneously eluted from NeutrAvidin resin and denatured by incubation in 1x glycoprotein denaturing buffer (New England Biolabs) containing 50 mM dithiothreitol for 30 minutes at 50˚C. Eluates were divided into 15 μl aliquots and digested with 1 unit of endo-β-N-acetylglucosaminidase H (endo H) or peptide-N-glycosidase F (PNGase F) in manufacturer-supplied buffers (New England Biolabs) at 37˚C for 2 h.

Flow cytometry

Staining protocols for flow cytometry have been described previously [335]. $GABA_A$ receptor subunits were detected with antibodies to human α1 subunits (N-terminus, clone BD24, Millipore; 2.5 μg/ml), human α3 subunits (N-terminal residues 29-43, polyclonal, Alomone; 1.5 μg/ml), or the HA epitope tag (clone 16B12, Covance; 2.5 μg/ml). The Molecular Probes Monoclonal Antibody Labeling Kit (Invitrogen), used per manufacturer instructions, was previously used to directly conjugate Alexa647 fluorophores to anti-α1 subunit and anti-HA tag antibodies. Following antibody incubation, cells were washed three times with FACS buffer and either fixed with 2 % w/v paraformaldehyde, 1 mM EDTA diluted in PBS (anti-α1, anti-HA) or

incubated with anti-mouse-IgG1 secondary antibody conjugated to the Alexa 647 fluorophore (Invitrogen; anti-α3) before additional washing and fixation.

For total cellular protein detection, cells were permeabilized for 15 minutes with Cytofix/Cytoperm (BD Biosciences) and washed twice with 1 x PermWash (BD Biosciences) before antibody incubation. For these experiments, all antibodies were diluted to 2.5 μg/ml in PermWash. After antibody incubation, cells were washed four times in PermWash and twice in FACS buffer before fixation with 2 % w/v paraformaldehyde, 1 mM EDTA diluted in PBS.

Fluorescence intensity (FI) of all samples was determined using an LSR II 5-laser flow cytometer (BD Biosciences) and analyzed offline with FlowJo 7.5 (Tree Star). For each sample, 50,000 total events were acquired; non-viable cell populations, determined in control experiments by staining with 7-amino-actinomycin D, were excluded from analysis. For all experiments, the net FI of samples was determined by subtracting the mean FI of cells transfected with blank pcDNA(3.1+) vector from the mean FI of cells expressing $GABA_A$ receptor subunits. The relative fluorescence intensity ("relative FI") for each condition was calculated by normalizing the net FI of each experimental condition to the net FI of cells expressing wildtype β3 subunits.

Whole cell electrophysiology

Whole cell voltage-clamp recordings were performed at room temperature on lifted HEK293T cells 24-72 hrs after transfection with $GABA_A$ receptor subunits as described previously[367]. Briefly, cells were bathed in an external solution containing 142 mM NaCl, 1 mM $CaCl_2$, 8 mM KCl, 6 mM $MgCl_2$, 10 mM glucose, and 10 mM HEPES (pH 7.4, ~325 mOsm), and recording electrodes were filled with an internal solution containing 153 mM KCl, 1 mM $MgCl_2$, 10 mM HEPES, 5 mM EGTA, 2 mM Mg^{2+}-ATP (pH 7.3, ~300 mOsm). All patch electrodes had a resistance of 1–2 MΩ. Cells were voltage-clamped at -20 mV using an Axopatch 200B amplifier (Axon Instruments, Union City, CA). A rapid exchange system (open tip exchange times ~ 400 μs), composed of a four-barrel square pipette attached to a Perfusion

Fast-Step (Warner Instruments Corporation, Hamden, CT) and controlled by Clampex 9.0 (Axon Instruments), was used to apply GABA to lifted whole cells. All currents were low-pass filtered at 2 kHz, digitized at 5-10 kHz, and analyzed using the pCLAMP 9 software suite.

Single-channel electrophysiology

Cell-attached single-channel recording was performed as described previously[367]. Briefly, HEK293T cells expressing $GABA_A$ receptor subunits were bathed in an external solution containing 140 mM NaCl, 2 mM $CaCl_2$, 5 mM KCl, 1 mM $MgCl_2$, 10 mM glucose, and 10 mM HEPES (pH 7.4). Recording electrodes were filled with an internal solution containing 1mM GABA, 120 mM NaCl, 0.1 mM $CaCl_2$, 5 mM KCl, 10 mM $MgCl_2$, 10 mM glucose, and 10 mM HEPES (pH 7.4), and electrode potential was held at +80 mV. The electrodes were polished to a resistance of 10-20 MΩ.

Single channel currents were amplified and low-pass filtered at 2 kHz using an Axopatch 200B amplifier, digitized at 20 kHz using Digidata 1322A, and saved using pCLAMP 9 software (Axon Instruments). Data were analyzed using TAC 4.2 and open time and amplitude histograms were generated using TACFit (Bruxton Corporation, Seattle, WA) as described previously (10). The number of components required to fit the duration histograms was increased until an additional component did not significantly improve the fit[377]. Single channel openings occurred as bursts of one or more openings or clusters of bursts. Bursts were defined as one or more consecutive openings that were separated by closed times that were shorter than a specified critical duration (t_{crit}) prior to and following the openings[378]. A t_{crit} of 5 ms was used in the current study. Clusters were defined as a series of bursts preceded and followed by closed intervals longer than a specific critical duration ($t_{cluster}$). A $t_{cluster}$ of 10 ms was used in this study.

Homology modeling

Multiple sequence alignments of human $GABA_A$ receptor α1, β3, and γ2L subunits and the human nicotinic acetylcholine receptor (nAChR) α1 subunit were performed using ClustalW (European Bioinformatics Institute, Hinxton, UK). Structural models of $GABA_A$ receptor N-terminal domains were generated with SWISS-MODEL[379], using the crystal structure of the nAChR α1 subunit (PDB ID 2qc1)[153] as a template. Point mutations were introduced into the β3 subunit sequence using DeepView/Swiss-PdbViewer 4.02 (Swiss Institute of Bioinformatics, Lausanne, Switzerland), and SWISS-MODEL project files containing the mutated target sequence and the superposed template structure were submitted. For heteropentamers, subunits were threaded in the order γ2L-β3-α1-β3-α1 onto the *Lymnaea stagnalis* acetylcholine binding protein (AChBP) crystal structure (PDB ID 1i9b)[98] used as a template. All models were energy-optimized using GROMOS96 in default settings within DeepView/Swiss-PdbViewer, and the most likely conformations were presented here.

Statistical analysis

Statistical analysis was performed using Prism version 5.04 (GraphPad Software, La Jolla, CA). Student's two-tailed *t* test or one-way analysis of variance (ANOVA) with Tukey's and/or Bonferroni's post-tests was used as appropriate to determine statistical significance among transfection conditions. Levels of significance were indicated in figure legends, and all data were expressed as mean ± S.E.M.

Results

Cotransfection of the mutant β3(G32R) subunit with α1 or α3 and γ2L^{HA} subunits was associated with increased β3 subunit and decreased γ2L^{HA} subunit surface expression.

Because the β3(G32R) mutation was reported to reduce the current density of heterologously expressed α1β3γ2L receptors[310], we sought to determine whether the mutation

reduced surface expression of the $GABA_A$ receptor subunits under similar conditions. First, we transiently co-expressed α1, $\gamma2L^{HA}$, and either wildtype β3 or mutant β3(G32R) subunit cDNAs at a 1:1:1 ratio in HEK293T cells and assessed surface expression of all subunits using surface biotinylation and Western blotting.

Immunoblotting revealed two major differences between β3 and β3(G32R) subunit proteins (Figure 2A). First, although both wildtype and mutant subunits migrated as three bands with molecular masses of approximately 51, 47, and 43 kDa, the distribution of protein among those bands differed considerably (Figure 2A1). Specifically, a larger fraction of mutant subunits migrated at the higher molecular masses. Second, surprisingly mutant β3(G32R) subunit surface levels were increased significantly (154 ± 15 % of wildtype, $n = 17$, $p < 0.01$) (Figure 2A2).

Because it would be highly unusual for a mutation to cause both an increase in surface receptor number and a reduction in current density, we first addressed the differences in wildtype and mutant subunit expression levels. Increases in β3 subunit surface expression could reflect either a change in receptor subunit composition, including production of α1β3 receptors and/or β3 subunit homomers, or an overall increase in surface α1β3γ2L receptor number. To distinguish between these two possibilities, we first examined the differences in wildtype and mutant partnering subunit expression levels. Immunoblotting for surface levels of partnering subunits suggested that α1 subunit levels did not change but $\gamma2L^{HA}$ subunit levels decreased when co-expressed with β3(G32R) rather than β3 subunits (data not shown), indicating a potential change in receptor subunit composition. Because the reduction of $\gamma2L^{HA}$ surface levels was subtle, we employed flow cytometry to confirm and quantify changes in subunit expression levels. In these experiments, we also included a condition modeling heterozygous expression of β3(G32R) subunits, in which an equimolar mixture of both β3 and β3(G32R) subunit cDNA was cotransfected with α1 and $\gamma2L^{HA}$ subunit cDNAs (see Methods for exact subunit cDNA ratios and concentrations). Consistent with the prior immunoblotting data, α1 subunit surface levels did not differ significantly in the heterozygous or homozygous mutant conditions (Figure 2B), but $\gamma2L^{HA}$

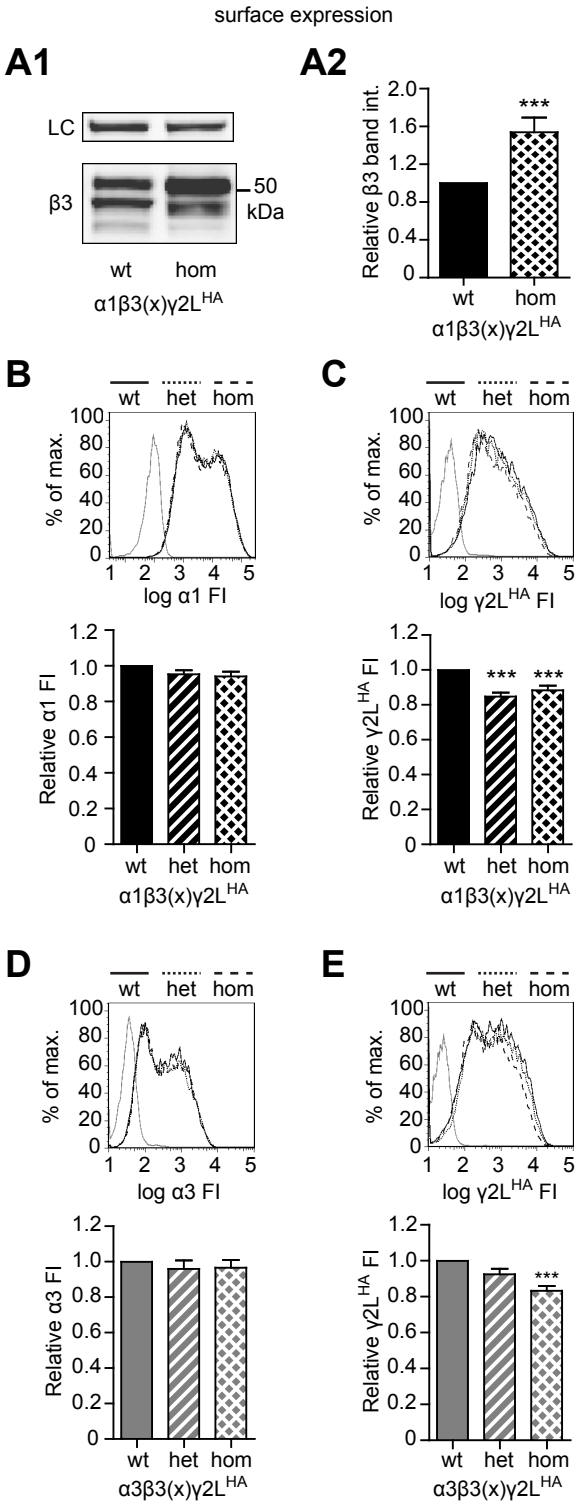
surface expression
A1
LC
β3
50 kDa
wt
hom
α1β3(x)γ2L^HA
A2
Relative β3 band int.
***
wt
hom
α1β3(x)γ2L^HA
B
wt het hom
% of max.
log α1 FI
Relative α1 FI
wt het hom
α1β3(x)γ2L^HA
C
wt het hom
% of max.
log γ2L^HA FI
Relative γ2L^HA FI
***
***
wt het hom
α1β3(x)γ2L^HA
D
wt het hom
% of max.
log α3 FI
Relative α3 FI
wt het hom
α3β3(x)γ2L^HA
E
wt het hom
% of max.
log γ2L^HA FI
Relative γ2L^HA FI
***
wt het hom
α3β3(x)γ2L^HA

Figure 2

Figure 2. Cells expressing α1 or α3, β3(G32R), and γ2L^{HA} subunits had higher surface levels of β3 subunits and lower surface levels of γ2L^{HA} subunits compared to cells expressing α1 or α3, β3(wt), and γ2L^{HA} subunits.

A1. Surface protein was isolated from HEK293T cells transfected with equimolar amounts of α 1, γ2LHA, and either wildtype or G32R mutant (hom) β3 $GABA_A$ receptor subunit cDNA, separated by SDS-PAGE, and evaluated using Western blots. The upper panel presents staining for Na+/K+ ATPase as a loading control (LC), and the lower panel presents staining for β3 subunits (see Methods for antibody descriptions). **A2.** Surface protein levels of β3 subunits were quantified in HEK293T cells transfected with equimolar amounts of α1, γ2L^{HA}, and either wildtype or G32R mutant (hom) β3 $GABA_A$ receptor subunits. Integrated band intensities of all β3 subunits were determined, summed, and normalized to integrated band intensities of Na+/K+ ATPase for the same sample. The normalized intensities of β3 subunits were then expressed as proportions of wildtype β3 subunit intensities. Statistical significance was determined using Student's two-tailed paired t-test. **B-C.** Flow cytometry was used to evaluate surface protein levels of α1 (B) and γ2L^{HA} (C) subunits in HEK293T cells transfected with α1, γ2L^{HA}, and wildtype and/or G32R mutant β3 $GABA_A$ receptor subunit cDNA. Wildtype and homozygous mutant (hom) expression were modeled by transfecting 1 μg each of α1, γ2L^{HA}, and either wildtype or G32R mutant (hom) β3 subunit cDNA. Heterozygous mutant expression (het) was modeled by transfecting 1 μg each of α1 and γ2L^{HA} cDNA together with 0.5 μg each of β3 and β3(G32R) subunit cDNA. Upper panels present fluorescence intensity histograms; the abscissa indicates fluorescence intensity (FI) in arbitrary units plotted on a logarithmic scale, and the ordinate indicates percentage of maximum cell count (% of max). Histograms for cells transfected with blank vector (solid gray line), or wt (solid black line), het (dotted black line), and hom (dashed black line) subunit combinations are overlaid. Lower panels present normalized fluorescence intensities for each expression condition. Mean fluorescence intensities from cells transfected with blank vector alone ("mock") were subtracted from mean fluorescence intensities of wt, het, and hom expression conditions. All mock-subtracted fluorescence intensities were normalized to the mock-subtracted fluorescence intensity of the wt expression condition. **D-E.** Flow cytometry was used to evaluate surface protein levels of α3 (D) and γ2L^{HA} (E) subunits in HEK293T cells transfected with α3, γ2L^{HA}, and wildtype and/or G32R mutant β3 subunit cDNA. All panels are presented as described in B-C, but in all cases α3 subunit cDNA was substituted for α1 subunit cDNA. Statistical significance was determined using one-way ANOVA with Tukey's post-test. *** indicates $p < 0.001$ compared to wt.

subunit surface levels were decreased slightly in both heterozygous (84.8 ± 2.2 % of wildtype, n = 10, $p < 0.001$) and homozygous mutant (87.1 ± 2.4 % of wildtype, n = 16, $p < 0.001$) conditions (Figure 2C).

We chose to co-express α1 and γ2 subunits because they are the most widely expressed subunits of their respective families in whole brain; however, subunit expression patterns vary widely among brain regions. Several studies have indicated that absence seizures frequently involve dysfunction in the thalamic reticular nucleus (nRT), where the α3 subunit subtype predominates and β3 subunit expression is also high [57]. Consequently, we also examined changes in partnering subunit expression levels using α3 rather than α1 subunit cDNA. Results resembled those obtained using α1 subunits; that is, α3 subunit surface levels did not differ significantly among wildtype, heterozygous, and homozygous mutant receptors (Figure 2D), but $\gamma2L^{HA}$ subunit surface levels decreased in both heterozygous and homozygous mutant conditions, although the reduction was significant only in the homozygous mutant condition (Figure 2E).

Changes in subunit surface expression could reflect alterations in subunit production, subunit stability, or receptor trafficking. Therefore, we also assessed total cellular subunit levels (Figure 3) in the same conditions used to study surface expression (Figure 2). Interestingly, coexpressing α1, β3(G32R) and $\gamma2L^{HA}$ subunits yielded no significant changes in β3 (Figure 3 A1, A2), α1 (Figure 3B), or $\gamma2L^{HA}$ (Figure 3C) subunit total cellular expression among wildtype and heterozygous and homozygous mutant transfections. Likewise, coexpressing α3, β3(G32R) and $\gamma2L^{HA}$ subunits yielded no significant changes in α3 (Figure 3D) or $\gamma2L^{HA}$ (Figure 3E) subunit total cellular expression.

The β3 subunit mutation, G32R, affected subunit surface expression independent of glycosylation.

To this point, we observed two principal effects of the β3 subunit mutation, G32R. First, mutant and wildtype receptors had different surface expression patterns (specifically, a small

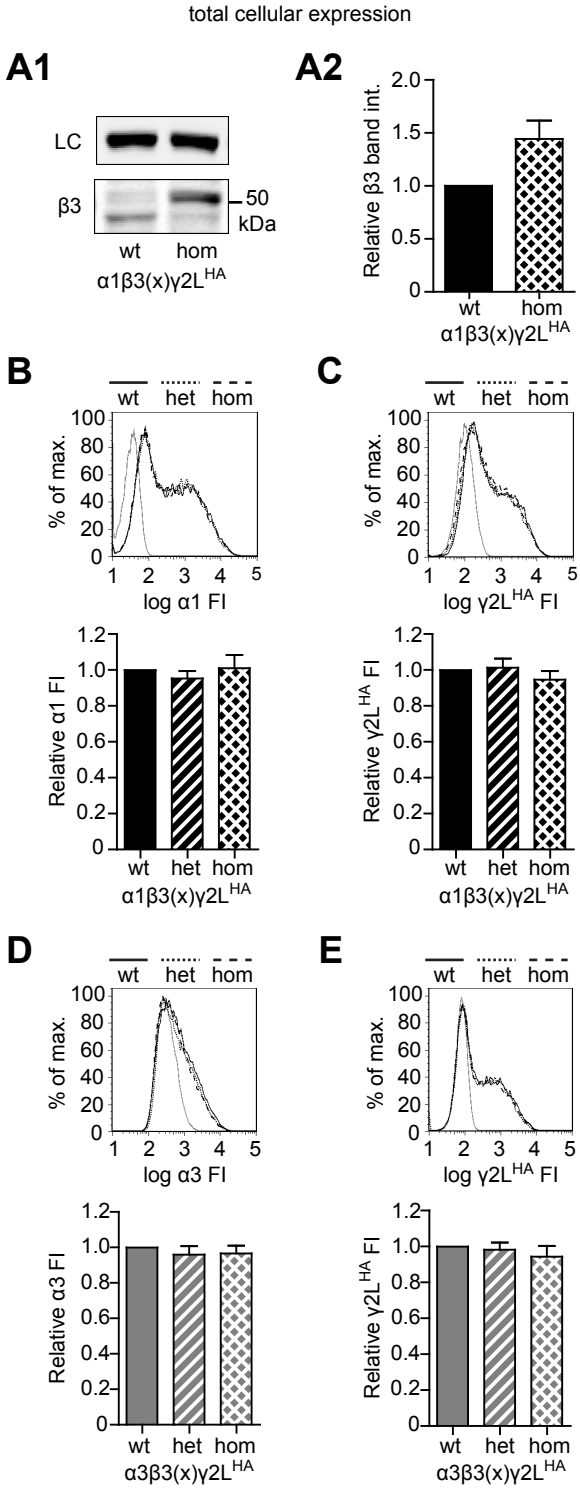
total cellular expression
A1
LC
β3
50 kDa
wt hom
α1β3(x)γ2L^HA
A2
Relative β3 band int.
wt hom
α1β3(x)γ2L^HA
B
wt het hom
% of max.
log α1 FI
Relative α1 FI
wt het hom
α1β3(x)γ2L^HA
C
wt het hom
% of max.
log γ2L^HA FI
Relative γ2L^HA FI
wt het hom
α1β3(x)γ2L^HA
D
wt het hom
% of max.
log α3 FI
Relative α3 FI
wt het hom
α3β3(x)γ2L^HA
E
wt het hom
% of max.
log γ2L^HA FI
Relative γ2L^HA FI
wt het hom
α3β3(x)γ2L^HA

Figure 3

Figure 3. The β3(G32R) mutation did not significantly affect total cellular levels of $GABA_A$ receptor subunits in cells expressing α1 or α3, β3, and γ2L^{HA} subunits.

A1. Total cell lysates (40 μg) were obtained from HEK293T cells transfected with equimolar amounts of α1, γ2LHA, and either wildtype or G32R mutant (hom) β3 subunit cDNA, separated by SDS-PAGE, and evaluated using Western blots. The upper panel presents staining for Na+/K+ ATPase as a loading control (LC), and the lower panel presents staining for β3 subunits (see Methods for antibody descriptions). **A2.** Total cellular levels of β3 subunits were quantified in HEK293T cells transfected with equimolar amounts of α1, γ2L^{HA}, and either wildtype or G32R mutant (hom) β3 $GABA_A$ receptor subunits. Integrated band intensities of all β3 subunit populations were determined, summed, and normalized to integrated band intensities of Na+/K+ ATPase for the same sample. The normalized intensities of β3 subunits were then expressed as proportions of wildtype β3 subunit intensities. Statistical significance was determined using Student's two-tailed paired t-test. **B-C.** Flow cytometry was used to evaluate total cellular levels of α1 (B) and γ2L^{HA} (C) subunits in HEK293T cells transfected with α1, γ2L^{HA}, and wildtype and/or G32R mutant β3 subunit cDNA and permeabilized before staining with fluorescently-conjugated antibodies. Wildtype (wt), heterozygous (het), and homozygous (hom) expression patterns were modeled as described for Figure 1. Upper panels present fluorescence intensity histograms; the x axis indicates fluorescence intensity (FI) in arbitrary units plotted on a logarithmic scale, and the y axis indicates percentage of maximum cell count (% of max). Histograms for cells transfected with blank vector (solid gray line), or wt (solid black line), het (dotted black line), and hom (dashed black line) subunit combinations are overlaid. Lower panels present normalized fluorescence intensities for each expression condition. Mean fluorescence intensities from cells transfected with blank vector alone ("mock") were subtracted from mean fluorescence intensities of wt, het, and hom expression conditions. All mock-subtracted fluorescence intensities were normalized to the mock-subtracted fluorescence intensity of the wt expression condition. **D-E.** Flow cytometry was used to evaluate total cellular levels of α3 (D) and γ2L^{HA} (E) subunits in HEK293T cells transfected with α1, γ2L^{HA}, and wildtype and/or G32R mutant β3 $GABA_A$ receptor subunit cDNA and permeabilized before staining with fluorescently-conjugated antibodies. All panels are presented as described in B-C, but in all cases α3 subunit cDNA was substituted for α1 subunit cDNA. Statistical significance was determined using one-way ANOVA with Tukey's post-test.

decrease in γ2L subunit levels and a large increase in β3 subunit levels); these changes suggested a partial replacement of α1β3γ2L receptors by α1β3 receptors and β3 subunit homopentamers. Second, β3(G32R) subunits were more likely than β3 subunits to migrate at the highest of three distinct molecular mass populations. However, it remained unclear if there was a causal relationship between these two phenomena.

Because the mutant subunit had been reported to be hyperglycosylated, we hypothesized that the multiple β3 subunit bands represented differently glycosylated protein populations, where individual sequons may or may not be occupied by a glycan, occupancy patterns may or may not be uniform within a protein population (e.g., among all β3(G32R) subunits), and the glycans themselves may contain different combinations of monosaccharides. To determine if the multiple β3 subunit bands represented differently glycosylated protein populations and to characterize β3 subunit *N*-glycans, we isolated surface protein from HEK293T cells expressing α1, $\gamma 2L^{HA}$, and either β3 or β3(G32R) subunits and compared the migration patterns of β3 and β3(G32R) subunits that were undigested (U); digested with endoglycosidase H (endo H), which cleaves only high-mannose, unprocessed glycans; or digested with peptide *N*-glycosidase F (PNGaseF), which removes all *N*-glycans regardless of modification (Figure 4A). After digestion with PNGaseF (F), both β3 and β3(G32R) subunits migrated as one 43 kDa band, indicating that the G32R mutation did indeed increase *N*-glycosylation of at least one of the three β3 subunit sequons (Figure 4A, lanes 3 and 6). Interestingly, β3 and β3(G32R) subunits also displayed different endo H digestion patterns (H); after endo H digestion, a substantial population of β3 subunits migrated at 43 kDa and thus were fully endo H sensitive, but virtually none of the β3(G32R) subunits migrated at 43 kDa and thus were endo H resistant. Therefore, the G32R mutation increased the efficiency of both addition and processing of *N*-glycans.

We recently established that partnering subunit incorporation could alter glycosylation patterns of β2 subunits[335]. Thus, it was possible that the increased endo H resistant population of β3(G32R) subunits reflected increased formation of α1β3 and/or β3 receptor isoforms. To assess

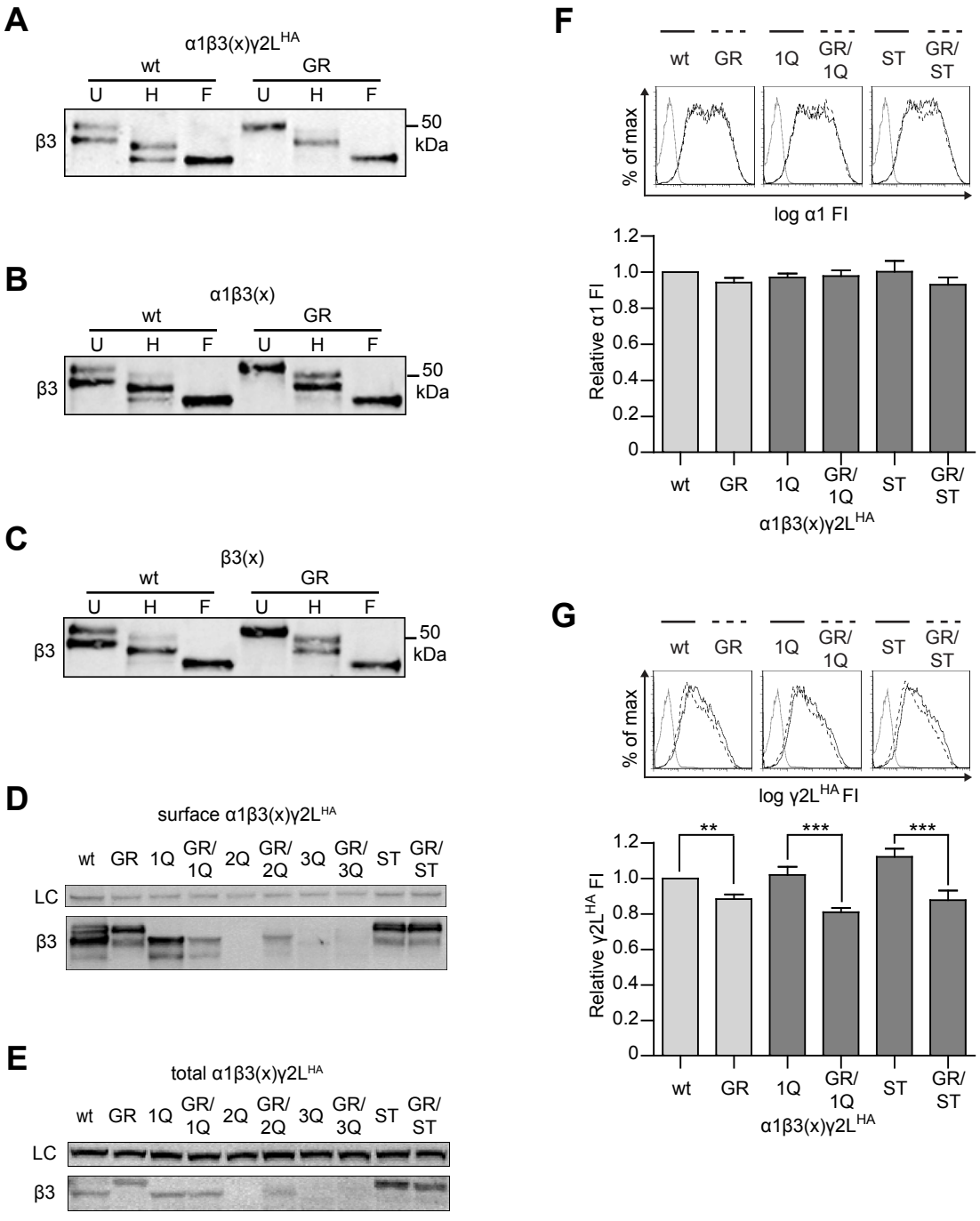
A
α1β3(x)γ2L^HA
wt
GR
U H F U H F
β3
50 kDa
B
α1β3(x)
wt
GR
U H F U H F
β3
50 kDa
C
β3(x)
wt
GR
U H F U H F
β3
50 kDa
D
surface α1β3(x)γ2L^HA
wt GR 1Q GR/ 1Q 2Q GR/ 2Q 3Q GR/ 3Q ST GR/ ST
LC
β3
E
total α1β3(x)γ2L^HA
wt GR 1Q GR/ 1Q 2Q GR/ 2Q 3Q GR/ 3Q ST GR/ ST
LC
β3
F
wt GR 1Q GR/ 1Q ST GR/ ST
% of max
log α1 FI
Relative α1 FI
1.2
1.0
0.8
0.6
0.4
0.2
0
wt GR 1Q GR/ 1Q ST GR/ ST
α1β3(x)γ2L^HA
G
wt GR 1Q GR/ 1Q ST GR/ ST
% of max
log γ2L^HA FI
Relative γ2L^HA FI
**
***
***
1.2
1.0
0.8
0.6
0.4
0.2
0
wt GR 1Q GR/ 1Q ST GR/ ST
α1β3(x)γ2L^HA

Figure 4

Figure 4. The β3(G32R) mutation increased glycosylation of Asn-33 and reduced γ2L^{HA} subunit surface expression independent of glycosylation at Asn-33.

A. Surface protein was isolated from HEK293T cells expressing equimolar amounts of α1, γ 2L^{HA}, and either β3 or β3(G32R) subunits and left undigested (U) or digested with endoglycosidase H (H) or peptide N-glycosidase F (F). **B.** Surface protein was isolated from HEK293T cells expressing equimolar amounts of α1 and either β3 or β3(G32R) subunits and left undigested (U) or digested with endoglycosidase H (H) or peptide N-glycosidase F (F). **C.** Surface protein was isolated from HEK293T cells expressing equimolar amounts of either β3 or β3(G32R) subunits and left undigested (U) or digested with endoglycosidase H (H) or peptide N-glycosidase F (F). **D-E.** Surface (D) or total cellular (E) protein was isolated from HEK293T cells expressing equimolar amounts of α1, γ2L^{HA}, and different β3 subunits. The β3 subunit cDNA constructs were modified to inactivate (with an Asn to Gln mutation) or enhance (with a Ser to Thr mutation) the putative N-glycosylation sites of β3 subunits. In lane 1, the β3 subunit had no mutations (wt), and in lane 2, the β3 subunit had the G32R mutation only (GR). The three glycosylation sites (N33, N105, and N174) were inactivated individually in the absence (lane 3, 1Q; lane 5, 2Q; and lane 7, 3Q) or the presence (lane 4, GR/1Q; lane 6, GR/2Q; lane 8, GR/3Q) of the G32R mutation. The first glycosylation site was also enhanced in either the absence (lane 9, ST) or the presence (lane 10, GR/ST) of the G32R point mutation. The upper panel presents staining for Na+/K+ ATPase as a loading control (LC), and the lower panel presents staining for β3 subunits. **F-G.** Surface levels of α1 (F) and γ2L^{HA} (G) subunits in cells expressing α1, γ2LHA, and glycosylation sequon mutant β3 subunits were determined using flow cytometry. The β3 subunit transfected in each condition is labeled as described in panels D and E. Upper panels present fluorescence intensity histograms in which the abscissa denotes fluorescence intensity in arbitrary units graphed on a logarithmic scale (log FI) and the ordinate denotes percentage of maximum cell count (% of max). Fluorescence intensity histograms from mock-transfected cells (solid gray line) are overlaid with histograms from cells expressing α1, γ2L^{HA}, and β3 subunits that either lacked (solid black line) or contained (dashed black line) the G32R point mutation. In the left panels, either β3(wt, solid) or β3(G32R) (GR, dashed) subunit cDNAs were transfected; in the middle panels, either β3(N33Q) (1Q, solid) or β3(G32R/N33Q) (GR/1Q, dashed) subunit cDNAs were transfected; and in the right panels, either β3(S35T) (ST, solid) or β3(G32R/S35T) (GR/ST, dashed) subunit cDNAs were transfected. The lower panels present normalized fluorescence intensities for each expression condition. Mean fluorescence intensities from cells transfected with blank vector alone ("mock") were subtracted from mean fluorescence intensities of cells transfected with α1, γ2L^{HA}, and the indicated β3 subunits. All mock-subtracted fluorescence intensities were normalized to the mock-subtracted fluorescence intensity of the cells expressing β3 subunits. One-way ANOVA with Bonferroni's post-test was used to compare normalized fluorescence intensities of each glycosylation sequon pair (i.e., wt v. GR, 1Q v. GR/1Q, and ST v. GR/ST). ** $p < 0.01$; *** $p < 0.001$.

this possibility, we studied the digestion pattern of wildtype β3 and mutant β3(G32R) subunits after transfecting α1 and β3 (Figure 4B) or only β3 (Figure 4C) subunit cDNA. We found that the increased glycosylation and glycan processing of β3(G32R) mutant subunits compared to β3 subunits persisted in the absence of α1 and/or γ2L partnering subunits. Interestingly, the proportion of endo H sensitive β3 subunits did decrease with the number of subunits expressed; that is, endo H sensitivity was greatest in $\alpha1\beta3\gamma2L^{HA}$ receptors, lower in α1β3 receptors, and lowest in β3 receptors.

These results demonstrating altered glycosylation of β3(G32R) subunits contradicted *in silico* analysis. We used NetNGlyc 1.0 to establish that the G32R mutation did not change the occupancy potential of N105 (0.7904) or N174 (0.6229), but it slightly *reduced* the occupancy potential of N33 (β3 0.5947, β3(G32R) 0.5239) (data not shown). Similarly, meta-analyses have concluded that sequons with Arg at the -1 position are considerably less likely to be glycosylated than sequons with Gly at the -1 position[380]. Finally, although hypoglycosylation disorders frequently cause severe pathology[376], to our knowledge there are no reports of increased glycosylation adversely affecting function or trafficking of other receptors.

After confirming that β3 and β3(G32R) subunits had different glycosylation patterns, we sought to determine if the increased glycosylation and glycan processing of β3(G32R) mutant subunits were indeed responsible for changes in subunit surface trafficking. To identify the occupancy of a particular sequon for both wildtype and mutant receptors, we mutated each potentially glycosylated asparagine residue (N-glycosylation sites N33, N105, and N174) individually to glutamine in wildtype β3 and mutant β3(G32R) subunits, thereby creating glycosylation-defective subunits[335, 375, 381, 382]. We could not eliminate the possibility that these point mutations themselves could alter receptor assembly or function; however, we compared the characteristics of glycosylation-defective subunits bearing or lacking the G32R mutation. Furthermore, in a previous study we addressed several concerns regarding this method [335].

Consistent with previous results, β3 and β3(G32R) subunits displayed clear differences in molecular mass distribution when all three glycosylation sites remained intact. If this difference reflected increased glycosylation of β3(G32R) subunits at one specific site (i.e., N33, N105, or N174), inactivating that site with an Asn to Gln mutation ("NQ mutation") should yield proteins with identical molecular mass distributions. Moreover, the 51 kDa band, which presumably represented triply-glycosylated proteins, should disappear in any subunit bearing an NQ mutation. Therefore, we coexpressed α1 and $\gamma 2L^{HA}$ subunits with each wildtype/glycosylation-deficient β3 subunit (N33Q, N105Q, and N174Q; labeled as 1Q, 2Q, and 3Q, respectively) and each mutant/glycosylation-deficient β3 subunit (G32R/N33Q, G32R/N105Q, and G32R/N174Q; labeled as GR/1Q, GR/2Q, and GR/3Q, respectively (Figure 4D and 4E). Immunoblotting for wildtype β3 subunit surface and total protein yielded several interesting results. Most strikingly, inactivating the second or third glycosylation site (2Q or 3Q) drastically reduced expression of wildtype β3 subunits; indeed, expression of β3(2Q) subunits was nearly abolished. While intriguing, these deficits in protein expression made it impossible to compare the glycosylation patterns of these second- and third- glycosylation site mutants in the presence or absence of the G32R mutation and, thus, to determine conclusively if the molecular mass shifts in glycosylation-competent β3(G32R) subunits were due to increased occupancy of the second or third glycosylation sites. Nonetheless, these data indirectly suggest that glycosylation of N105 or N174 was not responsible for the molecular mass shift; given that disruption of these sites so drastically reduced protein expression, it seems likely that both sites are usually glycosylated and therefore could not have their occupancy increased by the G32R mutation.

Inactivating the first glycosylation site (1Q) produced remarkably different effects (Figure 4D and 4E). First, β3(N33Q) subunit expression levels were not significantly reduced compared to wildtype β3 subunit levels. Conversely, combining the G32R and N33Q mutations (GR/1Q) significantly reduced surface and total β3 subunit levels relative to both β3 and β3(N33Q) subunit levels. Despite the difference in overall β3 subunit levels, β3(N33Q) and

β3(G32R/N33Q) subunits had similar molecular mass distributions, suggesting that the G32R mutation may indeed have facilitated N33 glycosylation.

The β3 subunit constructs with NQ mutations allowed us to examine the effects of the G32R mutation in the absence of *N*-glycosylation at specific sequons. However, when all glycosylation sites were intact, the G32R mutation appeared to increase β3 subunit glycosylation; therefore, it was valuable to examine the effects of the mutation when both wildtype β3 and mutant β3(G32R) subunits had increased glycosylation. It is not possible to force glycosylation of individual sequons, but it is well known that NXT sequons are much more likely than NXS sequons to accept *N*-glycans. As described above, expression of glycosylation-deficient constructs indicated that the N33 site (sequon: NMS) was more likely to be occupied in the presence of the G32R mutation. Therefore, we hypothesized that β3 subunits in which Ser 35 was mutated to Thr (β3(S35T) subunits; ST) would exhibit a glycosylation pattern similar to that of β3(G32R) subunits. As shown in Figure 4D and 4E, the S35T mutation did increase glycosylation of β3 subunits, but the G32R mutation did not increase glycosylation further; that is, β3(S35T) and β3(G32R/S35T) subunits exhibited similar molecular mass distributions. Taken together, these results indicated that the G32R mutation increased β3 subunit *N*-glycosylation at N33.

However, it remained unclear whether glycosylation at N33 was responsible for decreased $\gamma 2L^{HA}$ subunit surface incorporation. We therefore evaluated levels of partnering subunits when coexpressed with β3(N33Q), β3(G32R/N33Q), β3(S35T), or β3(G32R/S35T) subunits. Surface levels of α1 subunits remained similar regardless of the coexpressed β3 subunit construct (Figure 4F). Conversely, $\gamma 2L^{HA}$ subunit surface levels decreased whenever the coexpressed β3 subunit contained the G32R mutation, but without regard to glycosylation site inactivation or strengthening (Figure 4G). Thus, these data suggested that glycosylation was not the mechanism by which the G32R mutation reduced γ2L subunit incorporation and, potentially, $GABA_A$ receptor function.

Presence of a basic residue at position 32 reduced surface expression levels of γ2L subunits and increased glycosylation at Asn-33.

If the change in glycosylation was not responsible for altered subunit expression patterns seen with mutant β3(G32R) subunits, some other property of the point mutation itself, such as charge, must have been causative. To investigate the effects of charge at residue 32, we mutated the β3 subunit residue G32 to lysine, glutamine, or glutamate (G32K, G32Q, and G32E, respectively). We co-expressed each of these β3 subunits individually with α1 and γ2L subunits and evaluated glycosylation patterns of β3 subunits and surface levels of all subunits (Figure 5). Interestingly, our results suggested that glycosylation of N33 clearly depended upon the charge of residue 32. Thus, 32.0 ± 3.9% of all wildtype β3 subunit surface protein was fully glycosylated (i.e., migrated at 51 kDa), compared to 67.4 ± 5.9 % of β3(G32R) and 56.7 ± 5.4 % of β3(G32K) subunit proteins (Figure 5 A1, A2). In contrast, 42.0 ± 4.9 % of β3(G32Q) subunit surface protein and only 2.8 ± 0.9 % of β3(G32E) subunit surface protein was fully glycosylated.

As in previous experiments, α1 subunit surface levels changed minimally when coexpressed with any β3 subunit (Figure 5B). Surprisingly, however, α1 subunit surface levels did decrease significantly when coexpressed with β3(G32K) subunits (89% of wildtype; $p < 0.05$). Conversely, $\gamma 2L^{HA}$ subunit surface levels were correlated with charge at β3 subunit residue 32. Specifically, $\gamma 2L^{HA}$ subunit surface levels decreased significantly when the coexpressed β3 subunit had a positively-charged residue (arginine or lysine) at position 32 (GK, 79.2 ± 3.3 % of wildtype, $n = 12$, $p < 0.001$), but $\gamma 2L^{HA}$ subunit surface levels decreased only slightly when the coexpressed β3 subunit had an uncharged residue at the same position (GQ, 93.5 ± 3.4 % of wildtype, $n = 12$) and did not change when the coexpressed β3 subunit had a negatively charged residue (GE, 1.02 ± 4.0 % of wildtype, $n = 11$). Taken together, these data (Figures 4 and 5) indicated that the positive charge introduced by the G32R mutation was responsible both for increasing N33 glycosylation and for decreasing $\gamma 2L^{HA}$ subunit incorporation; however, these two phenomena were not causally related to one another.

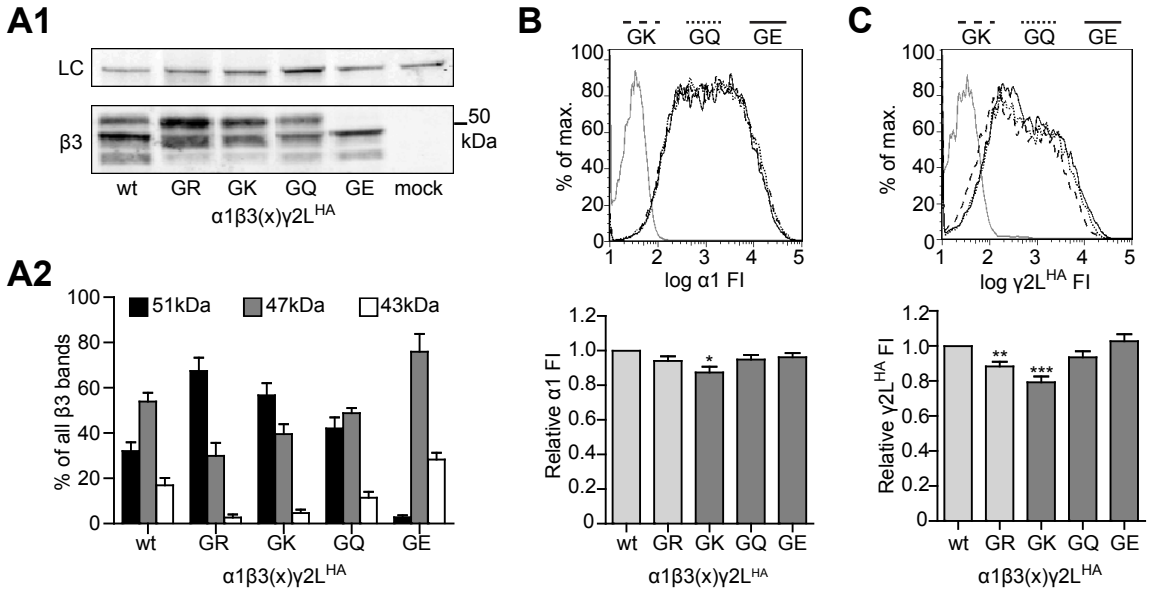

Figure 5. Presence of a basic residue at position 32 of β3 subunits increased β3 subunit glycosylation at Asn-33 and reduced γ2LHA subunit incorporation into surface α1β3γ2LHA GABAA receptors.

A1. Surface proteins were isolated from HEK293T cells expressing equimolar amounts of α1, γ 2LHA, and different β3 subunits. In lane 1, the β3 subunit was not mutated (wt), and in lane 2, the β3 subunit contained the G32R mutation (GR). In lanes 3, 4, and 5, Gly 32 was mutated to lysine (GK), glutamine (GQ), or glutamate (GE), respectively. The upper panel presents staining for Na+/K+ ATPase as a loading control (LC), and the lower panel presents staining for β3 subunits. The β3 subunits migrated as three populations, with bands seen at approximately 51, 47, and 43 kDa. **A2.** Integrated intensity was calculated for all β3 subunit bands and normalized to the integrated band intensity of the Na+/K+ ATPase. The normalized integrated intensities for each β3 subunit band were summed, and the proportions of β3 protein migrating at 51 kDa (black), 47 kDa (gray), and 43 kDa (white) were calculated. **B-C.** Surface levels of α1 (B) and γ2LHA(C) subunits in cells expressing α1, γ2LHA, and Gly32 mutant β3 subunits were determined using flow cytometry. Upper panels present fluorescence intensity histograms in which the abscissa denotes fluorescence intensity in arbitrary units graphed on a logarithmic scale (FI) and the ordinate denotes percentage of maximum cell count (% of max). Fluorescence intensity histograms from mock-transfected cells (solid gray line) are overlaid with histograms from cells expressing α1, γ2LHA, and either β3(G32K) (dashed black line), β3(G32Q) (dotted black line), or β3(G32E) (solid black line) subunits. Lower panels present normalized fluorescence intensities for each condition. Mean fluorescence intensities from cells transfected with blank vector alone ("mock") were subtracted from mean fluorescence intensities of cells transfected with α1, γ2LHA, and the indicated β3 subunits. All mock-subtracted fluorescence intensities were normalized to the mock-subtracted fluorescence intensity of the cells expressing β3 subunits. Statistical analysis was performed using one-way ANOVA with Tukey's post-test. ** $p < 0.01$, *** $p < 0.001$ compared to wildtype.

The G32R mutation reduced current density independent of glycosylation.

Up to now, we observed that the G32R mutation caused glycosylation-independent changes in subunit expression patterns that could reduce the function of αβγ $GABA_A$ receptors; however, those changes were not large enough to account for the reduction in current amplitude that was previously reported[310]. This discrepancy suggested that expression of β3(G32R) subunits might also affect receptor gating. Furthermore, although subunit expression patterns depended upon charge at residue 32 rather than glycosylation at residue 33, any such changes in gating might still be glycosylation-dependent.

To determine how mutant β3(G32R) subunits affected $GABA_A$ receptor function, we used a rapid exchange system to apply 1 mM GABA for 400 ms to lifted HEK293T cells coexpressing α1, γ2L, and β3, β3(G32R), β3(N33Q), or β3(G32R/N33Q) subunits (Figure 6A). Wildtype receptors displayed a current density of 845.8 ± 33.93 pA/pF (n = 34), nearly 50% higher than current density of receptors containing mutant β3(G32R) subunits (454.3 ± 57.46 pA/pF, n = 32, $p < 0.001$ compared to wildtype) (Figure 6A, 6B); this difference was consistent with previously reported data[310]. When N33 glycosylation was abolished by introducing the β3(N33Q) subunit mutation alone, current density also decreased (411.7 ± 19.61 pA/pF, n = 21, $p < 0.001$ compared to wildtype). However, when the G32R mutation was introduced together with the N33Q mutation, current density decreased further (160.4 ± 46.99 pA/pF, n = 13, $p < 0.001$ compared to wildtype and $p < 0.01$ compared to the β3(N33Q) subunit alone). These results suggested that although eliminating N33 glycosylation by introducing the N33Q mutation itself reduced current density (due to either the absence of the glycan or the presence of the point mutation), the CAE-associated β3(G32R) subunit mutation also impaired receptor function independent of N33 glycosylation.

In summary, both β3(G32R) and β3(N33Q) point mutations significantly reduced current densities of α1β3γ2L receptors. However, the effects of these mutations were additive, indicating

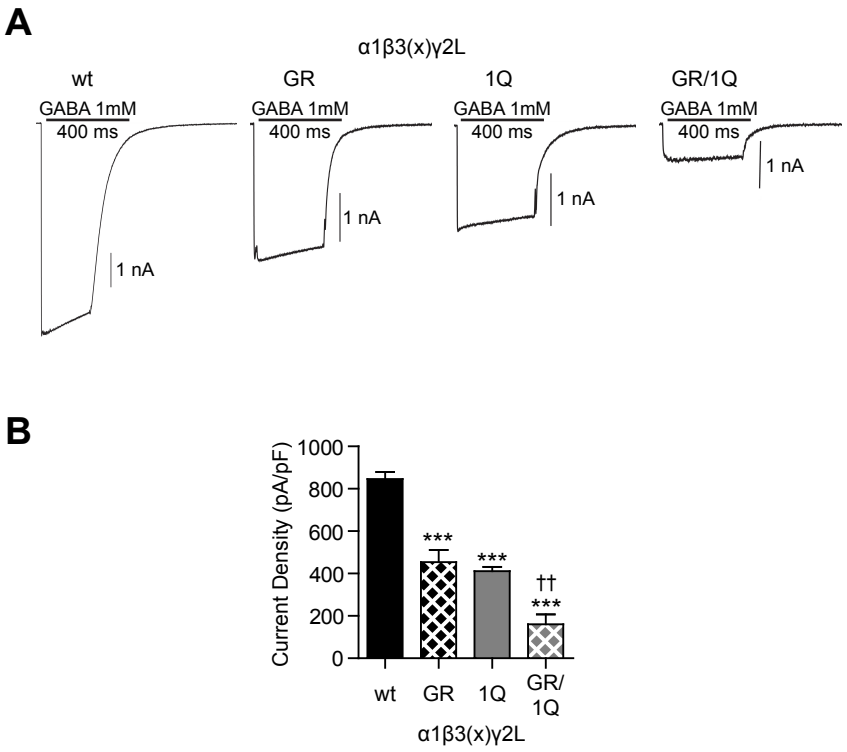

Figure 6. The β3(G32R) mutation reduced current density from α1β3γ2L receptors even if the first glycosylation site was inactivated.

A. Currents were recorded from lifted whole HEK293T cells transfected with equimolar amounts of α1, γ2L, and either β3(wt), β3(G32R), β3(N33Q), or β3(G32R/N33Q) subunit cDNAs (wt, GR, 1Q, and GR/1Q, respectively). Cells voltage-clamped at -20 mV and subjected to a 400 ms pulse of 1 mM GABA. Subunit identity and length of GABA application (black line) are indicated above the current traces. Scale bar = 1 nA. **B.** Mean current densities (pA/pF) from cells expressing α1, γ2L, and either β3(wt), β3(G32R), β3(N33Q), or β 3(G32R/N33Q) subunits were calculated*** indicates $p < 0.001$ compared to wt, and †† and ††† indicate $p < 0.01$ and $p < 0.001$, respectively, compared to NQ.

that the G32R point mutation reduced current density even when N33 was not glycosylated. Taken together, these data suggest that the G32R mutation reduced current density by a mechanism that was independent of increasing N33 glycosylation and furthermore that this region of the N-terminal α-helix could play a role in channel gating.

Presence of a charged residue at position 32 of the β3 subunit reduced current density of α1β3γ2L receptors.

To this point, we demonstrated that the G32R mutation increased glycosylation at β3 subunit residue N33, altered $GABA_A$ receptor assembly, and reduced current density. Contrary to previous hypotheses, the changes in subunit expression and receptor function were not due to increased β3 subunit glycosylation; the changes in subunit expression instead could be attributed to introduction of positive charge at residue 32. Therefore, we investigated whether or not the charge of residue 32 was also responsible in part for the lower current densities observed in α1β3(G32R)γ2L receptors. We applied 1 mM GABA for 4 s to lifted HEK293T cells coexpressing α1, γ2L, and either β3, β3(G32R), β3(G32K), β3(G32E), or β3(G32Q) subunits and determined current densities (Figure 7A). As expected, α1β3(G32R)γ2L receptor current densities were lower ($p < 0.001$) (GR, 409 ± 11 pA/pF, n = 8) than those of α1β3γ2L receptors (wt, 903 ± 22 pA/pF, n = 8) (Figure 7B). When residue 32 was mutated to another basic residue (i.e., G32K), α1β3(G32K)γ2L receptor current densities were also significantly reduced (GK, 577 ± 66 pA/pF, n = 13, $p < 0.01$). Interestingly, current densities were also reduced in α1β3(G32E)γ2L receptors; that is, when residue 32 was mutated to an acidic amino acid (GE, 606 ± 98 pA/pF, n=10, $p < 0.05$). However, when residue 32 was mutated to a large but neutral amino acid (i.e., G32Q), receptor current density did not differ significantly from that of wildtype receptors (GQ, 870 ± 35 pA/pF, n = 10). Thus, receptor function was altered due to introduction of a charged residue at this position. It is possible that the charged residues can form new salt bridges that altered channel function (this hypothesis is further addressed below).

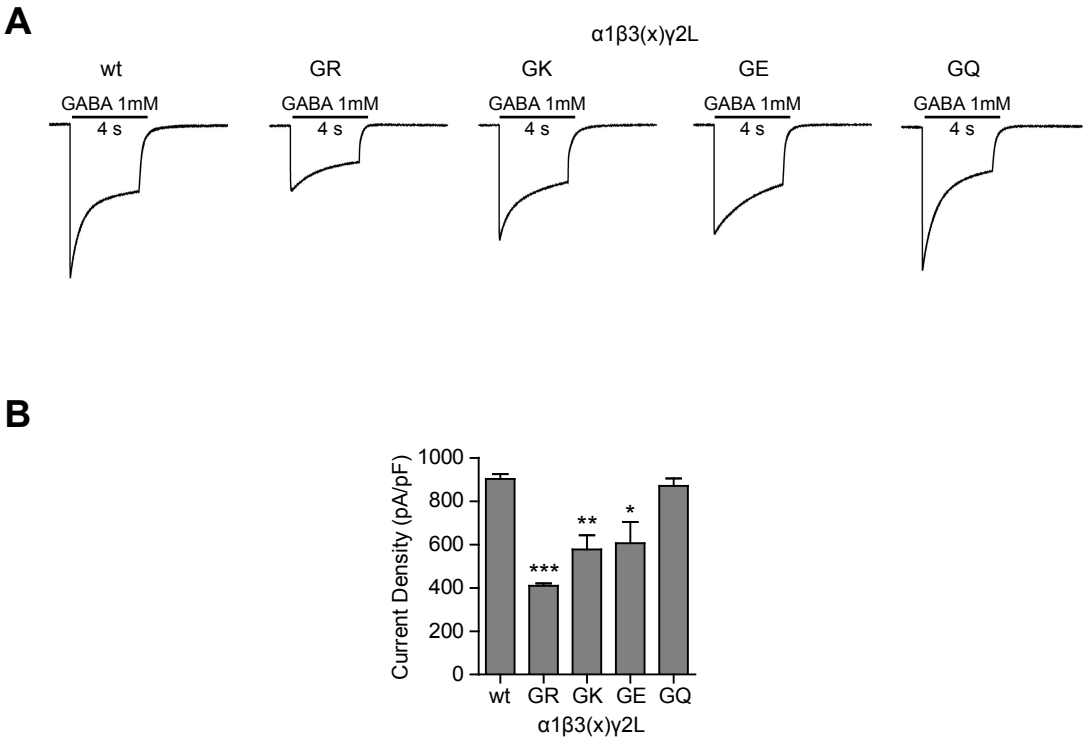

Figure 7. Introduction of a charged residue at position 32 reduced current amplitudes in α1β3γ2L GABA$_A$ receptors.

A. Currents were recorded from lifted whole HEK293T cells transfected with equimolar amounts of α1, γ2L, and either β3, β3(G32R), β3(G32K), β3(G32E), or β3(G32Q) subunit cDNAs (wt, GR, GK, GE, and GQ, respectively). Cells were voltage-clamped at -20 mV and subjected to a 4 s pulse of 1 mM GABA. Subunit identity and length of GABA application (black line) are indicated above the current traces. Scale bar = 1 nA. **B.** Mean current density (pA/pF) from cells expressing α1, γ2L, and either β3, β3(G32R), β3(G32K), β3(G32E), or β 3(G32Q) subunits were calculated. All data are presented as mean ± S.E.M., and significance was determined using one-way ANOVA with Tukey's post-test. *, **, and *** indicate $p < 0.05$, 0.01, and 0.001, respectively, compared to wildtype.

α1β3(G32R)γ2L receptors were more likely to enter short open states and had reduced mean open times.

The α1β3(G32R)γ2L^{HA} receptors displayed many macroscopic kinetic changes (slightly slower activation, faster desensitization, and faster deactivation) that were consistent with reduced charge transfer; however, most of these changes were not significant and could not explain the nearly 50% reduction of current density in mutant compared to wildtype receptors. Consequently, we employed cell-attached single-channel recording to examine the microscopic kinetic properties of α1β3γ2L receptors containing β3 or β3(G32R) subunits (Figure 8A). Wildtype and mutant receptors had identical single channel amplitudes (Figure 8B), but mutant receptors had significantly reduced mean open times (Figure 8C). The reduction was not due to alterations of open time constants themselves, because the open duration histograms of wildtype and mutant receptors (Figure 8D) both were fitted best by three time constants whose mean durations did not change (Figure 8E). However, the relative contributions of the time constants did change (Figure 8F); specifically, the relative proportion of the shortest open state was significantly increased in mutant receptors (α1β3γ2L receptors τ1% = 23.1 ± 3.3 %; α1β3(G32R)γ2L receptors τ1% = 78.4 ± 4.2 %; n = 4, $p < 0.001$). Therefore, the G32R mutation reduced $GABA_A$ receptor-mediated inhibition both by introducing a positive charge that discouraged formation of high-functioning α1β3γ2L receptors in favor of low-functioning α1β3 receptors and β3 homopentameric receptors and by inducing those α1β3γ2L receptors to enter shorter open states, thereby reducing mean single channel open time.

The β3(G32R) mutation was predicted to alter salt bridges and conformation at β3-γ2 and β3-β3 subunit interfaces

To gain insight into the mechanism by which the β3(G32R) mutation affected receptor assembly and channel gating, we performed homology modeling of wildtype and mutant receptors using the nAChR α1 subunit extracellular domain structure (PDB ID 2qc1)[153] as a template (Figure 10). In α1β3γ2L receptor isoforms, the major structural changes induced by the

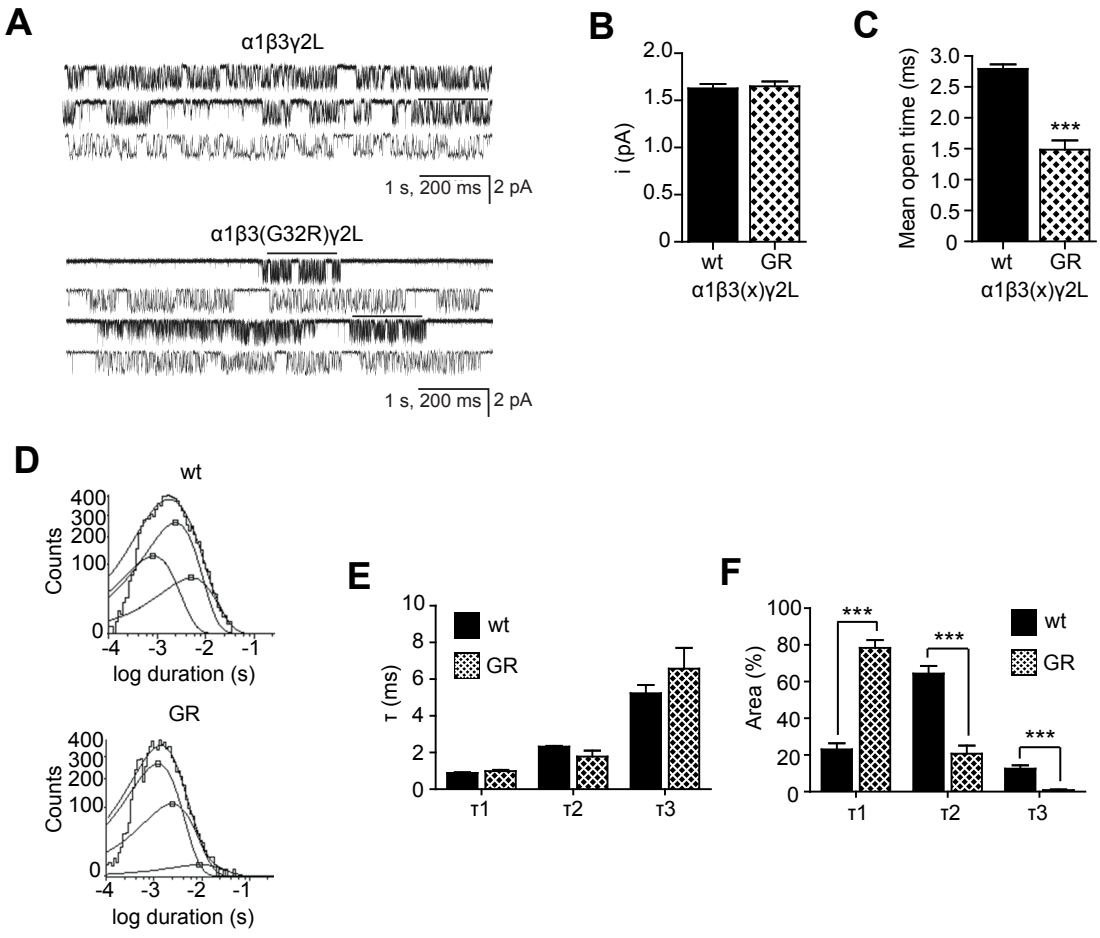

Figure 8. The G32R mutation reduced mean single-channel open time of α1β3γ2L GABAA receptors by promoting occupancy of shorter-lived open states.

A. Single-channel currents were recorded from HEK293T cells expressing α1, γ2L, and either β 3 (upper panel) or β3(G32R) (lower panel) subunits. Recording was conducted in the cell-attached configuration, with cells voltage-clamped at +80 mV and 1 mM GABA present in the recording electrode. **B.** Single-channel conductance (pA) was calculated for α1β3γ2L and α 1β3(G32R)γ2L GABAA receptors. **C.** Mean open time (ms) was calculated for α1β3γ2L and α 1β3(G32R)γ2L GABAA receptors. **D.** Frequency histograms of channel open durations were best fitted with three exponential functions. The left panel presents histograms for α1β3γ2L receptors and the right panel presents histograms for α1β3(G32R)γ2L receptors. **E.** Means of the three open durations (ms) were calculated. **F.** The relative contribution (%) of each open state was calculated. All data are expressed as mean ± S.E.M., and significance was calculated using two-tailed Student's t-test. *** indicates $p < 0.001$ compared to wt.

β3(G32R) mutation occurred at the interface between the principal (+) side of the γ2L subunit and the complementary (-) side of the β3 subunit (γ2-β3 interface). In both α1β3γ2L (Figure 9A) and α1β3(G32R)γ2L (Figure 9B) receptors, all subunits were predicted to begin with a random coil leading into an α-helix. However, the G32R mutation induced a conformational change in the β3 subunit α-helix, causing the random coil to project in a slightly different direction. Moreover, the side-chain of Arg 32 extended across the γ2-β3 subunit interface, forming a salt bridge with γ2 subunit residue Asp 123, which lies in a motif previously established to be necessary for γ2-β3 subunit interaction[92].

Because both α1β3(G32K)γ2L and α1β3(G32E)γ2L receptors also displayed reduced current densities, we performed homology modeling of these isoforms as well. These mutations also induced structural changes primarily at the γ2-β3 subunit interface. Interestingly, the side-chain of the β3 subunit residue K32 angled toward the cell membrane and formed a salt bridge with the γ2 subunit residue E217, which participates in a salt bridge network disrupted by the epilepsy-associated γ2(R82Q) mutation[316] (Figure 9C). The side-chain of the β3 subunit residue E32, conversely, extended toward the γ2 subunit but did not come within 4Å of any γ2 subunit atoms (Figure 9D).

We demonstrated that β3(G32R) subunits were expressed on the cell surface at much higher levels than β3 subunits, suggesting that mutant subunits might assemble into homopentamers. Consequently, we also created homology models of β3 and β3(G32R) homopentameric receptors. Unsurprisingly, structural changes occurred at subunit interfaces. Strong salt bridges existed at the interface of wildtype β3 subunits (Figure 10A), but when R32 was introduced (Figure 10B), its side chain formed three new salt bridges with D94 of the adjacent β3(G32R) subunit. In summary, homology modeling provided a potential explanation for the changes in subunit surface expression associated with the β3 subunit G32R mutation. All structural changes occurred at subunit interfaces, suggesting that the point mutation could perturb subunit oligomerization.

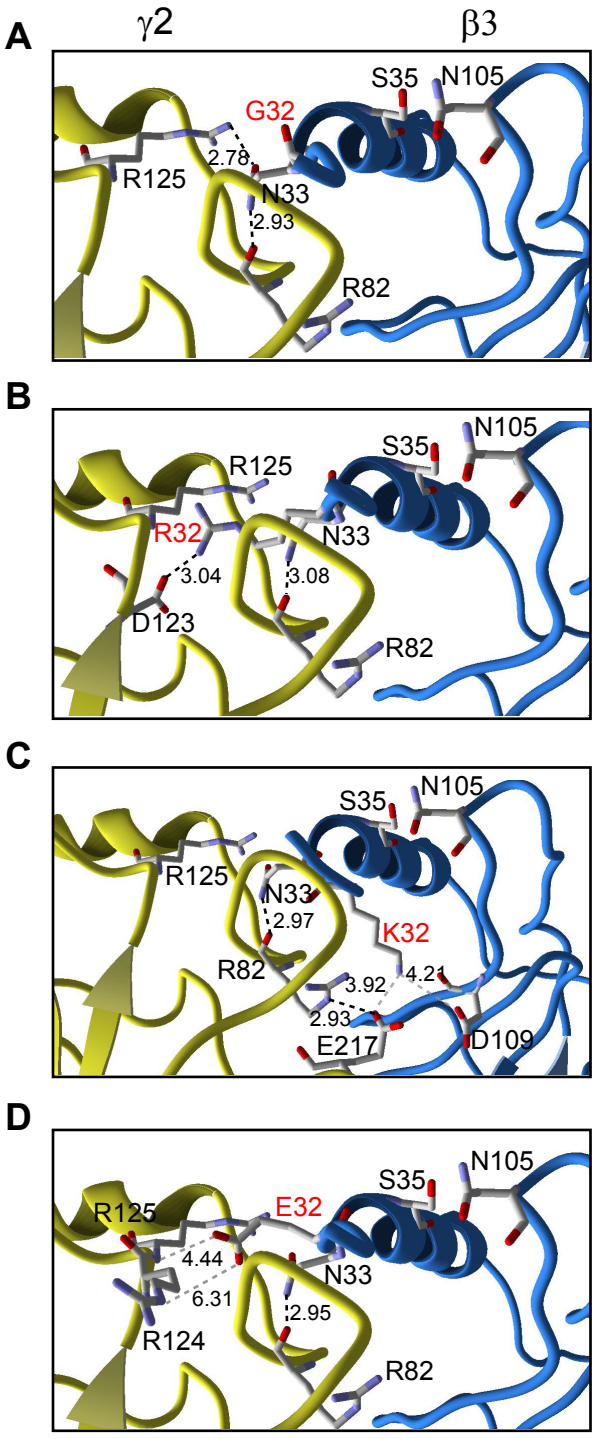
A
γ2
β3
S35
N105
G32
2.78
R125
N33
2.93
R82
B
N105
S35
R125
R32
N33
3.04
3.08
D123
R82
C
S35
N105
R125
N33
2.97
K32
R82
3.92
4.21
2.93
E217
D109
D
N105
S35
R125
E32
4.44
N33
6.31
2.95
R124
R82

Figure 9

Figure 9. β3(G32) mutations changed conformation and salt bridge formation at the γ2-β3 interface of heteropentameric α1β3γ2L receptors.

Three-dimensional models of α1, β3, and γ2 subunit extracellular domains were created (see Methods) and threaded onto the *Lymnaea stagnalis* acetylcholine binding protein structure in the order γ2-β3-α1-β3-α1 to model ternary heteropentameric α1β3γ2L receptors. Point mutations were introduced into β3 subunit structures and the resulting energy-minimized models were examined for structural changes. **A.** A portion of the interface between the γ2 subunit (yellow) and the wildtype β3 subunit (blue) is presented. The perspective is from outside the receptor, such that the synaptic cleft would be located at the top of the figure. Residues discussed in the text, including the mutated G32, the first glycosylation sequon residues N33 and S35, and the second glycosylation site N105, are labeled, and predicted salt bridges are indicated by dotted lines. Adjacent numbers indicate the distance in angstroms between the two atoms forming the salt bridge. Two γ2 subunit residues are also identified: R125, which is predicted to form a salt bridge with β3(N33); and R82, which was mutated to Q in a family with GEFS+. Side-chains are colored in the CPK scheme; that is, carbon atoms are grey, oxygen atoms are red, and nitrogen atoms are blue. **B-D.** Views of the γ2-β3 interface in α1β3(G32R)γ2L (B), α1β3(G32K)γ2L (C), and α1β3(G32E)γ2L (D) receptors are presented as in panel A. Salt bridges longer than 3.5 Å are indicated by grey dotted lines, while salt bridges shorter than 3.5 Å are indicated by black dotted lines.

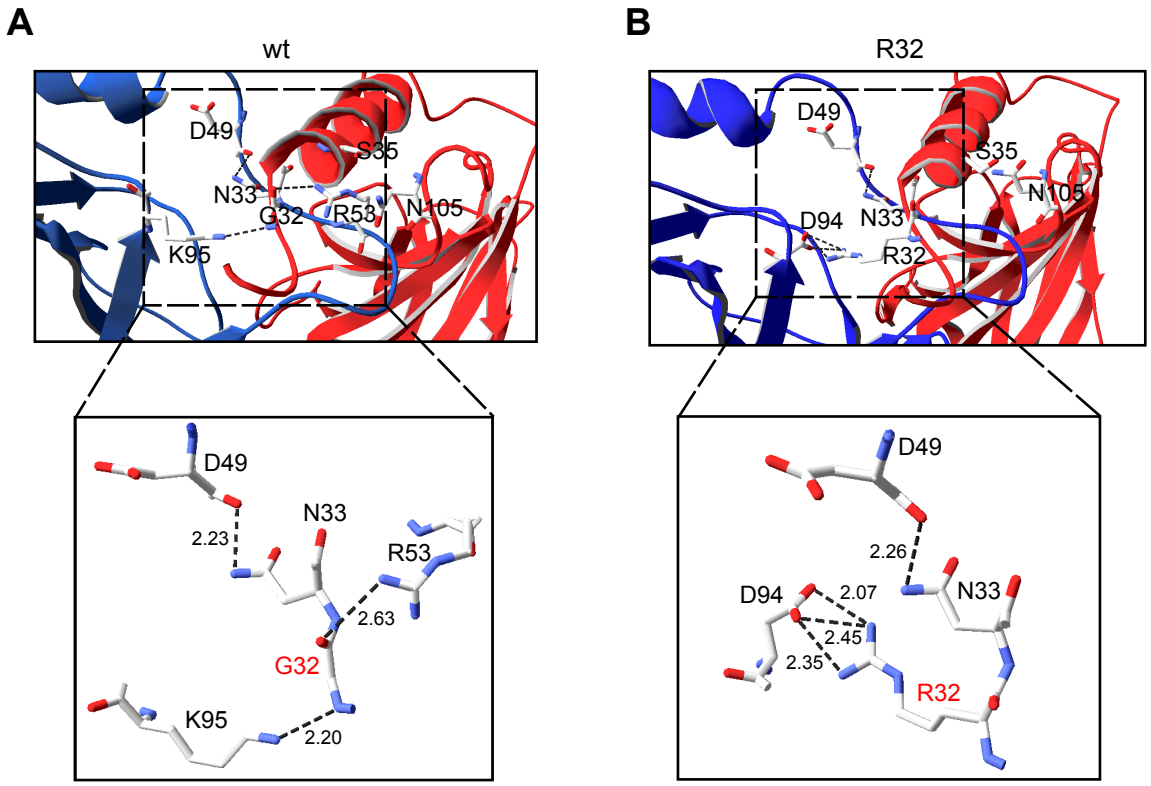

Figure 10. The β3(G32R) mutation changed salt bridge formation at the β3-β3 interface of homopentameric receptors.

Three-dimensional models of β3 homopentamers were constructed as described in Figure 10. **A.** The upper panel illustrates a portion of the interface between two wildtype β3 subunits. Although the two subunits are identical, one is presented in red and one in blue for clarity. The lower panel presents a magnification of the area boxed in the upper panel. **B.** The upper panel illustrates a portion of the interface between two β3(G32R) subunits, and the lower panel presents a magnification of the area boxed in the upper panel.

Discussion

The N-terminal α-helix: new roles in receptor assembly and gating?

A large body of work exists documenting the $GABA_A$ receptor subunit domains that are responsible for receptor assembly and trafficking, GABA binding, and coupling of agonist binding to channel gating[167]. However, the distal N-terminal domain, which comprises a random coil followed by an α-helix, has not been demonstrated to be important for these processes. In fact, the helix was entirely absent in recently-discovered prokaryotic nAChR homologs[156, 383]. Helical integrity was shown to be necessary for proper biogenesis of nAChR α7 subunits, but most residues could be mutated without affecting subunit expression[384]. In our experiments, multiple point mutations of G32 and N33 residues in the distal α-helix of β3 subunits caused changes in assembly as well as gating that were not attributable fully to the glycosylation changes induced by the mutations. Our results suggest that unexpectedly the N-terminal α1-helix may be important for assembly and function of $GABA_A$ receptors containing β3 subunits.

The β3 subunit G32R mutation and receptor heterogeneity

Our data suggested that the G32R mutation promoted formation of binary α1β3 receptors and β3 homopentamers and decreased formation of ternary α1β3γ2L receptors. Wildtype β3 subunits are known to assemble more promiscuously than most other $GABA_A$ receptor subunits in heterologous systems; β3 subunits reached the cell surface when expressed alone, and both β3 and γ2L subunits were detected on the cell surface when coexpressed together without an α subunit[90]. We obtained similar results when β3 subunits were coexpressed with β, δ, ε, or θ subunits (data not shown). In contrast, β2 subunits are retained intracellularly and degraded in the absence of coexpressed α subunits even though β2 and β3 subunits have very similar sequences. In previous studies, four amino acid residues (G171, K173, E179, R180) conferred

the ability to form β3 subunit homopentamers[90]. According to our model, these residues are also predicted to lie on the (-) face of β3 subunits, but are much closer to the cell membrane than the G32 residue. Thus, we may have uncovered a previously unknown role for the N-terminal α-helix in regulating β3 homopentamer assembly.

β3 subunit glycosylation: patterns and their dependence on receptor subunit composition

Although we have shown that hyperglycosylation ultimately was not responsible for the effects of the β3(G32R) mutation on receptor assembly and function, our studies elucidate the characteristics and importance of β3 subunit *N*-glycosylation. We demonstrated that all three *N*-glycosylation sites on wildtype β3 subunits could be glycosylated in HEK293T cells, though many β3 subunits were not glycosylated at N33. Importantly, other investigators have observed similar β3 subunit glycosylation patterns in mouse cortical neurons (M.J. Gallagher, private communication). Interestingly, we also showed that β3 subunits retain some unprocessed, high-mannose glycans despite being assembled into receptors and trafficked to the cell surface. This occurred in all tested receptor isoforms (i.e., β3, α1β3, and α1β3γ2L); however, the proportion of β3 subunits containing endo H sensitive glycans was correlated with the number of different subunits expressed. We recently observed a similar phenomenon in β2 subunits. In heterologous systems, all β2 subunit bands were endo H resistant when only α1 and β2 subunits were coexpressed, but an endo H sensitive population appeared if γ2 subunits were added. Furthermore, β2 subunits from heterozygous γ2 subunit knockout mice, which may form α1β2 receptors due to γ2 subunit deficiency, had a larger endo H resistant population than β2 subunits from wildtype mice (W.Y. Lo, A.H. Lagrange, C.C. Hernandez, K.N. Gurba, and R.L. Macdonald, in review). Taken together, these findings suggest that incorporation of non-β subunits might alter β subunits such that their glycans become accessible for modification in the Golgi apparatus. It will be interesting to determine if glycan structure contributes to the characteristic current properties of binary and ternary receptors.

Although the G32R mutation appeared to promote increased assembly of binary α1β3 and homopentameric β3 receptors, and those isoforms promoted glycan maturation, the G32R mutation also affected glycan processing independent of receptor stoichiometry. All wildtype receptors (i.e., β3, α1β3, and α1β3γ2L) contained at least a small population of β3 subunits that were fully endo H sensitive. However, that population virtually disappeared in the corresponding mutant receptor isoforms. It may be worthwhile to investigate whether microheterogeneity (i.e., sugar composition) as well as macroheterogeneity (i.e., sequon occupancy) of *N*-glycans can affect receptor function.

Altered salt bridge formation and receptor conformation may be responsible for changes in assembly, glycosylation, and gating, leading to reduced $GABA_A$ receptor-mediated inhibition.

Because $GABA_A$ receptors have not been crystallized, homology models are limited to nAChR[97, 153] and AChBP[98, 385] templates, many of which have poor resolution in their N-terminal domains. Therefore, while homology models of $GABA_A$ receptors are necessarily speculative, they nonetheless provide valuable insight regarding potential interactions. In our models, mutating the G32 residue to R32 induced formation of new salt bridges at the γ2-β3 and β3-β3 interfaces in ternary and homopentameric receptors, respectively. The β3-β3 salt bridges were particularly strong, and would likely increase the affinity of homodimer formation. This, in turn, could promote formation of isoforms containing a β3-β3 interface. Such interfaces are not predicted to exist in ternary receptors, which are thought to have a γ-β-α-β-α orientation (anticlockwise as viewed from the synaptic cleft)[328, 340]. However, in binary receptors, the γ2 subunit presumably is replaced by either an α1 or a β3 subunit; the latter would introduce a β3-β3 interface. It is possible that the salt bridges introduced by the G32R mutation promote β3(G32R) subunit homodimerization, which in turn could "seed" the formation of $(\alpha1)_2(\beta3)_3$ and β3 receptor isoforms, thereby increasing β3 subunit surface expression. It is somewhat less clear how salt bridge formation between R32 and γ2(D123) could discourage incorporation of γ2 subunits;

however, it is important to note that salt bridges can be destabilizing[386], and that γ2 subunit (122-129) integrity was essential for γ2-β3 subunit interaction[92]. It is also worth mentioning that the epilepsy-associated mutation γ2(R82Q), which has been shown to disrupt receptor assembly[100, 316] is located in the γ2 subunit loop nearest to the N-terminal domain of the β3 subunit α-helix. Indeed, point mutations throughout this loop impaired γ2 subunit incorporation. Thus, it is possible that any structural changes in this area, whether on γ2 or β3 subunits, could disturb an important assembly domain and result in preferential expression of low efficacy binary αβ3 receptors and homopentameric β3 receptors instead of high efficacy ternary αβ3γ2 receptors, thereby causing disinhibition.

How might the β3(G32R) mutation contribute to epileptogenesis?

The electroencephalographic signature of an absence seizure involves generalized, synchronous spike-wave activity, reflecting oscillations in thalamocortical circuits. The location of the seizure discharge origin within these circuits remains a subject of debate[387], making it difficult to predict how changes in the function of a particular ion channel could initiate seizures. However, it is known that both thalamic reticular nucleus and cortex (particularly somatosensory cortex) participate in synchronized activity. Importantly, the β3 subunit subtype predominates in the reticular nucleus throughout life and in cortex during development[45, 49, 57].

It was recently demonstrated that tonic GABAergic current is paradoxically increased in thalamocortical neurons from two rat models of absence epilepsy[388], whereas we discovered many changes wrought by the G32R mutation that decreased mutant receptor function. This could indicate that the G32R mutation might primarily promote hyperexcitability through cortical and/or postsynaptic (i.e., phasic current-mediating) $GABA_A$ receptors. If so, this could suggest a reason for this mutation being associated with childhood absence epilepsy, because cortical β3 subunit expression declines throughout childhood. Thus, it is possible that deficits in $GABA_A$ receptors containing β3 subunits could affect children more significantly than adults because in

children, a substantial proportion of cortical receptors contain β3 subunits. Subsequently, associated epilepsy syndromes might remit as β2 subunits displace β3 subunits in adulthood.

CHAPTER V

THE GABRA6 MUTATION, R46W, ASSOCIATED WITH CHILDHOOD ABSENCE EPILEPSY, ALTERS α6β2γ2L and α6β2δ $GABA_A$ RECEPTOR CHANNEL GATING AND EXPRESSION

Abstract

A $GABA_A$ receptor α6 subunit mutation, R46W, was identified as a susceptibility gene that may contribute to the pathogenesis of childhood absence epilepsy (CAE), but the molecular basis for alteration of $GABA_A$ receptor function is unclear. The R46W mutation is located in a region homologous to a $GABA_A$ receptor γ2 subunit missense mutation, R82Q, which is associated with CAE and febrile seizures in humans. To determine how this mutation reduces GABAergic inhibition, we expressed wild-type (α6β2γ2L and α6β2δ) and mutant (α6(R46W)β2γ2L and α6(R46W)β2δ receptors in HEK 293T cells in order to characterize their whole-cell and single-channel currents and surface and total expression levels. Our results indicated that the R46W mutation impaired gating and assembly of both α6(R46W)β2γ2L and α6(R46W)β2δ receptors by complex mechanisms. Compared to wild-type currents, α6(R46W)β2γ2L and α6(R46W)β2δ receptors had a reduced current density, α6(R46W)β2γ2L currents desensitized to a greater extent and deactivated at a slower rate, α6(R46W)β2δ receptors did not desensitize but deactivated faster and both α6(R46W)β2γ2L and α6(R46W)β2δ single channel current mean open times and burst durations were reduced. Surface levels of coexpressed α6(R46W), β2 and δ, but not γ2L, subunits were decreased. "Heterozygous" coexpression of α6(R46W) and α6 subunits with β2 and γ2L subunits produced intermediate macroscopic current amplitudes by increasing incorporation of wild-type and decreasing incorporation of mutant subunits into receptors trafficked to the surface. Taken together, these

findings suggest that, similar to the γR82Q mutation, the CAE-associated α6(R46W) mutation could cause neuronal disinhibition and thus increase susceptibility to generalized seizures through a reduction of αβγ and αβδ receptor function and expression.

Introduction

$GABA_A$ receptors, the major mediators of inhibition in the mammalian central nervous system, belong to the Cys-loop ion channel superfamily, which includes glycine, nicotinic acetylcholine (nAChR), and serotonin 5-HT_3 receptors. $GABA_A$ receptor subunits have a large N-terminal extracellular domain and four transmembrane segments (M1, M2, M3, M4) that are homologous to the ACh binding protein (AChBP) N-terminal domain[98] and the transmembrane domain of the *Torpedo marmorata* ACh receptor (AChR)[389]. $GABA_A$ receptors are formed by pentameric assembly of 19 different subunit subtypes (α1-α6, β1-β3, γ1-γ3, δ, ε, π, θ, and ρ1-ρ3), although the majority of receptors are thought to be αβγ and αβδ receptor isoforms that mediate both phasic inhibitory synaptic transmission and tonic perisynaptic inhibition[390].

Idiopathic epilepsy syndromes are primarily genetic diseases. They are characterized by typical seizure types and EEG abnormalities that are not associated with structural brain lesions[391]. Mutations or variants associated with idiopathic generalized epilepsies (IGEs) have been identified in *GABRA1*, *GABRB3*, *GABRG2* and *GABRD* genes[392]. A novel $GABA_A$ receptor α6 subunit mutation, R46W, was recently described in an IGE cohort study in a patient with childhood absence epilepsy (CAE)[393], but no evidence of channel impairment was reported. The mutation is located in a region homologous to that of the $GABA_A$ receptor γ2 subunit mutation, R82Q (R43Q in the mature peptide), which is associated with CAE and febrile seizures in humans[314, 394]. Mutant γ2(R82Q) subunits reduced both surface α1β2γ2(R82Q) receptor levels[395] and receptor currents[313], suggesting impairment of both assembly and function of $GABA_A$ receptors.

Homology modeling of the N-terminal extracellular domain of human β2-α6-β2-α6-γ2 and β2-α6-β2-α6-δ $GABA_A$ receptors suggested that the R46W mutation (Figure 1*A* and Figure 10*C*) is located within a loop (L1) between the α-helix and the β1-sheet (Figure 1*B*), where it contributes to the α-β, α-γ and α-δ subunit interfaces in assembled receptors. In contrast, the γ2 subunit mutation, R82Q, (Figure 1*A*) only contributes to the γ-α interface. Sequence alignment of the AChBP with the α-helix-L1-β1-sheet region of human α6, γ2L, β2 and δ subunits and the *T. marmorata* AChR α1 subunit showed conserved structural relationships (Figure 1*B*).

To gain further insights into the effects of the R46W mutation on $GABA_A$ receptor function and assembly, we studied the gating properties and surface expression of α6β2γ2, α6/α6(R46W)β2γ2, α6(R46W)β2γ2, α6β2δ, α6/α6(R46W)β2δ and α6/α6(R46W)β2δ subunits expressed in HEK293T cells. We found that the R46W mutation impaired gating and assembly of both α6(R46W)β2γ2L and α6(R46W)β2δ receptors and substantially reduced the current density of both receptors. In addition, surface levels of coexpressed α6(R46W), β2 and δ subunits, but not γ2L subunits, were decreased. These findings suggested that the CAE-associated α6(R46W) mutation could cause neuronal disinhibition and thus increase susceptibility to generalized seizures through a reduction of αβγ and αβδ receptor function and expression, sharing a mechanism with the γR82Q mutation linked with CAE in humans.

Materials and Methods

cDNA constructs

cDNAs encoding human α6, β2, γ2L and delta $GABA_A$ receptor subunit subtypes (GenBank accessions NM000811, NM000813, NM198904, and NM000815, respectively) were subcloned into the plasmid expression vector pcDNA3.1 (Invitrogen, Carlsbad, CA) using standard techniques. The human α6 subunit mutation, R46W, was generated by site-directed

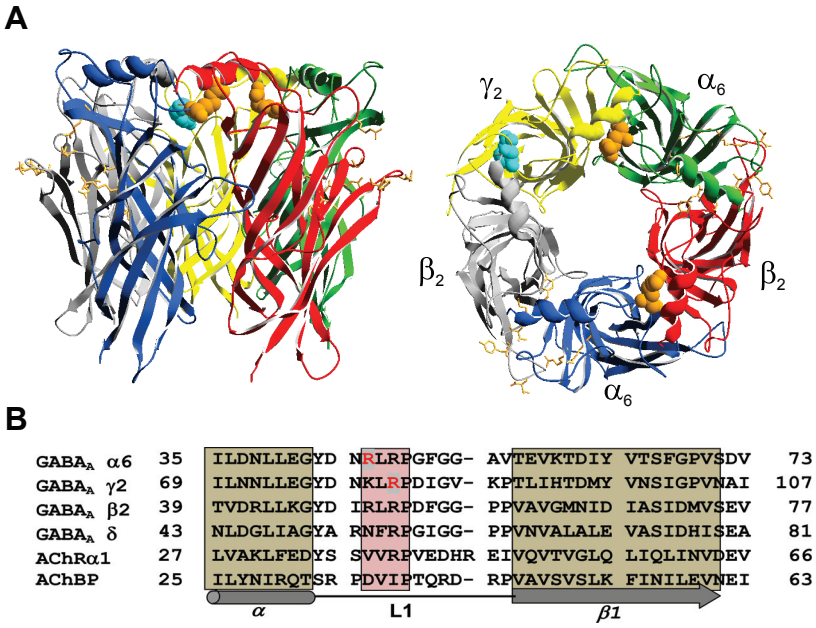

Figure 1. The α6 subunit mutation, R46W, contributes to the α/β and α/γ subunit interfaces in assembled GABA$_A$ receptors.

A. A structural model of the N-terminal extracellular domain of human β2α6β2α6γ2 receptors viewed from outside the pentamer (left panel) and orthogonal toward the membrane (right panel) was developed. Mutations at α6R46 (in orange) and γ2R82 (in aqua) on the L1-loop at the α/β, α/γ, and γ/β interfaces are shown in a space-fill representation. Residues involved in GABA binding at the β/α interface are shown as well (in orange in a stick representation). B. Sequence alignments of the α-helix, L1-loop and the β1-sheet domain of human α6, β2, γ2 and δ subunits from the GABAR family, the nicotinic acetylcholine receptor α1 subunit (AChRα1) and the acetylcholine-binding protein (AChBP) are presented. The basic charged residues linked to CAE are shown in red within a pink box representing conserved residues into the L1-loop, and the light grey boxes represent residues in the α-helix and β1-sheet across the subunits.

mutagenesis using the QuikChange Site-Directed Mutagenesis Kit (Stratagene, La Jolla, CA) and verified by sequencing. FLAG (DYKDDDDK) or HA (YPYDVPDYA) epitopes were inserted between amino acids 4 and 5 of the mature α6, γ2L and d subunits, so that subunit total and cell surface expression could be determined by flow cytometry. In this study all mutations were specified in the immature peptide, which has been the convention in the literature for α1, β3 and δ subunit mutations and variants but not for γ2 subunit mutations, which have generally been identified in the mature peptide[392].

Cell culture and transfections

Human embryonic kidney cells (HEK293T) were grown in 100 mm tissue culture dishes (Corning) in DMEM, supplemented with 10% fetal bovine serum at 37□C in 5% CO2 / 95% air For electrophysiological experiments, cells were plated onto poly-L-lysine–coated (cell-attached and excised outside-out patches) or non-coated (lifted whole cells) coverglass chips and transfected with 0.3 mg of each subunit plasmid in a ratio of $1^{\alpha6}:1^{\beta2}:1^{\gamma2L/\delta}$ (wild-type or homozygous mutant α6 subunit expression) or $0.5^{\alpha6}:0.5^{\alpha6(R46W)}:1^{\beta2}:1^{\gamma2L/\delta}$ (heterozygous wild-type and mutant α6 subunit expression) using the FuGENE 5 transfection reagent (Roche Applied Science, Indianapolis IN) according to the manufacturer's instructions. The terms "heterozygous" and "homozygous" are used solely to refer to mixed wild-type and mutant α6 subunit or pure mutant α6 subunit transfection, respectively. Cells were used 24–72 h after transfection. As a marker for successfully transfected cells, cDNA encoding green fluorescent protein was cotransfected together with the subunits of interest. For the surface expression measurement using flow cytometry, cells were first passaged onto 60 mm dishes and transfected 24 h later with 1 μg of each subunit in a ratio of 1:1:1 (homozygous α6 subunit expression) or 0.5:0.5:1:1 (heterozygous α6 subunit expression) with FuGENE 5 transfection reagent as previously described [95]. Experiments were performed over the subsequent 2–3 d.

Whole cell electrophysiology

Whole cell voltage-clamp recordings were performed on lifted cells or outside-out membrane patches excised from transfected HEK293T cells as described previously[360]. Cells were bathed in an external solution consisting of (mM): NaCl 142, $CaCl_2$ 1, KCl 8, $MgCl_2$ 6, glucose 10, HEPES 10 (pH 7.4, ~ 325 mOsm). Glass micropipettes were pulled from thin-walled borosilicate glass (World Precision Instruments, Sarasota, FL) using a P2000 laser electrode puller (Sutter Instruments, San Rafael, CA) and fire polished with a microforge (Narishige, East Meadow, NY). Patch electrodes had resistances of 1–2 MΩ when filled with an internal solution consisting of (mM): KCl 153, $MgCl_2$ 1, HEPES 10, EGTA 5, Mg^{2+}-ATP 2 (pH 7.3, ~300 mOsm). This combination of external and internal solutions produced a chloride equilibrium potential of ~ 0 mV. Lifted cells were voltage-clamped at –20 mV and outside-out membrane patches at – 50 mV using an Axopatch 200B amplifier (Axon Instruments, Union City, CA). No voltage-dependent changes in kinetics were detected between -20 and -50 mV. GABA was applied to the lifted cells and/or excised macropatches using four-barrel square glass pipettes (Friedrich and Dimmock, Millville, NJ) attached to a Warner SF-77B Perfusion Fast-Step (Warner Instrument Corporation, Hamden, CT), which was commanded by Clampex 9.0 software (Axon Instruments). The solution exchange time across the open electrode tip was ~400 μs. All experiments were performed at room temperature (22-23°C).

Currents were low-pass filtered at 2 kHz, digitized at 5–10 kHz, and analyzed using the pCLAMP 9 software suit. Current amplitudes and 10–90% rise times were measured using Clampfit 9. Desensitization and deactivation current time courses were fitted using the Levenberg-Marquardt least squares method with up to four component exponential functions of the form $\sum a_n e^{(-t/\tau n)}+C$, where n is the number of the exponential components, t is time, a is the relative amplitude, τ_n is the time constant, and C is the residual current at the end of the GABA application. Additional components were accepted only if they significantly improved the fit, as

determined by an *F*-test on the sum of squared residuals. The time course of deactivation was summarized as a weighted time constant, defined by the following expression$\sum a_n\tau n/\sum a_n$. The extent of desensitization was measured as (fitted peak-current − fitted steady-state current) / (fitted peak current). Numerical data were expressed as mean ± SEM. Statistical analysis was performed using Prism version 5.04 (GraphPad Software, La Jolla, CA). Statistical significance was taken as $p < 0.05$, using unpaired two-tailed Student's *t* test or one-way ANOVA as appropriate.

Single channel electrophysiology

Single-channel currents were recorded in cell-attached configuration as described before[396]. Cells were bathed in an external solution consisting of (mM): 140 NaCl, 5 KCl, 1 $MgCl_2$, 2 $CaCl_2$, 10 glucose, and 10 HEPES (pH 7.4). During recording, 1 mM GABA was present in the electrode solution consisting of (mM): 120 NaCl, 5 KCl, 10 MgCl2, 0.1 $CaCl_2$, 10 glucose, and 10 HEPES (pH 7.4). The electrode potential was held at +80 mV. All experiments were conducted at room temperature.

Single channel currents were amplified and low-pass filtered at 2 kHz using an Axopatch 200B amplifier, digitized at 20 kHz using Digidata 1322A, and saved using pCLAMP 9. Data were analyzed using TAC 4.2 (Bruxton Corporation, Seattle, WA). Open and closed events were analyzed using the 50% threshold detection method. All events were carefully checked visually before being accepted. Only patches showing no overlaps of simultaneous openings were accepted. Open and closed time histograms as well as amplitude histograms were generated using TACFit 4.2 (Bruxton Corporation, Seattle, WA). Single-channel amplitudes (*i*) were calculated by fitting all-point histograms with single- or multi-Gaussian curves. The difference between the fitted "closed" and "open" peaks was taken as *i*. Duration histograms were fitted with exponential components in the form:$\sum (A_i /\tau_i) e^{(-t/\tau_i)}$, where A and τ are the relative area and the time constant of the *i* component, respectively, and *t* is the time. The mean open time was then

calculated as follows: $\sum A_i \tau_i$. The number of components required to fit the duration histograms was increased until an additional component did not significantly improve the fit[377]. Single channel openings occurred as bursts of one or more openings or clusters of bursts. Bursts were defined as one or more consecutive openings that were separated by closed times that were shorter than a specified critical duration (t_{crit}) prior to and following the openings[378]. A t_{crit} duration of 5 ms was used in the current study. Clusters were defined as a series of bursts preceded and followed by closed intervals longer than a specific critical duration ($t_{cluster}$). A $t_{cluster}$ of 10 ms was used in this study. Data were expressed as the mean ± SEM. Statistical analysis was performed as described in the previous section.

Flow cytometry

Cells were harvested ~48 hours after transfection using 37ºC trypsin-EDTA and placed immediately on ice in 4ºC FACS buffer (Ca^{2+}/Mg^{2+} -free PBS with 2% FBS and 0.05% NaN_3). Cells were then pelleted by centrifugation, resuspended in 4ºC FACS buffer, and transferred to 96-well polystyrene V-bottom plates. For measurements of subunit surface expression, cells were stained for 1 h on ice using primary antibodies diluted in 4ºC FACS buffer and then washed 3 times in 4ºC FACS buffer. Where necessary, cells were then stained for 1 h on ice using fluorophore-conjugated secondary antibodies before fixation in 2% w/v paraformaldehyde diluted in PBS. For measurements of total cellular expression, cells were harvested as described for surface staining. Prior to staining, however, cells were permeabilized for 15 min using Cytofix/Cytoperm fixation/permeabilization buffer and washed 2 times using Perm/Wash staining buffer (BD Biosciences; San Jose, CA). Samples were then stained using primary antibodies diluted in 4ºC Perm/Wash for 1 h on ice before being washed 4 times in 4ºC Perm/Wash, 2 times in 4ºC FACS buffer, and fixed in 2% w/v paraformaldehyde.

Expression levels were measured using a LSRII 3-laser flow cytometer (BD Biosciences, Sparks, MD). Data were acquired using FACS-Diva™ (BD Biosciences) and analyzed offline

using FlowJo 7.5.5 (Tree Star Inc., Ashland, OR). For each condition, 30,000 cells were analyzed. Non-viable cells were excluded from analysis based on forward- and side-scatter properties, as determined in separate experiments by 7-amino-actinomycin-D staining. For each condition, the mean fluorescence obtained from staining cells transfected with empty pcDNA 3.1 was subtracted and the data were normalized to the wild-type α6β2γ2L/δ condition for comparison. Statistical significance was determined using a Student's unpaired *t*-test.

Homology modeling

Three-dimensional models of human α6, β2, γ2 and δ subunit N-terminal domains were generated using the crystal structure of the N-terminal domain of the nAChR α subunit[153] as a template (Protein Database accession number 2qc1) using the program SWISS-MODEL[379]. The initial sequence alignments between $GABA_A$ receptor subunits and the nAChR α subunit were generated with full-length multiple alignments using ClustalW (European Bioinformatics Institute, Hinxton, UK). Then the alignment of a 212-residue core of N-terminal domains of $GABA_A$ receptor subunits with residues of the N-terminal domain of nAChR α subunit were submitted for automated comparative protein modeling implemented in the program suite incorporated in SWISS-MODEL (http://swissmodel.expasy.org/SWISS-MODEL.html) using the $GABA_A$ receptors sequence as a target protein and the nAChR sequence as a template structure. The α6 mutant structural model was individually made by selecting the mutation desired using the program DeepView/Swiss-PdbViewer 4.02 (Swiss Institute of Bioinformatics, Lausanne, Switzerland). SWISS-MODEL project files containing the target sequence with a single mutation, and the superposed template structure, then were modeled and submitted in the program. To generate pentameric $GABA_A$ receptor homology models, α6, β2 and γ2 or d subunit N-terminal domain models were assembled in a counter clockwise β2-α6-β2-α6-γ2/δ order by superposition onto the acetylcholine binding protein as a template (Protein Database accession number 1i9b)[98]. The resulting models were subsequently energy-optimized using GROMOS96 in default settings

within DeepView/Swiss-PdbViewer. The models with the most likely conformation were presented here.

Reagents

Reagents used included GABA (Sigma, Aldrich, St. Louis, MO), DMEM (Invitrogen), fetal bovine serum (Gibco, Billings, MT), penicillin/streptomycin (Invitrogen), trypsin/EDTA (Gibco). Mouse monoclonal anti-β2/3 antibody (Clone 62-3G1) was obtained from Upstate (Lake Placid, NY) and used at a dilution of 1:100 (surface) or 1:200 (total). Mouse monoclonal anti-HA antibody (clone 16B12) and Alexa647 labeling kits were obtained from Invitrogen and conjugated per manufacturer instructions; the product was used at a dilution of 1:200 (surface) or 1:400 (total). Two different anti-FLAG antibodies (both clone M2) were used to verify results and optimize signal; conjugated anti-FLAG-Alexa647 antibody was obtained from Cell Signaling Technology (Beverly, MA) and used at a dilution of 1:50 (surface) and 1:100 (total), and unconjugated anti-FLAG antibody was obtained from Sigma-Aldrich and used at dilution of 1:1000 (surface). Surface staining with unconjugated antibodies was followed by secondary antibody staining with Alexa647-conjugated goat anti-mouse IgG1 antibody (Invitrogen) as described previously. Total staining with unconjugated anti-β2/3 was performed using Alexa647-conjugated Zenon (Invitrogen) per manufacturer instructions.

Results

The α6 subunit mutation, R46W, decreased current amplitude and altered the time course of transient α6β2γ2L receptor currents.

We initially characterized the effect of the R46W mutation on macroscopic α6β2γ2L receptor currents. Whole-cell currents were elicited from lifted HEK293T cells cotransfected with human β2 and γ2L subunits and wild-type α6 or mutant α6(R46W) subunits by applying a saturating GABA concentration (1 mM) for 400 ms using a rapid concentration jump technique

(Figure 2*A*). Peak α6(R46W)β2γ2L receptor current density (89 ± 14 pA/pF, n = 18 $p < 0.001$) was reduced relative to peak α6β2γ2L receptor current density (395 ± 53 pA/pF, n = 21) (Figure 2*A*, *B*). To characterize the effects of the R46W mutation on macroscopic current kinetic properties (rate of activation (10 – 90% rise time), desensitization (current relaxation in the present of saturating agonist) and deactivation (current relaxation after removal of agonist)) of α6(R46W)β2γ2L currents, we applied a saturating GABA concentration (1 mM) for 400 ms to excised outside out patches obtained from cells expressing wild-type and mutant receptors (Figure 2*C*). Again peak mutant receptor currents were smaller (400 ± 29.6 pA) than wild-type receptor currents (1427 ± 298 pA, $p < 0.001$). Mutant receptor current activation was slower than wild-type receptor current activation ($p < 0.01$, Table 1), and desensitization of mutant receptor currents was slightly more extensive (35 ± 2 %) than that of wild-type receptor currents (29 ± 2 %, $p < 0.05$, Figure 2*D*, top left panels). Interestingly the increased extent of desensitization was not accompanied by a decrease in the relative contribution of the residual currents ($p > 0.05$, Figure 2*D*, bottom left panel, Table 1). Both wild-type and mutant receptor currents desensitized with fast and slow exponential components (Figure 2*D*, top central and right panels). The fast component time constant (t_1; $p < 0.001$, Table 1) and relative contribution (a_1; $p < 0.001$, Table 1) for mutant receptor currents was much smaller than that for wild-type receptor currents (Figure 2*D*, top right panels), but no differences in time constant (t_2) or relative contribution (a_2) of the second exponential component were found ($p > 0.05$, Figure 2D, bottom right panels, Table 1).

Deactivation of mutant receptor currents was significantly slower than for wild-type receptor currents (Figure 2*E*, left panel). The slowing of mutant receptor current deactivation was due to larger deactivation time constants t_1 and t_2 ($p < 0.01$, $p < 0.05$, Table 1, Figure 2*E*, middle and right panels) resulting in a larger weighted decay time constant ($p < 0.01$, Table 1, Figure 2*E*, left panel). No differences were found in the relative contribution (a_1) of the first deactivation component for wild-type or mutant receptors ($p > 0.05$, Table 1). The longer deactivation time

Table 1. Macroscopic kinetics of α6β2γ2L currents after 400ms applications of 1mM GABA

	Excised outside-out macropatches (n)	
	wt (26)	**R46W (22)**
Rise time 10-90% (ms)	1.84 ± 0.12	2.56 ± 0.25**
Desensitization		
Extent (%)	29 ± 2	35 ± 2*
τ1 (ms)	37.9 ± 5.93	2.36 ± 0.46***
τ2 (ms)	460 ± 38.7	488 ± 66.5
a1 (%)	15 ± 2	10 ± 1*
a2 (%)	34 ± 4	42 ± 4
Residual (%)	50 ± 5	49 ± 5
Deactivation		
τ1 (ms)	47.3 ± 3.77	93.0 ± 14.3**
τ2 (ms)	176 ± 17.4	268 ± 42.2*
a1 (%)	60 ± 5	68 ± 5
τ-weight (ms)	79.4 ± 3.48	111 ± 9.22**

Values represent mean ± SEM. *, **, and *** indicate $p < 0.05$, $p < 0.01$, and $p < 0.001$ respectively (unpaired t-test) compared to wild-type.

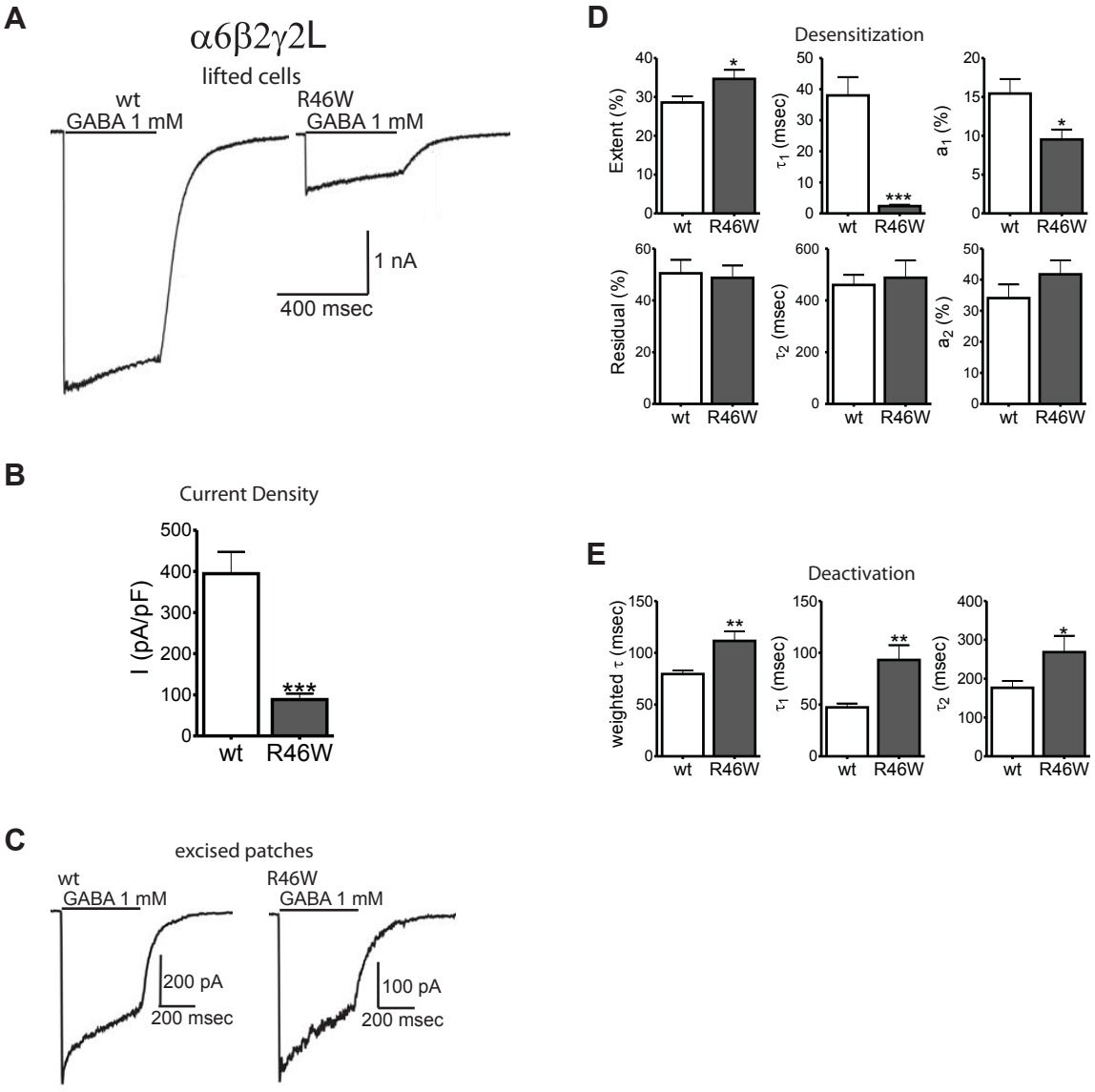

Figure 2. The R46W mutation evoked small α6β2γ2L receptor currents with slowed activation and deactivation macroscopic kinetics.

A. Current responses to 400 ms pulses of 1 mM GABA to lifted cells containing wild-type (wt) and mutant R46Wα6β2γ2Lreceptors are shown. B. Current densities of wild-type (white bars) and mutant R46W(grey bars) α6β2γ2L receptors evoked by 400 ms pulses of 1 mM GABA to lifted cells are shown. C. Current responses to 400 ms pulses of 1 mM GABA to excised patches cells containing wild-type and mutant R46W α6β2γ2L receptors. D and E. Summary of macroscopic kinetic parameters obtained from currents evoked by 400 ms pulses of 1 mM GABA to excised patches for both wild-type (white bars) and mutant R46W (grey bars) α6β2γ2L receptors. Values represent mean ± S.E.M. Differences between wild-type and mutant channels are shown as *, ** and ***, which indicate $p < 0.05$, $p < 0.01$ and $p < 0.001$ (unpaired t-test).

course displayed by mutant receptor currents may have been related to increased time for equilibration among desensitized states[168].

The α6 subunit mutation, R46W, decreased mean open time but increased opening frequency of single channel α6β2γ2L currents.

Modifications of macroscopic current kinetic properties can be due to alterations in single channel gating properties. Thus, steady-state on-cell single channel recordings of α6β2γ2L or α6(R46W)β2γ2L receptors were obtained in the continuous presence of GABA (1 mM). Single channel openings and complex bursting patterns were recorded from both wild-type (Figure 3*A*, wt) and mutant (Figure 3*A*, R46W) receptors. Wild-type receptor channels displayed brief bursts of openings and frequent prolonged (1 to 2 s) clusters of bursts; in contrast, mutant receptor channel openings occurred as single events and frequent brief bursts of openings. In addition, there was a small but significant difference between wild-type and mutant single channel current amplitudes (Figure 3*A, B*). Mutant receptor single channel openings were briefer than wild-type receptor single channel openings ($p < 0.01$, Table 2). This difference might represent a variation in the main conductance state of α6β2γ2L receptors, which was 21-27 pS. Similar results were found in our previous reports for αβγ receptors expressed in mouse L929 cells[276, 377]. Indeed, to rule out the possibility that these conductance levels were due to the presence of αβ receptor currents, single channel α6β2 currents were recorded from HEK293T cells in the presence of GABA (1 mM). α6β2 receptors opened to a main current amplitude of 0.86 ± 0.11 pA (n = 5, $p <$ 0.001 vs. wild-type, $p < 0.01$ vs. R46W), consistent with an ~ 12 pS channel conductance and in agreement with conductance levels for single channel α1β2 currents reported previously[276]. The twofold difference in current amplitudes between α6β2 and α6β2γ2L single channel excludes the presence of a binary receptor population in our recordings.

To further address how the α6 subunit mutation, R46W, affected channel gating, we measured mean open time and opening frequency of both wild-type and mutant receptor single

Table 2. Kinetic properties of α6β2γ2L and α6β2δ single-channel currents

	α6β2γ2L (n)		α6β2δ (n)	
	wt (8)	**R46W (6)**	**wt (7)**	**R46W (6)**
Channel amplitude (pA)	1.76 ± 0.09	1.36 ± 0.05**	1.69 ± 0.02	1.62 ± 0.05
Mean open time (ms)	1.09 ± 0.08	0.88 ± 0.04*	1.2 ± 0.11	0.89 ± 0.05*
Opening frequency (s^{-1})	3.76 ± 0.42	8.42 ± 0.35***	10.1 ± 1.81	2.77 ± 0.54**
Open time constants				
τ_{o1} (ms)	0.62 ± 0.04	0.56 ± 0.05	0.6 ± 0.02	0.44 ± 0.02***
τ_{o2} (ms)	0.75 ± 0.09	0.61 ± 0.06	0.86 ± 0.08	0.58 ± 0.02*
τ_{o3} (ms)	2.28 ± 0.31	1.81 ± 0.12	2.18 ± 0.17	2.17 ± 0.12
a_{o1} (%)	25 ± 3	78 ± 6***	14 ± 1	25 ± 2***
a_{o2} (%)	71 ± 4	19 ± 5***	81 ± 2	71 ± 2**
a_{o3} (%)	4 ± 2	3 ± 1	5 ± 1	4 ± 1
Intraburst closed time constant				
τ_{c1} (ms)	1.37 ± 0.17	1.21 ± 0.13	0.75 ± 0.05	0.59 ± 0.04
τ_{c2} (ms)	5.40 ± 0.72	6.53 ± 1.03	4.79 ± 0.49	2.53 ± 0.50*
ac_1 (%)	50 ± 4	28 ± 4**	11 ± 1	7 ± 2
ac_2 (%)	36 ± 4	45 ± 3	22 ± 3	15 ± 3
Burst kinetics				
Openings per burst	3.03 ± 0.24	2.27 ± 0.26	1.75 ± 0.21	1.33 ± 0.12
P_o	0.010 ± 0.003	0.013 ± 0.002	0.018 ± 0.002	0.003 ± 0.001***
Duration (ms)	6.66 ± 0.57	3.8 ± 0.12**	2.90 ± 0.11	1.43 ± 0.12
Frequency (s^{-1})	1.28 ± 0.13	3.93 ± 0.39***	6.02 ± 1.29	2.18 ± 0.48*
τ_1 (ms)	0.82 ± 0.03	0.74 ± 0.04	0.61 ± 0.04	0.54 ± 0.04
τ_2 (ms)	10.1 ± 1.00	6.68 ± 0.43*	5.87 ± 0.76	3.23 ± 0.21*
a_1 (%)	35 ± 2	50 ± 2***	64 ± 2	82 ± 2***
a_2 (%)	65 ± 2	51 ± 2***	36 ± 2	18 ± 2***

Values represent mean ± SEM. *, **, and *** indicate $p < 0.05$, $p < 0.01$, and $p < 0.001$ respectively (unpaired t-test) compared to wild-type.

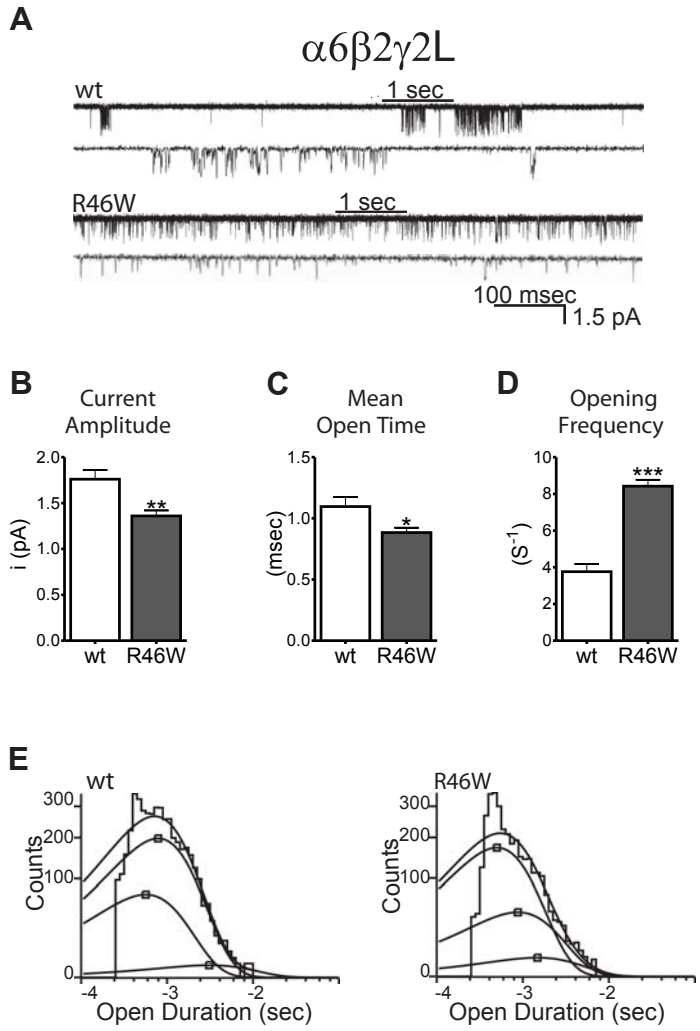

Figure 3. The R46W mutation affected gating efficacy by decreasing mean open time of single channel α6β2γ2L currents.

A. Steady state single channel currents were obtained from cell-attached patches containing wild-type (wt) and mutant R46W α6β2γ2L receptors. Patches were voltage clamped at +80 mV and continuously exposed to 1 mM GABA. Note that the upper traces in panel A (1 S, black bars) were expanded below them. B-D. Single channel kinetics for both wild-type (white bars) and mutant R46W (grey bars) α6β2γ2Lreceptors are shown. E. Representative open duration histograms for both wild-type and mutant R46W α6β2γ2L receptors were fitted to three exponential functions. Values represent mean ± S.E.M. Differences between wild-type and mutant channels are shown as *, ** and ***, which indicate $p < 0.05$, $p < 0.01$ and $p < 0.001$ (unpaired t-test).

channel currents. Overall, mutant receptor channels displayed lower mean open times (Figure 3*C*) and higher opening frequencies (Figure 3*D*) than wild-type receptor channels ($p < 0.05$, $p < 0.001$, Table 2). Open time distributions from wild-type and mutant receptors were fitted best by three exponential components (Figure 3*E*). While there were no significant differences among the three open-time constants (t_{o1}, t_{o2} and t_{o3}) from wild-type and mutant receptors ($p > 0.05$, Table 2), there was a significant shift in the relative occurrence of the three components (a_{o1}, a_{o2} and a_{o3}) that accounted for the differences in mean open time of wild-type and mutant receptors. Mutant receptor single channel openings were dominated by the shortest open state, accounting for ~ 78 % of the relative area (a_{o1}) ($p < 0.001$, Table 2). In contrast, wild-type receptor single channel openings contained a short open state that accounted for only ~ 25 % of the single channel openings, and a longer open state that accounted for ~ 71 % of the relative area (a_{o2}) ($p < 0.001$, Table 2). No differences were found in the relative area of the longest open state (a_{o3}) ($p > 0.05$, Table 2).

The α6 subunit mutation, R46W, decreased burst duration and increased burst frequency of α6β2γ2L single channel currents.

In response to saturating concentrations of GABA, $GABA_A$ receptor channels display bursts of fast transitions between open and closed states prior to unbinding of agonist or entering into desensitized states. To determine the effects of the R46W mutation on single channel bursts, we analyzed the intraburst kinetics of single channel currents from α6β2γ2L and α6(R46W)β2γ2L receptor channels. First, we focused on the two briefest closed time constants that most likely represent closures within bursts of channel activity. Interestingly, both intraburst closed time constants (t_{c1} and t_{c2}) for mutant receptors were similar to those found for wild-type receptors ($p > 0.05$, Table 2), but the relative contribution of the brief component (a_{c1}) for mutant receptors was significantly reduced relative to wild-type receptors ($p < 0.01$, Table 2). Thus, agonist activation of mutant receptors produced single channel currents with bursts that usually

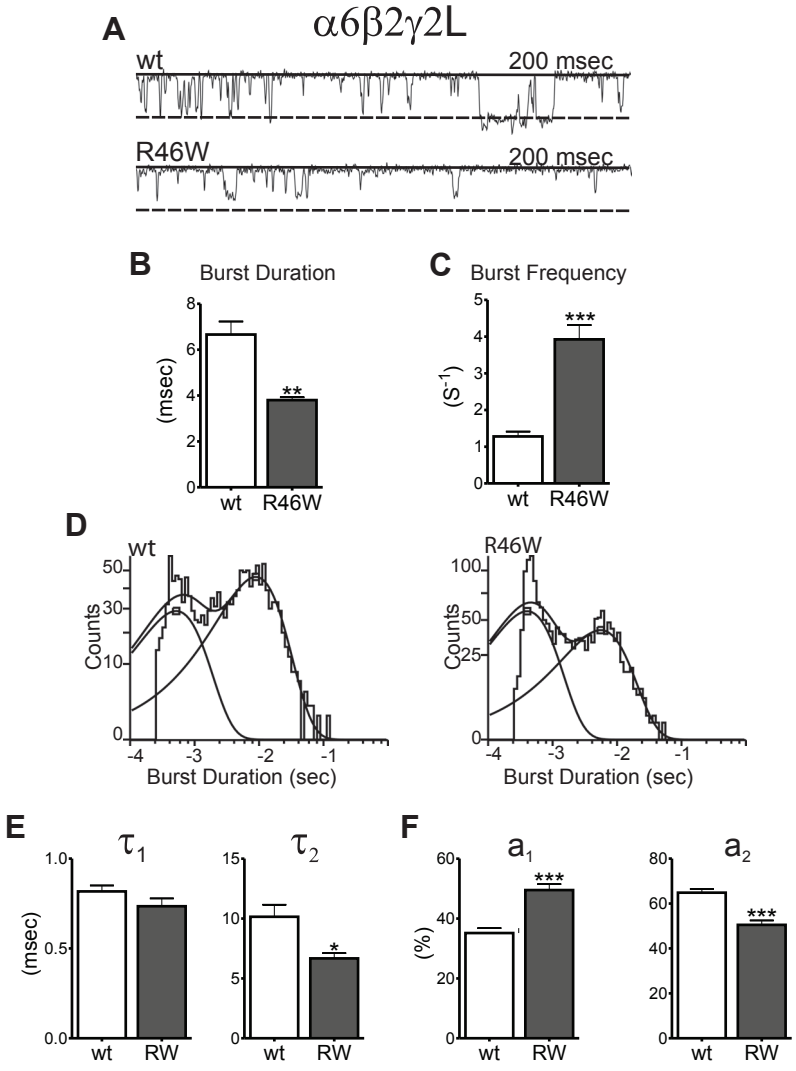

Figure 4. Mutant α6(R46W)β2γ2L receptor channel bursts occurred as brief single openings, which decreased single channel current burst durations.

A. Representative steady state single channel current traces from cell-attached patches containing wild-type (wt) and mutant R46W (RW) α6β2γ2L receptors. Patches were voltage clamped at +80 mV and continuously exposed to 1 mM GABA. **B-C.** Comparison of burst kinetics for both wild-type (white bars) and mutant R46W (grey bars) α6β2γ2L receptors are shown. **D.** Representative burst duration histograms for both wild-type and mutant R46W receptors were fitted to two exponential functions. **E-F.** Time constants (τ) and representative areas (a) of burst duration histograms for both wild-type (white bars) and mutant R46W receptors (grey bars) are shown. Values represent mean ± S.E.M. Differences between wild-type and mutant channels are shown as *, ** and ***, which indicate $p < 0.05$, $p < 0.01$ and $p < 0.001$ (unpaired t-test).

occurred as single openings or brief bursts of openings and closings, while wild-type receptors produced single-channel openings that contained prolonged bursts of brief openings. The duration of bursts were reduced for mutant receptors relative to wild-type receptors (see representative 200 ms traces of bursting wild-type (Figure 4*A*, wt) and mutant (Figure 4*A*, R46W) receptor currents). Further analysis showed that burst durations of mutant receptor currents were significantly reduced relative to wild-type receptor currents ($p < 0.01$, Table 2, Figure 4*B*), and this difference was associated with a slight reduction of openings per burst ($p > 0.05$, Table 2) and a substantial increase in burst frequency of mutant receptor currents ($p < 0.001$, Table 2, Figure 4*C*).

The burst duration frequency distributions were fitted best by two exponential functions for both wild-type and mutant receptors (Figure 4*D*). However there were no differences in the time constants for the short-duration burst component (t_1) for the receptors ($p > 0.05$, Table 2, Figure 4*E*, left panel), but the time constant for the longer-duration burst component (t_2) was significant reduced for mutant receptors ($p < 0.05$, Table 2, Figure 4*E*, right panel). In addition, with mutant receptors there was a shift in the distribution of the two populations of burst durations due to an increase in the relative proportion of bursts with short duration (a_1) and a reduction in the relative proportion of longer bursts (a_2) ($p < 0.001$, Table 2, Figure 4*F*). Taken together, mutant receptor burst durations were reduced due to reduction of the time that the channel spends in the open state.

The α6 subunit mutation, R46W, decreased surface expression of α6β2γ2L receptors.

To gain insight into the effects of the α6 subunit mutation, R46W, on $GABA_A$ receptor assembly, wild-type $\alpha6^{FLAG}$ and mutant $\alpha6(R46W)^{FLAG}$ subunits were coexpressed in HEK293T cells, and surface and total expression levels of each subunit were assessed using flow cytometry (Figure 5*A*, *C*). Coexpression of $\alpha6(R46W)^{FLAG}$ with β2 and $\gamma2L^{HA}$ subunits resulted in a significant reduction of both $\alpha6(R46W)^{FLAG}$ and β2, but not $\gamma2L^{HA}$, subunits on the cell surface

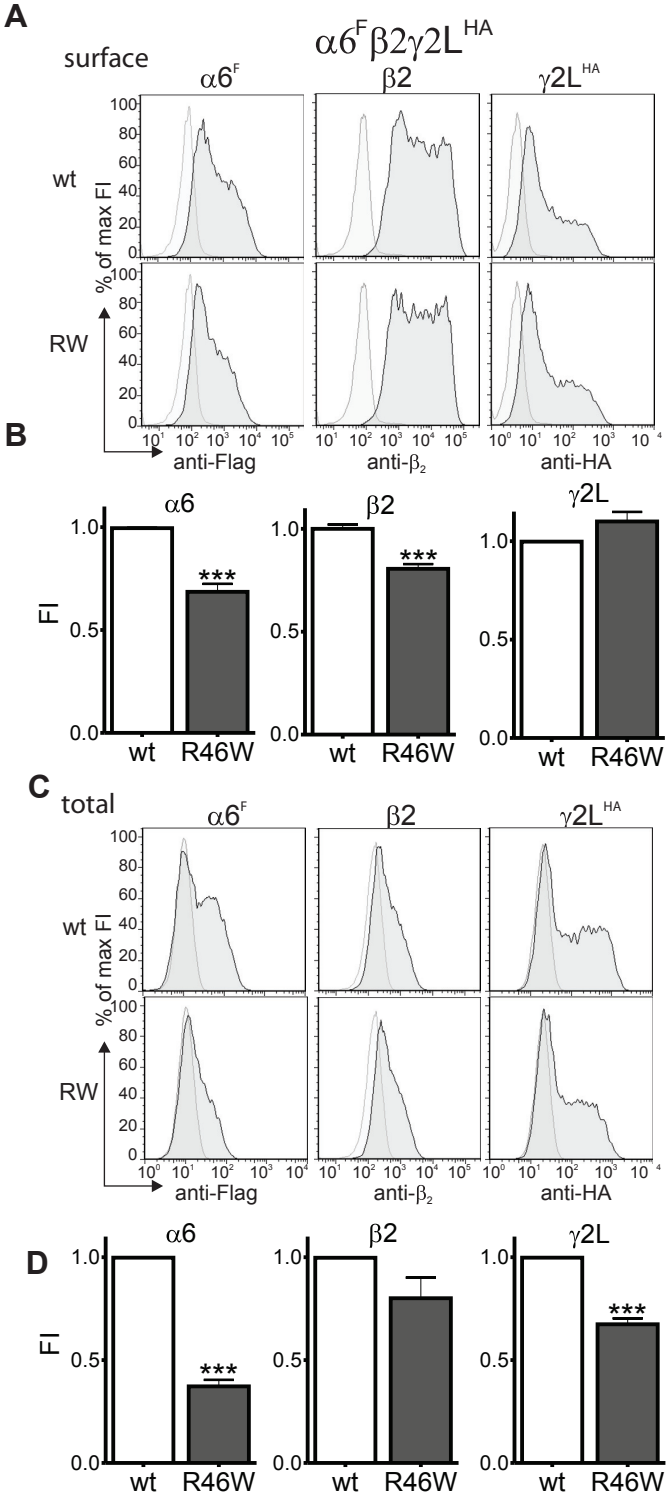

Figure 5. The R46W mutation decreased surface expression of α6 and β2, but not γ2L subunits of α6β2γ2L receptors.

A. $GABA_A$ receptor $\alpha6^F$, $\alpha6^F$(R46W), β2 and $\gamma2L^{HA}$ subunit cell surface levels were measured by flow cytometry for cells coexpressing wild-type (wt) and mutant R46W α6β2γ2L receptors. Representative histograms of positively transfected cells (dark grey) were superimposed on those from mock transfected cells (light grey) and shown for surface expression. Note that the abscissa has a log-scale. **B.** The mean fluorescence intensity (FI) of α6, β2, and γ2L subunits surface expression was quantified for wild-type (white bars) and mutant R46W receptors (grey bars). **C.** $GABA_A$ receptor $\alpha6^F$, $\alpha6^F$(R46W), β2 and $\gamma2L^{HA}$ subunit total cellular levels were measured by flow cytometry for cells coexpressing wild-type and mutant R46W α6β2γ2L receptors. Representative histograms of positively transfected cells (dark grey) were superimposed on those from mock transfected cells (light grey). **D.** The mean fluorescence intensity (FI) of $\alpha6^F$, β2, and $\gamma2L^{HA}$ subunit total cell expression was quantified as well (wild-type as white bars, and mutant receptors as grey bars). Values represent mean ± S.E.M. Differences between wild-type and mutant channels are shown as ***, which indicate $p < 0.001$ (unpaired t-test).

(Figure 5*A*). Cell surface levels of mutant α6(R46W)^{FLAG} subunits were reduced compared to wild-type α6^{FLAG} subunits (0.69 ± 0.04, n = 10 compared to 1.00 ± 0.002, n = 10, respectively, $p < 0.001$, Figure 5*B*, left panel), and β2 subunits were also reduced compared to control subunits when coexpressed with mutant α6(R46W)^{FLAG} subunits (0.81 ± 0.02, n = 10 compared to 0.995 ± 0.002, n = 10, respectively, $p < 0.001$, Figure 5*B*, middle panel). No differences were found in surface levels of γ2L^{HA} subunits (1.10 ± 0.05, n = 10 compared to 0.998 ± 0.001 n = 10, respectively, $p > 0.05$, Figure 5*B*, right panel).

Total cellular levels of coexpressed α6^{FLAG} or α6(R46W)^{FLAG} and β2, and γ2L^{HA} subunits were measured by permeabilizing cell membranes prior to staining (Figure 5*C*). Comparable to surface levels, when coexpressed with β2 and γ2L^{HA} subunits total expression of α6(R46W)^{FLAG} subunits was reduced significantly relative to α6^{FLAG} subunits (0.37 ± 0.03, n = 10 compared to 1.0 ± 0.001, n = 10, respectively, $p < 0.001$, Figure 5*D*, left panel). Interestingly, this reduction was associated with a reduction of total levels of γ2L^{HA} subunits (0.67 ± 0.03, n = 10, $p < 0.001$, Figure 5*D*, right panel), but with no changes in total levels of coexpressed β2 subunits (0.80 ± 0.10, n = 7, $p > 0.05$, Figure 5*D*, middle panel).

These results suggested that the R46W mutation impaired expression and surface trafficking of α6 subunits. Moreover, α6(R46W) subunits had a dominant negative effect on partnering subunits, reducing surface expression of β2 subunits and total cellular expression of γ2L subunits. Importantly, though total α6(R46W) subunit levels were reduced, some α6(R46W) subunits could be successfully assembled with β2 and γ2L subunits into α6(R46W)β2γ2L receptors that were trafficked to the cell surface. However, because expression levels of α6(R46W), β2 and γ2L subunits were not affected equally, it is likely that the mutation led to production of surface receptors with altered stoichiometry.

Heterozygous coexpression of mutant α6(R46W) and wild-type α6 subunits with β2 and γ2L subunit produced intermediate macroscopic receptor current amplitudes.

Most epilepsy-associated $GABA_A$ receptor subunit mutations were found in heterozygous patient. Therefore, we repeated the preceding experiments in conditions representing heterozygous expression of wild-type α6 and mutant α6(R46W) subunits (50/50 mix of wild-type and mutant α6 subunits). First, we compared wild-type α6β2γ2L, heterozygous α6/α6(R46W)β2γ2L and homozygous mutant α6(R46W)β2γ2L receptor whole-cell currents elicited from lifted HEK293T cells evoked by application of 4 s concentration jumps of saturating GABA (1 mM) (Figure 6*A*). Heterozygous receptor currents were larger (Figure 6*A* insert panel, $p < 0.001$, Table 3) and desensitized more extensively (Figure 6*B* middle panel, $p < 0.01$, Table 3) than homozygous mutant receptor currents. In addition, the 10-90% activation rise time was shorter than for homozygous receptor currents (Figure 6*B* left panel, $p < 0.001$, Table 3). When compared with wild-type receptors, heterozygous receptors had decreased maximal peak current density with no differences in the extent of desensitization or activation (Figure 6*A* insert panel and *B*, Table 3).

The desensitization time courses of wild-type, heterozygous and homozygous mutant receptor currents were fitted best by four exponential components (Table 3). Despite the fact that both heterozygous and homozygous mutant receptor currents exhibited a significantly slower third component exponential time constant (t_3) than wild-type receptor currents ($p < 0.05$, Table 3), heterozygous receptors displayed similar desensitization component distribution values (a_1, a_2, a_3 and a_4) and residuals compared to wild-type receptor currents ($p > 0.05$, Table 3), but significantly different than from homozygous mutant receptor currents ($p < 0.01$, Table 3, Figure 6*B* right panel). Moreover, heterozygous receptor currents deactivated faster than homozygous mutant receptor currents ($p < 0.01$, Table 3), but with kinetic properties similar to those of wild-type receptors.

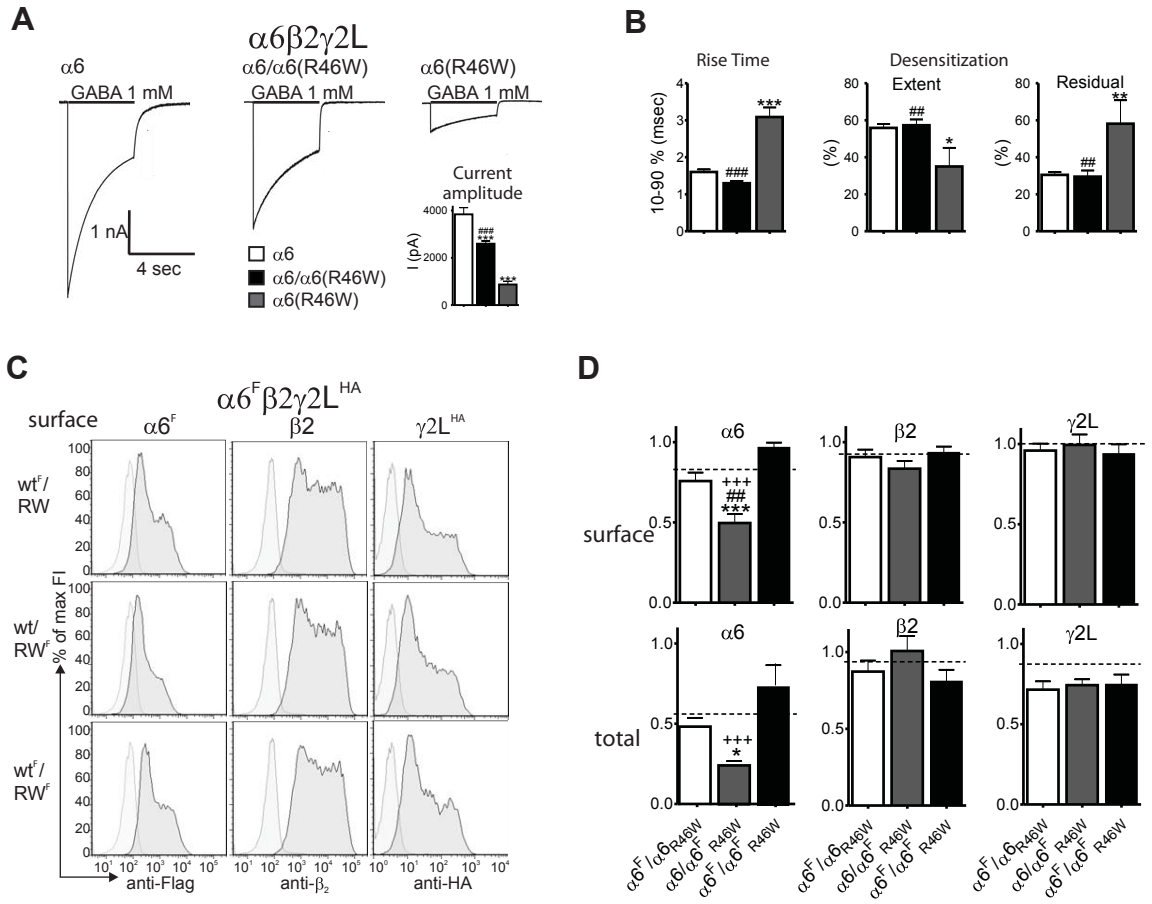

Figure 6. Heterozygous coexpression of mutant α6(R46W) and wild-type α6 subunits produced intermediate macroscopic receptor current amplitudes by assembling a mixed fraction of wild-type/mutant receptors on the surface.

A. Current responses to long (4 s) applications of 1 mM GABA to lifted cells containing wild-type α6β2γ2L, heterozygous α6/α6(R46W)β2γ2L and α6(R46W)β2γ2L receptors are shown. In the inset, current amplitudes for α6 (white bar), α6/α6(R46W) (black bar) and α6(R46W) (grey bar) subunit-containing receptors are shown. **B.** The 10-90% rise time, extent of desensitization and residual current for currents evoked by 4 S pulses of 1 mM GABA are presented for wild-type, heterozygous and mutant α6β2γ2L receptors. **C.** Surface levels of heterozygous $\alpha6^{FLAG}$/α6(R46W) (wt^F/RW), α6/α6(R46W)^{FLAG} (wt/RW^F), and $\alpha6^{FLAG}$/α6(R46W)^{FLAG} (wt^F/RW^F) subunits coexpressed with α2 and $\gamma2L^{HA}$ subunits were measured using flow cytometry. Histograms of positively transfected cells (dark grey) were superimposed on those from mock transfected cells (light grey). **D.** The mean of fluorescence intensity (FI) of $\alpha6^F$, β2, and $\gamma2L^{HA}$ subunit surface and total levels were quantified for heterozygous $\alpha6^{FLAG}$/α6(R46W), α6/α6(R46W)^{FLAG}, and $\alpha6^{FLAG}$/α 6(R46W)^{FLAG} subunit combinations. Dashed lines represent half-tagged $\alpha6^F$/α6 levels. Values represent mean ± S.E.M.. *, ** and *** indicate $p < 0.05$, $p < 0.01$ and $p < 0.001$ (one-way ANOVA) statistically different from wild-type levels (α6 or α6F/α6), respectively. ## and ### indicate $p < 0.01$ and $p < 0.001$ (one-way ANOVA) statistically different from α6(R46W) or $\alpha6^F$/α6(R46W). +++ indicate $p < 0.001$ (one-way ANOVA) statistically different from α6/α6(R46W)^F.

With heterozygous coexpression of mutant α6(R46W) and wild-type α6 subunits with β2 and γ2L subunits, there was increased incorporation of wild-type subunits over mutant subunits.

To gain insight into the assembly fate of wild-type α6 and mutant α6(R46W) subunits with heterozygous expression, we coexpressed α6, α6(R46W), β2, and $\gamma2L^{HA}$ subunit cDNA at a molar ratio of 0.5 : 0.5 : 1: 1 (see Methods) and evaluated subunit expression levels using flow cytometry (Figure 6C). To distinguish wild-type and mutant subunits, we differentially tagged α6 and α6(R46W) subunits with the FLAG epitope. Specifically, we determined surface levels of wild-type and mutant α6 subunits coexpressed with β2 and γ2L subunits when only the wild-type subunit ($\alpha6^{FLAG}$/α6(R46W), Figure 6D top left panel, white bar), only the mutant subunit (α6/$\alpha6(R46W)^{FLAG}$, Figure 6D top left panel, grey bar) or both subunits ($\alpha6^{FLAG}$/$\alpha6(R46W)^{FLAG}$, Figure 6D top left panel, black bar) were FLAG-tagged.

With the "half-tagged" subunits, we compared FLAG-tagged subunit levels obtained with heterozygous expression to those obtained with coexpression of "half tagged" wild-type $\alpha6^{FLAG}$/α6 subunits (Figure 6*D*, dotted line). Heterozygous expression of half-tagged $\alpha6^{FLAG}$/α6(R46W) subunits (Figure 6*D*, top panel, white bars) resulted in no significant difference in surface levels of $\alpha6^{FLAG}$ (0.76 ± 0.05, n = 7, $p > 0.05$, Figure 6*D*, left top panel), β2 (0.91 ± 0.05, n = 8, $p > 0.05$, Figure 6*D*, middle top panel) or $\gamma2L^{HA}$ (0.96 ± 0.04, n = 8, $p > 0.05$, Figure 6*D*, right top panel) subunits, when compared to coexpression of half-tagged $\alpha6^{FLAG}$/α6 subunits ($\alpha6^{FLAG}$ = 0.83 ± 0.05, n = 7, β2 = 0.92 ± 0.02, n = 7, and $\gamma2L^{HA}$ = 1.00 ± 0.03, n = 7, respectively, Figure 6D, top panels, dotted lines). These results suggested that incorporation of wild-type $\alpha6^{FLAG}$, β2 and $\gamma2L^{HA}$ subunits into heterozygous receptors was not affected by the presence of the mutant subunit or the FLAG tag.

Heterozygous expression of half-tagged α6/$\alpha6(R46W)^{FLAG}$ subunits, however, resulted in a significant reduction of surface $\alpha6(R46W)^{FLAG}$ subunits (0.50 ± 0.06, n = 7, Figure 6*D*, left top panel grey bar) relative to those obtained with wild-type $\alpha6^{FLAG}$/α6 subunits ($p < 0.001$, Figure 6*D*, left top panel, black bar) and with heterozygous $\alpha6^{FLAG}$/α6(R46W) subunits ($p < 0.01$, Figure

6*D*, left top panel, white bar) levels. These results suggest that with heterozygous expression, both wild-type and mutant α6 subunits could be incorporated into surface-trafficked receptors, but that wild-type subunits were preferred over mutant subunits.

With "full-tagged" heterozygous $\alpha6^{FLAG}/\alpha6(R46W)^{FLAG}$ subunit coexpression, there was a small, non-significant increase in α6 subunit levels on the cell surface (0.97 ± 0.03, n = 6, Figure 6*D*, left top panel, black bar) relative to those obtained with half-tagged $\alpha6^{FLAG}/\alpha6(R46W)$ subunit coexpression (Figure 6*D*, left top panel, white bar), again suggesting that with heterozygous expression, wild-type subunits are incorporated into the receptors much more successfully than mutant subunits.

As would be expected if the FLAG epitope did not disrupt overall assembly of the receptors, no significant differences were found in the surface expression levels of β2 (Figure 6*D*, middle panel) (0.84 ± 0.04, n = 8, grey bar, and 0.93 ± 0.04, n = 6, black bar) or γ2L (Figure 6*D*, right panel) (0.99 ± 0.07, n = 8, grey bar, and 0.94 ± 0.06, n = 6, black bar) subunits with heterozygous coexpression of either $\alpha6/\alpha6(R46W)^{FLAG}$ or $\alpha6^{FLAG}/\alpha6(R46W)^{FLAG}$ subunits, respectively. Moreover, in all heterozygous conditions, neither β2 nor γ2L subunit surface expression was reduced compared to levels obtained with coexpression of "half tagged" wild-type $\alpha6^{FLAG}/\alpha6$ subunits (Figure 6D, upper middle and right panels, all bars compared to dotted line). These data indicate that heterozygous expression of α6(R46W) subunits did not reduce surface expression levels of β2 or γ2L subunits.

Using a similar approach, total cellular expression of heterozygous $\alpha6^{FLAG}/\alpha6(R46W)$, $\alpha6/\alpha6(R46W)^{FLAG}$, and $\alpha6^{FLAG}/\alpha6(R46W)^{FLAG}$ subunits coexpressed with β2, and $\gamma2L^{HA}$ subunits was measured (Figure 6*D*, bottom panels). Similar to the cell surface results obtained for heterozygous coexpression of $\alpha6^{FLAG}/\alpha6(R46W)$ with β2, and $\gamma2L^{HA}$ subunits, no differences were found in total expression of $\alpha6^{FLAG}$ (0.49 ± 0.06, n = 8, $p > 0.05$, Figure 6*D*, left bottom panel, white bar), β2 (0.87 ± 0.07, n = 5, $p > 0.05$, Figure 6*D*, middle bottom panel, white bars)

and $\gamma 2L^{HA}$ (0.72 ± 0.05, n = 8, $p > 0.05$, Figure 6*D*, right bottom panel, white bar) subunits, when compared to those obtained with coexpression of half-tagged $\alpha 6^{FLAG}/\alpha 6$ subunits ($\alpha 6^{FLAG}$ = 0.56 ± 0.08, n = 7, β2 = 0.94 ± 0.15, n = 4, and $\gamma 2L^{HA}$ = 0.88 ± 0.08, n = 7, respectively, dotted lines).

Coexpression of $\alpha 6/\alpha 6(R46W)^{FLAG}$ subunits, however, resulted in a larger reduction of total FLAG expression (0.25 ± 0.03, n = 8, Figure 6*D*, left bottom panel, grey bar) than with either half-tagged wild-type ($\alpha 6^{FLAG}/\alpha 6$ = 0.56 ± 0.08, n = 7, $p < 0.05$, Figure 6D, left bottom panel, dotted line) or heterozygous $\alpha 6^{FLAG}/\alpha 6(R46W)$ ($p > 0.05$, Figure 6*D*, left bottom panel, white bar) subunits. Again, when $\alpha 6^{FLAG}/\alpha 6(R46W)^{FLAG}$ subunits were coexpressed, there was an increase in total expression levels of FLAG expression (0.74 ± 0.14, n = 6, Figure 6*D*, left bottom panel, black bar) relative to those obtained with expression of $\alpha 6(R46W)^{FLAG}$ subunits ($p < 0.001$, Figure 6*D*, left bottom panel, grey bar), indicating that both wild-type and mutant subunits were expressed. Similar to expression of $\alpha 6^{FLAG}/\alpha 6(R46W)^{FLAG}\beta 2\gamma 2L^{HA}$ receptors on the cell surface, there was also more total cell wild-type α6 subunits (~ 66%) than mutant α6(R46W) subunits (~ 34%).

As with surface expression, no significant differences were found for total expression levels of β2 (Figure 6*D*, middle bottom panel) (1.00 ± 0.09, n = 5, grey bar, and 0.81 ± 0.08, n = 3, black bar) or γ2L (Figure 6*D*, right bottom panel) (0.74 ± 0.04, n = 8, grey bar, and 0.75 ± 0.06, n = 6, black bar) subunits with heterozygous coexpression of either $\alpha 6/\alpha 6(R46W)^{FLAG}$ or $\alpha 6^{FLAG}/\alpha 6(R46W)^{FLAG}$ subunits, respectively. Taken together, these data suggest that when α6 and α6(R46W) subunits are "heterozygously" coexpressed with β2 and γ2L subunits, all subunits are expressed, and the number of $GABA_A$ receptors on the cell surface is not affected. Those receptors may contain α6 and/or α6(R46W) subunits, but expression and incorporation of wild-type α6 subunits is preferred.

The α6 subunit mutation, R46W, decreased macroscopic α6β2δ receptor current amplitude by reducing single channel mean open time and opening frequency.

The α6 subunit has been shown to coassemble with both γ2 and δ subunits. To determinate the effect of the α6 subunit mutation, R46W, on the macroscopic kinetic properties of α6β2δ currents, we compared wild-type α6β2δ and mutant α6(R46W)β2δ whole-cell currents elicited from lifted HEK293T cells by applying 4 s concentration jumps of saturating GABA (1 mM) (Figure 7*A*). Wild-type α6β2δ currents were smaller and desensitized less (Figure 7*D*, Table 3) than α6β2γ2L receptor currents, consistent with the macroscopic properties of α6β3δ and α6β3γ2L receptor currents reported previously[397]. Mutant α6(R46W)β2δ receptor currents also had much smaller peak currents and less whole-cell current desensitization than mutant α6(R46W)β2γ2 receptor currents (Table 3). Mutant α6(R46W)β2δ receptor currents were reduced substantially relative to wild-type α6β2δ receptor currents ($p < 0.001$, Table 3, Figure 7*A, B*), and their activation was slower than wild-type receptor currents ($p < 0.001$, Table 3, Figure 7*C*). While wild-type α6β2δ receptor currents exhibited some slow desensitization that was best fitted by four exponential functions (Table 3), mutant α6(R46W)β2δ currents displayed negligible macroscopic desensitization ($p < 0.001$, Table 3, Figure 7*D*). In addition, mutant α6(R46W)β2δ receptor currents had significantly faster current deactivation than wild-type α6β2δ receptor currents ($p < 0.001$, Table 3, Figure 7*E*).

The severe alteration of macroscopic properties of α6(R46W)β2δ receptor currents should be due to altered single channel currents. Thus, mutant α6(R46W)β2δ and wild-type α6β2δ single channel currents evoked by steady state application of 1 mM GABA were compared. Wild-type single channels opened in prolonged bursts (Figure 7*F*, top panel), while mutant single channels opened less frequently in brief bursts (Figure 7*F*, bottom panel). The single channel open duration histograms for wild-type and mutant receptors were fitted best by the sum of three exponential functions (Figure 7*G*). For both wild-type and mutant single channel current open duration histograms, the time constant (t_{o3}) and relative contribution (a_{o3}) of the longest open state

Table 3. Macroscopic kinetic properties of α6β2γ2L and α6β2δ currents evoked by 4-second applications of 1 mM GABA

	α6β2γ2L (n)			α6β2δ (n)	
	wt (15)	**R46W (7)**	**wt/R46W (18)**	**wt (11)**	**R46W (6)**
Rise time 10-90% (ms)	1.60 ± 0.07	3.09 ± 0.26***	1.30 ± 0.07###	2.82 ± 0.28	7.04 ± 1.23***
Current density (pA/pF)	4.27 ± 31.6	96.8 ± 14.7***	289 ± 13***###	130 ± 5.66	2.84 ± 0.29
Desensitization					
Extent (%)	56 ± 2	35 ± 10*	57 ± 3##	34 ± 4	2 ± 1***
τ_1 (ms)	2.32 ± 0.56	1.89 ± 0.39	1.92 ± 0.61	7.20 ± 2.53	NA
τ_2 (ms)	190 ± 35.1	171 ± 34.1	278 ± 41	85.2 ± 39.2	NA
τ_3 (ms)	528 ± 71.5	1312 ± 448*	1138 ± 155*	1606 ± 246	NA
τ4 (ms)	2533 ± 386	2322 ± 287	2742 ± 257	2739 ± 378	NA
a_1 (%)	2 ± 0.3	12 ± 3***	2 ± 0.4###	6 ± 2	NA
a_2 (%)	3 ± 0.4	17 ± 6**	9 ± 2#	8 ± 2	NA
a_3 (%)	31 ± 7	5 ± 3*	33 ± 6#	7 ± 3	NA
a4 (%)	45 ± 5	43 ± 11	50 ± 4	33 ± 6	NA
Residual (%)	31 ± 1	58 ± 13**	30 ± 3##	52 ± 7	NA
Deactivation					
τ_1 (ms)	75.1 ± 6.04	120 ± 28.1*	55 ± 3.45###	333 ± 10.6	14.0 ± 3.15***
τ_2 (ms)	430 ± 38.2	1050 ± 280**	400 ± 55###	1280 ± 153	403 ± 237**
a_1 (%)	88. ± 3	89 ± 3	90 ± 2	81 ± 3	71 ± 10
τ_{weight} (ms)	96.2 ± 9.62	184 ± 65*	67 ± 3.14##	425 ± 10.4	25.0 ± 9.97***

Values represent mean ± SEM. *, **, and *** indicate $p < 0.05$, $p < 0.01$, and $p < 0.001$ respectively (unpaired t-test or one-way ANOVA) compared to wild-type. #, ##, and ### indicate $p < 0.05$, $p < 0.01$, and $p < 0.001$ respectively (unpaired t-test or one-way ANOVA) compared to R46W.

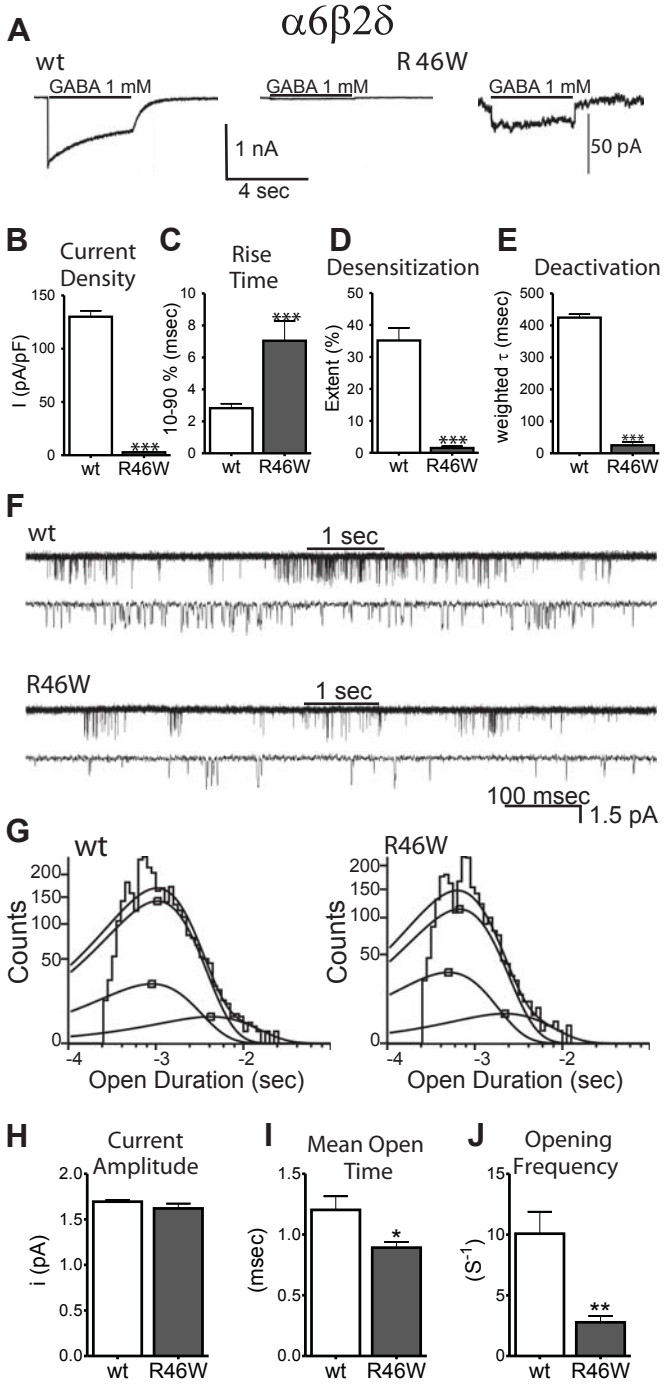

Figure 7. The R46W mutation had a greater effect on the function of α6β2δ than on α6β2γ2L receptors.

A. Current responses to long (4 s) applications of 1 mM GABA to lifted cells containing wild-type (wt) and mutant (R46W) α6β2δ receptors are shown. Note that the right trace (1 nA bar scale) of the R46W current was expanded to the left (50 pA bar scale) to demonstrate the mutant current amplitude. **B-E.** Current density, 10-90% rise time, desensitization extent and deactivation rate were measured during 4 S pulses of 1 mM GABA for both wild-type (white bars) and mutant (grey bars) receptors. **F.** Steady state single channel currents were obtained from cell-attached patches containing wild-type (wt) and mutant (R46W) α6β2δ receptors. Patches were voltage clamped at +80 mV and continuously exposed to 1 mM GABA. Note that the upper traces in panel A (1 s, black bars) were expanded below them. G. Representative open duration histograms were plotted for both wild-type and mutant R46W α6β2δ receptors and were fitted to three exponential functions. H-J. Current amplitude (H), mean open time (I) and opening frequency (J) for both wild-type (white bars) and mutant R46W (grey bars) α6β2δ receptors are shown. Values represent mean ± S.E.M. Differences between wild-type and mutant channels are shown as *, ** and ***, which indicate $p < 0.05$, $p < 0.01$ and $p < 0.001$ (unpaired t-test).

were similar ($p > 0.05$, Table 2). The shortest and intermediate open states of mutant single channel currents, however, had time constants (t_{o1} and t_{o2}) that were briefer than for wild-type receptor currents ($p < 0.001$, $p < 0.05$, Table 2). Moreover, there was a shift in the relative contributions of both brief open states (a_{o1} and a_{o2}) for mutant single channel currents that was due to increased frequency of occurrence of the fastest component and reduced frequency of occurrence of the slowest component (Figure 7*G* right panel) ($p < 0.001$, $p < 0.01$, Table 2). Thus, mutant single channel currents had significantly reduced mean open time relative to that of wild-type α6β2δ currents ($p < 0.05$, Table 2, Figure 7*I*), and their opening frequency was only about one third of wild-type channel opening frequency ($p < 0.01$, Table 2, Figure 7*J*). In contrast, there was no alteration of the main conductance state of mutant channels (~ 25 pS) when compared to wild-type channels (~ 26 pS) ($p > 0.05$, Table 2, Figure 7*H*).

The α6 subunit mutation, R46W, decreased both burst duration and frequency of α6β2δ receptor currents.

Both α6β2δ and α6(R46W)β2δ receptor channels opened in bursts (Figure 8). Wild-type channels (Figure 8*A*, top panel) opened with single brief openings and bursts of longer openings, while mutant channels opened with very brief openings (Figure 8A, bottom panel). Since a major determinant of burst structure is the time constants of the two shortest closed states that occur within bursts (t_{c1} and t_{c2}), we compared the frequency of occurrence of these intraburst closures between wild-type and mutant receptor channels. Mutant receptors had shorter intraburst closures than wild-type receptors ($p < 0.05$, Table 2), but no differences were found in the relative occurrence (a_{c1} and a_{c2}) of these closures ($p > 0.05$, Table 2). Interestingly, the overall relative contribution of intraburst closures for both wild-type and mutant d subunit-containing receptors were only 1/3 of the wild-type and mutant γ2L subunit-containing receptors (Table 2). This is consistent with the propensity of α6β2δ receptors to open in bursts of brief openings, and for α6β2γ2L receptors to open in clusters of bursts [272, 377].

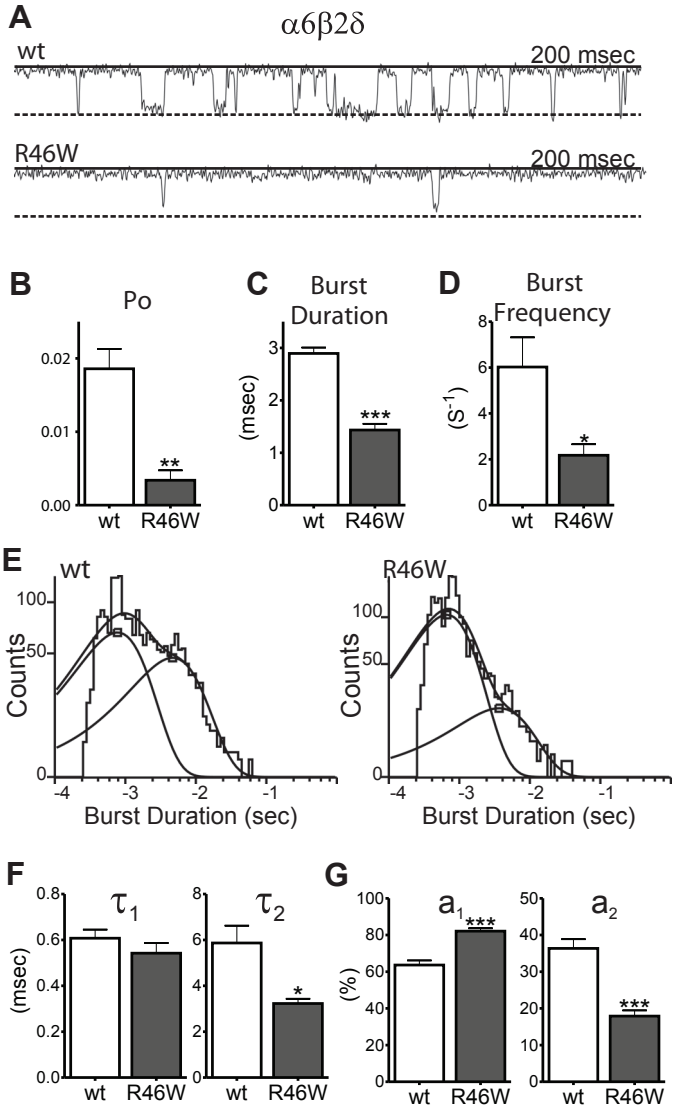

Figure 8. The R46W mutation decreased both burst duration and frequency of α6β2δ receptor currents.

A. Representative steady state single channel burst traces from cell-attached patches containing wild-type (wt) and mutant R46W α6β2δ receptors are presented. Patches were voltage clamped at +80 mV and continuously exposed to 1 mM GABA. **B-D.** Comparison of burst kinetics for both wild-type (white bars) and mutant R46W (grey bars) receptors are shown. **E.** Representative burst duration histograms for both wild-type and mutant R46W α6β2δ receptors were fitted to two exponential functions. **F, G.** Time constants (τ) and representative areas (a) of burst duration histograms for both wild-type (white bars) and mutant R46W receptors (grey bars) are presented. Values represent mean ± S.E.M. Differences between wild-type and mutant channels are shown as *, ** and ***, which indicate $p < 0.05$, $p < 0.01$ and $p < 0.001$ (unpaired t-test).

Consistent with the shorter mean open duration, α6(R46W)β2δ channel burst durations were reduced when compared to wild-type channels ($p < 0.001$, Table 2, Figure 8*C*). In addition, the time that α6(R46W)β2δ channels spent within the burst (Po) was much less than that of control channels ($p < 0.01$, Table 2, Figure 8*B*), and the burst frequency of mutant channels was also less than that of wild-type channels ($p < 0.05$, Table 2, Figure 8*D*). Furthermore, mutant channels had a small reduction of the number of openings per burst compared to wild-type channels ($p > 0.05$, Table 2).

Similar to γ2L subunit-containing $GABA_A$ receptors, for both wild-type α6β2δ and mutant α6(R46W)β2δ channels, the burst duration frequency distributions were fitted best by two exponential functions (Figure 8*E*). Again, there were no differences in the time constants (t_1 and t_2) for the short-duration bursts (t_1) for wild-type and mutant channels ($p > 0.05$, Table 2, Figure 8*F*, left panel), and the time constant for the longer burst component (t_2) was reduced for the mutant channel ($p < 0.05$, Table 2, Figure 8*F*, right panel). Again, mutant receptors shifted the distribution of the two populations of burst durations by increasing the relative proportion of bursts with short duration (a_1) and reducing the relative proportion of longer bursts (a_2) ($p < 0.001$, Table 2, Figure 8*G*). In summary, the α6 subunit mutation, R46W, substantially impaired the gating of α6β2δ channels that resulted in reduced macroscopic currents and altered kinetic properties.

The α6 subunit mutation, R46W, decreased surface expression of α6β2δ receptors.

As described previously, both macroscopic and microscopic kinetic properties of α6β2δ receptors were impaired by the α6(R46W) subunit mutation. Primarily we found a substantial reduction in α6(R46W)β2δ current density, which was due in part to the mutation's effect to reduce mean channel open time but could be due also to reduced expression of αβδ receptors on the cell surface. To determine how expression of mutant α6(R46W) subunits affected expression of α6β2δ receptors, homozygous wild-type $\alpha6^{FLAG}$ or mutant $\alpha6(R46W)^{FLAG}$ subunits were

coexpressed with β2 and δ^{HA} subunits in HEK293T cells, and surface and total cell expression levels of each subunit ($\alpha6^{FLAG}$, $\alpha6(R46W)^{FLAG}$, β2, and $\gamma2L^{HA}$) were assessed using flow cytometry.

In contrast to the results obtained for α6β2γ2L receptors, coexpression of $\alpha6(R46W)^{FLAG}$ with β2, and δ^{HA} subunits resulted in a general reduction of α6, β2 and δ subunits on the cell surface (Figure 9*A*). Cell surface levels of $\alpha6(R46W)^{FLAG}$ (0.63 ± 0.03, n = 9,), β2 (0.72 ± 0.02, n = 10), and δ^{HA} (0.59 ± 0.01, n = 10) subunit levels were all lower ($p < 0.001$) than those determined for coexpression of wild-type $\alpha6^{FLAG}$ with β2 and δ^{HA} subunits ($\alpha6^{FLAG}$ 0.997 ± 0.001, n = 9; β2 0.99 ± 0.001, n = 10; δ^{HA} 1.00 ± 0.001, n = 10) (Figure 9*B*). Moreover, total expression of $\alpha6(R46W)^{FLAG}$ subunits (0.44 ± 0.03, n = 10, $p < 0.001$, Figure 9*C* and *D*, left panels) was half that of wild-type $\alpha6^{FLAG}$ subunits (0.999 ± 0.001, n = 10). , This reduction was associated with a reduction of δ^{HA} subunit total levels (0.81 ± 0.05, n = 10, and 0.99 ± 0.001, n = 10, respectively, $p < 0.01$, Figure 9*C* and *D*, right panels) but no changes in coexpressed β2 subunits (0.96 ± 0.09, n = 7, and 0.997 ± 0.001, n = 10, respectively, $p > 0.05$, Figure 9*C* and *D*, middle panels). In summary, the R46W mutation caused a major reduction of surface expression of all subunits in αβδ receptors.

Heterozygous coexpression of $\alpha6^{FLAG}$/α6(R46W) with β2 and d^{HA} subunits resulted in no significant difference in α6 subunits (0.64 ± 0.02, n = 7, $p > 0.05$), and a small reduction of β2 (0.85 ± 0.03, n = 8, $p < 0.05$) and δ^{HA} (0.78 ± 0.02, n = 8, $p < 0.001$) subunits (Figure 9*E*, top panels) on the cell surface, when compared to half-tagged $\alpha6^{FLAG}$/α6 subunits (0.61 ± 0.02, n = 7, 1.01 ± 0.04, n = 7, and 0.99 ± 0.04, n = 7, respectively, dotted lines). Coexpression of α6/$\alpha6(R46W)^{FLAG}$ subunits, however, resulted in a larger reduction of α6 subunits (0.28 ± 0.03, n = 7) relative to both half-tagged ($p < 0.001$) and heterozygous $\alpha6^{FLAG}$/α6(R46W) ($p < 0.001$) receptors on the cell surface (Figure 9*E*, left top panel) and was associated with a reduction of β2

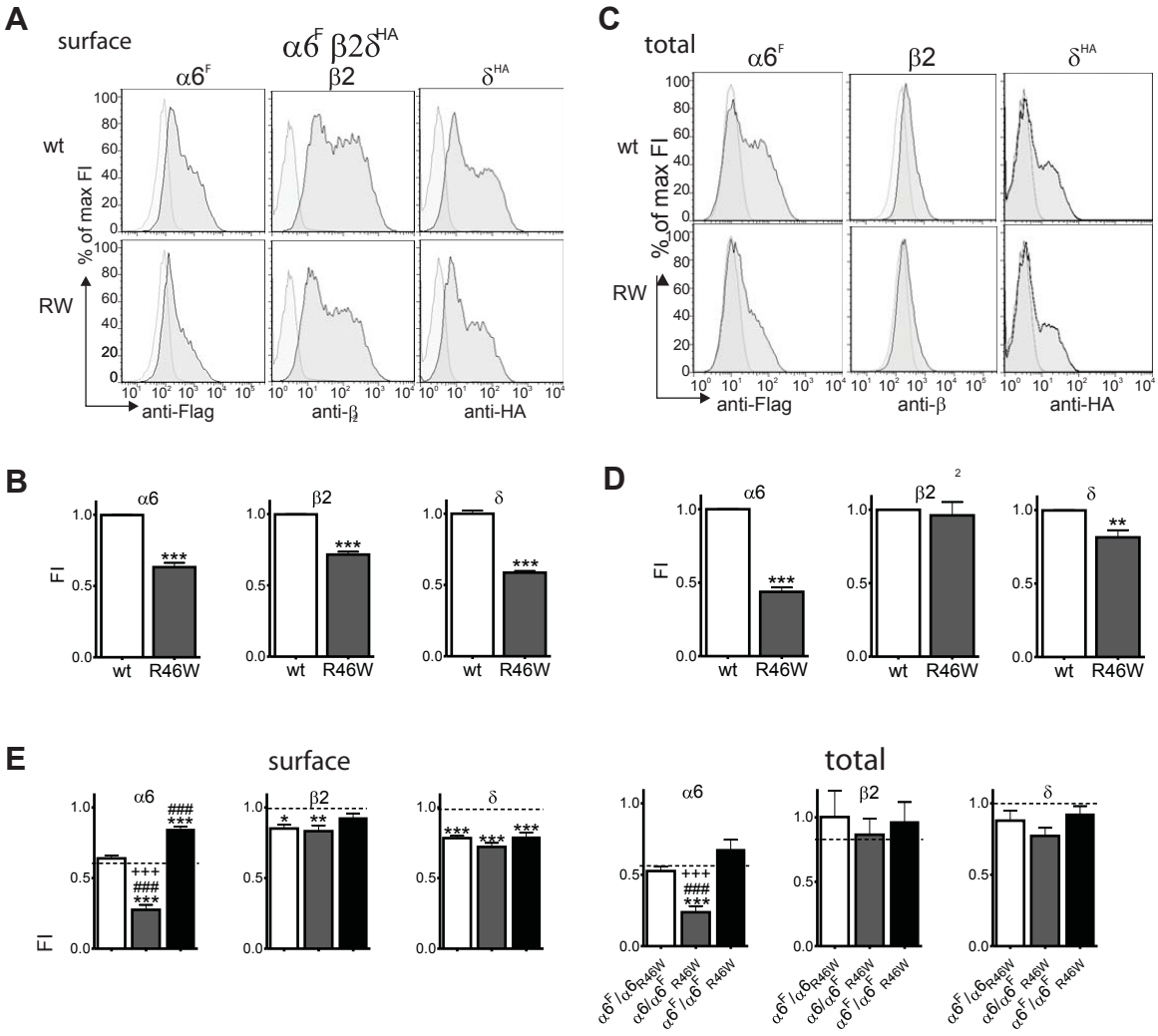

Figure 9. The R46W mutation decreased surface expression of all subunits in αβδ-containing receptors.

A. $GABA_A$ receptor $\alpha6^F$, α6F(R46W), β2 and δ^{HA} subunit surface levels were measured by flow cytometry for cells coexpressing wild-type (wt) and mutant R46W α6β2δ receptors. Representative histograms of positively transfected cells (dark grey) were superimposed on those from mock transfected cells (light grey) and are shown for surface expression. Note that the abscissa is a log scale. **B.** mean fluorescence intensity (FI) of α6, β2 and δ subunit surface levels was quantified for both wild-type (white bars) and mutant receptors (grey bars). **C.** $GABA_A$ receptor $\alpha6^F$, $\alpha6^F$(R46W), β2 and δ^{HA} subunit total cellular expression levels were measured by flow cytometry for cells coexpressing wild-type and mutant R46W α6β2δ receptors. Representative histograms of positively transfected cells (dark grey) were superimposed on those from mock transfected cells (light grey). **D.** mean fluorescence intensity (FI) of $\alpha6^F$, β2 and δ^{HA} subunit total levels was quantified as described above (wild-type as white bars, and mutant receptors as grey bars). **E.** mean fluorescence intensity (FI) of $\alpha6^F$, β2 and δ^{HA} subunit surface and total expression was quantified for heterozygous $\alpha6^F/\alpha6$(R46W), $\alpha6/\alpha6(R46W)^F$ and $\alpha6^F/\alpha6(R46W)^F$ α6β2δ receptor. Dashed lines represent $\alpha6^F/\alpha6$ surface or total levels.

(0.83 ± 0.04, n = 8, $p < 0.01$) and δ^{HA} (0.72 ± 0.03, n = 8, $p < 0.001$) subunit surface levels relative to half-tagged wild-type subunits, respectively (Figure 9*E*, middle and right top panels)

When full-tagged $\alpha6^{FLAG}/\alpha6(R46W)^{FLAG}$ subunits were coexpressed, α6 subunit levels were increased on the cell surface (0.84 ± 0.02, n = 6) when compared to those obtained with $\alpha6/\alpha6(R46W)^{FLAG}$ subunit coexpression ($p < 0.001$), and were slightly increased compared to FLAG levels with both half-tagged $\alpha6^{FLAG}/\alpha6$ ($p < 0.001$) and heterozygous $\alpha6^{FLAG}/\alpha6(R46W)$ ($p < 0.001$) expression (Figure 9*E*, left top panel). No differences were found in surface expression levels of β2 subunits (0.93 ± 0.03, n = 6, $p > 0.05$) coexpressed with $\alpha6^{FLAG}/\alpha6(R46W)^{FLAG}$ subunits (Figure 9*E*, right middle panel), but a reduction in surface levels of δ^{HA} subunits (0.79 ± 0.03, n = 6, $p < 0.001$) was found when compared to the half-tagged condition (Figure 9*E*, right top panel). As with αβγ receptors, these results suggested that in heterozygous α6/α6(R46W)β2δ receptors, mutant subunits were incorporated into the surface-trafficked receptors less efficiently than wild-type subunits. Specifically, in heterozygous α6/α6(R46W)β2δ receptors, about 2/3 of all surface α6 subunits were wild-type and 1/3 were mutant (Figure 9*E* left top panel).

We also measured the total cellular expression of heterozygous $\alpha6/\alpha6(R46W)\beta2\delta^{HA}$ receptors (Figure 9*E*, bottom panels). Similar to the results obtained for heterozygous expression of $\alpha6^{FLAG}/\alpha6(R46W)\beta2\gamma2L^{HA}$ receptors, no differences were found in total expression of α6 (0.53 ± 0.03, n = 7, $p > 0.05$), β2 (1.00 ± 0.20, n = 5, $p > 0.05$) or δ^{HA} (0.88 ± 0.07, n = 8, $p > 0.05$) subunits when compared to half-tagged $\alpha6^{FLAG}/\alpha6$ subunit total expression (0.56 ± 0.03, n = 7; 0.83 ± 0.05, n = 4; and 1.00 ± 0.04, n = 7; respectively, dotted lines), and no significant differences were found in total expression levels of β2 (0.87 ± 0.12, n = 5 and 0.96 ± 0.15, n = 3) or δ^{HA} (0.77 ± 0.06, n = 8, and 0.92 ± 0.06, n = 6) subunits with heterozygous coexpression with either $\alpha6/\alpha6(R46W)^{FLAG}$ or $\alpha6^{FLAG}/\alpha6(R46W)^{FLAG}$ subunits, respectively (Figure 9*E*, middle and right bottom panels). Coexpression of $\alpha6/\alpha6(R46W)^{FLAG}$ subunits, however, resulted in a lower levels of total α6 subunits (0.24 ± 0.04, n = 8) than of either half-tagged $\alpha6^{FLAG}/\alpha6$ ($p < 0.001$) or

heterozygous $\alpha6^{FLAG}/\alpha6(R46W)$ ($p < 0.001$) subunits (Figure 9*E*, left bottom panel). Moreover, when full-tagged $\alpha6^{FLAG}/\alpha6(R46W)^{FLAG}$ subunits were coexpressed, there was an increase of total FLAG levels (0.68 ± 0.07, $n = 6$) when compared to FLAG levels with $\alpha6/\alpha6(R46W)^{FLAG}$ coexpression ($p < 0.001$). Similar results were observed for total expression of α6 subunits (wild-type α6 subunits ~ 2/3 and mutant α6(R46W) subunits~ 1/3) in α6/α6(R46W)β2γ2L receptors (Figures 6*D* and 9*E*, left bottom panels).

Discussion

We determined the functional consequences of the $GABA_A$ receptor α6 subunit missense mutation, R46W, which was found in a patient with childhood absence epilepsy (CAE) and atonic seizures[393]. The mutation is located in the N-terminus of the α6 subunit in a region homologous to a γ2 missense mutation, R82Q, which was reported in patients affected with both CAE and febrile seizures[314, 394]. The γ2 subunit mutation, R82Q, reduced current amplitude without altering current time course by impairing primarily receptor trafficking, thus reducing receptor surface expression[313, 395]. In contrast we found that the α6 subunit mutation, R46W, affected both gating properties and trafficking of human α6β2γ2 and α6β2δ receptors.

The α6 subunit mutation, R46W, impaired gating of α6β2γ2 and α6β2δ receptors.

While the α6(R46W) subunit mutation reduced the current density of γ2 subunit-containing $GABA_A$ receptors by ~25%, the mutation reduced the current density of δ subunit-containing receptors by 98% when compared with wild-type receptors. In addition to having reduced current amplitude, α6(R46W)β2γ2 currents displayed more macroscopic desensitization and slower deactivation kinetics. In contrast, α6(R46W)β2δ currents did not desensitize and deactivated rapidly. The mutation slowed activation rates of both α6β2γ2 and α6β2δ currents to a similar extent. The mutation also produced similar changes in the single channel properties of

α6β2γ2 and α6β2δ receptors, reducing both mean open time and burst duration. A reduction in current density could be produced by reduction of channel density on the cell surface (an issue discussed later) and/or by reduction of the time the channel spends in the open state. As a result, inhibitory postsynaptic current (IPSC) amplitudes would be reduced, potentially causing disinhibition and development of epilepsy. Reduced $GABA_A$ receptor function with mutations linked to CAE was also described with mutations of γ2(R82Q) and β3(G32R) $GABA_A$ receptor subunits[310, 313, 317]. All of these mutations are located in the N-terminal extracellular subunit domain between the α-helix and the first β-sheet. Within this domain, the γ2(R82Q) mutation is predicted to be located at the γ(+)/β(-) subunit interface, and the β3(G32R) subunit mutation is predicted to be located at the γ(+)/β(-) and α(+)/β(-) subunit interfaces in assembled receptors. In HEK293 cells, Bianchi et al (2002a) found that α1β3γ2(R82Q) receptors had reduced macroscopic peak currents and single channel mean open duration, and Tanaka et al (2008) reported that α1β3(G32R)γ2 receptors had reduced current density. Goldschen-Ohm et al (2010) reported that $GABA_A$ receptors containing the γ2(R82Q) mutation had slowed deactivation by slowing recovery from desensitization and GABA unbinding, but without changes in the conductance of the channel. We conclude that both of these mutations affect channel function through structural conformational changes in the extracellular domain that links to channel gating and desensitization-deactivation coupling, thus likely altering the amplitude and duration of IPSCS.

Once GABA binds to $GABA_A$ receptors, rearrangements at the binding site trigger transitions among open, closed, and desensitized states, thereby coupling gating, desensitization and deactivation [12, 360, 398, 399]. Our results demonstrate that the R46W mutation affects gating efficacy and desensitization-deactivation coupling of both γ and δ subunit-containing $GABA_A$ receptors. For γ subunit-containing receptors, gating efficacy was decreased by reducing burst duration. This makes the channel open in brief bursts and can prolong channel deactivation.

Desensitization is usually coupled to deactivation in γ2 subunit-containing $GABA_A$ receptors. In contrast, with δ subunit-containing $GABA_A$ receptors, the smaller opening/burst frequencies predict faster deactivation of the channel. The R46W mutation affected macroscopic desensitization and deactivation, but the effects were channel is governed by the subunit that completes the pentameric receptor. This is important since γ (synaptic) and δ (extrasynaptic) subunit-containing $GABA_A$ receptors confer different properties to the synapse.

The α6(R46W) subunit mutation impaired assembly and/or trafficking of both α6β2γ2 and α6β2δ receptors.

Multiple motifs for efficient subunit folding and receptor assembly have been described in the N-terminal extracellular domains of $GABA_A$ receptor subunits[86, 90, 92, 329]. These motifs are structurally conserved among $GABA_A$ receptor subunits and involve intermolecular binding interactions between side chains of residues located on subunit interfaces. The α6(R46W) mutation is located at the α(+) interface of $GABA_A$ receptors. Thus, this mutation could impair oligomerization at the α(+)/γ(-), α(+)/δ(-), and α1(+)/β(-) subunit interfaces, potentially impairing assembly or altering the stoichiometry of receptors.

The α6(+) subunit face was reported to interact with a group of residues at the γ(-) subunit interface that are homologous to residues at the (-) face of β subunits where the missense mutation γ2(R82Q) disrupts a highly conserved inter-subunit contact site[92, 100]. Hales and colleagues suggested that the mutant γ2(R82Q) subunit has impaired oligomerization at the γ2(+)/β2(-) subunit interface during receptor assembly[100]. This failure of assembly and folding of mutant γ2(R82Q) subunits result in retention of the mutant subunit in the endoplasmic reticulum (ER) and reduction of surface expression levels of α1β2γ2 receptors[395, 400]. We found that coexpression of mutant α6(R46W) subunits decreased surface expression levels of all partnering subunits in αβδ receptors, and α and β subunits in αβγ receptors, suggesting misfolding of excess subunits and later ER retention and degradation[395]. It was proposed that non-degraded or residual

mutant $GABA_A$ receptor α1(A322D) subunits linked to juvenile myoclonic epilepsy produced a dominant negative effect by association and retention of wild-type receptor subunits [308]. However, heterozygous coexpression of mutant α6(R46W) and wild-type α6 subunits restored ~ 68% of the macroscopic current amplitude by expressing more wild-type than mutant subunits and assembling α6/α6(R46W)β2γ2L receptors on the cell surface. Thus, mutant α6(R46W) subunits can access the cell surface and form $GABA_A$ receptors with different subunit arrangements. Although the presumed stoichiometry of ternary $GABA_A$ receptors is 2α, 2β and 1γ/δ subunits[329], the assembly and trafficking of other subunits to the cell surface is restricted to a limited number of receptor stoichiometries[81, 86, 276]. Using concatenated subunits it was suggested that the α1(A322D) subunit mutation, which impaired these interactions, produced asymmetrical subunit composition of functional heteromeric $GABA_A$ receptors on the cell surface[401]. It seems that the α6(R46W) subunit mutation could also impair intersubunit binding interactions differently at the α6β2 and α6γ/δ interfaces, differently affecting the subunit arrangement of $GABA_A$ receptors expressed on the cell surface.

Mutation of R46 in the α helix loop 1 zone weakens interactions at the interfaces of γ2, δ and β2 subunits and alters channel function through structural conformational changes in the extracellular domain that mediate links to channel gating and desensitization.

Structural studies showed a common mechanism for translating ligand binding to channel gating for Cys-loop ligand ion channels[97, 402-404]. These included conformational rearrangements of the C-loop within the ligand binding pocket followed by movements of loops 2 and 7 (Cys loop) where critical residues interact upon agonist binding. These conformational rearrangements in the binding zone are transmitted to the coupling zone through interactions between the β1–β2 loop and the M2–M3 linker, which propagate structural movements from the binding site to the transmembrane domains allowing channel opening. It is possible that the R46W mutation in the α helix-Loop 1 zone of the α6 subunit weakens the interactions at the interfaces of γ2, δ and β2 subunits, propagating allosteric conformational changes through the rigid β-strands, causing

rearrangements within the coupling zone of α6β2γ2/δ receptors. Thus this mutation could affect channel function through structural conformational changes in the extracellular domain that links to channel gating and desensitization. It was proposed that the missense mutation γ2(R82Q) eliminates benzodiazepine binding to the putative benzodiazepine-binding site at the α-γ interface[405], which is on the opposite side of the γ subunit (γ2(-)), through allosteric conformational change of a salt-bridge network existing between this arginine and charged residues at the γ2(+)/β2(-) interface of α1β2γ2 $GABA_A$ receptors. Charge reversal or neutralization of the residues positioned in this salt-bridge network impaired $GABA_A$ receptor macroscopic kinetics and diazepam sensitivity of α1β2γ2 receptors expressed in HEK293 cells[317]. At the homologous position of α6(R46), a comparative structural model of the extracellular domain of α1β2γ2 receptors based on homology with the crystal structure of the nAChR[97, 406] suggested that the arginine (α1R29) shares bonding interactions between the side chains of acidic (β2D89, α1D27) and amide (α1N28, γ2N101) residues at the interfaces of β2(-) and γ2(-) subunits that stabilizes the tertiary structure of the subunits. These residues were identified as a part of a conserved assembly motif in α1 subunits[92]. Homology modeling of the N-terminal extracellular domain of α6β2γ2 and α6β2δ receptors shows a lack (α6D44, γN71, β2D41, β2D113 and δD45) of interactions between the side chains in the interfaces of α6(+) and β2(-), γ2(-), or δ(-) subunits when the α6 subunit R46 is mutated to W46 (Figure 10), which might first change the surface accessible area of the residues between the interfaces of the subunits, and second propagate intramolecular and/or intermolecular allosteric conformational changes through the rigid β-strands, causing rearrangements within the coupling zone of $GABA_A$ receptors. Moreover, when an agonist binds to these receptors, conformational changes trigger the "capping motion" of the C-loop in toward the channel over the agonist, which couples agonist binding to channel gating[402, 404]. A similar mechanism was proposed to occur at the homologous structural region of the C-loop of α1β2γ2 $GABA_A$ receptors[407]. Hence electrostatic interactions between charged residues of loop-B and loop-C might be involved in the C-loop mobility during activation of $GABA_A$

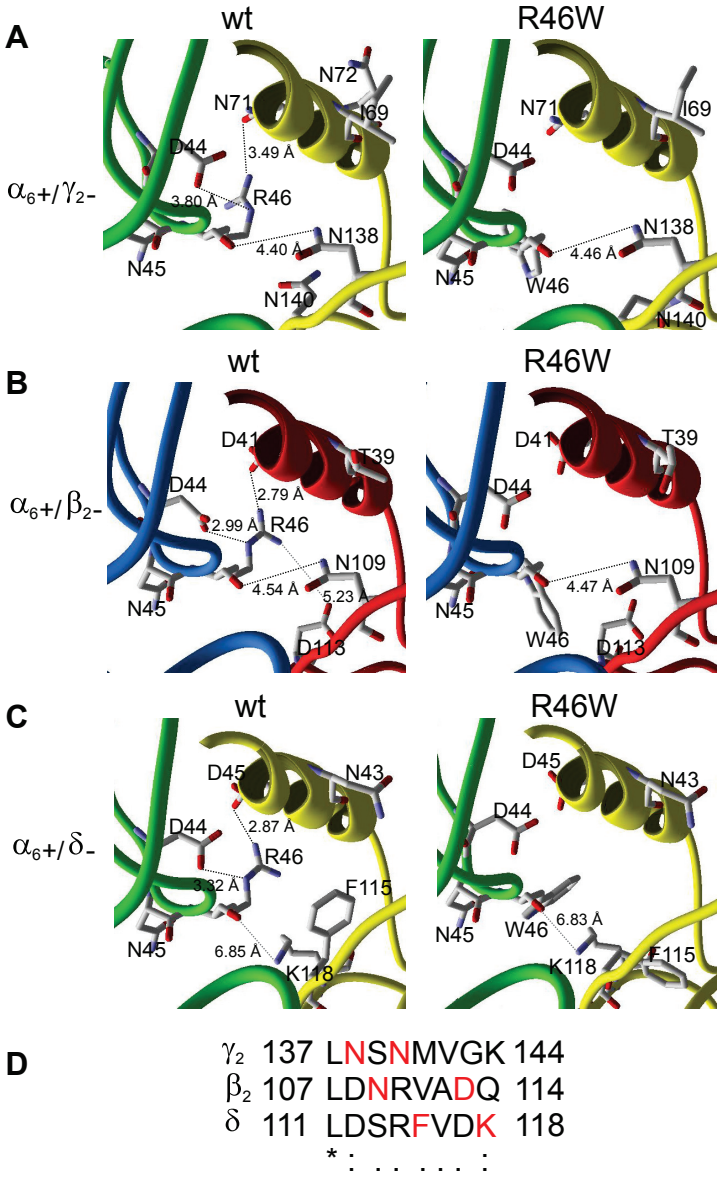

Figure 10. Mutation of α6R46 in the α-helix-Loop-1 zone weakens interactions at the interfaces of γ2, β2 and δ subunits.

A-C. Close view of the α-helix-Loop-1 zone of the structural modelling of the GABAA receptor at the interface between α6(+) and γ2(-), β2(-) and δ(-) subunits showing the predicted interactions (< 4.60 Å, black dotted lines; and >4.60 Å, grey dotted lines) between side chains of α 6R46 (wt, left panels) and α6W46 (R46W, right panels). Note that γ2N71, β2D41 and δD45 are conserved residues into the α-helix across the GABAR subunits (see Figure 1B). The backbones of subunits are represented as coloured ribbons as showed in Figure 1A (α6 in green and blue, β2 in red, and γ2 and δ in yellow) and labelled residues as CPK representation. **D.** Sequence alignment of the putative homologous assembly motif at human γ2(-), β2(-) and δ(-) subunit interfaces is presented. Predicted residues at the interfaces are in red. "*", ":" and "." means that residues are identical, conserved or semi-conserved in all sequences in the alignment.

receptors and could be affected by structural changes transmitted through the β-strands by either modification of glycosylation sites[335] or by nearby point mutations located at the top of the N-terminal extracellular domain of the receptor as suggested for the missense mutation γ2(R82Q)[317] and the α6(R46W) mutation (this study).

Pathophysiological consequences of GABRA6 mutations in CAE.

It may be assumed that in pathological conditions, all neural networks are susceptible to amplification or intensification of aberrant signals from disinhibited neuronal networks. However, the functional consequences of these networks for epileptogenesis in the cerebellum are unclear. Early work[408, 409], which failed to demonstrate any behavioral phenotype in mice lacking $GABA_A$ receptor α6 subunits; however, we cannot necessarily discount the possibility of the presence of absence seizures in these models since the detection of such events sometimes requires a phenotypic criterion such as abnormal EEG (generalized spike-wave discharges) rather than a simple observable behavior. Nonetheless, the lack of α6 subunits caused a dramatic reduction in δ subunit protein levels in the cerebellum of α6 knockout mice[408]. We found that the R46W mutation caused a similar reduction of surface expression of δ subunits, which unveils a critical role of this residue for properly assembling/trafficking of functional $GABA_A$ receptors. Likewise, a point mutation in a residue critical for benzodiazepine binding to α6 subunits (R100) conferred diazepam-mediated potentiation of α6(Q100)β2γ2 GABA-activated currents and reduced the impairment of postural reflexes produced by benzodiazepine agonists such as diazepam in alcohol non-tolerant rats[410-412]. We suggest that the R46W mutation may increase susceptibility to epilepsy syndromes such as CAE through a reduction of α6βγ and α6βδ receptor function and expression in the cerebellum. However, it is unclear whether or not and if so how the mutated α6 protein contributes to the pathogenesis of the epilepsy syndrome. Further validation of the mutant subunit *in vivo* will be required to determine whether this mutation contributes to shaping the disease phenotype.

CHAPTER VI

$GABA_A$ RECEPTOR BIOGENESIS IS IMPAIRED BY THE γ2 SUBUNIT FEBRILE SEIZURE-ASSOCIATED MUTATION, *GABRG2(R177G)*

Abstract

A missense mutation in the $GABA_A$ receptor γ2L subunit, R177G, was reported in a family with complex febrile seizures (FS). To gain insight into the mechanistic basis for these genetic seizures, we explored how the R177G mutation altered the properties of recombinant α1β2γ2L $GABA_A$ receptors expressed in HEK293T cells. Using a combination of electrophysiology, flow cytometry, and immunoblotting, we found that the R177G mutation decreased GABA-evoked whole-cell current amplitudes by decreasing cell surface expression of α1β2γ2L receptors. This loss of receptor surface expression resulted from endoplasmic reticulum (ER) retention of mutant γ2L(R177G) subunits, which unlike wild-type γ2L subunits, were degraded by ER-associated degradation (ERAD). Interestingly, when compared to the condition of homozygous γ2L(R177G) subunit expression, disproportionately low levels of γ2L(R177G) subunits reached the cell surface with heterozygous expression, indicating that wild-type γ2L subunits possessed a competitive advantage over mutant γ2L(R177G) subunits for receptor assembly and/or forward trafficking. Inhibiting protein synthesis with cycloheximide demonstrated that the R177G mutation primarily decreased the stability of an intracellular pool of unassembled γ2L subunits, suggesting that the mutant γ2L(R177G) subunits competed poorly with wild-type γ2L subunits due to impaired subunit folding and/or oligomerization. These findings support an emerging body of literature implicating defects in $GABA_A$ receptor biogenesis in the pathogenesis of idiopathic generalized epilepsies (IGEs).

Introduction

Idiopathic generalized epilepsies (IGEs) include a wide variety of epilepsy syndromes, ranging from relatively benign forms such as simple febrile seizures (FS) to catastrophic syndromes such as Dravet syndrome [310, 413]. The most common childhood seizures are FS[414], with a prevalence as high as 5% in children under the age of six[415]. Although FS typically do not occur after six years of age, patients experiencing FS have an increased risk of epilepsy later in life[416, 417], and many clinically heterogeneous IGEs present in childhood as FS[416]. As a result, they have been grouped into the generalized epilepsy with FS plus (GEFS+) spectrum of IGEs**.** Many IGEs likely have a genetic component, with monogenic mutations in voltage-gated (CACNB4, KCNQ2, KCNQ3, SCN1A and SCN1B) and ligand-gated (CHRNA4, CHRNB2, GABRA1, GABRB3, and GABRG2) ion channel subunits having been identified in families with various IGE syndromes[391, 418-420].

In the $GABA_A$ receptor γ2 subunit, we previously reported the R177G mutation in a family with complex FS occurring with an autosomal dominant inheritance pattern[421]. Understanding the effects of this mutation was of particular interest, as introduction of glycine residues is known to increase conformational freedom[422], and adjacent to this residue there is already a conserved glycine at position 176. The R177G mutation might therefore amplify existing conformational freedom in this region of the γ2 subunit. Since channel gating is mediated by subunit conformational changes, which are in turn highly dependent upon the integrity of local structural motifs[166, 167, 423], this additional flexibility might change the kinetic properties of receptors containing mutant γ2(R177G) subunits. Alternatively, if increased conformation freedom were to cause subunit instability and misfolding, the mutation might impair assembly and/or trafficking of γ2 subunit-containing receptors, thereby reducing the number of functional $GABA_A$ receptors on the cell surface.

Since $GABA_A$ receptors are the primary mediators of fast inhibitory synaptic transmission in the mammalian brain, and the γ2 subunit is an important determinant of both $GABA_A$ receptor current kinetics[168] and synaptic targeting[136, 137], we hypothesized that the R177G mutation promoted neuronal hyperexcitability via loss of GABAergic inhibition due to impaired receptor function and/or biogenesis. To explore these possibilities, we characterized the effects of the γ2 subunit R177G mutation on the properties of recombinant α1β2γ2L $GABA_A$ receptors transiently expressed in HEK293T cells. Using a combination of patch clamp recording, flow cytometry, and immunoblotting, we evaluated the effects of the mutation on $GABA_A$ receptor current kinetics, surface trafficking, and subunit maturation, respectively. We identified a novel mechanism underlying loss of GABAergic inhibition whereby mutant γ2L(R177G) subunits are retained in the ER and degraded by the ubiquitin-proteasome system after failing to "compete" with wild-type subunits for incorporation into functional receptors.

Materials and Methods

Cell culture and expression of recombinant $GABA_A$ receptors

HEK293T cells (a gift from P. Connely, COR Therapeutics, San Francisco, CA) were cultured in Dulbecco's Modified Eagle's Medium with 10% Fetal Bovine Serum, 100 IU / ml penicillin, and 100 μg / ml streptomycin (Invitrogen, Carlsbad, CA) and maintained at 37 °C in humidified 5% CO_2 / 95% air.

The cDNAs encoding human $GABA_A$ receptor α1, β2S, and γ2L subunits were individually subcloned into the pcDNA3.1 expression vector. The γ2L subunit R177G mutation was introduced using the QuikChange site-directed mutagenesis kit (Stratagene, La Jolla, CA) and confirmed by DNA sequencing. Note that all point mutation residues are numbered according to their position in the immature human subunit (i.e., including the signal peptide). Due to the lack of a highly specific, commercially available antibody for a native extracellular

epitope on the γ2L subunit, FLAG (DYKDDDDK) or HA (YPYDVPDYA) epitopes were inserted between amino acids 4 and 5 of the mature γ2L subunit so that subunit surface expression could be monitored with flow cytometry or immunoblotting (see Results).

Using Fugene6 (Roche Diagnostics, Indianapolis, IN) according to the manufacturer's recommended protocol, cells were cotransfected with α1, β2, and either "wild-type" γ2L (α1 : β2 : γ2L cDNA ratio of 0.3 μg : 0.3 μg : 0.3 μg), "heterozygous" γ2L/γ2L(R177G) (α1 : β2 : γ2L : γ2L(R177G) cDNA ratio of 0.3 μg : 0.3 μg : 0.15 μg : 0.15 μg), or "homozygous" γ2L(R177G) (α1 : β2 : γ2L(R177G) cDNA ratio of 0.3 μg : 0.3 μg : 0.3 μg) subunits. Note that subsequent sections use the terms wild-type, heterozygous, and homozygous as shorthand for these transfection conditions rather than to imply a specific genotype. For electrophysiology experiments, subunit cDNAs were cotransfected with 1 μg of pHook-1 (Invitrogen, Carlsbad, CA), a surface antigen used for immunomagnetic selection 24-30 hours after transfection, as previously described [343]. For all transfection conditions, empty pcDNA3.1 vector was added such that a total of 0.9 μg of subunit cDNA was used for each experimental condition. Mock transfection conditions included 0.9 μg of empty pcDNA 3.1 expression vector cDNA.

Electrophysiology

Cells were plated onto 35-mm culture dishes (Corning Life Sciences, Acton, MA), and positively transfected cells were selected with an immunomagnetic selection technique described previously[343]. For macropatch recordings, the 35-mm dishes were coated with collagen in acetic acid (Sigma-Aldrich, St. Louis, MO) and allowed to dry under UV light before plating. Recordings were made 18-24 hours after cell selection in an external bath solution consisting of (in mM): NaCl 142, KCl 8, $MgCl_2$ 6, $CaCl_2$ 1, HEPES 10, glucose 10 (pH adjusted to 7.4 using NaOH; 318-328 mOsm). The intrapipette solution consisted of (in mM): KCl 153, $MgCl_2$ 1, MgATP 2, HEPES 10, EGTA 5 (pH was adjusted to 7.3 using KOH; 305-312 mOsm). The solutions were designed such that the chloride equilibrium potential was approximately 0 mV.

Cells were held at a membrane potential of -20 mV for lifted whole cell recordings and -50 mV for macropatch recordings. Recording pipettes were made of thin-walled (whole cell) or thick-walled (macropatch) borosilicate glass (World Precision Instruments, Pittsburgh, PA) pulled with a P-2000 laser puller (Sutter Instruments, San Rafael, CA) and fire polished with a microforge (Narishige, East Meadow, NY) to resistances of 0.8-1.5 MΩ (whole cell) or 5-8 MΩ (macropatches) when filled with internal solution. Currents were elicited from lifted whole cells or excised outside-out macropatches using the concentration-jump technique[424]. The 10-90% open tip solution exchange times were consistently < 1 ms for whole cell recordings and < 500 μs for macropatch recordings. Data were acquired at 20 kHz using an Axopatch 200-B (Molecular Devices, Sunnyvale, CA), filtered at 2 kHz, and analyzed offline using pClamp 9. For macropatch recordings, current desensitization time courses were fitted using the Levenberg-Marquardt least squares method to the form $\sum a_n e^{(-t/\tau_n)}$, where *n* is the number of exponential components, *a* is the relative (fractional) amplitude of the component at time = 0, *t* is time, and τ is the time constant. The number of components was incremented until additional components did not significantly improve the fit as determined by an F-test performed on residuals. For the time course of current deactivation, a weighted sum ($a_f * \tau_f + a_s * \tau_s$) was used. Data were represented as the mean ± SEM, and statistical significance was determined using a Student's unpaired *t*-test with Welch's correction for unequal variance.

Flow cytometry

Surface and total cellular expression of $GABA_A$ receptor subunits was evaluated by flow cytometry as previously described[335, 367, 425]. Briefly, cells were harvested 48 hours after transfection using 37 ºC trypsin/EDTA (Gibco, Carlsbad, CA) and 4ºC FACS buffer composed of phosphate-buffered saline (Mediatech, Herndon, FA), 2% fetal bovine serum (Gibco), and 0.05% sodium azide (VWR, Weschester, PA). Cells were then transferred to 96-well plates for antibody

staining. For total protein staining, samples were first fixed and permeabilized using the Cytofix/Cytoperm kit from BD Biosciences (San Jose, CA).

The human α1 antibody (Clone BD24) was obtained from Millipore (Temecula, CA), conjugated to the Alexa-647 fluorophore using a kit (Invitrogen, Carlsbad, CA), and used at a dilution of 1:200. The β2/3 antibody (Clone 62-3G1) was obtained from Millipore (Billerica, MA), but could not be directly conjugated to fluorophore without substantially reducing its affinity. Thus, after staining at a 1:100 dilution, the samples were stained again for 1 hour using rabbit anti-mouse IgG1 Alexa-647-conjugated secondary antibody (Invitrogen) at a 1:500 dilution, pelleted and resuspended three times in FACS buffer, and pelleted and resuspended in 2% PFA. Since high-affinity antibodies against an extracellular domain of the γ2 subunit were unavailable, N-terminal FLAG-tagged γ2L ($\gamma2L^{FLAG}$) or HA-tagged subunits were employed. The FLAG antibody (Clone M2) was obtained from Perkin Elmer (Boston, MA) as an allophycocyanin conjugate and used at a dilution of 1:200, and the HA antibody was obtained from Covance and used at a dilution of 1:5000. Antibodies were diluted in FACS buffer for surface staining and Permwash for total staining.

Samples were run on a BectonDickson FACS Calibur flow cytometer and data were acquired using CellQuest (BD Biosciences, San Jose, CA). For each staining condition, at least 50,000 events were recorded, and data were analyzed offline using FlowJo 7.1. The mean fluorescence intensity (FI) of the experimental cells was normalized to the wild-type α1β2γ2L condition for comparison ("Relative FI"). In all experiments, cells were transfected also with an equivalent amount of blank pcDNA3.1 vector as a control for the transfection proceedure (mock condition). Statistical significance was determined using a Student's unpaired *t*-test or ANOVA with Tukey's post-test, as appropriate.

For cycloheximide and lactacystin experiments, cells were prepared and transfected as described above, except that cells were transfected in 10-cm culture dishes and split 24 hours later into separate 6-cm culture dishes for drug application. Cycloheximide (Supelco, Bellefonte, PA)

and lactacystin (Boston Biochem, Cambridge, MA) were dissolved in DMSO (Sigma) and diluted 1:1000 into the culture dish to final concentrations of 100 μg / mL and 10 μM on the day of the experiment. For control experiments, DMSO was added to the culture dish.

Protein digestion and immunoblotting

Transfected cells (as described above) were lysed 48 hours after transfection in RIPA buffer composed of: 10 mM Tris, 150 mM NaCl, 1 mM EDTA, 0.25% sodium deoxycholate, and 1% NP-40 (pH adjusted to 7.4). All reagents were obtained from Sigma. A Complete Mini™ protease inhibitor cocktail tablet (Roche Diagnostics, Mannheim, Germany) was added to the RIPA buffer on the day of the experiment. The protein concentration of each sample was determined with a protein assay dye (BioRad, Hercules, CA) on a spectrophotometer measuring absorbance at 595 nm against a standard curve generated with BSA. For each sample, 25 μg of protein was included, and sample volumes were adjusted with lysis buffer. Samples were digested with Endo H or PNGase F with 1x dilution of G7 or G5 reaction buffer, respectively (New England BioLabs, Beverly, MA). Undigested samples were incubated with 1x G7 reaction buffer and RIPA buffer in place of enzyme. Digestion proceeded for 3 hours at 37º C and was stopped with 5% β-mercaptoethanol (Sigma) in 5x sample buffer (BioRad). Samples were loaded onto a 10% acrylamide gel for SDS-page electrophoresis at 100 V for 4-5 hours and transferred to a PVDF membrane (Millipore). Membranes were blocked in 0.5% non-fat milk in Tris-Buffered Saline with 0.2% Tween (TTBS) and incubated in mouse anti-HA antibody (Covance, Berkeley, CA) and Na^+/K^+ ATPase α-chain as a loading control (Abcam, Cambridge, MA). Membranes were secondarily probed with a goat anti-mouse antibody conjugated to HRP (Jackson ImmunoResearch, West Grove, PA). Membranes were washed and incubated with a chemiluminescent reagent (GE/Amersham Life Sciences, Piscataway, NJ) before exposure with a chemiimager. Band density was determined using BioRad's Quantity One software. Statistical significance was determined using a Student's paired *t*-test.

Sequence alignment and homology modeling

Multiple sequence alignments of human $GABA_A$ receptor subunits and the glutamate-gated chloride channel were performed using ClustalW (European Bioinformatics Institute, Hinxton, UK). Structural models of $GABA_A$ receptor α1, β2, and γ2 subunits were generated with SWISS-MODEL[379], using the crystal structure of the *C. elegans* glutamate-gated chloride channel (GluCl; PDB ID 3rhw) as a template[159]. Point mutations were introduced into the γ2 subunit sequence using DeepView/Swiss-PdbViewer 4.02 (Swiss Institute of Bioinformatics, Lausanne, Switzerland), and project files containing the mutated target sequence and the superposed template structure were submitted to SWISS-MODEL. Completed subunits were threaded onto the GluCl crystal structure in the order γ2L-β2-α1-β2-α1. All models were subjected to energy minimization within DeepView/Swiss-Pdb Viewer using GROMOS96 in default settings, and the most likely conformations were presented here.

Results

Whole cell current density was reduced by expression of mutant γ2L(R177G) subunits.

GABA-evoked currents (1 mM application for 4 s) were obtained from lifted HEK293T cells cotransfected with $GABA_A$ receptor α1, β2, and either wild-type γ2L, an equimolar mixture of wild-type γ2L and mutant γ2L(R177G) ("heterozygous"), or mutant γ2L(R177G) ("homozygous") subunits (Figure 1A; see Methods for subunit cDNA ratios and concentrations for each condition). Peak current densities obtained from cells expressing wild-type γ2L subunits (539.6 $\pm$ 62 pA/pF, n = 10) were greater than those obtained from cells expressing mutant γ2L(R177G) subunits in the heterozygous condition (377.4 $\pm$ 39 pA/pF, n = 13, n.s.) and significantly greater than those obtained from cells expressing mutant γ2L(R177G) subunits in the homozygous condition (220.6 $\pm$ 90 pA/pF, n = 9, $p < 0.01$). The difference in current density

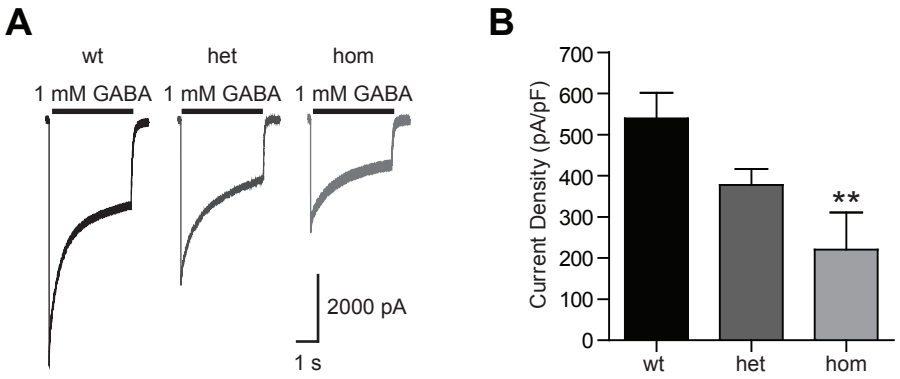

Figure 1. Cells expressing α1, β2, and mutant γ2L(R177G) subunits had reduced current density compared to cells expressing α1, β2, and wild-type γ2L subunits.
A. GABA-evoked (1 mM; 4 sec) currents were obtained from lifted HEK293T cells expressing α1, β2, and either wild-type γ2L (wt), heterozygous γ2L/γ2L(R177G) (het), or homozygous γ2L(R177G) (hom) subunits. **B.** Cells expressing either heterozygous or homozygous γ2L(R177G) subunits had reduced current density compared to those expressing wild-type γ2L subunits. * $p < 0.05$, ** $p < 0.01$ when compared to the wild-type condition.

from cells expressing homozygous as compared to heterozygous mutant γ2L(R177G) subunits was not statistically significant (Figure 1B).

Currents obtained from cells coexpressing α1β2γ2L or α1β2γ2L(R177G) subunits had similar kinetic properties.

To compare the macroscopic kinetic properties of wild-type and mutant $GABA_A$ receptor currents, GABA-evoked currents (1 mM application for 400 ms) were obtained from outside-out macropatches excised from cells coexpressing α1, β2, and either γ2L or γ2L(R177G) subunits. Wild-type and homozygous mutant receptors yielded currents with similar rates of activation (10-90% rise times of <1.5 ms; data not shown), as well as similar time courses of desensitization and deactivation (Figure 2A). Desensitization was consistently biphasic, with time constants of 9.0 $\pm$ 1.0 and 141 $\pm$ 36 ms for wild-type (n = 3) and 7.9 $\pm$ 2.2 ms and 85 $\pm$ 5.1 ms for homozygous mutant (n = 4) receptors, respectively (Figure 2B). There was a similar contribution of each exponential component (Figure 2C).

Coexpression of mutant γ2L(R177G) subunits increased α1 and β2 and decreased γ2L subunit surface levels.

The observation that peak current amplitudes were reduced in the context of unchanged macroscopic current kinetics suggested that the R177G mutation decreased $GABA_A$ receptor surface levels without altering subunit composition or stoichiometry. To test this hypothesis, flow cytometry was used to analyze the surface levels of α1, β2, and γ2L subunits when cotransfected in either wild-type, heterozygous, or homozygous γ2L subunit combinations.

Surface α1 subunit levels were increased slightly in the heterozygous condition (117.5 $\pm$ 4.0% of wild-type, n = 11-12, $p < 0.05$), but not in the homozygous condition (Figure 3A). Surface β2 levels trended toward an increase in the heterozygous condition (138.3 $\pm$ 10% of wild-type, n = 6, and increased significantly in the homozygous condition (146.0 $\pm$ 16% of wild-type, n = 6, $p < 0.05$) (Figure 3B). These trends in surface α1 and β2 subunit levels were similar when

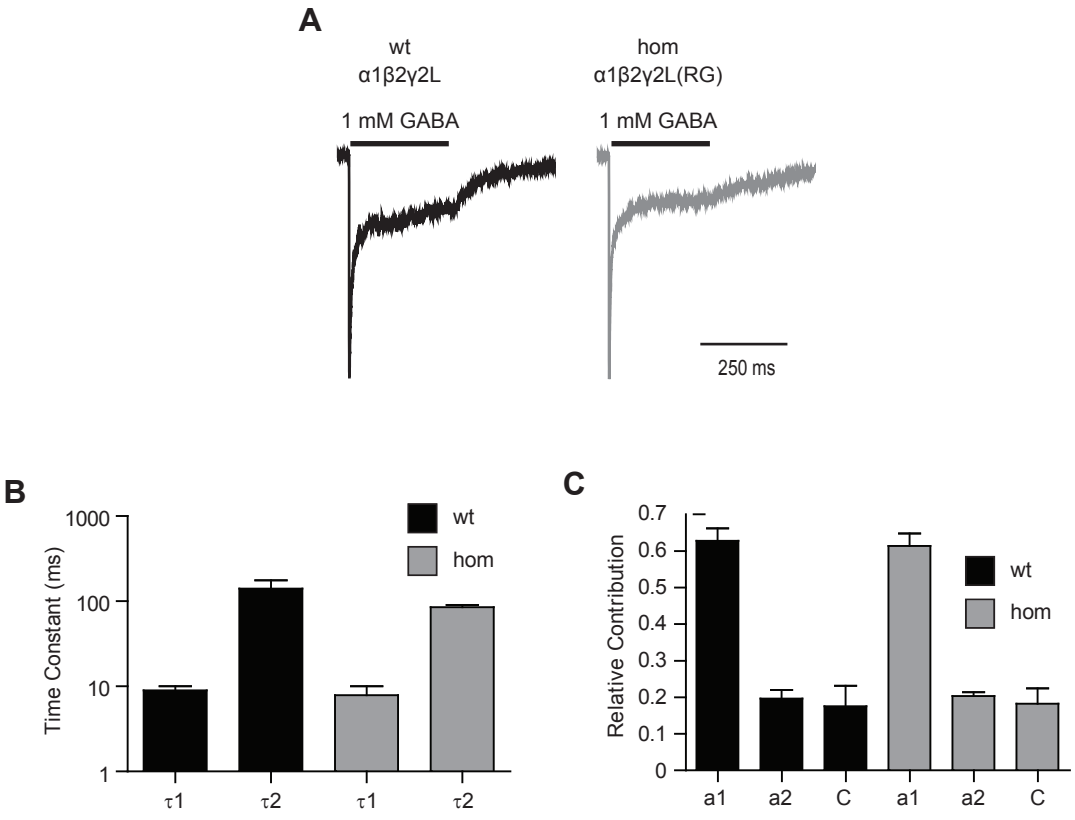

Figure 2. The time course of macroscopic desensitization was similar for currents recorded from cells expressing α1, β2, and either wild-type γ2L or mutant γ2L(R177G) subunits.

A. GABA-evoked (1 mM; 400 ms) currents were recorded from outside-out macropatches excised from HEK 293T cells coexpressing α1, β2, and either wild-type γ2L (wt; black) or homozygous mutant γ2L(R177G) (hom; grey) subunits. Each trace represents the average of 3-5 currents evoked from the same cell. **B.** Currents recorded from cells expressing wild-type γ2L and homozygous mutant γ2L(R177G) subunits were analyzed to determine time constants of macroscopic desensitization. **C.** Currents recorded from cells expressing wild-type γ2L and homozygous mutant γ2L(R177G) subunits were analyzed to determine the relative contribution of each desensitization component.

untagged γ2L or γ2L(R177G) subunits were used (data not shown). In contrast, $\gamma2L^{FLAG}$ subunit surface levels were decreased in both heterozygous (80.0 ± 3.0% of wild-type, n = 7, $p < 0.001$) and homozygous (40.0 ± 4.0% of wild-type, n = 7, $p < 0.001$) conditions (Figure 3C). The $\gamma2L^{FLAG}$ levels were also significantly different in the heterozygous and homozygous conditions ($p < 0.001$). Thus, despite the appearance of unaltered macroscopic current kinetics, the γ2L(R177G) mutation likely altered the subunit composition and/or stoichiometry of $GABA_A$ receptors expressed on the cell surface.

In parallel experiments, HEK293T cells were permeabilized before staining to determine the total cellular levels of $\gamma2L^{FLAG}$ and/or $\gamma2L(R177G)^{FLAG}$ subunits (Figure 3D). Total FLAG staining was not reduced significantly in the heterozygous condition, but was reduced significantly in the homozygous condition (72.5 ± 9.0% of wild-type, n = 6, $p < 0.05$) (Figure 3D). However, the R177G mutation decreased surface $\gamma2L^{FLAG}$ subunit levels to a greater extent than total $\gamma2L^{FLAG}$ subunit levels (compare Figure 3C with Figure 3D), suggesting that mutant γ2L(R177G) subunits had either decreased rates of forward trafficking or increased rates of surface internalization.

Receptors containing wild-type γ2L subunits were preferentially trafficked to the cell surface with coexpression of mutant γ2L(R177G) and wild-type γ2L subunits.

To determine the relative contributions of wild-type γ2L and mutant γ2L(R177G) subunits in the context of heterozygous expression, the subunits were differentially tagged with the FLAG epitope (i.e., $\gamma2L^{FLAG}$/γ2L(R177G) or γ2L/$\gamma2L(R177G)^{FLAG}$). Following co-transfection with α1 and β2 subunits, surface (Figure 4A) and total (Figure 4B) FLAG levels were analyzed using flow cytometry. For comparison, the following conditions were evaluated in each experiment: 1) "wt[half-FLAG]", corresponding to α1β2$\gamma2L^{FLAG}$/γ2L subunit coexpression; 2) "het[wt-FLAG]", corresponding to α1β2$\gamma2L^{FLAG}$/γ2L(R177G) subunit coexpression; 3) "het[RG-FLAG]", corresponding to α1β2γ2L/$\gamma2L(R177G)^{FLAG}$ subunit coexpression; and 4) "mock",

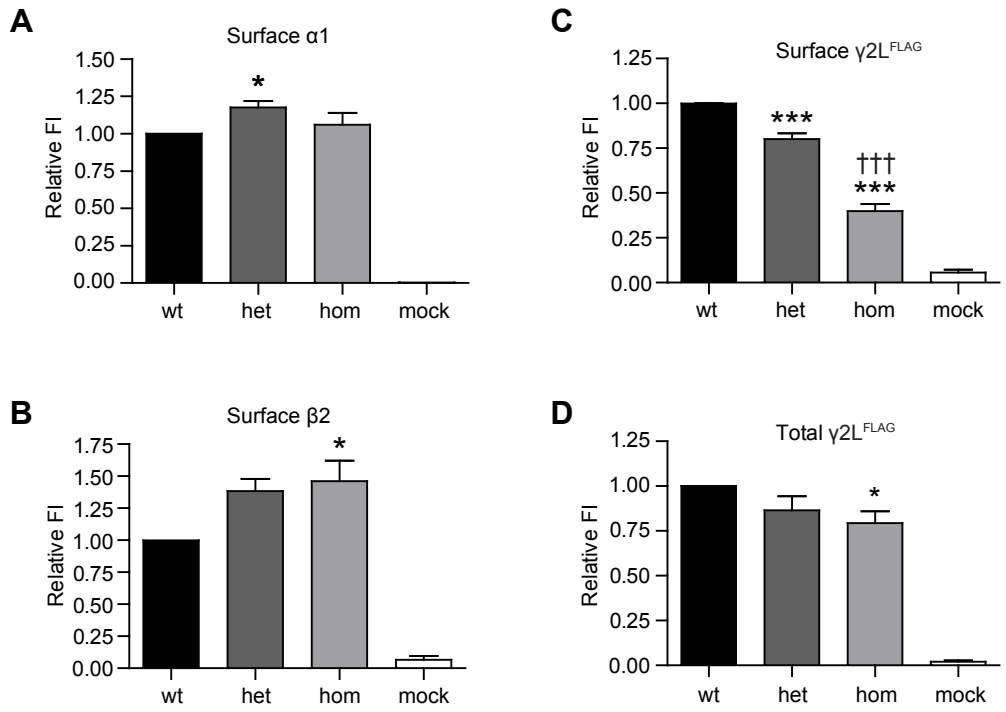

Figure 3. The R177G mutation decreased cellular expression levels of the γ2L^{FLAG}, but not the α1 or β2, subunits in heterozygous and homozygous transfection conditions.
A-C. Surface expression levels of the α1 (Panel A), β2 (Panel B), and γ2L^{FLAG} (Panel C) subunits were evaluated by flow cytometry for wild-type ("wt"; α1β2γ2L^{FLAG}), heterozygous mutant ("het"; α1β2γ2L^{FLAG}/γ2L(R177G)^{FLAG}), homozygous mutant ("hom"; γ2L(R177G)^{FLAG}), and "mock" transfection conditions. **D.** Total cellular expression levels of the γ2L^{FLAG} subunit were evaluated by flow cytometry for wild-type, heterozygous, homozygous, and mock transfection conditions. Relative fluorescence intensity (Relative FI) was calculated by normalizing the fluorescence intensity obtained for each condition to that of wild-type. * $p < 0.05$, ** $p < 0.01$, *** $p < 0.001$ when compared to the wild-type condition; ††† $p < 0.001$ when compared to the heterozygous condition.

corresponding to expression of empty pcDNA3.1 vector (see Materials and Methods for cDNA concentrations and ratios for each condition).

In the wt[half-FLAG] condition, surface $\gamma 2L^{FLAG}$ subunit levels were approximately half (52.4 $\pm$ 1.0%, n = 7) of the wt[all-FLAG] condition (Figure 3C), indicating that tagged and untagged subunits competed equally for surface expression (Figure 4A). When wild-type $\gamma 2L^{FLAG}$ subunits were coexpressed with untagged mutant γ2L(R177G) subunits (het[wt-FLAG] condition), surface FLAG levels were increased slightly compared to the wt[half-FLAG] condition (60.0% $\pm$ 2% of wt[all-FLAG] levels; $p < 0.001$, n = 7). In contrast, when mutant $\gamma 2L(R177G)^{FLAG}$ subunits were coexpressed with untagged wild-type γ2L subunits (het[RG-FLAG]), surface FLAG levels were decreased substantially (9.0 $\pm$ 1% of wt[all-FLAG] levels; $p < 0.001$, n = 7) (Figure 4A). The combined surface levels of the het[wt-FLAG] and het[RG-FLAG] conditions were similar to the surface levels observed for the original heterozygous condition, where wild-type and mutant subunits were both FLAG-tagged (Figure 3). Thus, in the heterozygous condition, the wild-type γ2L subunit was the predominant γ2L subunit on the cell surface. Of note, while mutant subunit surface levels in the homozygous condition were substantially reduced compared to the wild-type condition (Figure 3C), they were much higher than mutant subunit levels in the heterozygous condition (het[RG-FLAG], Figure 4A), even when corrected for the higher (i.e., double) concentration of mutant cDNA used to transfect for the homozygous condition (see Methods). This suggested that the presence of wild-type subunits further compromised the ability of mutant γ2L(R177G) subunits to reach the cell surface.

To determine if this phenomenon was limited to the surface receptor pool or if the entire cellular pool of receptors was similarly affected, the differential epitope tagging approach was again employed, but cells were permeabilized prior to staining for the FLAG epitope (Figure 4B). The FLAG tag did not affect total cellular expression of γ2L subunits, as the wt[half-FLAG] condition yielded total levels that were half (48.3 $\pm$ 4%, n = 5) of the wt[all-FLAG] condition. In contrast to surface expression patterns (Figure 4A), total cellularexpression levels (Figure 4B)

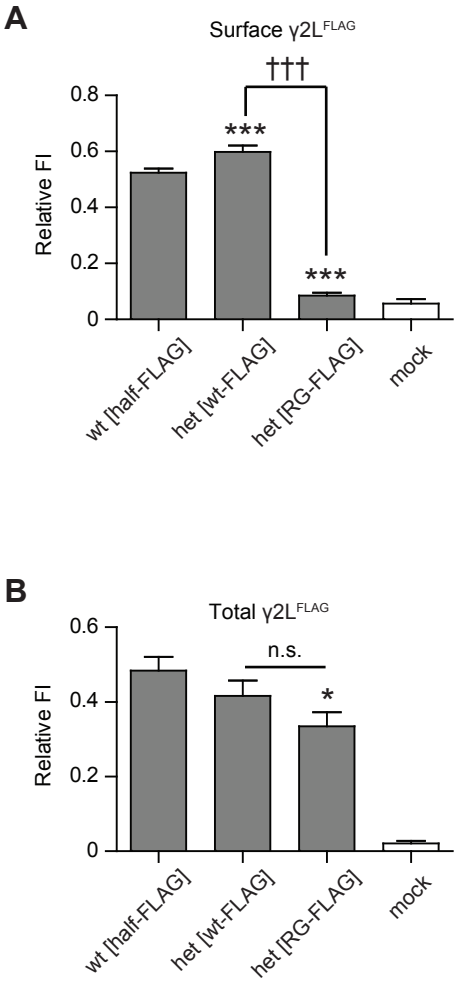

Figure 4. Differential epitope tagging allowed for the relative contributions of wild-type γ2L and mutant γ2L(R177G) subunits to be evaluated in the heterozygous transfection condition.

Surface (Panel **A**) and total (Panel **B**) expression levels of $\gamma 2L^{FLAG}$ subunits were evaluated by flow cytometry for the heterozygous transfection condition ($\alpha 1\beta 2\gamma 2L/\gamma 2L(R177G)$) when either wild-type γ2L subunits ("het[wt-FLAG]') or mutant γ2L(R177G) subunits ("het[RG-FLAG]") was tagged with the FLAG epitope. For comparison, the wild-type transfection condition ($\alpha 1\beta 2\gamma 2L$) was also evaluated when half of the γ2L subunits ("wt[half-FLAG]") contained the FLAG epitope. "Mock" transfected cells contained empty pcDNA3.1 vector. * $p < 0.05$, *** $p < 0.001$ when compared to the wt[half-FLAG] condition. ††† $p < 0.001$ when compared to the het[wt-FLAG] condition.

were similar in the het[wt-FLAG] condition (41.6 ± 4% of wt[all-FLAG] levels, n = 5). Total levels were slightly lower in the het[RG-FLAG] condition (33.5 ± 4% of wt[all-FLAG] levels, $p < 0.05$ when compared to wt[half-FLAG] condition and $p > 0.05$ when compared to the het[wt-FLAG] condition = 5). Thus, the R177G mutation primarily compromised surface expression of mutant γ2L(R177G) subunits.

The γ2L subunit R177G mutation reduced protein maturation.

The results in the previous sections demonstrated that the R177G mutation reduced γ2L subunit surface levels to a greater extent than total levels, suggesting that the mutation impaired assembly, forward trafficking, or surface stability of receptors containing γ2L(R177G) subunits. Since the *N*-glycosylation pattern of membrane proteins reflects their progression through the secretory pathway, these possibilities were explored using enzymes that specifically deglycosylate proteins at different stages of processing. For example, Endoglycosidase H (Endo H) removes only high-mannose (core or immature) *N*-glycans, which are added to proteins in the ER before transport to the Golgi apparatus (where further glycan modification, including mannose removal, confers Endo H resistance). Thus, proteins that are Endo H resistant must have reached at least the trans-Golgi network[426]. In contrast, Peptide N-Glycosidase F (PNGase F) cleaves all *N*-linked carbohydrate modifications[427]. By comparing the glycosylation patterns following treatment with Endo H and PNGase F, the effect of the R177G mutation on γ2L subunit trafficking could be determined. For example, reduced mature fractions would suggest impaired assembly and/or forward trafficking. In contrast, unchanged mature fractions would suggest decreased surface stability.

Western blots of undigested lysates from wild-type ($\alpha1\beta2\gamma2L^{HA}$), heterozygous ($\alpha1\beta2\gamma2L^{HA}/\gamma2L(R177G)^{HA}$), and homozygous ($\alpha1\beta2\gamma2L(R177G)^{HA}$) subunit combinations showed specific bands at 45 and 40 kDa (Figure 5A, lanes U). In the wild-type condition, both bands were similar in density, while in heterozygous and homozygous conditions, the 40 kDa

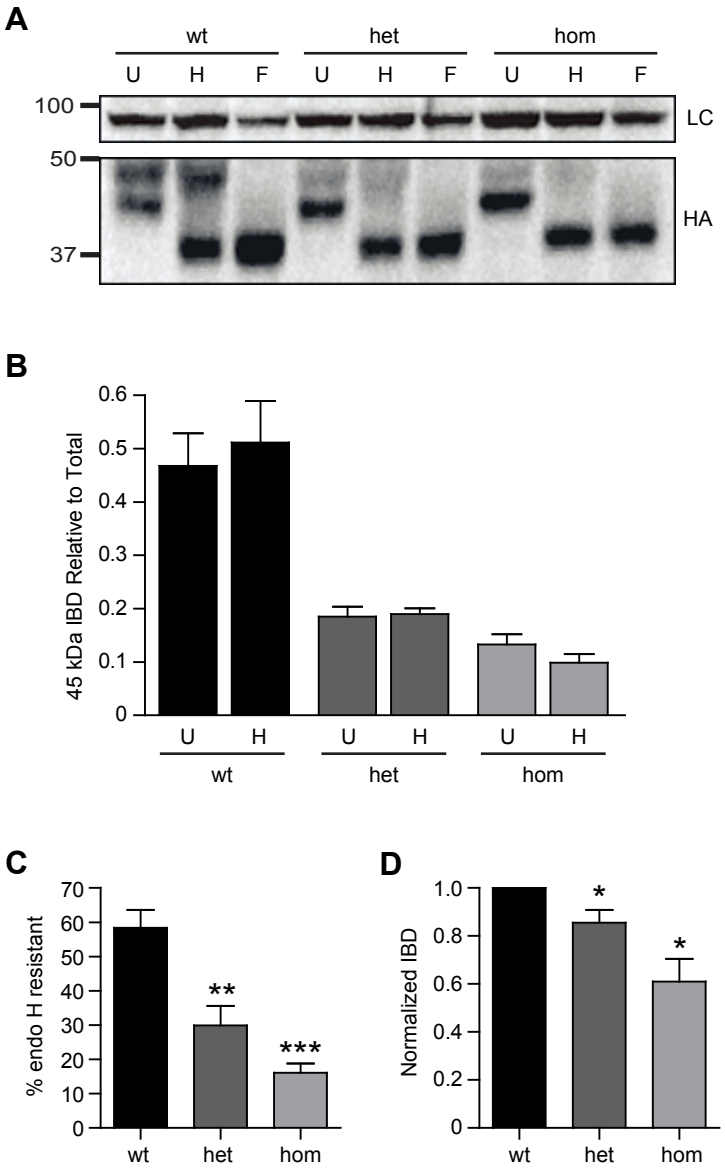

Figure 5. Mutant γ2L(R177G) subunits matured less efficiently than wild-type γ2L subunits.

A. Western blots were performed on whole cell lysates from HEK293T cells cotransfected with α1, β2, and either wild-type $\gamma 2L^{HA}$ (wt), heterozygous mutant $\gamma 2L^{HA}/\gamma 2L(R177G)^{HA}$ (het), or homozygous mutant $\gamma 2L(R177G)^{HA}$ (hom) subunits. Staining of the Na+/K+ ATPase α chain was used as a loading control (visible at ~100 kDa). **B.** The integrated band density (IBD) of the 45 kDa band in undigested and Endo H digested wt, het, and hom samples was calculated and normalized to the IBD of the PNGase F band. **C.** The fraction of Endo H insensitive protein was determined for each condition by dividing the IBD of the 45 kDa band in the Endo H lane by the IBD of the 37 kDa band in the PNGase F lane. **D.** The PNGase F sensitive band in the heterozygous and homozygous conditions was quantified using densitometry and normalized to the IBD of the wild-type condition. * $p < 0.05$, ** $p < 0.01$, *** $p < 0.001$ compared to the wild-type condition.

band was denser than the 45 kDa band. In all conditions, Endo H digestion shifted the 40 kDa band to 37 kDa, but did not affect the 45 kDa band, suggesting that the 40 kDa band represented "immature" $\gamma 2L^{HA}$ subunits while the 45 kDa band represented "mature" $\gamma 2L^{HA}$ subunits (Figure 5A, lanes H). This was confirmed by comparing the integrated band density (IBD) of the 45 kDa band before (lanes U) and after (lanes H) Endo H digestion (Figure 5B). To quantify the fraction of mature $\gamma 2L^{HA}$ subunits in each condition, the IBD of the Endo H-resistant band (45 kDa, lanes H) was compared to the IBD of the single fully-digested PNGase F band (37 kDa, lanes F) (Figure 5C). While the fraction of mature $\gamma 2L^{HA}$ subunits in the wild-type condition was 58 ± 5 % ($n = 5$), the fractions of mature $\gamma 2L^{HA}$ subunits in the heterozygous and homozygous conditions were only 30 ± 6 % ($n = 4$, $p < 0.01$) and 16 ± 3 % ($n = 4$, $p < 0.001$), respectively, supporting the hypothesis that mutant γ2L(R177G) subunits had impaired assembly and/or forward trafficking. Of note, these experiments also supported the prior observation made with flow cytometry that the R177G mutation decreased total γ2L subunit levels (Figure 3D). Indeed, relative to the IBD of the wild-type γ2L subunit PNGase band (Figure 5A; wt lane F), IBDs of γ2L subunit PNGase bands (Figure 5A; het and hom lanes F) were decreased in both heterozygous (85.5 ± 5% of wild-type levels, $n = 4$, $p < 0.05$) and homozygous (61.0 ± 9% of wild-type levels, $n = 4$, $p < 0.05$) conditions (Figure 5D).

Maturation of mutant γ2L(R177G) subunits was further compromised in the presence of wild-type γ2L subunits.

The flow cytometry results demonstrated that the trafficking deficiency observed for mutant γ2L(R177G) subunits was exacerbated in the presence of wild-type γ2L subunits (Figure 4). To determine if this phenomenon reflected wild-type γ2L subunits having a competitive advantage over mutant γ2L(R177G) subunits at the level of the ER, we combined the specificity of the HA immunoblots for mature and immature γ2L subunit proteins with the differential epitope tagging paradigm and determined the relative maturity of wild-type γ2L and mutant

γ2L(R177G) subunits in the context of heterozygous expression. This was accomplished by co-transfecting α1 and β2 subunits with equivalent amounts of either $\gamma2L^{HA}$ and γ2L(R177G) (het[wt-HA] condition) or γ2L and $\gamma2L(R177G)^{HA}$ (het[RG-HA] condition) subunits.

As in the previous section, each transfection condition produced two specific bands at molecular masses of 40 kDa and 45 kDa, corresponding to immature and mature γ2L subunits, respectively (Figure 6A). To determine the relative contributions of wild-type and mutant subunits to total cellular levels in the heterozygous condition, the IBD of mature and immature bands were background-subtracted and summed. The total IBD of HA-tagged wild-type subunits (het[wt-HA]; 22.2 $\pm$ 1.4, n = 3) was greater than that of HA-tagged mutant subunits (het[RG-HA]; 11.2 $\pm$ 0.2, n = 3, $p < 0.05$) (Figure 6B). Although not statistically significant, this trend was also present in the flow cytometry data (Figure 4B). To determine the mature subunit fraction, the IBD of the 45 kDa band was divided by the summed IBD of the 45 and 40 kDa bands (Figure 6C). In the het[wt-HA] condition, the fractions of mature (54.1 $\pm$ 2 %, n = 3) and immature $\gamma2L^{HA}$ subunits (45.6 $\pm$ 2 %, n = 3) were similar. However, in the het[RG-HA] condition, the fraction of mature $\gamma2L(R177G)^{HA}$ subunits (11.8 $\pm$ 1 %, n = 3) was substantially lower than the fraction of immature $\gamma2L(R177G)^{HA}$ subunits (88.2 $\pm$ 1 %, n = 3) (Figure 6B). Moreover, the mature mutant fraction in the heterozygous condition was less than the mature mutant fraction in the homozygous condition (compare Figure 5C and 6C), supporting the conclusion that assembly and/or forward trafficking of mutant subunits was further compromised in the presence of wild-type subunits.

Mutant γ2L(R177G) subunits were degraded prior to assembly with other $GABA_A$ receptor subunits by ER associated degradation (ERAD).

The results in the previous sections demonstrated that the R177G mutation decreased γ2L subunit surface levels. This decrease was associated with retention of mutant γ2L(R177G) subunits in the ER. However, the basis for the ER retention of mutant subunits remained unclear.

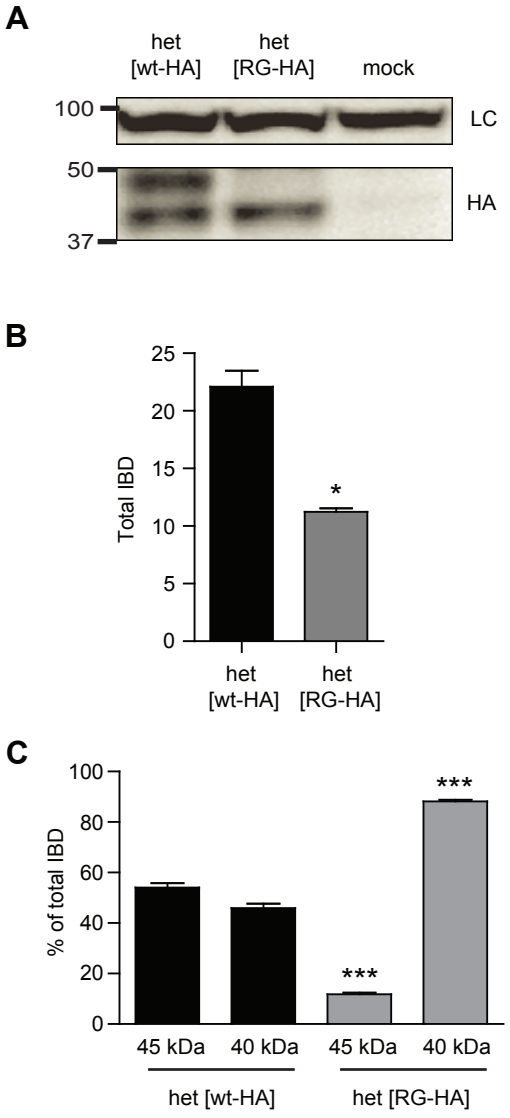

Figure 6. Differential epitope-tagging was used to independently assess maturation of wild-type γ2L and mutant γ2L(R177G) subunits in the heterozygous transfection condition.

A. Western blots were performed on whole cell lysates from HEK293T cells transfected with heterozygous subunit combinations that included wild-type ("het[WT-HA]"; α1β2γ 2LHA/γ2L(R177G)) or mutant ("het[RG-HA]"; α1β2γ2L/γ2L(R177G)HA) γ2L subunits tagged with the HA epitope. Staining of the Na+/K+ ATPase α chain was used as a loading control (visible at ~100 kDa). As shown in Figure 5A, staining for the HA epitope yielded specific bands at ~45 kDa and ~40 kDa, and a non-specific band at ~50 kDa (evident by its presence in the lane from the "mock" transfection condition). **B.** The total HA-specific signal in each of the transfection conditions was determined by adding the IBDs of the 45 kDa and 40 kDa bands. **C.** The relative contributions of the 45 kDa and 40 kDa bands in each transfection condition were determined by dividing the IBD of each band by the total IBD shown in Panel B. * $p < 0.05$, *** $p < 0.001$ when compared to the het[WT-HA] condition.

One possibility was that mutant γ2L subunits failed to form ternary receptors with coexpressed subunits. Alternatively, ER retention could have been secondary to failed forward trafficking of assembled ternary receptors. To explore these possibilities, transfected HEK293T cells were treated with 100 μg/ml cycloheximide (CHX) to prevent synthesis of $GABA_A$ receptor subunits. Then, the stability of surface and total cellular pools of wild-type and mutant γ2L subunits was compared to stability of partnering α1 subunits using flow cytometry.

For both wild-type and homozygous mutant conditions, α1 and $\gamma2L^{FLAG}$ subunit surface levels were relatively stable during a four hour incubation in CHX (Figure 7A, B). Similarly, total levels were also stable for α1 subunits in both wild-type and homozygous mutant conditions (Figure 7C). In contrast, total levels of $\gamma2L^{FLAG}$ subunits declined over the four hour incubation period (Figure 7D). The half-life of $\gamma2L(R177G)^{FLAG}$ subunits was only ~1 hour (total levels were reduced by 45.9 $\pm$ 8% (n = 6) after 60 minutes), as compared to a half-life of ~3 hours for wild-type $\gamma2L^{FLAG}$ subunits (total levels were reduced by 44.4 $\pm$ 10% (n = 9) after 180 minutes) (Figure 7D). The observation that total, but not surface, levels of $\gamma2L^{FLAG}$ subunits declined in the presence of CHX indicated that the rapidly degraded fraction was localized intracellularly. In addition, given the absence of associated change in α1 subunit levels, this rapidly degraded fraction likely represented an intracellular pool of "unassembled" $\gamma2L^{FLAG}$ subunits. Moreover, since mutant γ2L subunits were degraded more rapidly than wild-type γ2L subunits, the results suggest that the R177G mutation decreased γ2L subunit stability prior to oligomerization with other $GABA_A$ receptor subunits. Note that the different stabilities of α1 and $\gamma2L^{FLAG}$ subunits could not be attributed to the presence of the FLAG epitope, as $\alpha1^{FLAG}$ subunit levels were similar at each time point to those of untagged α1 subunits when coexpressed with β2 and γ2L subunits (not shown).

Multiple prior studies have demonstrated that $GABA_A$ receptor subunits retained in the ER, particularly those that are misfolded, are ultimately subjected to ERAD by the ubiquitin-proteasome system (Gallagher et al., 2007). To determine if this was also true for γ2L(R177G)

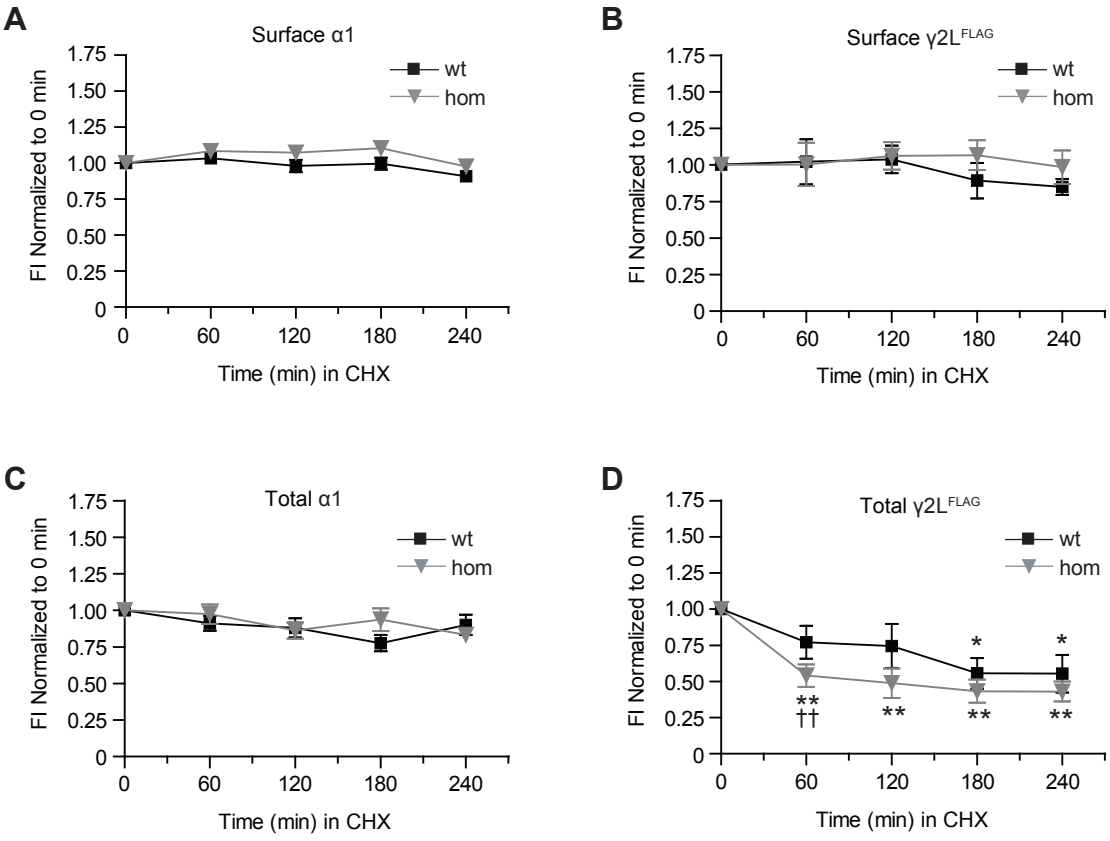

Figure 7. Mutant γ2L(R177G)^{FLAG} subunits were degraded more rapidly than wild-type γ2L^{FLAG} subunits.

A, B. Surface levels of α1 (Panel A) and γ2L^{FLAG} (Panel B) subunits were stable over four hours in the presence of cycloheximide (CHX) both for wild-type (α1β2γ2L^{FLAG}; black line) and homozygous mutant (α1β2γ2L(R177G)^{FLAG}; grey line) transfection conditions. **C, D.** Total cellular levels of α1 subunits (Panel C), but not γ2L^{FLAG} subunits (Panel D), were stable over four hours in the presence of CHX for both wild-type and homozygous mutant transfection conditions. The degradation rate was higher for mutant γ 2L(R177G)^{FLAG} than for wild-type γ2L^{FLAG} subunits. *$p < 0.05$, ** $p < 0.01$ when compared to Time 0 of same transfection condition. ++ $p < 0.01$ when compared to the wild-type condition at the same time point.

subunits, cells were incubated with the proteasomal inhibitor, lactacystin, and the CHX assay described in the previous section was repeated. Because lactacystin has previously been shown to require 60 minutes to reach maximal levels in cultured cells[428], cells were preincubated with 10 μM lactacystin before treatment with CHX. In the presence of lactacystin, total wild-type $\gamma2L^{FLAG}$ subunit levels declined in a manner similar to that observed after incubation in CHX alone (Figure 8A). In contrast, total levels of mutant $\gamma2L(R177G)^{FLAG}$ subunits did not decrease significantly after 240 minutes in the presence of lactacystin (Figure 8B). Thus, while mutant $\gamma2L^{FLAG}$ subunits were subjected to ERAD, degradation of wild-type $\gamma2L^{FLAG}$ subunits was not proteasome-mediated.

Absence of a basic amino acid at the 177 position of the γ2 subunit caused subunit misfolding.

The observation that mutant but not wild-type γ2L subunits underwent ERAD suggested that the R177G mutation caused subunit misfolding. To investigate this possibility, we performed sequence alignments, mutagenesis studies, and homology modeling of wild-type and mutant γ2 subunits. Sequence analysis revealed that the R177 residue was conserved among γ2 subunits of multiple species and basic residues also occupied this position in other γ subunits (Figure 9A). In contrast, other $GABA_A$ receptor and Cys-loop family member subunits had polar and charged amino acid residues at homologous positions. To determine if a basic residue was required at the 177 position in the γ2 subunit, other residues (glutamate (E), valine (V), and lysine (K)) were introduced at this position and coexpressed with α1 and β2 subunits. Subunit subunit surface levels were then evaluated using flow cytometry (Figure 9B). While surface levels of the $\gamma2L(R177E)^{FLAG}$ and $\gamma2L(R177V)^{FLAG}$ mutants were significantly reduced (41.1 $\pm$ 2% and 49.2 + 4% of wild-type levels, respectively; $n = 7\text{-}10$, $p < 0.001$), the γ2L(R177K) mutation produced no change in surface levels. Thus, it appeared that normal surface trafficking of γ2 subunits required the presence of a basic residue at position 177.

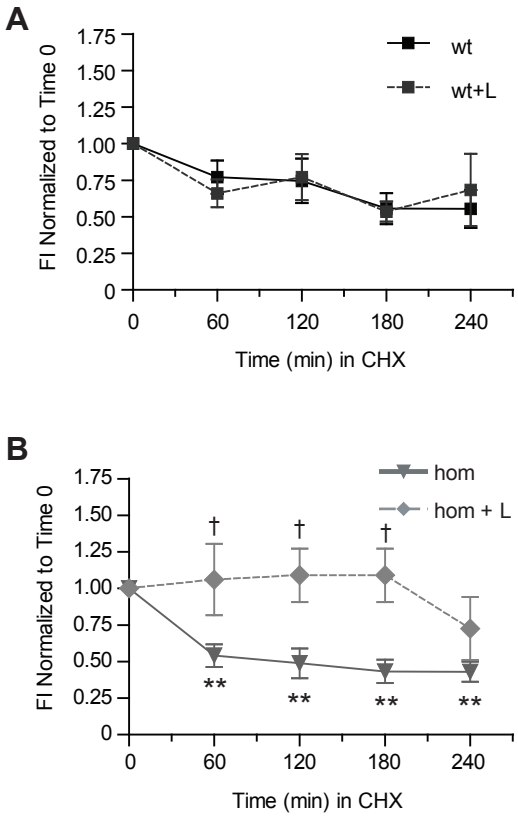

Figure 8. Proteasomal inhibition by lactacystin prevented degradation of mutant γ2L(R177G)^{FLAG}, but not wild-type γ2L^{FLAG}, subunits.

Total cellular expression of wild-type γ2L^{FLAG} (Panel **A**) or homozygous mutant γ 2L(R177G)^{FLAG} (Panel **B**) subunits when coexpressed with α1 and β2 subunits in HEK 293T cells was evaluated by flow cytometry following treatment with cycloheximide either alone (CHX; solid line) or in the presence of lactacystin (L; dashed line). ** $p < 0.01$ when compared to Time 0 of same transfection condition. + $p < 0.05$ when compared to the CHX-only condition at same time point.

Interestingly, the R177 residue is located in a highly conserved region at the amino-terminal end of β-strand 6 (Figure 9A). Charged residues can contribute to the hydrogen bonding that is essential for for beta sheet stability[429, 430], suggesting that loss of positive charge at this position could adversely affect protein structure. Indeed, two informatics tools predicted that this point mutation would be damaging. The SIFT (Sorting Intolerant from Tolerant) algorithm [431] predicted that the R177G mutation would be damaging with a score of 0.03 (zero is most damaging), and the PolyPhen 2.0 algorithm[432] predicted that the R177G mutation would be "possibly damaging" with a score of 0.888 (data not shown).

To determine if the R177G mutation might alter the tertiary or quaternary structure of $GABA_A$ receptors, homology modeling of α1β2γ2 and α1β2γ2(R177G) isoforms was performed using the *C. elegans* glutamate-gated chloride channel structure as a template (Figure 9C, D) [159]. The model predicted that R177 would form hydrogen bonds with T120 in β-strand 2 and W173 in β strand 5 (Figure 9C), but neither bond would be formed with G177 (Figure 9D). Because the formation and stability of β-sheets is highly dependent upon hydrogen bonding between residues of adjacent β-strands, this loss would be expected to destabilize secondary and tertiary structure of γ2(R177G) subunits [433].

Discussion

The γ2 subunit mutation, R177G, decreased GABA-evoked current amplitudes by decreasing $GABA_A$ receptor surface levels.

In this study, we investigated the pathogenesis of FS by determining how the γ2 subunit mutation, R177G, altered $GABA_A$ receptor biogenesis and physiological properties. Our results demonstrated that α1β2γ2L $GABA_A$ receptors containing mutant γ2(R177G) subunits had smaller peak current densities, which occurred not because of changes in receptor biophysical properties, but rather because of decreases in receptor surface expression. This, in turn, resulted from ER

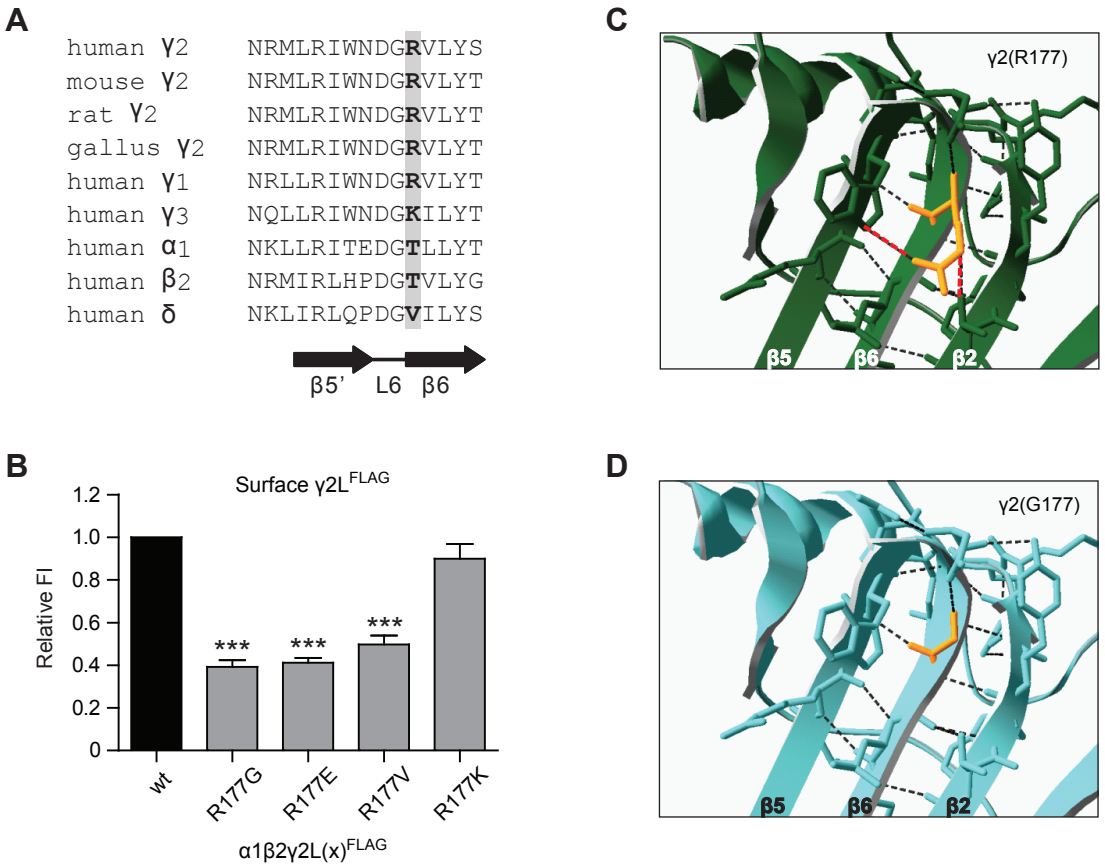

Figure 9. R177 was highly conserved among GABA$_A$ receptor γ2 subunits and formed hydrogen bonds with neighboring β-strands.

A. The sequences of GABA$_A$ receptor subunits from various species and families were aligned and secondary structure was determined by homology to the glutamate-gated chloride channel (GluCl). Residues homologous to human γ2 subunit R177 are bolded and highlighted in gray. Local secondary structure elements are indicated below the alignment. **B.** Surface levels of R177 mutant γ2L^{FLAG} subunits (R177V, R177E, and R177K) were evaluated using flow cytometry. **C.** Homology modeling of α1β2γ2 receptors was performed using the GluCl structure as a template. The image illustrates a portion of the γ2 subunit N-terminal domain including (from left to right) beta strands 5, 6, and 2. Hydrogen bonds among these sheets are indicated by black dashed lines, and the hydrogen bonds disrupted by the R177G mutation are indicated by red dashed lines. The R177 residue is colored orange. **D.** Homology modeling of α1β2γ2(R177G) receptors was performed and presented as in panel C.

retention of misfolded mutant γ2(R177G) subunits. The misfolded subunits underwent ERAD, as previously demonstrated for other $GABA_A$ receptor mutations associated with IGEs[100, 307, 395]. Ultimately, the smaller current density of α1β2γ2L(R177G) receptors is predicted to decrease GABAergic phasic inhibition and lower the seizure threshold by promoting neuronal hyperexcitability.

Mutant γ2L(R177G) subunits were trafficked to the cell surface less efficiently in the heterozygous than in the homozygous condition.

Surface expression of α1β2γ2L receptors was significantly reduced by "homozygous" expression of γ2L(R177G) subunits. However, the trafficking deficit caused by the R177G mutation was considerably more severe in the presence of wild-type γ2 subunits (i.e., γ2L(R177G) expression levels were much lower in heterozygous than homozygous conditions), emphasizing the importance of evaluating the heterozygous condition when characterizing the effects of disease-causing mutations. The most likely explanation for this phenomenon was that wild-type γ2 subunits possessed a competitive advantage over mutant γ2(R177G) subunits for oligomerizing with partnering subunits, forward trafficking once assembled into pentamers, and/or remaining on the cell surface. The increased immature fraction of mutant γ2(R177G) subunits in the heterozygous condition suggested that this competitive advantage was present at the level of the ER. Because receptor assembly occurs in the ER membrane, this could have reflected either preferential incorporation of wild-type γ2 subunits into ternary receptors or preferential recruitment of wild-type α1β2γ2 receptors into the secretory pathway. However, the former seemed more likely since the R177G mutation appeared to destabilize the "unassembled" pool of γ2 subunits, consistent with decreased oligomerization efficiency.

The γ2L subunit R177G mutation altered the subunit composition and/or stoichiometry of $GABA_A$ receptors expressed on the cell surface.

In both heterozygous and homozygous mutant conditions, whole cell currents were smaller than those of the wild-type condition. While this was associated with lower surface levels of the γ2 subunit, surface levels of the α1 and β2 subunit surface levels were similar or higher, respectively. Because neither α1 nor β2 subunits can traffic to the cell surface when expressed individually[81, 276], and the putative stoichiometries of α1β2 and α1β2γ2 receptor isoforms are 2α:3β and 2α:2β:1γ, respectively[340], a likely explanation for these changes in surface expression involves the formation of a mixed population of binary α1β2 and ternary α1β2γ2L receptors in the presence of the γ2L(R177G) subunit. In other words, the mutant subunit seemed to oligomerize less efficiently with α1 and β2 subunits, allowing a β2 subunit to take the place of the mutant γ2 subunit.

We did not observe changes in the macroscopic current kinetics that would be consistent with the presence of α1β2 receptors on the cell surface (e.g., slower rise time, increased fast desensitization, or slower deactivation), but it should be noted that αβ receptor whole cell currents are between one sixth and one tenth the amplitude of αβγ receptor whole cell currents, depending on the subunit subtypes included[168, 434]. Consequently, unless α1β2 receptors constituted a significant portion of the surface pool, their contribution to the ensemble current would most likely be masked by the presence of α1β2γ2 receptors. The markedly different sensitivities of α1β2 and α1β2γ2 receptor peak currents to Zn^{2+} has been used to determine the contribution of α1β2 receptors to the peak current[419], but this approach is inherently confounded by the relatively slow rise time of α1β2 receptor currents [434].

Of note, the stoichiometries of α1β2 and α1β2γ2 receptors have been studied primarily with concatenated subunits[340]. Considering the known limitations of investigating subunit stoichiometry with the concatenated-subunit approach[435], and the fact that a subset of neuronal $GABA_A$ receptors has been suggested to contain multiple γ subunits[179, 436, 437], it is also possible

that the R177G mutation reduced surface levels of the γ2 subunit not by introducing an α1β2 receptor population, but rather by exchanging receptors containing multiple γ subunits for those containing a single γ subunit. This possibility will need to be addressed in future studies.

Loss of the required basic residue at the 177 position in the γ2 subunit may impair stability of β-sheets

Mutagenesis studies demonstrated that normal γ2 subunit surface expression required a basic residue at position 177. Although the subunit requirements for beta sheet formation are less well defined than those for alpha helix formation, it has been demonstrated that arginine and lysine residues are over-represented at the N-terminal cap (beginning) of β-strands, while glycine may act as a sheet terminator[433]. Although our models did not predict gross structural rearrangements, the location and relative sheet-forming propensities of the wild-type and mutant amino acids suggest a potential mechanism for misfolding of mutant γ2(R177G) subunits. Finally, all three γ2 subunit residues involved in the loss of hydrogen bonding (T120, W173, and R177) lie in regions that have been shown to contribute to α1-γ2 subunit interface formation[88, 92]. Structural disruption at these areas might impair subunit oligomerization and thus contribute to the apparent changes in stoichiometry.

What role does the γ2 subunit R177G mutation play in the pathogenesis of FS, and possibly, IGEs?

As has been demonstrated for other epilepsy-associated mutations in $GABA_A$ receptor subunits, the R177G mutation decreased $GABA_A$ receptor current amplitudes, an effect predicted to decrease the level of GABAergic inhibition and therefore to promote neuronal hyperexcitability. That being said, it remains unclear why the clinical phenotype of the R177G mutation was limited to FS. Although $GABA_A$ receptor surface expression levels have been reported to be temperature-sensitive in the context of other mutations in the γ2 subunit[395], this was not observed for the R177G mutation (data not shown). Interestingly, precipitation of FS in

rats has been linked to respiratory alkalosis[438]. Since the sensitivity of α1β2γ2L receptors to GABA is inversely related to ambient pH[439], one possibility is that the lower level of GABAergic inhibition imparted by the R177G mutation coupled with a change in the intracortical pH further reduced the seizure threshold. However, it should be emphasized that the R177G mutation may have only appeared to have a relatively homogeneous FS phenotype because of the small pedigree in which it was identified[421]. While most of the known GEFS+ mutations are associated with a heterogeneous group of epilepsies, most were also identified in much larger pedigrees. As such, it is possible that the R177G mutation could further impair neuronal inhibition in a larger population.

CHAPTER VI

CONCLUSIONS

Summary of experimental chapters

This dissertation investigated the assembly, trafficking, heterogeneity, and function of $GABA_A$ receptor isoforms that contained wild-type subunits and/or subunits bearing epilepsy-associated point mutations. Faced with two daunting problems – poor knowledge regarding assembly of the myriad potential $GABA_A$ receptor isoforms and no way to determine which epilepsy-associated mutations might be worth studying in animals – we turned to the high-throughput approach of heterologous expression combined with flow cytometry. We created cDNA constructs encoding most $GABA_A$ receptor subunit subtypes, added epitope tags as necessary, transfected various combinations into HEK293T cells (which do not express endogenous $GABA_A$ receptor subunits), and quantified expression patterns and levels using flow cytometry. To confirm that expressed subunits were incorporated into receptors and to gain insight into their arrangement, we employed fluorescence resonance energy transfer (FRET), which allowed us to determine subunit adjacency. After collecting basic information about wild-type and mutant receptors, we characterized them further using techniques including traditional biochemistry, electrophysiology, kinetic analysis, and homology modeling.

For even the most widely studied isoforms ($\alpha1\beta2$, $\alpha1\beta2\gamma2L^{HA}$ and $\alpha1\beta2\delta^{HA}$), we found remarkable properties that have not been reported previously (Chapter II, Chapter III). In Chapter II, we demonstrated that concatenated subunit constructs are not ideal for determining receptor stoichiometry and that differential tagging may constitute a better method. This approach suggested that there was not a homogeneous population of $\alpha1\beta2$ receptors; rather, they seemed to be a mixture of $2\alpha:3\beta$ and $3\alpha:2\beta$ isoforms. This phenomenon also occurs in $\alpha4\beta2$ nAChRs, where

the 3α:2β isoform preferentially assembles when α4 subunit cDNA is transfected in molar excess (and vice versa). Interestingly, α1β2 $GABA_A$ receptors did not behave similarly to α4β2 nAChRs; if anything, excess β subunit expression favored formation of 3α:2β isoforms. The exact ratio of α1 to β2 subunits remains unsettled, but it was clear that, whatever that ratio may be, it was altered little by subunit cDNA transfection ratios. However, the α1 subunit was clearly "rate-limiting" with regard to surface expression levels. Both α1 and β2 subunit surface expression increased proportionally with α1 subunit cDNA levels, but surface expression of both subunits declined when β2 subunit cDNA was transfected in molar excess. Finally, FRET patterns supported the conclusions regarding stoichiometry that were drawn from differential tagging. FRET occurred between individual α1 subunits, individual β2 subunits, and α1 and β2 subunits. It is universally agreed that there are two GABA binding sites per receptor; because these occur at β-α subunit interfaces, alternating α1 and β2 subunits must occupy four of the five positions in the receptor pentamer. For both α1-α1 and β2-β2 FRET to occur within a pentamer, the remaining position must contain an α1 subunit in some receptors and a β2 subunit in others. Interestingly, β2-β2 FRET was essentially eliminated when a γ2 subunit was coexpressed, but α1-α1 FRET persisted (albeit at lower levels).

The minimal requirement for GABA binding and surface expression is coexpression of both α and β subunits, but most $GABA_A$ receptor isoforms *in vivo* are thought to contain a third (non-α, non-β) subunit. Thus in Chapter III, we used similar strategies to address the assembly of α1β2γ2L and α1β2δ receptor isoforms and found similarly intriguing results. For instance, it appeared that both $\gamma2L^{HA}$ and δ^{HA} subunits were incorporated at the expense of β2 subunits and that δ^{HA} subunits were incorporated more efficiently, perhaps due to the fact that they were much more stable than $\gamma2L^{HA}$ subunits.

In Chapters IV-VI, we used these and other techniques to characterize the effects of three epilepsy-associated point mutations on $GABA_A$ receptor assembly and function. The GABRB3 mutation, G32R (Chapter IV), was associated with childhood absence epilepsy and was formerly

proposed to reduce receptor current density by increasing glycosylation of β3 subunits. However, we demonstrated that while the mutation did indeed reduce current density and increase occupancy of an adjacent *N*-glycosylation site, the latter phenomenon did not cause the former. Rather, the G32R mutation disfavored incorporation of γ2L subunits, likely by altering intersubunit salt bridges, and also made α1β3γ2L receptors more likely to enter short open states. The GABRA6 variant, R46W (Chapter V), was also associated with childhood absence epilepsy. The mutated arginine is located in a region homologous to the region of the well-studied γ2 subunit R82Q mutation, which causes ER retention of mutant γ2 subunits and thereby reduces αβγ2 receptor currents. We found that the R46W variant drastically reduced current density and changed kinetic properties of both α6β2γ2L and α6β2δ receptor isoforms. This was partially attributable to a decrease in surface receptor levels and/or changes in receptor stoichiometry. Interestingly, it appeared that the R46W variant altered stoichiometry of α6β2γ2L receptors but simply reduced overall surface expression of α6β2δ receptors, indicating that it is unwise to assume that a mutant subunit will have identical effects in different receptor isoforms. Finally, in the "heterozygous" condition, wild-type α6 subunits were preferentially incorporated into surface receptors, suggesting that the mutation might alter subunit structure such that α6(R46W) subunits had lower affinity for partnering β2, γ2L and/or δ subunits. The GABRG2 mutation, R177G (Chapter VI), was associated with a more diverse epilepsy phenotype, generalized epilepsy with febrile seizures plus (GEFS+). Both "heterozygous" α1β2γ2L/γ2L(R177G) receptors and "homozygous" α1β2γ2L(R177G) receptors had reduced current density but no apparent changes in macroscopic current kinetics. Similar to α6(R46W) mutant subunits, γ2L(R177G) mutant subunits were preferentially excluded from receptors in the "heterozygous" expression condition. The majority of γ2L(R177G) subunits were not trafficked beyond the endoplasmic reticulum and were then degraded by the proteasome. We could not conclusively establish cause and effect; that is, mutant subunits could have been sent to the proteasome because they were excluded from pentamers (an established fate of non-incorporated subunits), or they could have been targeted for

degradation (perhaps due to misfolding) and thus have been unavailable for incorporation. The R177 residue is located in a highly conserved region of the N-terminal domain, in a region that is likely to contribute to α-γ subunit interfaces. Mutagenesis indicated that positive charge at this position was required for normal subunit surface expression, but homology modeling did not identify a particular intersubunit salt bridge formed or broken by the point mutation. However, the R177G mutation did disrupt salt bridges between neighboring β-strands of the γ subunit, which could destabilize the mutant protein.

High-throughput assessment of receptor expression: promises and limitations

We anticipated that we would be able to characterize systematically and efficiently a substantial portion of the possible $GABA_A$ receptor isoforms. Within a single experiment, it is quite feasible to test thirty subunit combinations and to stain for all transfected subunits, even in ternary combinations. Prior reports suggest that many subunit combinations would not yield surface expression, so these preliminary screenings would reduce substantially the array of isoforms to be studied. The list of combinations yielding surface expression could be narrowed further by reviewing subunit coexpression patterns *in vivo*. Subsequently, receptor stoichiometry and subunit adjacency could be determined using differential tagging and FRET, respectively.

We remain confident that this approach will eventually succeed in providing copious amounts of information regarding receptor assembly. Unfortunately, the scope of this project was reduced somewhat by technical limitations, mostly relating to antibodies. Obviously, expression cannot be assessed without either subunit-specific antibodies or epitope tagging. The number of commercially available $GABA_A$ receptor subunit antibodies continues to increase, but we have discovered that many do not detect specific bands even on Western blots. Even fewer are suitable for flow cytometry; many antibodies are raised against the poorly-conserved subunit intracellular loops and thus cannot be used to assess surface expression, and high nonspecific staining impairs quantification. Consequently, we employed epitope tagging, but we remain concerned about this

approach. It is almost universally claimed that insertion of any epitope tag between the fourth and fifth amino acids of mature subunits will not affect trafficking or function of $GABA_A$ receptors[81, 130, 334]. However, in the course of these studies we have found that fluorescent proteins can cause abnormal subunit dimerization, that partnering subunit expression levels differed between wildtype and FLAG-tagged subunits, and that various tags altered receptor kinetics (data not shown). After careful evaluation, we determined that the HA and myc tags were the least disruptive to receptor assembly and function (though the FLAG epitope was surprisingly well-tolerated on γ subunits) and thus preferentially used those tags. Differential epitope tagging is a promising approach for determining receptor stoichiometry, but we admit that all such results should be thoroughly controlled and interpreted with caution due to the potentially disruptive effects of epitope tags. Another antibody-related technical limitation (albeit one that should be tractable) concerns direct conjugation of antibodies and fluorophores. High-throughput, quantitative FRET is invaluable for determining direct subunit adjacency. However, valid results require that antibodies be directly conjugated to fluorophores. Excellent conjugation kits are commercially available, and we used them successfully to conjugate many antibodies. To our dismay, however, several antibodies proved impossible to conjugate efficiently despite meeting all technical specifications. For this reason, the FRET studies presented here are limited to the α1β2, α1β2γ2L, and α1β2δ receptor isoforms (Chapters II and III).

The "alpha" of $GABA_A$ receptor assembly

One of the most intriguing patterns we observed was that α subunits appear to be a "constant" in many contexts. The cDNA levels of α1 subunits determined surface expression levels of both α1 and β2 subunits (Chapter II); α1 subunit levels remained stable while β2 subunits were apparently replaced by γ2L or δ subunits (Chapter III); and α subunit levels were not affected by mutations in β3 (Chapter IV) or γ2L (Chapter VI) subunits. Furthermore, α1-α1

subunit FRET was not wholly abolished by γ2L or δ subunit incorporation. Taken together, these paint a fascinating but puzzling picture of α subunit regulation of receptor assembly.

Although it is evident that α subunits play a critical, central role in pentamer formation and trafficking, it has been very difficult to establish a mechanism – or even to enumerate exactly what that role might be. As previously discussed, FRET patterns indicated that α1β2 receptors exist as a mixture of 3α:2β and 2α:3β populations, and differential epitope tagging suggested that the 3α:2β population would predominate. Confusingly, despite the α subunit advantage, it was β subunit levels that declined when γ2L or δ subunits were introduced. Finally, at peak γ2L or δ expression levels, some α1-α1 (but not β2-β2) subunit adjacency remained. There are a few potential explanations for these phenomena; admittedly, all are somewhat confusing and unlikely.

First, we need to consider how these "extra" α subunits were arranged. Our data indicated that many α subunits were present on the cell surface but did not establish conclusively how those subunits were organized – e.g., as monomers, homomultimers, or components of fully assembled pentameric receptors. Although it is possible that some α subunits were present as monomers, the strong α-α FRET patterns demonstrated that the majority of surface α subunits must be adjacent to at least one other α subunit. However, this does not prove that all adjacent α subunits were contained within 3α:2β (GABA-responsive) receptor pentamers; they could be assembled into homopentamers or lower-order homomultimers (although it is important to note that sucrose density centrifugation experiments indicated that nearly all α1 subunits were located in pentamers when α1 and β3 subunits were coexpressed)[329]. It was clear, however, that very few α1 subunits reached the cell surface in any arrangement when α1 subunit cDNA was transfected in isolation (Chapter III, Figure 1). Thus, if α1 subunits existed in homomultimers when α1 subunit cDNA was co-transfected with β2 (± γ2L or δ) subunit cDNA, β2 subunits would have to somehow promote the formation of α1 homomultimers. Particularly in light of the fact that excess β2 subunit expression did not significantly alter the α1/β2 subunit surface level ratio, this seems unlikely. However, we cannot yet exclude the unsettling possibility that a much larger α1

homopentamer population existed, but its contribution was underestimated because antibodies were sterically hindered from binding to all α1 subunits when they were in their native conformation. This could explain why the $\alpha1^{HA}/\beta2^{HA}$ subunit level ratio obtained using flow cytometry was substantially lower than the ratio obtained using denaturing SDS-PAGE and immunoblotting.

It is also possible that with α1 and β2 subunit co-transfection, all α1 subunits on the cell surface were in fact incorporated into 3α:2β or 2α:3β receptor pentamers. In light of the changes in expression, function, and adjacency (Chapter III, Figures 3-5) associated with transfecting increasing amounts of γ2L or δ subunit cDNA, this possibility has a few implications. First, because there were ranges of γ2L or δ subunit cDNA that produced decreases in β2 subunit expression but no change in α1 subunit expression, γ2L and δ subunits must preferentially replace the third β2 subunit of the 2α:3β pentamers. This theory is problematic for a few reasons. First, the functional signature of the persistent 3α:2β receptor population would have to be completely obscured by the αβγ/αβδ receptor population. This could occur because the αβγ/αβδ receptor populations produce far larger currents than the remaining αβ receptors or because the 3α:2β receptors are nonfunctional. The former possibility is somewhat plausible, particularly for αβγ receptors, and to our knowledge the second has never been proposed. That said, one of the studies that addressed receptor stoichiometry using functional assessment of the receptors formed by concatenated subunits concluded that 3α:2β receptors did not exist because the β2-α1 and α1-β2 tandems did not produce currents when coexpressed with α1 subunits[328]. (Of course, another group used the same technique but found precisely the opposite result[116], which was one reason we began the studies presented here.)

Finally, it is possible that the "extra" α subunits have a different role entirely. A recent study proposed that the short splice variant of γ2 subunits (γ2S) can act as an "external modulator" of receptor function by binding to the outside of a pentameric receptor, essentially serving as an accessory protein[337]. If α1 subunits could assume a similar role, many of the phenomena that we

observed could be explained. The "accessory" α subunits could promote receptor assembly and forward trafficking, which would account for the fact that α1 (but not β2) subunit overexpression increases both α1 and β2 subunit surface trafficking (Chapter II, Figure 4). If the accessory α1 subunits could not be replaced by β2 subunits, they could essentially "buffer" α1 subunit levels such that overall α subunit levels appeared to remain constant while γ2L or δ subunits replaced α1 subunits in 3α:2β pentamers and β2 subunits in 2α:3β pentamers. Furthermore, they would account for persistent α1-α1 subunit FRET in the presence of an otherwise apparently homogeneous α1β2γ2L/α1β2δ receptor population. As mentioned, sucrose density centrifugation indicated that all α subunits were in pentamers, but in principle even that could be reconciled with the accessory subunit theory if the interaction between the pentamer and the accessory subunits is relatively weak and was disrupted during the process of protein purification. That said, although this is an appealing theory, neither we nor the group reporting accessory γ2S subunits have provided any direct evidence that individual $GABA_A$ receptor subunits can bind to the outside of $GABA_A$ receptor pentamers. Ultimately, atomic force or electron microscopy would be required to advance this hypothesis beyond mere speculation.

The results discussed thus far have made it abundantly clear that α1 subunits guide $GABA_A$ receptor assembly in some fundamental way. However, we have not determined if the other five α subunits behave in a similar manner. Although α1 is the most abundant α subunit subtype in adult whole brain, each of the other α subunits predominates in particular brain regions or at particular times during development (Chapter I). As such, it will be interesting to repeat many of our experiments using other subtypes.

Finally, we had hoped to gain insight into the first steps of $GABA_A$ receptor assembly -- the initial oligomerization patterns of newly-synthesized subunits. When α1, β2, and γ2 subunits were coexpressed, assembly intermediates were not successfully detected. However, if we could initiate assembly, harvest cells at several time points shortly thereafter, and stain for intracellular FRET, we could determine if, for instance, α1 homomers form before other homomers or

heteromers. Thus, we have conducted pilot studies using inducible expression systems. The *tet*-on system worked poorly; significant subunit expression was detected in the absence of inducer. The RheoSwitch system has been more promising, but the inducing ligand is no longer commercially produced. Despite these setbacks, we hope that future optimization of inducible expression systems will allow us to determine the order of $GABA_A$ receptor subunit assembly and potentially determine why α subunits seem to direct receptor assembly.

Assembly of ternary $GABA_A$ receptor isoforms: α1β2γ2, α1β2δ, and beyond

The levels of both $\gamma 2L^{HA}$ and δ^{HA} subunit protein obtained from various amounts of subunit cDNA were quite surprising. Many groups who study $GABA_A$ receptors using heterologous expression have adamantly maintained that subunits not essential for surface trafficking (i.e., non-α, non-β subunits) must be transfected in molar excess in order to eliminate the binary (αβ) receptor population and to obtain a homogeneous ternary (e.g., αβγ) receptor population. Intuitively, this approach seems reasonable: we know that αβ receptors assemble efficiently in fibroblasts and oocytes, and two separate studies have used different approaches to identify αβ receptors in rodent brain. Sequential co-immunoprecipitation indicated that up to 50% of all α4 subunit-containing receptors in rat brain membranes did not contain γ1-3 or δ subunits[281]. Of course, this does not prove that these are binary receptors; they could actually contain γ and δ subunits that failed to immunoprecipitate, or they could be ternary receptors containing ε/θ/ρ subunits (though the low expression of those subtypes makes the latter possibility somewhat unlikely). Electrophysiology provided more direct evidence for the existence *in vivo* of binary αβ receptors. While αβγ receptors have primary conductances around 25-28 pS and are not inhibited by Zn^{++}, αβ receptors have primary conductances of approximately 11 pS and are inhibited strongly by Zn^{++}. Somata of cultured hippocampal pyramidal cells produced Zn^{++}-sensitive 11 pS single-channel currents[282]. Although it was not directly demonstrated, it is highly unlikely that these neurons would express no γ or δ subunits. Thus, it

stands to reason that αβ receptors might assemble efficiently enough to exclude subunits of other classes unless those subunits are present at levels capable of outcompeting α-β subunit association. Our studies, however, indicated that equivalent amounts of subunit coding sequences actually yield *excess* γ2L and δ subunit protein. Remarkably low δ subunit cDNA levels were required to produce peak δ subunit expression, and even γ2L subunits were not produced at strictly linear ratios. For instance, 0.3 μg of $\gamma2L^{HA}$ subunit cDNA produced 51.2 ± 11.3 % of the protein levels produced by 1 μg of $\gamma2L^{HA}$ subunit cDNA. It should be noted that this phenomenon does not seem to be restricted to heterologous expression systems; γ2 subunit heterozygous knockout mice had only a 20% reduction in γ2 subunit protein compared to wildtype mice. A simple explanation for this, of course, would be that most αβγ pentamers contain two α and β subunits but only one γ subunit and thus an equimolar subunit gene dose provides excess γ subunit protein. However, it will be interesting to determine if intersubunit affinity and/or receptor-associated proteins might play a role as well.

As was the case for binary αβ receptors, we have presented ternary receptor assembly studies with only a limited number of the available $GABA_A$ receptor subunits, and our results may not generalize to other subunit subtypes or classes. For instance, it appeared that the difference in $\gamma2L^{HA}$ and δ^{HA} subunit "potency" and degradation rates were intrinsic properties of the subunits themselves. However, it will be interesting to see if γ2L/δ titrations produce similar results when α4 subunits (which usually pair with δ subunits *in vivo*) are expressed in place of α1 subunits (which usually pair with γ subunits *in vivo*). In this case, it is possible that α4 and α1 subunits have different intersubunit binding affinities and that receptor assembly could affect the stability of γ2 and δ subunits differently.

In addition to demonstrating that very different amounts of γ2L and δ subunit cDNA were required to produce similar protein levels, the γ2L/δ subunit titration experiments clearly showed that as γ2L or δ subunit levels increased, β2 subunit levels declined more than α1 subunit levels, suggesting that γ2L and δ subunits replaced β2 subunits. Once again, however, different

subunits may produce different results – if β1/β3 subunits replace β2 subunits, or if ε/θ/π subunits replace γ2L/δ subunits, expression patterns may be very different. In fact, considering the reported properties of some of these subunits, it might be more surprising if expression patterns remained the same. Unlike β2 subunits, both β1 and β3 subunits can reach the cell surface when transfected alone[81, 90, 440]; ε subunits have been reported to do the same and to substitute for α, β, or γ subunits[101, 441]; and remarkably little is known about θ or π subunit assembly. We did in fact observe diverse assembly patterns when we conducted preliminary studies with some of these combinations. When we substituted β3 subunit cDNA for β2 subunit cDNA in the $\gamma 2L^{HA}$ subunit transfection experiments, we found that β3 levels did not drop nearly as dramatically; rather, both α1 and β3 subunit surface levels remained stable through equimolar α1:β3:γ2L subunit cDNA transfection (Figure 1A). However, this does not necessarily mean that ternary α1β3γ2L and α1β2γ2L receptors have different stoichiometries, because β3 homomers may exist even when other subunits are transfected.

We also expressed ε and π subunits in the presence of α1 and β2 subunits. Results indicated that ε subunits behaved similarly to δ subunits; that is, both α1 and β2 subunit levels were much lower with equimolar α1β2ε transfection than with α1β2 transfection, but β2 levels decreased more than α1 levels (Figure 1B). In contrast, both α1 and β2 subunit levels dropped as π subunit levels increased (Figure 1C). The latter was particularly surprising, because π subunit surface expression levels were particularly low; in fact, they were nearly undetectable if less than 0.3 μg of π^{HA} subunit cDNA was transfected. It should be noted that these results are preliminary and that further work will be required to truly determine the assembly patterns of ε, π, and θ subunits. In particular, it will be informative to see if αβε, αβπ, and αβθ receptors have FRET patterns similar to those of αβγ and αβδ receptors.

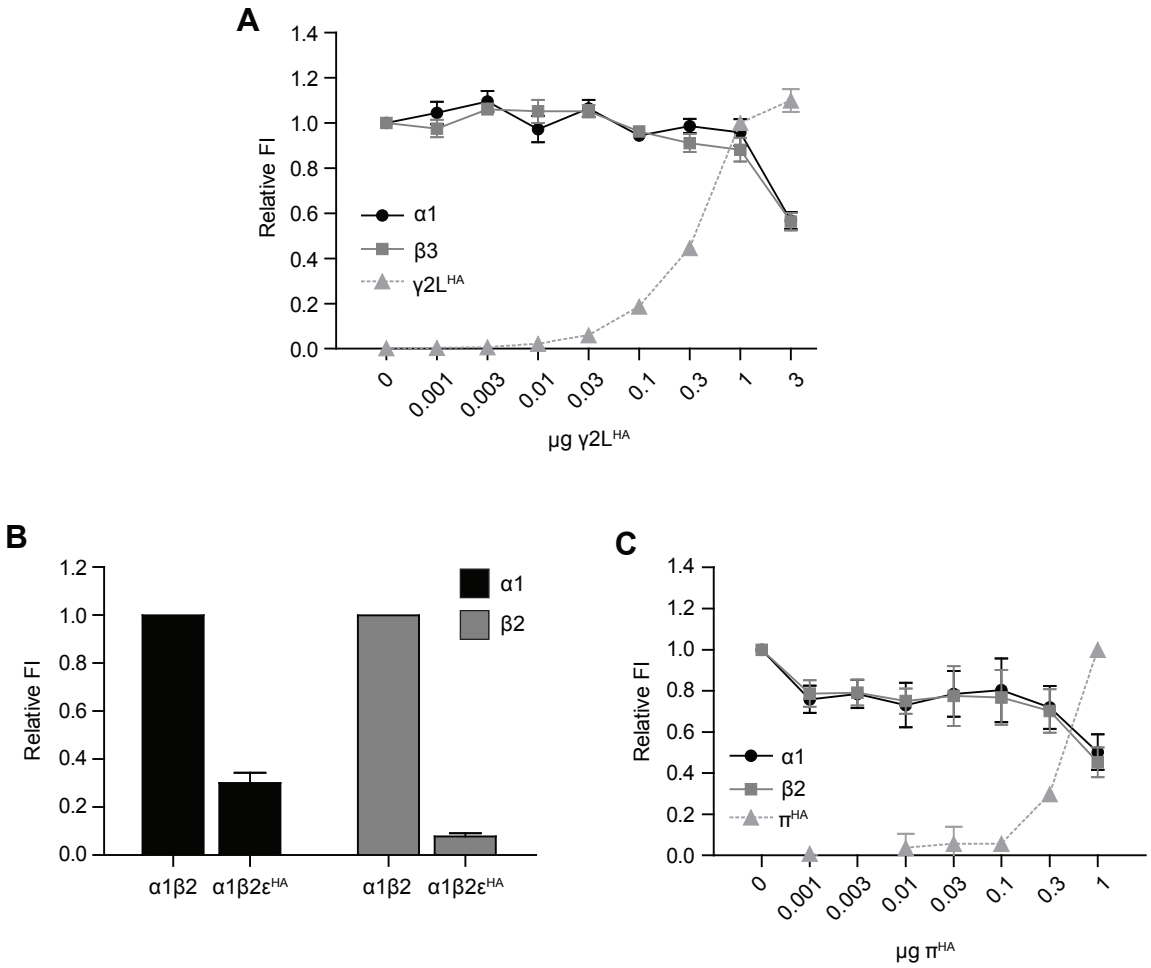

Figure 1. Expression patterns of other GABA$_A$ receptor isoforms

A. HEK293T cells were transfected with 1 μg each of α1 and β3 subunit cDNA and various amounts of γ2L subunit cDNA and subunit surface expression levels were measured using flow cytometry. Surface levels of α1 (black circles) and β3 (grey squares) subunits were normalized to levels at 0 μg γ2L subunit cDNA, and γ2L (grey triangles, dotted line) subunit levels were normalized to levels at 1 μg γ2L subunit cDNA. **B.** HEK293T cells were transfected with 1 μg each of α1 and β2 subunit cDNA with or without 1 μg ε subunit cDNA. Surface levels of α1 (black) and β2 (grey) subunits were measured using flow cytometry. **C.** HEK293T cells were transfected with 1 μg each of α1 and β2 subunit cDNA and various amounts of π subunit cDNA and subunit surface expression levels were measured using flow cytometry. Surface levels of α1 (black circles) and β3 (grey squares) subunits were normalized to levels at 0 μg π subunit cDNA, and π (grey triangles, dotted line) subunit levels were normalized to levels at 1 μg π subunit cDNA.

Rules were made to be broken: β3 and ε subunits

By reaching the cell surface as homomers, β3 and ε subunits already break the fundamental rules of assembly established in Chapters II and III. However, their unusual properties extend beyond their ability to forward traffic in the absence of partnering subunits. As shown in Figure 1A, β3 subunit levels did not drop as γ2L subunit levels increased to equimolar levels. Additionally, β3γ2 heteromers were reportedly expressed on the cell surface[90]. To determine if β3 subunits could form heteromultimers with other subunit subtypes, we measured surface levels of HA-tagged subunits when expressed alone or together with β3 subunits. We found that β3 subunit coexpression increased the surface expression of nearly all tested subunits (Figure 2A). Unsurprisingly, α subunit surface levels increased most dramatically, but γ2, δ, ε, and π subunit surface expression clearly increased as well. Thus, it seems probable that β3 subunits can oligomerize (and likely form pentamers) with most other subunit subtypes, thereby permitting forward trafficking in the absence of α subunits. However, future FRET and sucrose density centrifugation studies would be necessary to confirm this hypothesis.

It might seem that the indiscriminate oligomerization and trafficking induced by β3 subunits is simply an experimental curiosity because these atypical oligomers would cease to exist if α subunits were coexpressed. Interestingly, when comparing the properties of the three β subunits, we discovered indirect evidence that β3 subunits may produce unusual isoforms even when canonical αβγ receptors could assemble. We coexpressed α1 and $\gamma2L^{HA}$ subunits together with β1, β2 or β3 subunits and detected surface α1 and HA levels (Figure 2B). Because the β subunits were not epitope-tagged, their levels could not be compared directly, but we used an antibody capable of detecting both β2 and β3 (but not β1) subunits to confirm that they were properly expressed. The antibody did stain cells transfected with either β2 or β3 subunits (grey bars); although β3 subunit levels seemed much higher, it should be noted that the antibody epitope differs slightly between the two subunits, so relative quantification may be inaccurate.

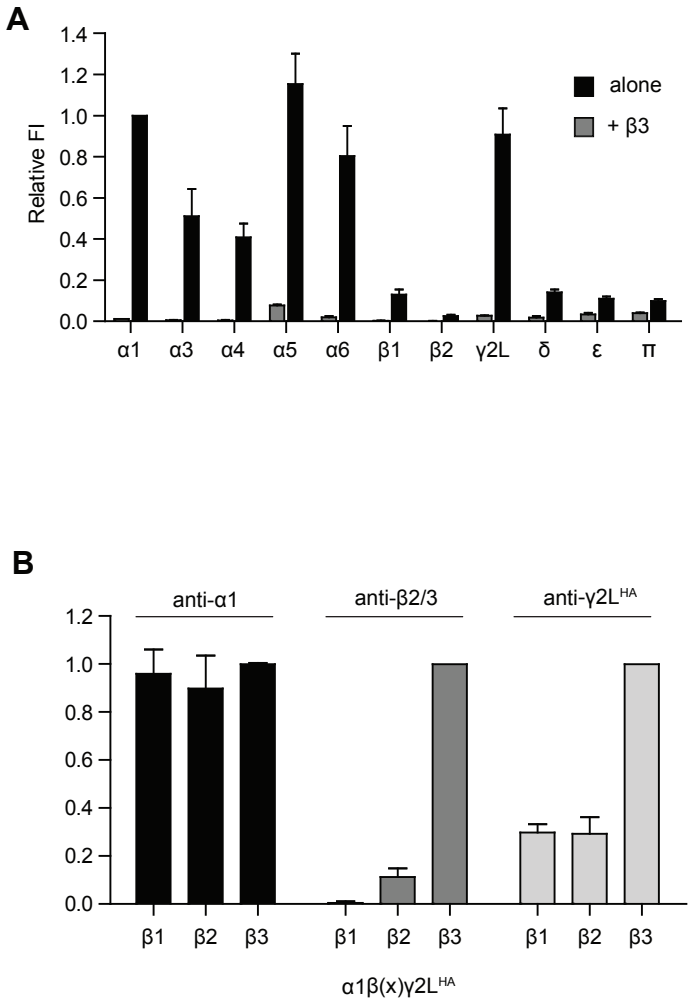

Figure 2. β3 subunits promote GABA$_A$ receptor heterogeneity.

A. Flow cytometry was used to measure surface levels of HA-tagged GABA$_A$ receptor subunits (x-axis) in HEK293T cells transfected with 1 μg of each subunit cDNA with (grey) or without (black) 1 μg of β3 subunit cDNA. **B.** Flow cytometry was used to measure surface levels of α1 (black) β2/3 (dark grey) or γ2L^{HA} (light grey) subunits in HEK293T cells transfected with 1 μg each of α1 and γ2L^{HA} subunit cDNAs together with β1 (left), β2 (center), or β3 (right) subunit cDNA.

Surface α1 subunit levels (black bars) were similar with any of the three β subunits, but surprisingly $\gamma 2L^{HA}$ levels (white bars) were significantly higher when coexpressed with β3 subunits rather than β1 or β2 subunits. The discrepancy between relative α1 and relative $\gamma 2L^{HA}$ levels indicates that β3 subunit expression cannot simply produce more receptors with the same stoichiometry as $\alpha 1\beta 1\gamma 2L^{HA}$ and $\alpha 1\beta 2\gamma 2L^{HA}$ receptors; if so, the α1 and $\gamma 2L^{HA}$ levels should rise proportionately. Considering that $\gamma 2L^{HA}$ subunits could not reach the cell surface alone (Chapter III, Figure 1) but could do so in the presence of β3 subunits[90], the simplest explanation is that a substantial number of $\beta 3\gamma 2L^{HA}$ heteromers persisted even when α1 subunits were available.

This raises several questions that remain to be answered. First, would α1 subunit cDNA levels be the "rate-limiting" component of α1β3 receptor assembly, or would the β3 subunit's inherent forward trafficking abilities essentially dictate surface expression levels? Second and more importantly, if receptor isoforms such as $\beta 3\gamma 2L^{HA}$ can exist in the presence of α subunits, could they also exist *in vivo*? The former question should be relatively easy to answer; the α1β2 subunit titrations (Chapter II, Figure 4) could simply be repeated using β3 rather than β2 subunit cDNA. The second question, though, presents considerably more problems. Historically, native receptor isoforms have been identified by sequential co-immunoprecipitation[57]. To identify native β3γ2 receptors with this method, it would be necessary to immunoprecipitate all α subunit subtypes expressed in a brain region and then co-immunoprecipitate β3 and γ2 subunits. Even if α subunit immunoprecipitation were perfect, this would prove only that β3γ2 oligomers exist, not that they were pentamers expressed on the cell surface. To establish that native β3 homopentamers exist, *all* non-β3 subunits would need to be immunoprecipitated before searching for pentamers. In summary, identifying these isoforms in brain tissue using established techniques would require (1) isolation of surface protein, (2) repeated immunoprecipitation, (3) sucrose density centrifugation to identify pentamers, and (4) a final immunoprecipitation/immunoblot to confirm that the correct subunits were found in the pentamers. Obviously, it would be arduous or even impossible to conduct these studies.

However, given the remarkably efficient surface expression of β3 homomers and β3γ2 heteromers in transfected cells, it would be extremely interesting to search for them *in vivo* if a more efficient method is invented.

In the absence of a more feasible method for identifying noncanonical $GABA_A$ receptor isoforms in brain, other heterologous experiments could be used to address how such isoforms might assemble – or be prevented from doing so. If non-α1 subunit-containing/β3 subunit-containing receptors do *not* exist *in vivo*, some neuronal regulatory mechanism must inhibit their formation. Thus, we could coexpress some of the many $GABA_A$ receptor-associated proteins with β3 subunits (± other non-α subunits) in HEK293T cells and see if any of those binding partners could eliminate surface expression of these unconventional isoforms.

Similar to β3 subunits, ε subunits have been reported to reach the cell surface independently[101], assemble promiscuously[441], and produce spontaneous currents in ternary receptors[442]. (Interestingly, it has been suggested that ε subunit residues homologous to those important for β3 subunit homo-oligomerization are necessary and sufficient for ε subunit self-exportation[101].) More surprisingly, while we were studying wild-type and mutant ε subunit-containing isoforms, we noticed that ε subunit-expressing cells displayed striking levels of cell death (data not shown). We assumed that this was due to overexpression (similar to the effects of 1:1:10 μg γ2L subunit cDNA co-transfection) and/or to the previously-reported spontaneous current. Unexpectedly, cell death persisted when very low levels of ε subunit cDNA were transfected, when ε subunits were expressed in the absence of α or β subunits (a condition that did not produce spontaneous currents in previous experiments), and when ε subunit-expressing cells were cultured in the presence of two different $GABA_A$ receptor antagonists. These results were somewhat bewildering, because there is no apparent reason for an ion channel subunit to be pro-apoptotic. As with β3 subunit heterogeneity, the ε subunit-induced cell death could be specific to transfected fibroblasts or generalizable to neurons – which would be extremely interesting. To begin addressing this question, we will transfect neurons with ε subunit cDNA and examine their

viability and morphology. If there is no effect, we could again co-express ε subunits and $GABA_A$ receptor-associated proteins in fibroblasts; if there is, this could be highly important in processes such as neuronal pruning, and it might be worth using optogenetics or lentivirus vector transduction to express ε subunits in regions of mouse brain that do not have endogenous ε subunit expression.

Characterization of epilepsy-associated mutations and variants: common themes?

Chapters IV-VI present extensive characterizations of three mutations and variants that were associated with different idiopathic generalized epilepsies. Two of these, GABRB3(G32R) and GABRG2(R177G), were clearly associated with epilepsy and EEG abnormalities in multigenerational families[310, 421]. The GABRA6(R46W) variant was identified by screening of unrelated epileptic patients; of the variant residues identified in that screen, this was the most evolutionarily conserved[393]. For these reasons, all seemed worthy of further study.

We hoped to find a common theme that would help us to predict the effects of other epilepsy mutations in the future. Notably, these mutations include one from each major $GABA_A$ receptor subunit family, so it would also be interesting if the mutations each had different effects, but ones that could theoretically result from the specific roles of each subunit class. The three mutations did in fact have some common elements; homology modeling predicted that each was located at or near a subunit interface, and each appeared to affect subunit incorporation or stoichiometry. Presumably, these effects contributed to the functional changes that were also seen in each mutant receptor. Interestingly, however, none of the three mutations was predicted to dramatically disrupt tertiary or quaternary structure, suggesting that relatively minor structural effects can have relatively major effects on receptor assembly and function.

Moving forward with mutations: should we then presume, and how should we begin?

As the cost of next-generation sequencing has decreased, it has become more feasible (and appealing) to perform genetic testing in hopes of delivering individualized treatment for various disorders. Consequently, the number of variants and mutations identified in generalized epilepsies is likely to increase rapidly, but it is far from certain that identifying more mutations will be useful to clinicians in the near future. Although it is potentially helpful to study genetic epilepsies by comprehensively characterizing mutations as we did in Chapters IV-VI, this method is currently too inefficient to provide viable diagnostic or treatment strategies for epileptic patients. It is even more unreasonable to create transgenic or knockin mice for each newly-discovered mutation, but animal models are the only way to study the complex network effects that are central to epileptogenesis. Finally, only about 2% of genetic epilepsies are monogenic. Thus, a means of prioritizing mutations and predicting their effects is greatly needed.

This problem is not unique to the field of epilepsy. All complex genetic traits that arise from combinations of rare variants will necessarily involve enormous data sets that are nearly impossible to interpret. For instance, autism researchers have struggled to make sense of the vast number of mutations, variants, and susceptibility loci that have been identified in various cohorts. As whole-exome sequencing and genome-wide association studies (GWAS) have become standard techniques, information has progressively outpaced interpretation. Aside from the fundamental problems of the large sample sizes and statistical tools necessary to detect significant associations, GWAS may simply leave the investigator with too many potential directions and no idea where to start.

A recent study highlighted the scope of this problem for idiopathic generalized epilepsies[327]. The authors sequenced 237 ion channel genes in hundreds of epileptic patients and non-epileptic controls. Surprisingly, cases and controls were mostly indistinguishable; neither the overall mutation load, nor the number of mutations predicted to be damaging, nor the number of

mutations present in known human epilepsy genes differed significantly between the groups. Indeed, the study found individual cases and controls with identical combinations of variants ("channotypes"). Ultimately, they concluded that network modeling would be required to understand how rare and common ion channel variants combine to produce hyperexcitability.

Several approaches have been proposed to address the similar problems that inevitably arise in GWAS of complex diseases[443]. These include pathway analysis, in which variants are sorted into known signaling pathways; meta-analysis, which can be used both to increase statistical power and to prioritize SNPs for subsequent studies (cumulative/Bayesian meta-analysis); and testing for epistasis, which could identify interactions that reduce the seizure threshold. The latter two might be most useful for epilepsy, considering that it is a disorder of neuronal hyperexcitability and therefore it may be wiser to focus on ion channels before complex signaling pathways. Undoubtedly, such investigations will yield fascinating results, but they are beyond the scope of our work. As such, we have chosen to address the complexity of epilepsy genetics in other ways.

Appendix 2 presents epilepsy-associated $GABA_A$ receptor subunit variants that were identified recently by several collaborators. We have narrowed a wider list to include only point mutations in subunit coding sequences, and we are beginning to screen mutant subunits for abnormal trafficking and/or function. The high-throughput technique of flow cytometry is particularly suited for this approach, and we hope that screening this wider set of variants will help us work toward our goal of predicting the effects of mutations in $GABA_A$ receptor subunits.

A few patterns were apparent when we mapped the variants that appeared only in cases (pink highlighting). First, remarkably few variants were found throughout most of the N-terminal domain; indeed, β-strands 1-6 contained no variants whatsoever. (Interestingly, even among previously-reported $GABA_A$ receptor epilepsy-associated mutations, only GABRG2(R177G) is located within that region, in β-strand 6.) Two variants were found in the loop connecting the N-terminal α-helix with the first β-strand (loop 1; L1), one residue with two variants was found in

the loop connecting β-strands 8 and 9 (loop 9; L9), and one variant was found in each of β-strands 7-10 (b7-b10). In contrast, 11 variants were found in the transmembrane domains (M1-M4). The remainder (20 variants) were concentrated in signal peptides (SP; six variants) and the cytoplasmic loop (loop; 13 variants) connecting the third and fourth transmembrane domains. Notably, two of the cytoplasmic loop variants were located in the predicted "MA" helix that is directly N-terminal to the fourth transmembrane domain and has been shown to affect receptor function[97].

Seventeen variants were reported to occur in both cases and controls, albeit at varying frequencies. Of these, one variant each was located in β-strands 1 and 8 (b1, b8); one was located in the third transmembrane domain (M3); and the remainder were located in the signal peptide (four variants), the random coil preceding the N-terminal α-helix (two variants), and the cytoplasmic loop (eight variants, two in the MA helix). In short, only 5 of 17 variants found in both cases and controls were located in structured $GABA_A$ receptor subunit domains, while 17 of 36 case-specific variants were located in structured domains or loops known to participate in subunit-subunit interactions.

However, it is by no means certain that mutations located in structured domains will be deleterious or that those located in unstructured domains will be benign. We used the Sorting Intolerant From Tolerant (SIFT)[431] and Polymorphism Phenotyping (PolyPhen)2.0[432] tools to predict whether or not a given missense mutation would adversely affect protein function. Because these algorithms depend heavily upon sequence conservation, it is perhaps unsurprising that the majority of variants predicted to be damaging were located in the transmembrane domains. Interestingly, the GABRE(Y38C) mutation found in both cases and controls was predicted to be damaging even though it is located in the random coil that is assumed to form the distal N-terminus of all $GABA_A$ receptor subunits.

It was also intriguing that 10 of 53 variants were located in signal peptides. This might simply indicate that there is little selective pressure in this region and that the variants are likely

to be benign. Alternatively, they could alter signal peptide cleavage, thereby changing localization or N-terminal structure of mutant subunits, but no change in cleavage site was predicted with high confidence by either the SignalP or the Signal CF algorithm[444, 445]. However, the GABRB3 mutations P11S and S15F also were not predicted to change signal peptide cleavage. These mutations were identified in multigenerational families with epilepsy[310, 446] and/or autism[296] and clearly reduced current density of α1β2γ2L $GABA_A$ receptor isoforms. However, we found no difference in surface expression levels large enough to explain such a current reduction, nor did we observe a shift in molecular weight (i.e., lack of signal peptide cleavage) after deglycosylation and SDS-PAGE. (Importantly, most $GABA_A$ receptor subunit signal peptides are longer than 20 amino acids, and we can detect shifts in molecular mass between β2 subunits containing or lacking the 9-aa HA epitope tag.) Similarly, preliminary studies of signal peptide variants listed in Appendix 2 have indicated few significant changes in subunit expression or current density, no detectible changes in molecular mass of protein backbones, and some changes in receptor kinetic properties. It is difficult to understand how a signal peptide mutation could affect receptor function without changing the sequence or trafficking of the mature protein, but the fact that the GABRB3(P11S) mutation has been found in multiple cohorts, in particular, suggests that the phenomenon is real and merits further study. As such, we are planning several further experiments. First, mass spectrometry could be used to determine if signal peptide cleavage is altered subtly enough to be undetectable with SDS-PAGE. Wild-type and mutant signal peptides could be coupled with reporter genes to assess any potential differences in rate or efficiency of subunit synthesis, and wild-type and mutant subunits could be expressed in cultured neurons to evaluate changes in subunit localization. Finally, a GABRB3(P11S) knockin mouse is currently being created. We eagerly await its arrival and plan to conduct full behavioral, histological, and electroencephalographic characterizations at the earliest opportunity.

Appendix 1: Annotated Alignment of $GABA_A$ Receptor Subunit Sequences

```
GABRB2-s          ------------------MWRVRKRGYFGIWS-FPLIIAAVCAQ---------------- 25    R3S
GABRB3v2          ------------------MCSGLLELLLLPIWLSWTLGTRGSEPR---------------- 26    P11S  S15F
GABRB1            ------------------MWTVQNRESLGLLSFPVMITMVCCAH---------------- 26
GABRQ             ------------------MGIRGMLRAAVILLLIRTWLAEGNYPSPIP----KFHFEFSSA 39
GABRD             ------------------MDAPARLLAPLLLLCAQQLRGTRAMNDIG-------------- 29    A3S
GABRP             ------------------MNYSLHLAFVCLSLFTERMCIQGSQFNV---------------- 28    V10M
GABRA1            --------MRKS---------PGLSDCLWAWILLLSTLTGR-------------------- 24    T20I
GABRA2            --------MKTK---------LNIYNMQFLLFVFLVWDPAR-------------------- 24
GABRA5            ----MDNGMFSG---------FIMIKNLLLFCISMNLSSHFG-------------------- 29
GABRA3            ----MIITQTSH---------CYMTSLGILFLINILPGTTGQGESRRQEPGDFVKQDIGG 47
GABRA4-iso1       --------MVSAKKVPAIALSAGVSFALLRFLCLAVCLNE---------------------- 32    A19T  L26M
GABRA6            --------MASS----------------LPWLCIILWLEN---------------------- 16
GABRG1            -MGPLKAFLFSPFLLRS---QSRGVRLVFLLLTLHLGNCVD----------KADDEDDE 45
GABRG2L           -MSSPNIWSTGSSVYSTPVFSQKMTVWILLLLSLYPGFTSQ----------KSDD-DYE 47    Q40X
GABRG3            ----------------------MAPKLLLLLCLFSGLHARS---------RKVEEDEYE 28
GABRE             MLSKVLPVLLGILLILQSRVEGPQTESKNEASSRDVVYGPQP---------QPLENQLLS 51    Y38C
GluCL-3RHW        ------------------------------------------------------------
CHRNA1-Tm         --------------------MILCSYWHVGLVLLLFSCCG---------------------- 20
CHRNA1-v1         ----------------------MEPWPL-LLLFSLCSAG---------------------- 16
ACHP-L            ----------------------MRRNIFCLACLWIVQACLS---------------------- 19
ACHBP-A           ----------------------MLVSVYLALLVACVGQAHS---------------------- 19
```

```
GABRB2-s          ---------SVNDPSNMSLVKETVDRLLKGYDIRLRPDFGGP-PVAVGMNIDIASIDMVS 75
GABRB3v2          ---------SVNDPCNMSFVKETVDKLLKGYDIRLRPDFGGP-PVCVGMNIDIASIDMVS 76    G32R
GABRB1            ---------STNEPSNMSYVKETVDRLLKGYDIRLRPDFGGP-PVDVGMRIDVASIDMVS 76
GABRQ             VPEVVLNLFNCKNCANEAVVQKILDRVLSRYDVRLRPNFGGA-PVPVRISIYVTSIEQIS 98
GABRD             ---------DYVGSNLEISWLPNLDGLIAGYARNFRPGIGGP-PVNVALALEVASIDHIS 79
GABRP             ----------EVGRSDKLS-LPGFENLTAGYNKFLRPNFGGE-PVQIALTLDIASISSIS 76
GABRA1            --SYGQPSLQDELKDNTTVFTRILDRLLDGYDNRLRPGLGER-VTEVKTDIFVTSFGPVS 81
GABRA2            --LVLANIQEDEAKNNITIFTRILDRLLDGYDNRLRPGLGDS-ITEVFTNIYVTSFGPVS 81
GABRA5            FSQMPTSSVKDETNDNITIFTRILDGLLDGYDNRLRPGLGER-ITQVRTDIYVTSFGPVS 88
GABRA3            LSPKHAPDIPDDSTDNITIFTRILDRLLDGYDNRLRPGLGDA-VTEVKTDIYVTSFGPVS 106
GABRA4-iso1       ----SPGQNQKEEKLCTENFTRILDSLLDGYDNRLRPGFGGP-VTEVKTDIYVTSFGPVS 87
GABRA6            ----ALGKLEVEGNFYSENVSRILDNLLEGYDNRLRPGFGGA-VTEVKTDIYVTSFGPVS 71    R46W
GABRG1            DLTVNKTWVLAPKI-HEGDITQILNSLLQGYDNKLRPDIGVR-PTVIETDVYVNSIGPVD 103
GABRG2L           DYASNKTWVLTPKV-PEGDVTVILNNLLEGYDNKLRPDIGVK-PTLIHTDMYVNSIGPVN 105   N79S R82Q  P83S
GABRG3            DSSSNQKWVLAPKS-QDTDVTLILNKLLREYDKKLRPDIGIK-PTVIDVDIYVNSIGPVS 86
GABRE             PETKSTETETGSRVCKLPEASRILNTILSNYDHKLRPGIGEK-PTVVTVEISVNSLGPLS 110   E52K  G66S
GluCL-3RHW        ----------------SDSKILAHLFTSGYDFRVRPPTDNGGPVVVSVNMLLRTISKID 43      S102A
CHRNA1-Tm         ------------LVLGSEHETRLVANLLENYNKVIRPVEHHTHFVDITVGLQLIQLINVD 68
CHRNA1-v1         ------------LVLGSEHETRLVAKLFKDYSSVVRPVEDHRQVVEVTVGLQLIQLINVD 64
ACHP-L            ----------------LDRADILYNIRQTSRPDVIPTQRDR-PVAVSVSLKFINILEVN 61
ACHBP-A           ----------------QANLMRLKSDLFNRSPMYPGPTKDDP--LTVTLGFTLQDIVKAD 61
                                  .         *         :   . .  :   .
```

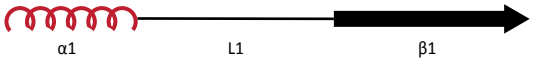

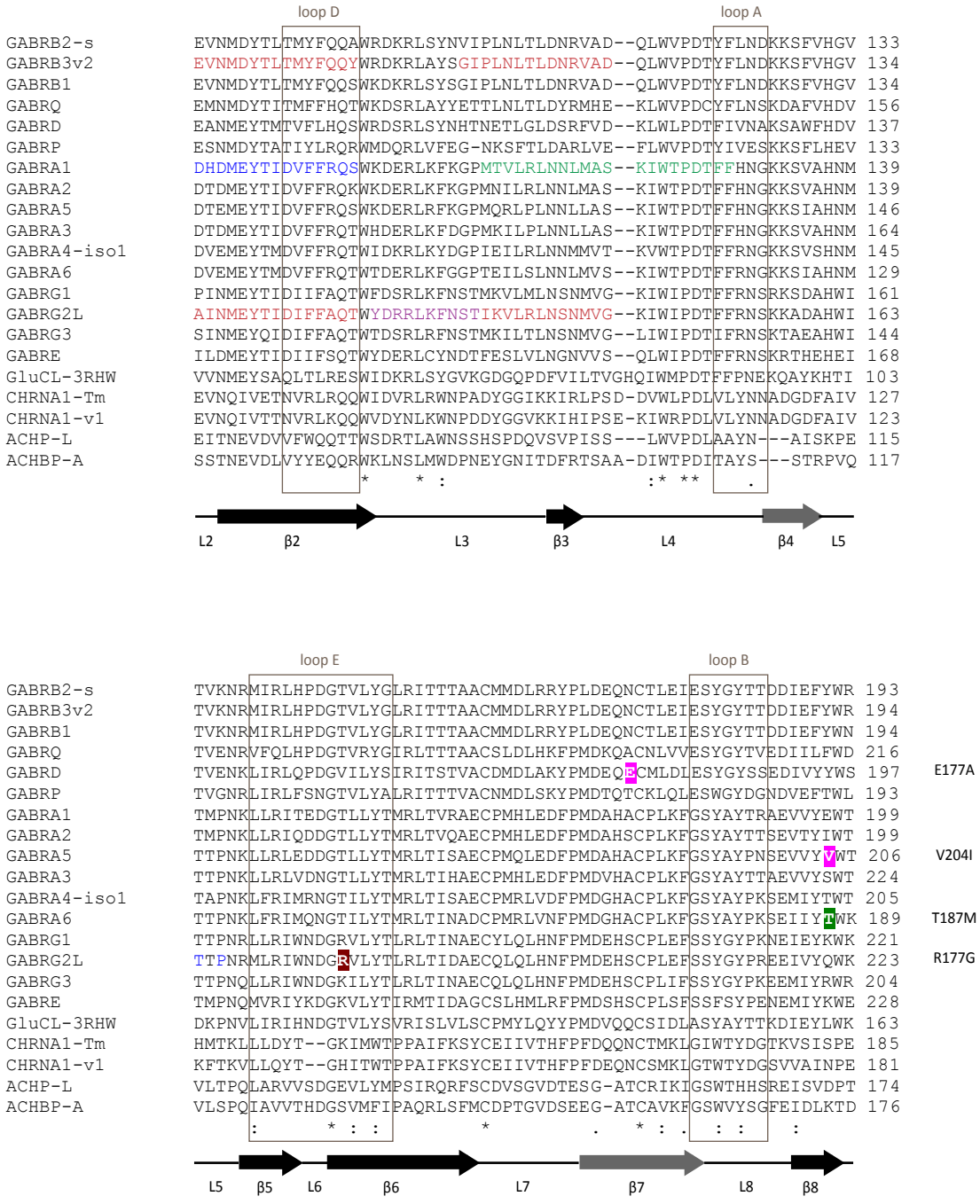
loop D
loop A
GABRB2-s EVNMDYTLTMYFQQAWRDKRLSYNVIPLNLTLDNRVAD--QLWVPDTYFLNDKKSFVHGV 133
GABRB3v2 EVNMDYTLTMYFQQYWRDKRLAYSGIPLNLTLDNRVAD--QLWVPDTYFLNDKKSFVHGV 134
GABRB1 EVNMDYTLTMYFQQSWKDKRLSYSGIPLNLTLDNRVAD--QLWVPDTYFLNDKKSFVHGV 134
GABRQ EMNMDYTITMFFHQTWKDSRLAYYETTLNLTLDYRMHE--KLWVPDCYFLNSKDAFVHDV 156
GABRD EANMEYTMTVFLHQSWRDSRLSYNHTNETLGLDSRFVD--KLWLPDTFIVNAKSAWFHDV 137
GABRP ESNMDYTATIYLRQRWMDQRLVFEG-NKSFTLDARLVE--FLWVPDTYIVESKKSFLHEV 133
GABRA1 DHDMEYTIDVFFRQSWKDERLKFKGPMTVLRLNNLMAS--KIWTPDTFFHNGKKSVAHNM 139
GABRA2 DTDMEYTIDVFFRQKWKDERLKFKGPMNILRLNNLMAS--KIWTPDTFFHNGKKSVAHNM 139
GABRA5 DTEMEYTIDVFFRQSWKDERLRFKGPMQRLPLNNLLAS--KIWTPDTFFHNGKKSIAHNM 146
GABRA3 DTDMEYTIDVFFRQTWHDERLKFDGPMKILPLNNLLAS--KIWTPDTFFHNGKKSVAHNM 164
GABRA4-iso1 DVEMEYTMDVFFRQTWIDKRLKYDGPIEILRLNNMMVT--KVWTPDTFFRNGKKSVSHNM 145
GABRA6 DVEMEYTMDVFFRQTWTDERLKFGGPTEILSLNNLMVS--KIWTPDTFFRNGKKSIAHNM 129
GABRG1 PINMEYTIDIIFAQTWFDSRLKFNSTMKVLMLNSNMVG--KIWIPDTFFRNSRKSDAHWI 161
GABRG2L AINMEYTIDIFFAQTWYDRRLKFNSTIKVLRLNSNMVG--KIWIPDTFFRNSKKADAHWI 163
GABRG3 SINMEYQIDIFFAQTWTDSRLRFNSTMKILTLNSNMVG--LIWIPDTIFRNSKTAEAHWI 144
GABRE ILDMEYTIDIIFSQTWYDERLCYNDTFESLVLNGNVVS--QLWIPDTFFRNSKRTHEHEI 168
GluCL-3RHW VVNMEYSAQLTLRESWIDKRLSYGVKGDGQPDFVILTVGHQIWMPDTFFPNEKQAYKHTI 103
CHRNA1-Tm EVNQIVETNVRLRQQWIDVRLRWNPADYGGIKKIRLPSD-DVWLPDLVLYNNADGDFAIV 127
CHRNA1-v1 EVNQIVTTNVRLKQQWVDYNLKWNPDDYGGVKKIHIPSE-KIWRPDLVLYNNADGDFAIV 123
ACHP-L EITNEVDVVFWQQTTWSDRTLAWNSSHSPDQVSVPISS---LWVPDLAAYN---AISKPE 115
ACHBP-A SSTNEVDLVYYEQQRWKLNSLMWDPNEYGNITDFRTSAA-DIWTPDITAYS---STRPVQ 117
L2 β2 L3 β3 L4 β4 L5
loop E
loop B
GABRB2-s TVKNRMIRLHPDGTVLYGLRITTTAACMMDLRRYPLDEQNCTLEIESYGYTTDDIEFYWR 193
GABRB3v2 TVKNRMIRLHPDGTVLYGLRITTTAACMMDLRRYPLDEQNCTLEIESYGYTTDDIEFYWR 194
GABRB1 TVKNRMIRLHPDGTVLYGLRITTTAACMMDLRRYPLDEQNCTLEIESYGYTTDDIEFYWN 194
GABRQ TVENRVFQLHPDGTVRYGIRLTTTAACSLDLHKFPMDKQACNLVVESYGYTVEDIILFWD 216
GABRD TVENKLIRLQPDGVILYSIRITSTVACDMDLAKYPMDEQECMLDIESYGYSSEDIVYYWS 197
GABRP TVGNRLIRLFSNGTVLYALRITTTVACNMDLSKYPMDTQTCKLQLESWGYDGNDVEFTWL 193
GABRA1 TMPNKLLRITEDGTLLYTMRLTVRAECPMHLEDFPMDAHACPLKFGSYAYTRAEVVYEWT 199
GABRA2 TMPNKLLRIQDDGTLLYTMRLTVQAECPMHLEDFPMDAHSCPLKFGSYAYTTSEVTYIWT 199
GABRA5 TTPNKLLRLEDDGTLLYTMRLTISAECPMQLEDFPMDAHACPLKFGSYAYPNSEVVYVWT 206
GABRA3 TTPNKLLRLVDNGTLLYTMRLTIHAECPMHLEDFPMDVHACPLKFGSYAYTTAEVVYSWT 224
GABRA4-iso1 TAPNKLFRIMRNGTILYTMRLTISAECPMRLVDFPMDGHACPLKFGSYAYPKSEMIYTWT 205
GABRA6 TTPNKLFRIMQNGTILYTMRLTINADCPMRLVNFPMDGHACPLKFGSYAYPKSEIIYTWK 189
GABRG1 TTPNRLLRIWNDGRVLYTLRLTINAECYLQLHNFPMDEHSCPLEFSSYGYPKNEIEYKWK 221
GABRG2L TTPNRMLRIWNDGRVLYTLRLTIDAECQLQLHNFPMDEHSCPLEFSSYGYPREEIVYQWK 223
GABRG3 TTPNQLLRIWNDGKILYTLRLTINAECQLQLHNFPMDEHSCPLIFSSYGYPKEEMIYRWR 204
GABRE TMPNQMVRIYKDGKVLYTIRMTIDAGCSLHMLRFPMDSHSCPLSFSSFSYPENEMIYKWE 228
GluCL-3RHW DKPNVLIRIHNDGTVLYSVRISLVLSCPMYLQYYPMDVQQCSIDLASYAYTTKDIEYLWK 163
CHRNA1-Tm HMTKLLLDYT--GKIMWTPPAIFKSYCEIIVTHFPFDQQNCTMKLGIWTYDGTKVSISPE 185
CHRNA1-v1 KFTKVLLQYT--GHITWTPPAIFKSYCEIIVTHFPFDEQNCSMKLGTWTYDGSVVAINPE 181
ACHP-L VLTPQLARVVSDGEVLYMPSIRQRFSCDVSGVDTESG-ATCRIKIGSWTHHSREISVDPT 174
ACHBP-A VLSPQIAVVTHDGSVMFIPAQRLSFMCDPTGVDSEEG-ATCAVKFGSWVYSGFEIDLKTD 176
L5 β5 L6 β6 L7 β7 L8 β8
E177A
V204I
T187M
R177G

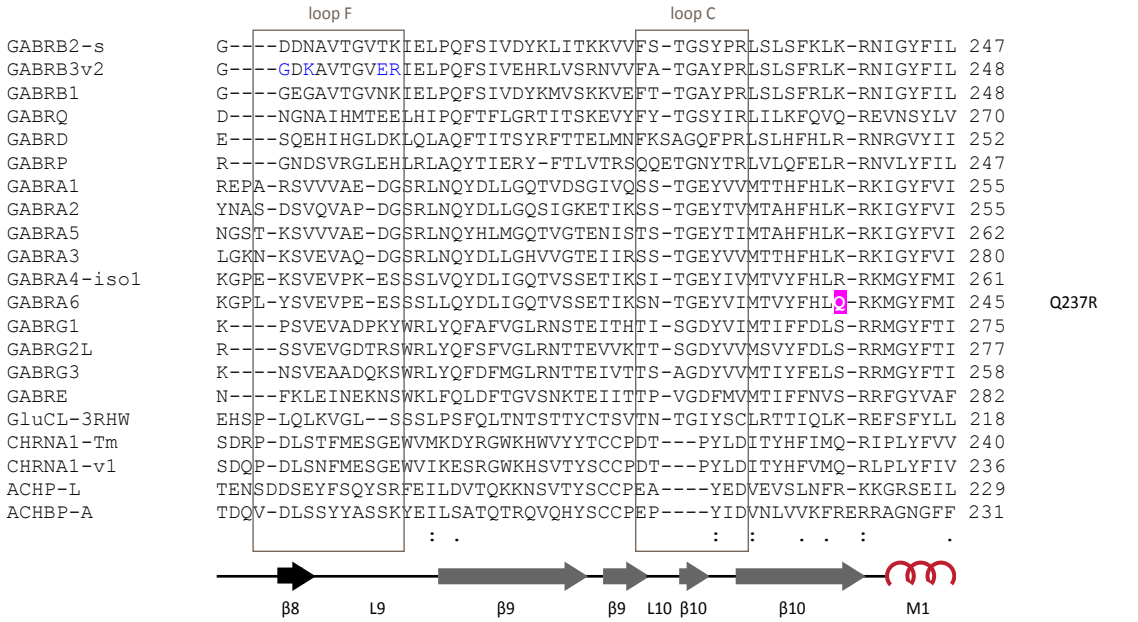
loop F
loop C
GABRB2-s G----DDNAVTGVTKIELPQFSIVDYKLITKKVVFS-TGSYPRLSLSFKLK-RNIGYFIL 247
GABRB3v2 G----GDKAVTGVERIELPQFSIVEHRLVSRNVVFA-TGAYPRLSLSFRLK-RNIGYFIL 248
GABRB1 G----GEGAVTGVNKIELPQFSIVDYKMVSKKVEFT-TGAYPRLSLSFRLK-RNIGYFIL 248
GABRQ D----NGNAIHMTEELHIPQFTFLGRTITSKEVYFY-TGSYIRLILKFQVQ-REVNSYLV 270
GABRD E----SQEHIHGLDKLQLAQFTITSYRFTTELMNFKSAGQFPRLSLHFHLR-RNRGVYII 252
GABRP R----GNDSVRGLEHLRLAQYTIERY-FTLVTRSQQETGNYTRLVLQFELR-RNVLYFIL 247
GABRA1 REPA-RSVVVAE-DGSRLNQYDLLGQTVDSGIVQSS-TGEYVVMTTHFHLK-RKIGYFVI 255
GABRA2 YNAS-DSVQVAP-DGSRLNQYDLLGQSIGKETIKSS-TGEYTVMTAHFHLK-RKIGYFVI 255
GABRA5 NGST-KSVVVAE-DGSRLNQYHLMGQTVGTENISTS-TGEYTIMTAHFHLK-RKIGYFVI 262
GABRA3 LGKN-KSVEVAQ-DGSRLNQYDLLGHVVGTEIIRSS-TGEYVVMTTHFHLK-RKIGYFVI 280
GABRA4-iso1 KGPE-KSVEVPK-ESSSLVQYDLIGQTVSSETIKSI-TGEYIVMTVYFHLR-RKMGYFMI 261
GABRA6 KGPL-YSVEVPE-ESSSLLQYDLIGQTVSSETIKSN-TGEYVIMTVYFHLQ-RKMGYFMI 245
Q237R
GABRG1 K----PSVEVADPKYWRLYQFAFVGLRNSTEITHTI-SGDYVIMTIFFDLS-RRMGYFTI 275
GABRG2L R----SSVEVGDTRSWRLYQFSFVGLRNTTEVVKTT-SGDYVVMSVYFDLS-RRMGYFTI 277
GABRG3 K----NSVEAADQKSWRLYQFDFMGLRNTTEIVTTS-AGDYVVMTIYFELS-RRMGYFTI 258
GABRE N----FKLEINEKNSWKLFQLDFTGVSNKTEIITTP-VGDFMVMTIFFNVS-RRFGYVAF 282
GluCL-3RHW EHSP-LQLKVGL--SSSLPSFQLTNTSTTYCTSVTN-TGIYSCLRTTIQLK-REFSFYLL 218
CHRNA1-Tm SDRP-DLSTFMESGEWVMKDYRGWKHWVYYTCCPDT---PYLDITYHFIMQ-RIPLYFVV 240
CHRNA1-v1 SDQP-DLSNFMESGEWVIKESRGWKHSVTYSCCPDT---PYLDITYHFVMQ-RLPLYFIV 236
ACHP-L TENSDDSEYFSQYSRFEILDVTQKKNSVTYSCCPEA----YEDVEVSLNFR-KKGRSEIL 229
ACHBP-A TDQV-DLSSYYASSKYEILSATQTRQVQHYSCCPEP----YIDVNLVVKFRERRAGNGFF 231
β8
L9
β9
β9
L10
β10
β10
M1

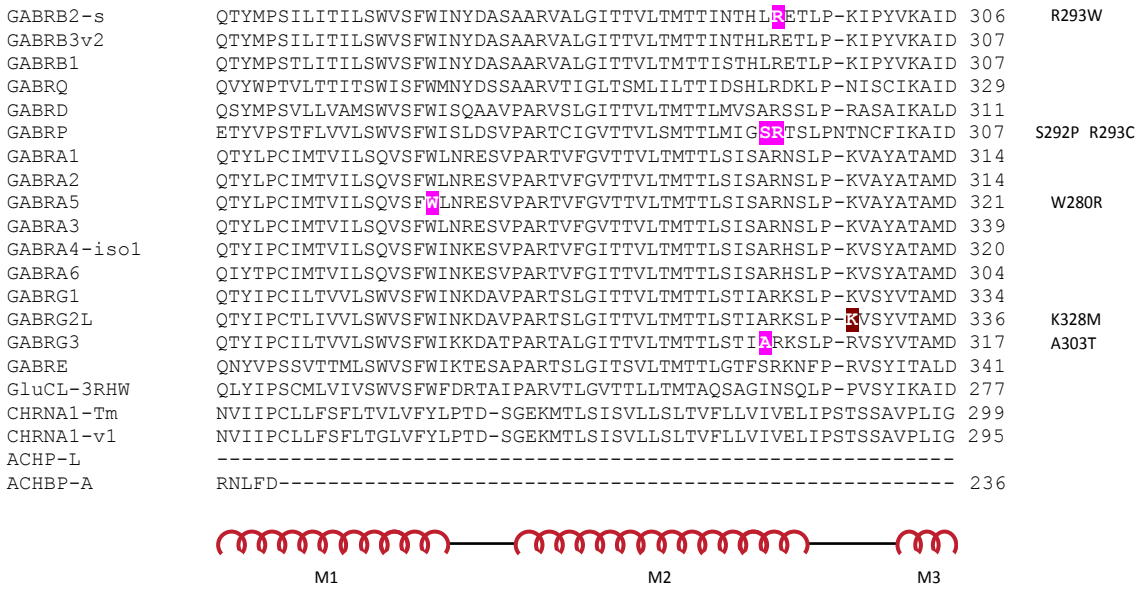
GABRB2-s QTYMPSILITILSWVSFWINYDASAARVALGITTVLTMTTINTHLRETLP-KIPYVKAID 306
R293W
GABRB3v2 QTYMPSILITILSWVSFWINYDASAARVALGITTVLTMTTINTHLRETLP-KIPYVKAID 307
GABRB1 QTYMPSTLITILSWVSFWINYDASAARVALGITTVLTMTTISTHLRETLP-KIPYVKAID 307
GABRQ QVYWPTVLTTITSWISFWMNYDSSAARVTIGLTSMLILTTIDSHLRDKLP-NISCIKAID 329
GABRD QSYMPSVLLVAMSWVSFWISQAAVPARVSLGITTVLTMTTLMVSARSSLP-RASAIKALD 311
GABRP ETYVPSTFLVVLSWVSFWISLDSVPARTCIGVTTVLSMTTLMIGSRTSLPNTNCFIKAID 307
S292P R293C
GABRA1 QTYLPCIMTVILSQVSFWLNRESVPARTVFGVTTVLTMTTLSISARNSLP-KVAYATAMD 314
GABRA2 QTYLPCIMTVILSQVSFWLNRESVPARTVFGVTTVLTMTTLSISARNSLP-KVAYATAMD 314
GABRA5 QTYLPCIMTVILSQVSFWLNRESVPARTVFGVTTVLTMTTLSISARNSLP-KVAYATAMD 321
W280R
GABRA3 QTYLPCIMTVILSQVSFWLNRESVPARTVFGVTTVLTMTTLSISARNSLP-KVAYATAMD 339
GABRA4-iso1 QTYIPCIMTVILSQVSFWINKESVPARTVFGITTVLTMTTLSISARHSLP-KVSYATAMD 320
GABRA6 QIYTPCIMTVILSQVSFWINKESVPARTVFGITTVLTMTTLSISARHSLP-KVSYATAMD 304
GABRG1 QTYIPCILTVVLSWVSFWINKDAVPARTSLGITTVLTMTTLSTIARKSLP-KVSYVTAMD 334
GABRG2L QTYIPCTLIVVLSWVSFWINKDAVPARTSLGITTVLTMTTLSTIARKSLP-KVSYVTAMD 336
K328M
GABRG3 QTYIPCILTVVLSWVSFWIKKDATPARTALGITTVLTMTTLSTIARKSLP-RVSYVTAMD 317
A303T
GABRE QNYVPSSVTTMLSWVSFWIKTESAPARTSLGITSVLTMTTLGTFSRKNFP-RVSYITALD 341
GluCL-3RHW QLYIPSCMLVIVSWVSFWFDRTAIPARVTLGVTTLLTMTAQSAGINSQLP-PVSYIKAID 277
CHRNA1-Tm NVIIPCLLFSFLTVLVFYLPTD-SGEKMTLSISVLLSLTVFLLVIVELIPSTSSAVPLIG 299
CHRNA1-v1 NVIIPCLLFSFLTGLVFYLPTD-SGEKMTLSISVLLSLTVFLLVIVELIPSTSSAVPLIG 295
ACHP-L ----------
ACHBP-A RNLFD---------- 236
M1
M2
M3

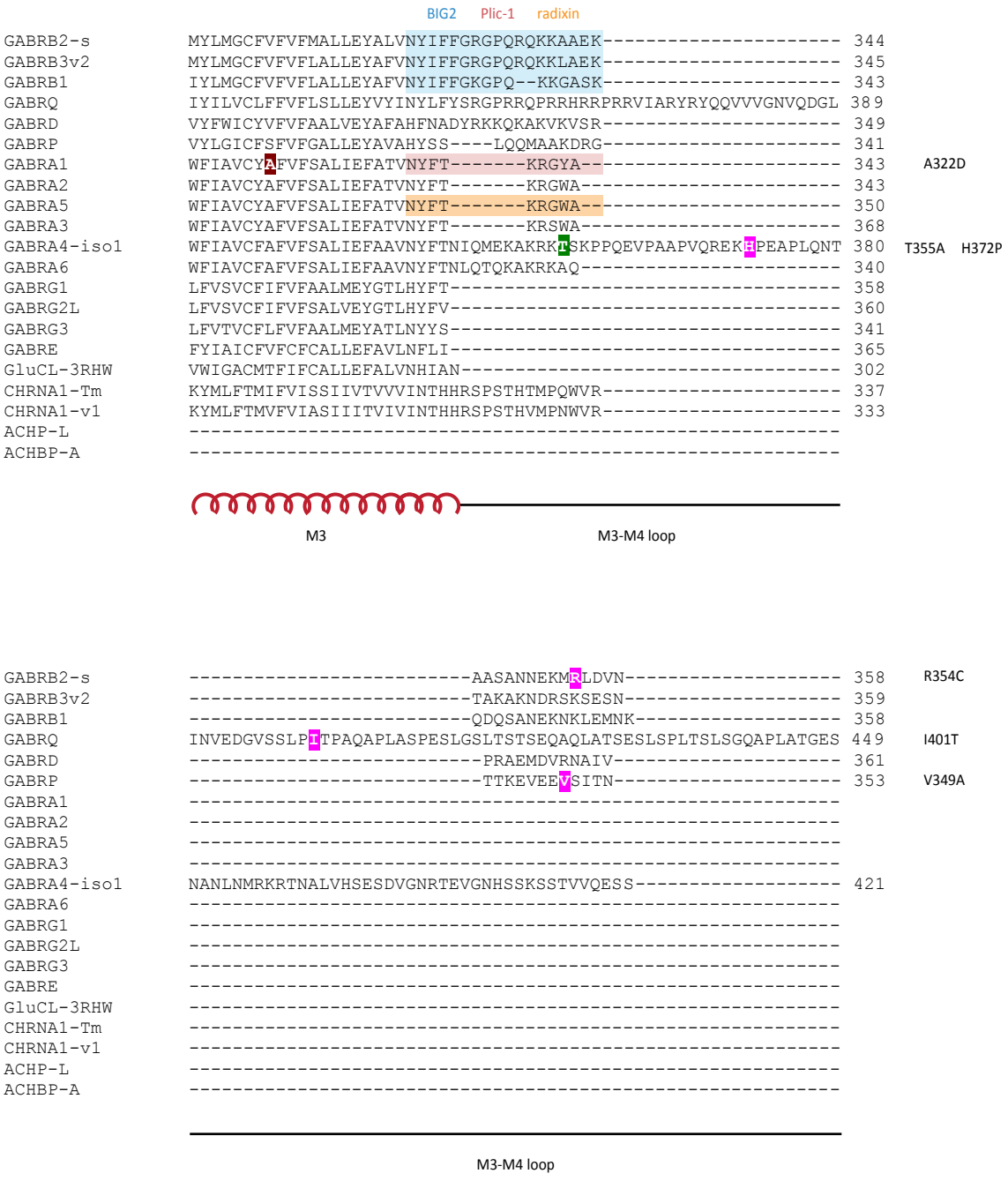
BIG2
Plic-1
radixin
GABRB2-s MYLMGCFVFVFMALLEYALVNYIFFGRGPQRQKKAAEK---------- 344
GABRB3v2 MYLMGCFVFVFLALLEYAFVNYIFFGRGPQRQKKLAEK---------- 345
GABRB1 IYLMGCFVFVFLALLEYAFVNYIFFGKGPQ--KKGASK---------- 343
GABRQ IYILVCLFFVFLSLLEYVYINYLFYSRGPRRQPRRHRRPRRVIARYRYQQVVVGNVQDGL 389
GABRD VYFWICYVFVFAALVEYAFAHFNADYRKKQKAKVKVSR---------- 349
GABRP VYLGICFSFVFGALLEYAVAHYSS----LQQMAAKDRG---------- 341
GABRA1 WFIAVCYAFVFSALIEFATVNYFT-------KRGYA-- ---------- 343 A322D
GABRA2 WFIAVCYAFVFSALIEFATVNYFT-------KRGWA---------- 343
GABRA5 WFIAVCYAFVFSALIEFATVNYFT-------KRGWA-- ---------- 350
GABRA3 WFIAVCYAFVFSALIEFATVNYFT-------KRSWA---------- 368
GABRA4-iso1 WFIAVCFAFVFSALIEFAAVNYFTNIQMEKAKRKTSKPPQEVPAAPVQREKHPEAPLQNT 380 T355A H372P
GABRA6 WFIAVCFAFVFSALIEFAAVNYFTNLQTQKAKRKAQ---------- 340
GABRG1 LFVSVCFIFVFAALMEYGTLHYFT---------- 358
GABRG2L LFVSVCFIFVFSALVEYGTLHYFV---------- 360
GABRG3 LFVTVCFLFVFAALMEYATLNYYS---------- 341
GABRE FYIAICFVFCFCALLEFAVLNFLI---------- 365
GluCL-3RHW VWIGACMTFIFCALLEFALVNHIAN---------- 302
CHRNA1-Tm KYMLFTMIFVISSIIVTVVVINTHHRSPSTHTMPQWVR---------- 337
CHRNA1-v1 KYMLFTMVFVIASIIITVIVINTHHRSPSTHVMPNWVR---------- 333
ACHP-L ----------
ACHBP-A ----------
M3
M3-M4 loop
GABRB2-s ----------AASANNEKMRLDVN---------- 358 R354C
GABRB3v2 ----------TAKAKNDRSKSESN---------- 359
GABRB1 ----------QDQSANEKNKLEMNK---------- 358
GABRQ INVEDGVSSLPITPAQAPLASPESLGSLTSTSEQAQLATSESLSPLTSLSGQAPLATGES 449 I401T
GABRD ----------PRAEMDVRNAIV---------- 361
GABRP ----------TTKEVEEVSITN---------- 353 V349A
GABRA1 ----------
GABRA2 ----------
GABRA5 ----------
GABRA3 ----------
GABRA4-iso1 NANLNMRKRTNALVHSESDVGNRTEVGNHSSKSSTVVQESS---------- 421
GABRA6 ----------
GABRG1 ----------
GABRG2L ----------
GABRG3 ----------
GABRE ----------
GluCL-3RHW ----------
CHRNA1-Tm ----------
CHRNA1-v1 ----------
ACHP-L ----------
ACHBP-A ----------
M3-M4 loop

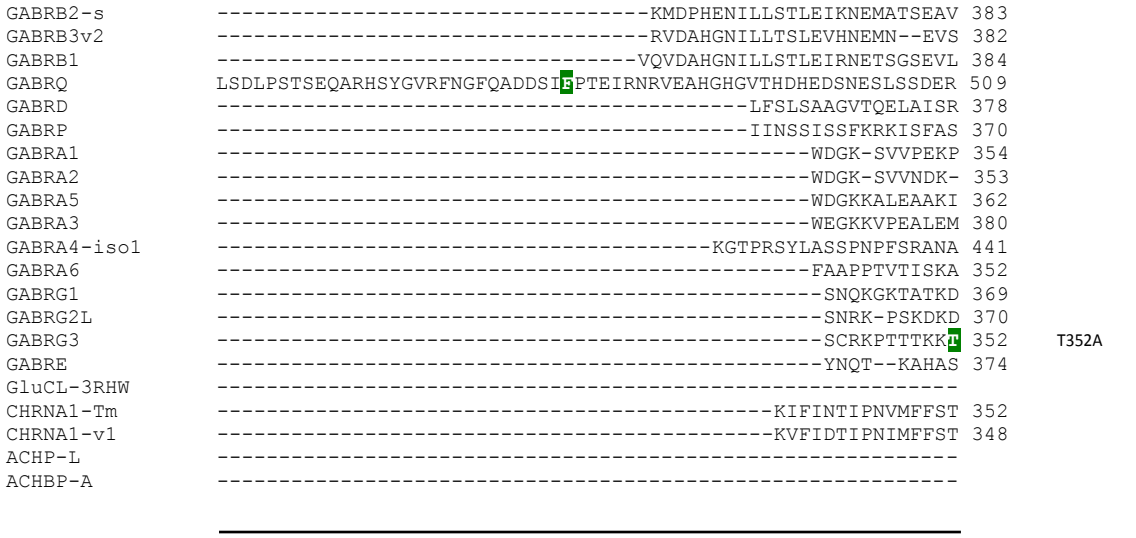
GABRB2-s ----------KMDPHENILLSTLEIKNEMATSEAV 383
GABRB3v2 ----------RVDAHGNILLTSLEVHNEMN--EVS 382
GABRB1 ----------VQVDAHGNILLSTLEIRNETSGSEVL 384
GABRQ LSDLPSTSEQARHSYGVRFNGFQADDSIEPTEIRNRVEAHGHGVTHDHEDSNESLSSDER 509
GABRD ----------LFSLSAAGVTQELAISR 378
GABRP ----------IINSSISSFKRKISFAS 370
GABRA1 ----------WDGK-SVVPEKP 354
GABRA2 ----------WDGK-SVVNDK- 353
GABRA5 ----------WDGKKALEAAKI 362
GABRA3 ----------WEGKKVPEALEM 380
GABRA4-iso1 ----------KGTPRSYLASSPNPFSRANA 441
GABRA6 ----------FAAPPTVTISKA 352
GABRG1 ----------SNQKGKTATKD 369
GABRG2L ----------SNRK-PSKDKD 370
GABRG3 ----------SCRKPTTTKKH 352
GABRE ----------YNQT--KAHAS 374
GluCL-3RHW ----------
CHRNA1-Tm ----------KIFINTIPNVMFFST 352
CHRNA1-v1 ----------KVFIDTIPNIMFFST 348
ACHP-L ----------
ACHBP-A ----------
T352A
M3-M4 loop

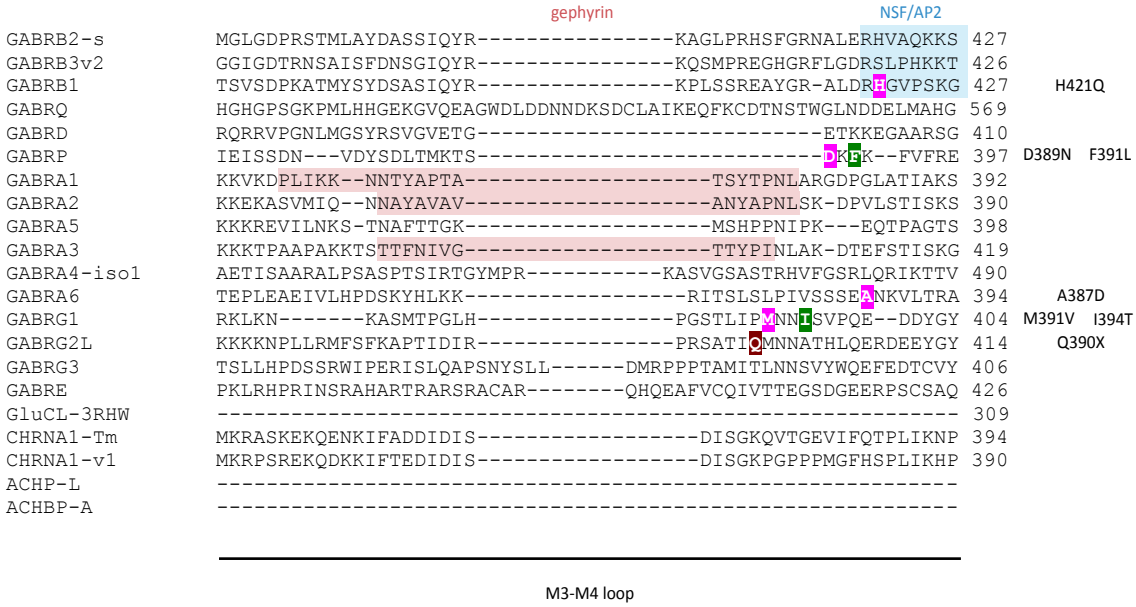
gephyrin
NSF/AP2
GABRB2-s MGLGDPRSTMLAYDASSIQYR----------KAGLPRHSFGRNALERHVAQKKS 427
GABRB3v2 GGIGDTRNSAISFDNSGIQYR----------KQSMPREGHGRFLGDRSLPHKKT 426
GABRB1 TSVSDPKATMYSYDSASIQYR----------KPLSSREAYGR-ALDRHGVPSKG 427
H421Q
GABRQ HGHGPSGKPMLHHGEKGVQEAGWDLDDNNDKSDCLAIKEQFKCDTNSTWGLNDDELMAHG 569
GABRD RQRRVPGNLMGSYRSVGVETG----------ETKKEGAARSG 410
GABRP IEISSDN---VDYSDLTMKTS----------DKEK--FVFRE 397
D389N F391L
GABRA1 KKVKDPLIKK--NNTYAPTA----------TSYTPNLARGDPGLATIAKS 392
GABRA2 KKEKASVMIQ--NNAYAVAV----------ANYAPNLSK-DPVLSTISKS 390
GABRA5 KKKREVILNKS-TNAFTTGK----------MSHPPNIPK---EQTPAGTS 398
GABRA3 KKKTPAAPAKKTSTTFNIVG----------TTYPINLAK-DTEFSTISKG 419
GABRA4-iso1 AETISAARALPSASPTSIRTGYMPR----------KASVGSASTRHVFGSRLQRIKTTV 490
GABRA6 TEPLEAEIVLHPDSKYHLKK----------RITSLSLPIVSSSEANKVLTRA 394
A387D
GABRG1 RKLKN-------KASMTPGLH----------PGSTLIPMNNISVPQE--DDYGY 404
M391V I394T
GABRG2L KKKKNPLLRMFSFKAPTIDIR----------PRSATIQMNNATHLQERDEEYGY 414
Q390X
GABRG3 TSLLHPDSSRWIPERISLQAPSNYSLL------DMRPPPTAMITLNNSVYWQEFEDTCVY 406
GABRE PKLRHPRINSRAHARTRARSRACAR--------QHQEAFVCQIVTTEGSDGEERPSCSAQ 426
GluCL-3RHW ---------- 309
CHRNA1-Tm MKRASKEKQENKIFADDIDIS----------DISGKQVTGEVIFQTPLIKNP 394
CHRNA1-v1 MKRPSREKQDKKIFTEDIDIS----------DISGKPGPPPMGFHSPLIKHP 390
ACHP-L ----------
ACHBP-A ----------
M3-M4 loop

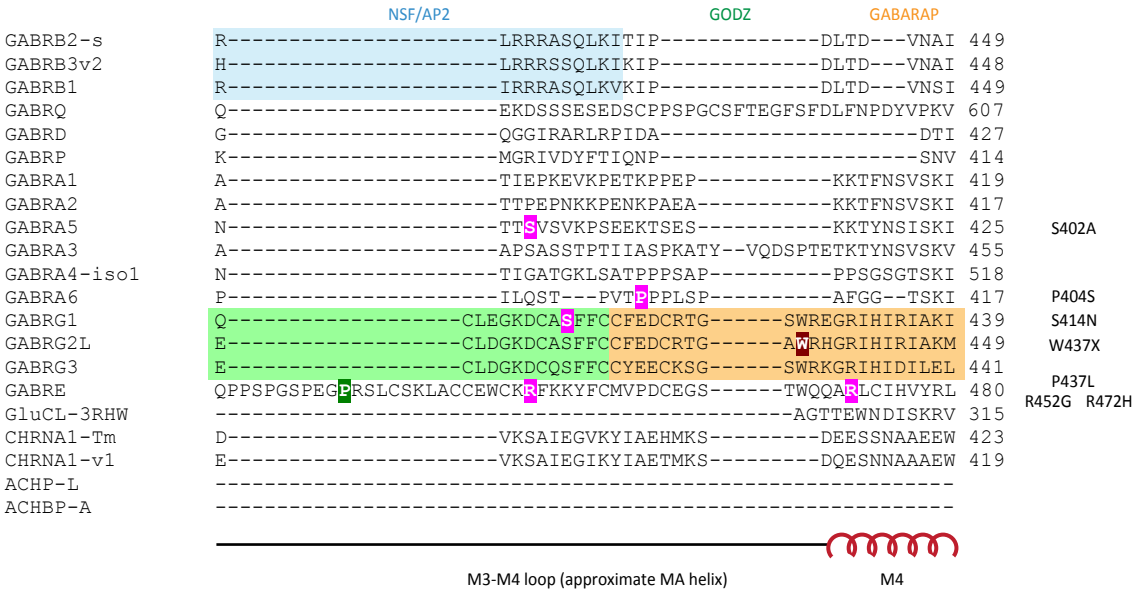

Mutations

New variants - controls only

New variants - controls and cases

inner sheet outer sheet

Interacts with α

Interacts with β

Interacts with γ

Interacts with α&β

Mutations

New variants – controls only

New variants – controls and cases

Appendix 2. Epilepsy-associated variants recently identified in GABAA receptor subunit genes

						Found in			Predictions	
gene		**ref AA**	**pos**	**mut AA**	**code**	**pts?**	**ctrls?**	**Region**	**PolyPhen**	**SIFT**
GABRA1	novel	Thr	20	Ile	T20I	yes	no	SP	benign	tolerated
GABRA1		Asp	219	Asn	*D219N*	yes	no	b9	poss	damaging
GABRA3		Thr	12	Asn	T12N			SP	benign	tolerated
GABRA4	rs16859837	Ala	19	Thr	A19T	yes	no	SP	benign	tolerated
GABRA4	novel	His	372	Pro	H372P	yes	no	loop	benign	tolerated
GABRA5	novel	Val	204	Ile	V204I	yes	no	b8	benign	tolerated
GABRA5	novel	Trp	280	Arg	W280R	yes	no	M2	prob	damaging
GABRA5	novel	Ser	402	Ala	S402A	yes	no	loop (MA)	benign	tolerated
GABRA5	novel	Pro	453	Leu	P453L	yes	no	C-tail	poss	tolerated
GABRA6		Arg	46	Trp	R46W	yes	no	L1	prob	damaging
GABRA6	novel	Gln	237	Arg	Q237R	yes	no	b10 (pre-M1)	benign	tolerated
GABRA6		Ala	387	Asp	A387D			loop	benign	tolerated
GABRA6		Pro	404	Ser	P404S			loop (MA)	benign	tolerated
GABRB1	rs41311286	His	421	Gln	H421Q	yes	no	loop	benign	
GABRB2		Arg	3	Ser	R3S			SP	benign	tolerated
GABRB2	novel	Arg	293	Trp	R293W	yes	no	M2	prob	damaging
GABRB2	rs41298406	Arg	354	Cys	R354C	yes	no	loop	prob	tolerated
GABRE		Gly	66	Ser	G66S	yes	no	helix 1	benign	tolerated
GABRE		Pro	437	Leu	P437L			loop	poss	tolerated
GABRE	rs61730044	Arg	452	Gly	R452G	yes	no	loop	benign	tolerated
GABRE	novel	Arg	472	His	R472H	yes	no	M4	benign	damaging
GABRE	novel	Ser	484	Leu	S484L	yes	no	M4	prob	damaging
GABRG1	novel	Ser	16	Arg	S16R	yes	no	SP	benign	
GABRG1		Met	391	Val	M391V	yes		loop	benign	
GABRG1	novel	Ser	414	Asn	S414N	yes	no	loop (MA)	poss	
GABRG2		Asn	79	Ser	N79S	yes	no	L1	benign	tolerated

GABRG2		Pro	83	Ser	P83S		yes			L1		prob	damaging
GABRG3	novel	Ala	303	Thr	A303T		yes	no		M2		prob	
GABRP		Val	10	Met	V10M					SP		benign	
GABRP	novel	Arg	200	Cys	R200C		yes	no		L9		prob	
GABRP	novel	Arg	200	His	R200H		yes	no		L9		benign	
GABRP	novel	Ser	292	Pro	S292P		yes	no		M2		prob	
GABRP	novel	Arg	293	Cys	R293C		yes	no		M2		prob	
GABRP	rs61733087	Val	349	Ala	V349A		yes	no		loop		benign	
GABRP	novel	Asp	389	Asn	D389N		yes	no		loop		poss	
GABRQ		Ile	401	Thr	I401T					loop		benign	
GABRQ		Leu	621	Ser	L621S					M4		prob	
GABRR1		Glu	412	Gly	E412G					loop			
GABRR2	novel	Val	294	Ile	V294I		yes	no		M1			
GABRR2	novel	Arg	287	His	R287H		yes	no		M1			
GABRR2		Glu	353	Asp	E353D					M3			
GABRA4	rs2229940	Leu	26	Met	L26M		yes	yes		SP		benign	tolerated
GABRA4	rs45546331	Thr	355	Ala	T355A		no	yes		loop		benign	tolerated
GABRA6	rs3811993	Thr	187	Met	T187M		yes	yes		b8		prob	tolerated
GABRA6	rs34907804	Pro	404	Ser	P404S		yes	yes		loop (MA)		benign	tolerated
GABRE		Tyr	38	Cys	Y38C		yes	yes		pre-a1 helix		prob	damaging
GABRE		Glu	52	Lys	E52K		yes	yes		pre-a1 helix		benign	tolerated
GABRE	rs45439991	Pro	437	Leu	P437L		yes	yes		loop (MA)		poss	tolerated
GABRE	rs1139916	Ser	102	Ala	S102A		yes	yes		b1		poss	damaging
GABRG1	novel	Ile	394	Thr	I394T		yes	yes		loop		benign	
GABRG3	rs2066712	Thr	352	Ala	T352A		yes	yes		loop		benign	
GABRP	novel	Val	10	Met	V10M		yes	yes		SP		benign	
GABRP	rs1063310	Phe	391	Leu	F391L		yes	yes		loop		benign	

GABRQ	rs3810651	Phe	478	Ile	F478I		yes	yes		loop		benign	
GABRR1	rs1186902	His	21	Arg	H21R		yes	yes		SP			
GABRR1	rs12200969	Met	20	Val	M20V		yes	yes		SP			
GABRR2	novel	Gln	352	Arg	Q352R		no	yes		M3			
GABRR2	rs282129	Thr	430	Met	T430M		yes	yes		loop			

PolyPhen: poss = possibly damaging; prob = probably damaging (using HumDiv algorithm)

Baylor study	other cohort

REFERENCES

1. DeFelipe, J. Neocortical neuronal diversity: chemical heterogeneity revealed by colocalization studies of classic neurotransmitters, neuropeptides, calcium-binding proteins, and cell surface molecules. *Cereb Cortex* **3**, 273-89 (1993).

2. Schousboe, A. & Waagepetersen, H.S. GABA: homeostatic and pharmacological aspects. *Prog Brain Res* **160**, 9-19 (2007).

3. Bu, D.F. et al. Two human glutamate decarboxylases, 65-kDa GAD and 67-kDa GAD, are each encoded by a single gene. *Proc Natl Acad Sci U S A* **89**, 2115-9 (1992).

4. Petroff, O.A. GABA and glutamate in the human brain. *Neuroscientist* **8**, 562-73 (2002).

5. Asada, H. et al. Cleft palate and decreased brain gamma-aminobutyric acid in mice lacking the 67-kDa isoform of glutamic acid decarboxylase. *Proc Natl Acad Sci U S A* **94**, 6496-9 (1997).

6. Asada, H. et al. Mice lacking the 65 kDa isoform of glutamic acid decarboxylase (GAD65) maintain normal levels of GAD67 and GABA in their brains but are susceptible to seizures. *Biochem Biophys Res Commun* **229**, 891-5 (1996).

7. Kash, S.F., Tecott, L.H., Hodge, C. & Baekkeskov, S. Increased anxiety and altered responses to anxiolytics in mice deficient in the 65-kDa isoform of glutamic acid decarboxylase. *Proc Natl Acad Sci U S A* **96**, 1698-703 (1999).

8. Kash, S.F. et al. Epilepsy in mice deficient in the 65-kDa isoform of glutamic acid decarboxylase. *Proc Natl Acad Sci U S A* **94**, 14060-5 (1997).

9. Pinal, C.S. & Tobin, A.J. Uniqueness and redundancy in GABA production. *Perspect Dev Neurobiol* **5**, 109-18 (1998).

10. Buddhala, C., Hsu, C.C. & Wu, J.Y. A novel mechanism for GABA synthesis and packaging into synaptic vesicles. *Neurochem Int* **55**, 9-12 (2009).

11. Mozrzymas, J.W., Zarnowska, E.D., Pytel, M. & Mercik, K. Modulation of GABA(A) receptors by hydrogen ions reveals synaptic GABA transient and a crucial role of the desensitization process. *J Neurosci* **23**, 7981-92 (2003).

12. Jones, M.V. & Westbrook, G.L. Desensitized states prolong GABAA channel responses to brief agonist pulses. *Neuron* **15**, 181-91 (1995).

13. Maconochie, D.J., Zempel, J.M. & Steinbach, J.H. How quickly can GABAA receptors open? *Neuron* **12**, 61-71 (1994).

14. Conti, F., Minelli, A. & Melone, M. GABA transporters in the mammalian cerebral cortex: localization, development and pathological implications. *Brain Res Brain Res Rev* **45**, 196-212 (2004).

15. Liu, Q.R., Lopez-Corcuera, B., Mandiyan, S., Nelson, H. & Nelson, N. Molecular characterization of four pharmacologically distinct gamma-aminobutyric acid transporters in mouse brain [corrected]. *J Biol Chem* **268**, 2106-12 (1993).

16. Madsen, K.K., White, H.S. & Schousboe, A. Neuronal and non-neuronal GABA transporters as targets for antiepileptic drugs. *Pharmacol Ther* **125**, 394-401 (2010).

17. Dalby, N.O. Inhibition of gamma-aminobutyric acid uptake: anatomy, physiology and effects against epileptic seizures. *Eur J Pharmacol* **479**, 127-37 (2003).

18. Kavanaugh, M.P., Arriza, J.L., North, R.A. & Amara, S.G. Electrogenic uptake of gamma-aminobutyric acid by a cloned transporter expressed in Xenopus oocytes. *J Biol Chem* **267**, 22007-9 (1992).

19. Gasnier, B. The loading of neurotransmitters into synaptic vesicles. *Biochimie* **82**, 327-37 (2000).

20. Bak, L.K., Schousboe, A. & Waagepetersen, H.S. The glutamate/GABA-glutamine cycle: aspects of transport, neurotransmitter homeostasis and ammonia transfer. *J Neurochem* **98**, 641-53 (2006).

21. Lu, J., Karadsheh, M. & Delpire, E. Developmental regulation of the neuronal-specific isoform of K-Cl cotransporter KCC2 in postnatal rat brains. *J Neurobiol* **39**, 558-68 (1999).

22. Rivera, C. et al. The K+/Cl- co-transporter KCC2 renders GABA hyperpolarizing during neuronal maturation. *Nature* **397**, 251-5 (1999).

23. Rivera, C. et al. BDNF-induced TrkB activation down-regulates the K+-Cl- cotransporter KCC2 and impairs neuronal Cl- extrusion. *J Cell Biol* **159**, 747-52 (2002).

24. Ludwig, A. et al. Neurturin evokes MAPK-dependent upregulation of Egr4 and KCC2 in developing neurons. *Neural Plast* **2011**, 1-8 (2011).

25. Ganguly, K., Schinder, A.F., Wong, S.T. & Poo, M. GABA itself promotes the developmental switch of neuronal GABAergic responses from excitation to inhibition. *Cell* **105**, 521-32 (2001).

26. Li, X. et al. Long-term expressional changes of Na+ -K+ -Cl- co-transporter 1 (NKCC1) and K+ -Cl- co-transporter 2 (KCC2) in CA1 region of hippocampus following lithium-pilocarpine induced status epilepticus (PISE). *Brain Res* **1221**, 141-6 (2008).

27. Coull, J.A. et al. Trans-synaptic shift in anion gradient in spinal lamina I neurons as a mechanism of neuropathic pain. *Nature* **424**, 938-42 (2003).

28. Jaenisch, N., Witte, O.W. & Frahm, C. Downregulation of potassium chloride cotransporter KCC2 after transient focal cerebral ischemia. *Stroke* **41**, e151-9 (2010).

29. Hyde, T.M. et al. Expression of GABA signaling molecules KCC2, NKCC1, and GAD1 in cortical development and schizophrenia. *J Neurosci* **31**, 11088-95 (2011).

30. Pin, J.P. et al. G-protein-coupled receptor oligomers: two or more for what? Lessons from mGlu and GABAB receptors. *J Physiol* **587**, 5337-44 (2009).

31. Padgett, C.L. & Slesinger, P.A. GABAB receptor coupling to G-proteins and ion channels. *Adv Pharmacol* **58**, 123-47 (2010).

32. Kohl, M.M. & Paulsen, O. The roles of GABAB receptors in cortical network activity. *Adv Pharmacol* **58**, 205-29 (2010).

33. Connolly, C.N. & Wafford, K.A. The Cys-loop superfamily of ligand-gated ion channels: the impact of receptor structure on function. *Biochem Soc Trans* **32**, 529-34 (2004).

34. Shimada, S., Cutting, G. & Uhl, G.R. gamma-Aminobutyric acid A or C receptor? gamma-Aminobutyric acid rho 1 receptor RNA induces bicuculline-, barbiturate-, and benzodiazepine-insensitive gamma-aminobutyric acid responses in Xenopus oocytes. *Mol Pharmacol* **41**, 683-7 (1992).

35. Russek, S.J. Evolution of GABA(A) receptor diversity in the human genome. *Gene* **227**, 213-22 (1999).

36. McLean, P.J., Farb, D.H. & Russek, S.J. Mapping of the alpha 4 subunit gene (GABRA4) to human chromosome 4 defines an alpha 2-alpha 4-beta 1-gamma 1 gene cluster: further evidence that modern GABAA receptor gene clusters are derived from an ancestral cluster. *Genomics* **26**, 580-6 (1995).

37. Russek, S.J. & Farb, D.H. Mapping of the beta 2 subunit gene (GABRB2) to microdissected human chromosome 5q34-q35 defines a gene cluster for the most abundant GABAA receptor isoform. *Genomics* **23**, 528-33 (1994).

38. Greger, V. et al. The gamma-aminobutyric acid receptor gamma 3 subunit gene (GABRG3) is tightly linked to the alpha 5 subunit gene (GABRA5) on human chromosome 15q11-q13 and is transcribed in the same orientation. *Genomics* **26**, 258-64 (1995).

39. Wagstaff, J., Chaillet, J.R. & Lalande, M. The GABAA receptor beta 3 subunit gene: characterization of a human cDNA from chromosome 15q11q13 and mapping to a region of conserved synteny on mouse chromosome 7. *Genomics* **11**, 1071-8 (1991).

40. Pape, J.R. et al. Expression of GABA(A) receptor alpha3-, theta-, and epsilon-subunit mRNAs during rat CNS development and immunolocalization of the epsilon subunit in developing postnatal spinal cord. *Neuroscience* **160**, 85-96 (2009).

41. Wilke, K., Gaul, R., Klauck, S.M. & Poustka, A. A gene in human chromosome band Xq28 (GABRE) defines a putative new subunit class of the GABAA neurotransmitter receptor. *Genomics* **45**, 1-10 (1997).

42. Petryshen, T.L. et al. Genetic investigation of chromosome 5q GABAA receptor subunit genes in schizophrenia. *Mol Psychiatry* **10**, 1074-88, 1057 (2005).

43. Sommer, B., Poustka, A., Spurr, N.K. & Seeburg, P.H. The murine GABAA receptor delta-subunit gene: structure and assignment to human chromosome 1. *DNA Cell Biol* **9**, 561-8 (1990).

44. Bailey, M.E., Albrecht, B.E., Johnson, K.J. & Darlison, M.G. Genetic linkage and radiation hybrid mapping of the three human GABA(C) receptor rho subunit genes: GABRR1, GABRR2 and GABRR3. *Biochim Biophys Acta* **1447**, 307-12 (1999).

45. Laurie, D.J., Wisden, W. & Seeburg, P.H. The distribution of thirteen GABAA receptor subunit mRNAs in the rat brain. III. Embryonic and postnatal development. *J Neurosci* **12**, 4151-72 (1992).

46. Poulter, M.O., Barker, J.L., O'Carroll, A.M., Lolait, S.J. & Mahan, L.C. Differential and transient expression of GABAA receptor alpha-subunit mRNAs in the developing rat CNS. *J Neurosci* **12**, 2888-900 (1992).

47. Fritschy, J.M., Paysan, J., Enna, A. & Mohler, H. Switch in the expression of rat GABAA-receptor subtypes during postnatal development: an immunohistochemical study. *J Neurosci* **14**, 5302-24 (1994).

48. Huntsman, M.M., Munoz, A. & Jones, E.G. Temporal modulation of GABA(A) receptor subunit gene expression in developing monkey cerebral cortex. *Neuroscience* **91**, 1223-45 (1999).

49. Fillman, S.G., Duncan, C.E., Webster, M.J., Elashoff, M. & Weickert, C.S. Developmental co-regulation of the beta and gamma GABAA receptor subunits with distinct alpha subunits in the human dorsolateral prefrontal cortex. *Int J Dev Neurosci* **28**, 513-9 (2010).

50. Alakuijala, A. et al. GABA receptor rho subunit expression in the developing rat brain. *Brain Res Dev Brain Res* **154**, 15-23 (2005).

51. Mejia, C. et al. Expression of GABArho subunits during rat cerebellum development. *Neurosci Lett* **432**, 1-6 (2008).

52. Yu, Z.Y., Wang, W., Fritschy, J.M., Witte, O.W. & Redecker, C. Changes in neocortical and hippocampal GABAA receptor subunit distribution during brain maturation and aging. *Brain Res* **1099**, 73-81 (2006).

53. Laurie, D.J., Seeburg, P.H. & Wisden, W. The distribution of 13 GABAA receptor subunit mRNAs in the rat brain. II. Olfactory bulb and cerebellum. *J Neurosci* **12**, 1063-76 (1992).

54. Wisden, W., Laurie, D.J., Monyer, H. & Seeburg, P.H. The distribution of 13 GABAA receptor subunit mRNAs in the rat brain. I. Telencephalon, diencephalon, mesencephalon. *J Neurosci* **12**, 1040-62 (1992).

55. Pirker, S., Schwarzer, C., Wieselthaler, A., Sieghart, W. & Sperk, G. GABA(A) receptors: immunocytochemical distribution of 13 subunits in the adult rat brain. *Neuroscience* **101**, 815-50 (2000).

56. Fritschy, J.M. & Mohler, H. GABAA-receptor heterogeneity in the adult rat brain: differential regional and cellular distribution of seven major subunits. *J Comp Neurol* **359**, 154-94 (1995).

57. Sieghart, W. & Sperk, G. Subunit composition, distribution and function of GABA(A) receptor subtypes. *Curr Top Med Chem* **2**, 795-816 (2002).

58. Gutierrez, A., Khan, Z.U. & De Blas, A.L. Immunocytochemical localization of gamma 2 short and gamma 2 long subunits of the GABAA receptor in the rat brain. *J Neurosci* **14**, 7168-79 (1994).

59. Moragues, N. et al. cDNA cloning and expression of a gamma-aminobutyric acid A receptor epsilon-subunit in rat brain. *Eur J Neurosci* **12**, 4318-30 (2000).

60. Moragues, N., Ciofi, P., Tramu, G. & Garret, M. Localisation of GABA(A) receptor epsilon-subunit in cholinergic and aminergic neurones and evidence for co-distribution with the theta-subunit in rat brain. *Neuroscience* **111**, 657-69 (2002).

61. Moragues, N., Ciofi, P., Lafon, P., Tramu, G. & Garret, M. GABAA receptor epsilon subunit expression in identified peptidergic neurons of the rat hypothalamus. *Brain Res* **967**, 285-9 (2003).

62. Hedblom, E. & Kirkness, E.F. A novel class of GABAA receptor subunit in tissues of the reproductive system. *J Biol Chem* **272**, 15346-50 (1997).

63. Skirzewski, M. et al. Enhanced GABAergic tone in the ventral pallidum: memory of unpleasant experiences? *Neuroscience* **196**, 131-46 (2011).

64. Dvoryanchikov, G., Huang, Y.A., Barro-Soria, R., Chaudhari, N. & Roper, S.D. GABA, its receptors, and GABAergic inhibition in mouse taste buds. *J Neurosci* **31**, 5782-91 (2011).

65. Mizuta, K. et al. GABAA receptors are expressed and facilitate relaxation in airway smooth muscle. *Am J Physiol Lung Cell Mol Physiol* **294**, L1206-16 (2008).

66. Johnson, S.K. & Haun, R.S. The gamma-aminobutyric acid A receptor pi subunit is overexpressed in pancreatic adenocarcinomas. *JOP* **6**, 136-42 (2005).

67. Takehara, A. et al. Gamma-aminobutyric acid (GABA) stimulates pancreatic cancer growth through overexpressing GABAA receptor pi subunit. *Cancer Res* **67**, 9704-12 (2007).

68. Zafrakas, M. et al. Systematic characterisation of GABRP expression in sporadic breast cancer and normal breast tissue. *Int J Cancer* **118**, 1453-9 (2006).

69. Ogurusu, T., Taira, H. & Shingai, R. Identification of GABAA receptor subunits in rat retina: cloning of the rat GABAA receptor rho 2-subunit cDNA. *J Neurochem* **65**, 964-8 (1995).

70. Ogurusu, T., Eguchi, G. & Shingai, R. Localization of gamma-aminobutyric acid (GABA) receptor rho 3 subunit in rat retina. *Neuroreport* **8**, 925-7 (1997).

71. Ogurusu, T., Yanagi, K., Watanabe, M., Fukaya, M. & Shingai, R. Localization of GABA receptor rho 2 and rho 3 subunits in rat brain and functional expression of homooligomeric rho 3 receptors and heterooligomeric rho 2 rho 3 receptors. *Receptors Channels* **6**, 463-75 (1999).

72. Boue-Grabot, E. et al. Expression of GABA receptor rho subunits in rat brain. *J Neurochem* **70**, 899-907 (1998).

73. Martinez-Delgado, G., Estrada-Mondragon, A., Miledi, R. & Martinez-Torres, A. An Update on GABArho Receptors. *Curr Neuropharmacol* **8**, 422-33 (2010).

74. Lopez-Chavez, A., Miledi, R. & Martinez-Torres, A. Cloning and functional expression of the bovine GABA(C) rho2 subunit. Molecular evidence of a widespread distribution in the CNS. *Neurosci Res* **53**, 421-7 (2005).

75. Steiger, J.L. & Russek, S.J. GABAA receptors: building the bridge between subunit mRNAs, their promoters, and cognate transcription factors. *Pharmacol Ther* **101**, 259-81 (2004).

76. Simon, J., Wakimoto, H., Fujita, N., Lalande, M. & Barnard, E.A. Analysis of the set of GABA(A) receptor genes in the human genome. *J Biol Chem* **279**, 41422-35 (2004).

77. Ohlson, J., Pedersen, J.S., Haussler, D. & Ohman, M. Editing modifies the GABA(A) receptor subunit alpha3. *RNA* **13**, 698-703 (2007).

78. Rula, E.Y. et al. Developmental modulation of GABA(A) receptor function by RNA editing. *J Neurosci* **28**, 6196-201 (2008).

79. Chen, Z.W., Fuchs, K., Sieghart, W., Townsend, R.R. & Evers, A.S. Deep amino acid sequencing of native brain GABAA receptors using high-resolution mass spectrometry. *Mol Cell Proteomics* **11**, M111 011445 (2012).

80. Gorrie, G.H. et al. Assembly of GABAA receptors composed of alpha1 and beta2 subunits in both cultured neurons and fibroblasts. *J Neurosci* **17**, 6587-96 (1997).

81. Connolly, C.N., Krishek, B.J., McDonald, B.J., Smart, T.G. & Moss, S.J. Assembly and cell surface expression of heteromeric and homomeric gamma-aminobutyric acid type A receptors. *J Biol Chem* **271**, 89-96 (1996).

82. Green, W.N. & Millar, N.S. Ion-channel assembly. *Trends Neurosci* **18**, 280-7 (1995).

83. Bollan, K., Robertson, L.A., Tang, H. & Connolly, C.N. Multiple assembly signals in gamma-aminobutyric acid (type A) receptor subunits combine to drive receptor construction and composition. *Biochem Soc Trans* **31**, 875-9 (2003).

84. Sarto-Jackson, I. & Sieghart, W. Assembly of GABA(A) receptors (Review). *Mol Membr Biol* **25**, 302-10 (2008).

85. Srinivasan, S., Nichols, C.J., Lawless, G.M., Olsen, R.W. & Tobin, A.J. Two invariant tryptophans on the alpha1 subunit define domains necessary for GABA(A) receptor assembly. *J Biol Chem* **274**, 26633-8 (1999).

86. Taylor, P.M. et al. Identification of residues within GABA(A) receptor alpha subunits that mediate specific assembly with receptor beta subunits. *J Neurosci* **20**, 1297-306 (2000).

87. Klausberger, T. et al. Alternate use of distinct intersubunit contacts controls GABAA receptor assembly and stoichiometry. *J Neurosci* **21**, 9124-33 (2001).

88. Sarto, I., Wabnegger, L., Dogl, E. & Sieghart, W. Homologous sites of GABA(A) receptor alpha(1), beta(3) and gamma(2) subunits are important for assembly. *Neuropharmacology* **43**, 482-91 (2002).

89. Bollan, K. et al. GABA(A) receptor composition is determined by distinct assembly signals within alpha and beta subunits. *J Biol Chem* **278**, 4747-55 (2003).

90. Taylor, P.M. et al. Identification of amino acid residues within GABA(A) receptor beta subunits that mediate both homomeric and heteromeric receptor expression. *J Neurosci* **19**, 6360-71 (1999).

91. Ehya, N., Sarto, I., Wabnegger, L. & Sieghart, W. Identification of an amino acid sequence within GABA(A) receptor beta3 subunits that is important for receptor assembly. *J Neurochem* **84**, 127-35 (2003).

92. Klausberger, T., Fuchs, K., Mayer, B., Ehya, N. & Sieghart, W. GABA(A) receptor assembly. Identification and structure of gamma(2) sequences forming the intersubunit contacts with alpha(1) and beta(3) subunits. *J Biol Chem* **275**, 8921-8 (2000).

93. Sarto, I. et al. A novel site on gamma 3 subunits important for assembly of GABA(A) receptors. *J Biol Chem* **277**, 30656-64 (2002).

94. Nymann-Andersen, J., Sawyer, G.W. & Olsen, R.W. Interaction between GABAA receptor subunit intracellular loops: implications for higher order complex formation. *J Neurochem* **83**, 1164-71 (2002).

95. Lo, W.Y., Botzolakis, E.J., Tang, X. & Macdonald, R.L. A conserved Cys-loop receptor aspartate residue in the M3-M4 cytoplasmic loop is required for GABAA receptor assembly. *J Biol Chem* **283**, 29740-52 (2008).

96. Klausberger, T. et al. Detection and binding properties of GABA(A) receptor assembly intermediates. *J Biol Chem* **276**, 16024-32 (2001).

97. Unwin, N. Refined structure of the nicotinic acetylcholine receptor at 4A resolution. *J Mol Biol* **346**, 967-89 (2005).

98. Brejc, K. et al. Crystal structure of an ACh-binding protein reveals the ligand-binding domain of nicotinic receptors. *Nature* **411**, 269-76 (2001).

99. Sarto-Jackson, I., Ramerstorfer, J., Ernst, M. & Sieghart, W. Identification of amino acid residues important for assembly of GABA receptor alpha1 and gamma2 subunits. *J Neurochem* **96**, 983-95 (2006).

100. Hales, T.G. et al. The epilepsy mutation, gamma2(R43Q) disrupts a highly conserved inter-subunit contact site, perturbing the biogenesis of GABAA receptors. *Mol Cell Neurosci* **29**, 120-7 (2005).

101. Jones, B.L. & Henderson, L.P. Trafficking and potential assembly patterns of epsilon-containing GABAA receptors. *J Neurochem* **103**, 1258-71 (2007).

102. Kleijnen, M.F. et al. The hPLIC proteins may provide a link between the ubiquitination machinery and the proteasome. *Mol Cell* **6**, 409-19 (2000).

103. Bedford, F.K. et al. GABA(A) receptor cell surface number and subunit stability are regulated by the ubiquitin-like protein Plic-1. *Nat Neurosci* **4**, 908-16 (2001).

104. Saliba, R.S., Pangalos, M. & Moss, S.J. The ubiquitin-like protein Plic-1 enhances the membrane insertion of GABAA receptors by increasing their stability within the endoplasmic reticulum. *J Biol Chem* **283**, 18538-44 (2008).

105. Salaun, C., Greaves, J. & Chamberlain, L.H. The intracellular dynamic of protein palmitoylation. *J Cell Biol* **191**, 1229-38 (2010).

106. Korycka, J. et al. Human DHHC proteins: a spotlight on the hidden player of palmitoylation. *Eur J Cell Biol* **91**, 107-17 (2012).

107. Rocks, O. et al. The palmitoylation machinery is a spatially organizing system for peripheral membrane proteins. *Cell* **141**, 458-71 (2010).

108. Keller, C.A. et al. The gamma2 subunit of GABA(A) receptors is a substrate for palmitoylation by GODZ. *J Neurosci* **24**, 5881-91 (2004).

109. Fang, C. et al. GODZ-mediated palmitoylation of GABA(A) receptors is required for normal assembly and function of GABAergic inhibitory synapses. *J Neurosci* **26**, 12758-68 (2006).

110. Mohrluder, J., Schwarten, M. & Willbold, D. Structure and potential function of gamma-aminobutyrate type A receptor-associated protein. *FEBS J* **276**, 4989-5005 (2009).

111. Wang, H., Bedford, F.K., Brandon, N.J., Moss, S.J. & Olsen, R.W. GABA(A)-receptor-associated protein links GABA(A) receptors and the cytoskeleton. *Nature* **397**, 69-72 (1999).

112. Knight, D. et al. The X-ray crystal structure and putative ligand-derived peptide binding properties of gamma-aminobutyric acid receptor type A receptor-associated protein. *J Biol Chem* **277**, 5556-61 (2002).

113. Coyle, J.E., Qamar, S., Rajashankar, K.R. & Nikolov, D.B. Structure of GABARAP in two conformations: implications for GABA(A) receptor localization and tubulin binding. *Neuron* **33**, 63-74 (2002).

114. Weiergraber, O.H. et al. Ligand binding mode of GABAA receptor-associated protein. *J Mol Biol* **381**, 1320-31 (2008).

115. Kittler, J.T. et al. The subcellular distribution of GABARAP and its ability to interact with NSF suggest a role for this protein in the intracellular transport of GABA(A) receptors. *Mol Cell Neurosci* **18**, 13-25 (2001).

116. Boileau, A.J., Pearce, R.A. & Czajkowski, C. Tandem subunits effectively constrain GABAA receptor stoichiometry and recapitulate receptor kinetics but are insensitive to GABAA receptor-associated protein. *J Neurosci* **25**, 11219-30 (2005).

117. Goto, H. et al. Direct interaction of N-ethylmaleimide-sensitive factor with GABA(A) receptor beta subunits. *Mol Cell Neurosci* **30**, 197-206 (2005).

118. Kanematsu, T. et al. Role of the PLC-related, catalytically inactive protein p130 in GABA(A) receptor function. *EMBO J* **21**, 1004-11 (2002).

119. Mizokami, A. et al. Phospholipase C-related inactive protein is involved in trafficking of gamma2 subunit-containing GABA(A) receptors to the cell surface. *J Neurosci* **27**, 1692-701 (2007).

120. Seo, K. et al. Genetic reduction of GABA(A) receptor gamma2 subunit expression potentiates the immobilizing action of isoflurane. *Neurosci Lett* **472**, 1-4 (2010).

121. Terunuma, M. et al. GABAA receptor phospho-dependent modulation is regulated by phospholipase C-related inactive protein type 1, a novel protein phosphatase 1 anchoring protein. *J Neurosci* **24**, 7074-84 (2004).

122. Morinaga, N., Moss, J. & Vaughan, M. Cloning and expression of a cDNA encoding a bovine brain brefeldin A-sensitive guanine nucleotide-exchange protein for ADP-ribosylation factor. *Proc Natl Acad Sci U S A* **94**, 12926-31 (1997).

123. Togawa, A., Morinaga, N., Ogasawara, M., Moss, J. & Vaughan, M. Purification and cloning of a brefeldin A-inhibited guanine nucleotide-exchange protein for ADP-ribosylation factors. *J Biol Chem* **274**, 12308-15 (1999).

124. Charych, E.I. et al. The brefeldin A-inhibited GDP/GTP exchange factor 2, a protein involved in vesicular trafficking, interacts with the beta subunits of the GABA receptors. *J Neurochem* **90**, 173-89 (2004).

125. Smith, M.J., Pozo, K., Brickley, K. & Stephenson, F.A. Mapping the GRIF-1 binding domain of the kinesin, KIF5C, substantiates a role for GRIF-1 as an adaptor protein in the anterograde trafficking of cargoes. *J Biol Chem* **281**, 27216-28 (2006).

126. Pozo, K. & Stephenson, F.A. GRIF-1-kinesin-1 interactions: a confocal microscopy study. *Biochem Soc Trans* **34**, 48-50 (2006).

127. Beck, M. et al. Identification, molecular cloning, and characterization of a novel GABAA receptor-associated protein, GRIF-1. *J Biol Chem* **277**, 30079-90 (2002).

128. Wang, Q. et al. Control of synaptic strength, a novel function of Akt. *Neuron* **38**, 915-28 (2003).

129. Xu, E. et al. Intra-islet insulin suppresses glucagon release via GABA-GABAA receptor system. *Cell Metab* **3**, 47-58 (2006).

130. Bogdanov, Y. et al. Synaptic GABAA receptors are directly recruited from their extrasynaptic counterparts. *EMBO J* **25**, 4381-9 (2006).

131. Yu, W. et al. Gephyrin clustering is required for the stability of GABAergic synapses. *Mol Cell Neurosci* **36**, 484-500 (2007).

132. Ramming, M. et al. Diversity and phylogeny of gephyrin: tissue-specific splice variants, gene structure, and sequence similarities to molybdenum cofactor-synthesizing and cytoskeleton-associated proteins. *Proc Natl Acad Sci U S A* **97**, 10266-71 (2000).

133. Saiyed, T. et al. Molecular basis of gephyrin clustering at inhibitory synapses: role of G- and E-domain interactions. *J Biol Chem* **282**, 5625-32 (2007).

134. Mammoto, A. et al. Interactions of drebrin and gephyrin with profilin. *Biochem Biophys Res Commun* **243**, 86-9 (1998).

135. Moss, S.J. & Smart, T.G. Constructing inhibitory synapses. *Nat Rev Neurosci* **2**, 240-50 (2001).

136. Essrich, C., Lorez, M., Benson, J.A., Fritschy, J.M. & Luscher, B. Postsynaptic clustering of major GABAA receptor subtypes requires the gamma 2 subunit and gephyrin. *Nat Neurosci* **1**, 563-71 (1998).

137. Schweizer, C. et al. The gamma 2 subunit of GABA(A) receptors is required for maintenance of receptors at mature synapses. *Mol Cell Neurosci* **24**, 442-50 (2003).

138. Alldred, M.J., Mulder-Rosi, J., Lingenfelter, S.E., Chen, G. & Luscher, B. Distinct gamma2 subunit domains mediate clustering and synaptic function of postsynaptic GABAA receptors and gephyrin. *J Neurosci* **25**, 594-603 (2005).

139. Tretter, V. et al. The clustering of GABA(A) receptor subtypes at inhibitory synapses is facilitated via the direct binding of receptor alpha 2 subunits to gephyrin. *J Neurosci* **28**, 1356-65 (2008).

140. Danglot, L., Triller, A. & Bessis, A. Association of gephyrin with synaptic and extrasynaptic GABAA receptors varies during development in cultured hippocampal neurons. *Mol Cell Neurosci* **23**, 264-78 (2003).

141. Brunig, I., Scotti, E., Sidler, C. & Fritschy, J.M. Intact sorting, targeting, and clustering of gamma-aminobutyric acid A receptor subtypes in hippocampal neurons in vitro. *J Comp Neurol* **443**, 43-55 (2002).

142. Kneussel, M. et al. Loss of postsynaptic GABA(A) receptor clustering in gephyrin-deficient mice. *J Neurosci* **19**, 9289-97 (1999).

143. Kneussel, M. et al. Gephyrin-independent clustering of postsynaptic GABA(A) receptor subtypes. *Mol Cell Neurosci* **17**, 973-82 (2001).

144. Tsukita, S. & Yonemura, S. ERM proteins: head-to-tail regulation of actin-plasma membrane interaction. *Trends Biochem Sci* **22**, 53-8 (1997).

145. Kittler, J.T. et al. Constitutive endocytosis of GABAA receptors by an association with the adaptin AP2 complex modulates inhibitory synaptic currents in hippocampal neurons. *J Neurosci* **20**, 7972-7 (2000).

146. Rapoport, I., Chen, Y.C., Cupers, P., Shoelson, S.E. & Kirchhausen, T. Dileucine-based sorting signals bind to the beta chain of AP-1 at a site distinct and regulated differently from the tyrosine-based motif-binding site. *EMBO J* **17**, 2148-55 (1998).

147. Smith, K.R. et al. Stabilization of GABA(A) receptors at endocytic zones is mediated by an AP2 binding motif within the GABA(A) receptor beta3 subunit. *J Neurosci* **32**, 2485-98 (2012).

148. Herring, D. et al. Constitutive GABAA receptor endocytosis is dynamin-mediated and dependent on a dileucine AP2 adaptin-binding motif within the beta 2 subunit of the receptor. *J Biol Chem* **278**, 24046-52 (2003).

149. Kittler, J.T. et al. Regulation of synaptic inhibition by phospho-dependent binding of the AP2 complex to a YECL motif in the GABAA receptor gamma2 subunit. *Proc Natl Acad Sci U S A* **105**, 3616-21 (2008).

150. Yuen, E.Y., Wei, J., Zhong, P. & Yan, Z. Disrupted GABA(A)R trafficking and synaptic inhibition in a mouse model of Huntington's disease. *Neurobiol Dis* **46**, 497-502 (2012).

151. Kittler, J.T. et al. Huntingtin-associated protein 1 regulates inhibitory synaptic transmission by modulating gamma-aminobutyric acid type A receptor membrane trafficking. *Proc Natl Acad Sci U S A* **101**, 12736-41 (2004).

152. Sheng, G. et al. Hypothalamic huntingtin-associated protein 1 as a mediator of feeding behavior. *Nat Med* **12**, 526-33 (2006).

153. Dellisanti, C.D., Yao, Y., Stroud, J.C., Wang, Z.Z. & Chen, L. Crystal structure of the extracellular domain of nAChR alpha1 bound to alpha-bungarotoxin at 1.94 A resolution. *Nat Neurosci* **10**, 953-62 (2007).

154. Warmuth, S., Zimmermann, I. & Dutzler, R. X-ray structure of the C-terminal domain of a prokaryotic cation-chloride cotransporter. *Structure* **17**, 538-46 (2009).

155. Hilf, R.J. & Dutzler, R. Structure of a potentially open state of a proton-activated pentameric ligand-gated ion channel. *Nature* **457**, 115-8 (2009).

156. Hilf, R.J. & Dutzler, R. X-ray structure of a prokaryotic pentameric ligand-gated ion channel. *Nature* **452**, 375-9 (2008).

157. Ernst, M., Brauchart, D., Boresch, S. & Sieghart, W. Comparative modeling of GABA(A) receptors: limits, insights, future developments. *Neuroscience* **119**, 933-43 (2003).

158. Ernst, M., Bruckner, S., Boresch, S. & Sieghart, W. Comparative models of GABAA receptor extracellular and transmembrane domains: important insights in pharmacology and function. *Mol Pharmacol* **68**, 1291-300 (2005).

159. Hibbs, R.E. & Gouaux, E. Principles of activation and permeation in an anion-selective Cys-loop receptor. *Nature* **474**, 54-60 (2011).

160. Zhu, Q. & Casey, J.R. Topology of transmembrane proteins by scanning cysteine accessibility mutagenesis methodology. *Methods* **41**, 439-50 (2007).

161. Xu, M. & Akabas, M.H. Identification of channel-lining residues in the M2 membrane-spanning segment of the GABA(A) receptor alpha1 subunit. *J Gen Physiol* **107**, 195-205 (1996).

162. Bali, M. & Akabas, M.H. The location of a closed channel gate in the GABAA receptor channel. *J Gen Physiol* **129**, 145-59 (2007).

163. Jensen, M.L. et al. The beta subunit determines the ion selectivity of the GABAA receptor. *J Biol Chem* **277**, 41438-47 (2002).

164. Khatri, A. & Weiss, D.S. The role of Loop F in the activation of the GABA receptor. *J Physiol* **588**, 59-66 (2010).

165. Wagner, D.A. & Czajkowski, C. Structure and dynamics of the GABA binding pocket: A narrowing cleft that constricts during activation. *J Neurosci* **21**, 67-74 (2001).

166. Kash, T.L., Jenkins, A., Kelley, J.C., Trudell, J.R. & Harrison, N.L. Coupling of agonist binding to channel gating in the GABA(A) receptor. *Nature* **421**, 272-5 (2003).

167. Kash, T.L., Trudell, J.R. & Harrison, N.L. Structural elements involved in activation of the gamma-aminobutyric acid type A (GABAA) receptor. *Biochem Soc Trans* **32**, 540-6 (2004).

168. Haas, K.F. & Macdonald, R.L. GABAA receptor subunit gamma2 and delta subtypes confer unique kinetic properties on recombinant GABAA receptor currents in mouse fibroblasts. *J Physiol* **514 (Pt 1)**, 27-45 (1999).

169. Tia, S., Wang, J.F., Kotchabhakdi, N. & Vicini, S. Distinct deactivation and desensitization kinetics of recombinant GABAA receptors. *Neuropharmacology* **35**, 1375-82 (1996).

170. Picton, A.J. & Fisher, J.L. Effect of the alpha subunit subtype on the macroscopic kinetic properties of recombinant GABA(A) receptors. *Brain Res* **1165**, 40-9 (2007).

171. Boileau, A.J., Evers, A.R., Davis, A.F. & Czajkowski, C. Mapping the agonist binding site of the GABAA receptor: evidence for a beta-strand. *J Neurosci* **19**, 4847-54 (1999).

172. Westh-Hansen, S.E. et al. Arginine residue 120 of the human GABAA receptor alpha 1, subunit is essential for GABA binding and chloride ion current gating. *Neuroreport* **10**, 2417-21 (1999).

173. Newell, J.G. & Czajkowski, C. The GABAA receptor alpha 1 subunit Pro174-Asp191 segment is involved in GABA binding and channel gating. *J Biol Chem* **278**, 13166-72 (2003).

174. Wagner, D.A., Czajkowski, C. & Jones, M.V. An arginine involved in GABA binding and unbinding but not gating of the GABA(A) receptor. *J Neurosci* **24**, 2733-41 (2004).

175. Boileau, A.J., Newell, J.G. & Czajkowski, C. GABA(A) receptor beta 2 Tyr97 and Leu99 line the GABA-binding site. Insights into mechanisms of agonist and antagonist actions. *J Biol Chem* **277**, 2931-7 (2002).

176. Pritchett, D.B., Luddens, H. & Seeburg, P.H. Type I and type II GABAA-benzodiazepine receptors produced in transfected cells. *Science* **245**, 1389-92 (1989).

177. Pritchett, D.B. & Seeburg, P.H. Gamma-aminobutyric acidA receptor alpha 5-subunit creates novel type II benzodiazepine receptor pharmacology. *J Neurochem* **54**, 1802-4 (1990).

178. Pritchett, D.B. et al. Importance of a novel GABAA receptor subunit for benzodiazepine pharmacology. *Nature* **338**, 582-5 (1989).

179. Benke, D., Honer, M., Michel, C. & Mohler, H. GABAA receptor subtypes differentiated by their gamma-subunit variants: prevalence, pharmacology and subunit architecture. *Neuropharmacology* **35**, 1413-23 (1996).

180. Wieland, H.A., Luddens, H. & Seeburg, P.H. A single histidine in GABAA receptors is essential for benzodiazepine agonist binding. *J Biol Chem* **267**, 1426-9 (1992).

181. Wingrove, P.B., Thompson, S.A., Wafford, K.A. & Whiting, P.J. Key amino acids in the gamma subunit of the gamma-aminobutyric acidA receptor that determine ligand binding and modulation at the benzodiazepine site. *Mol Pharmacol* **52**, 874-81 (1997).

182. Hanson, S.M. & Czajkowski, C. Structural mechanisms underlying benzodiazepine modulation of the GABA(A) receptor. *J Neurosci* **28**, 3490-9 (2008).

183. Jones-Davis, D.M., Song, L., Gallagher, M.J. & Macdonald, R.L. Structural determinants of benzodiazepine allosteric regulation of GABA(A) receptor currents. *J Neurosci* **25**, 8056-65 (2005).

184. Crestani, F. et al. Molecular targets for the myorelaxant action of diazepam. *Mol Pharmacol* **59**, 442-5 (2001).

185. Twyman, R.E., Rogers, C.J. & Macdonald, R.L. Differential regulation of gamma-aminobutyric acid receptor channels by diazepam and phenobarbital. *Ann Neurol* **25**, 213-20 (1989).

186. Twyman, R.E., Rogers, C.J. & Macdonald, R.L. Pentobarbital and picrotoxin have reciprocal actions on single GABAA receptor channels. *Neurosci Lett* **96**, 89-95 (1989).

187. Meera, P., Olsen, R.W., Otis, T.S. & Wallner, M. Etomidate, propofol and the neurosteroid THDOC increase the GABA efficacy of recombinant alpha4beta3delta and

alpha4beta3 GABA A receptors expressed in HEK cells. *Neuropharmacology* **56**, 155-60 (2009).

188. Drexler, B., Jurd, R., Rudolph, U. & Antkowiak, B. Distinct actions of etomidate and propofol at beta3-containing gamma-aminobutyric acid type A receptors. *Neuropharmacology* **57**, 446-55 (2009).

189. Hosie, A.M., Clarke, L., da Silva, H. & Smart, T.G. Conserved site for neurosteroid modulation of GABA A receptors. *Neuropharmacology* **56**, 149-54 (2009).

190. Hosie, A.M., Wilkins, M.E. & Smart, T.G. Neurosteroid binding sites on GABA(A) receptors. *Pharmacol Ther* **116**, 7-19 (2007).

191. Mihalek, R.M. et al. Attenuated sensitivity to neuroactive steroids in gamma-aminobutyrate type A receptor delta subunit knockout mice. *Proc Natl Acad Sci U S A* **96**, 12905-10 (1999).

192. Bianchi, M.T. & Macdonald, R.L. Neurosteroids shift partial agonist activation of GABA(A) receptor channels from low- to high-efficacy gating patterns. *J Neurosci* **23**, 10934-43 (2003).

193. Wohlfarth, K.M., Bianchi, M.T. & Macdonald, R.L. Enhanced neurosteroid potentiation of ternary GABA(A) receptors containing the delta subunit. *J Neurosci* **22**, 1541-9 (2002).

194. Jenkins, A. et al. Evidence for a common binding cavity for three general anesthetics within the GABAA receptor. *J Neurosci* **21**, RC136 (2001).

195. Hall, A.C., Rowan, K.C., Stevens, R.J., Kelley, J.C. & Harrison, N.L. The effects of isoflurane on desensitized wild-type and alpha 1(S270H) gamma-aminobutyric acid type A receptors. *Anesth Analg* **98**, 1297-304, table of contents (2004).

196. Jones, M.V. & Harrison, N.L. Effects of volatile anesthetics on the kinetics of inhibitory postsynaptic currents in cultured rat hippocampal neurons. *J Neurophysiol* **70**, 1339-49 (1993).

197. McKernan, R.M. et al. Sedative but not anxiolytic properties of benzodiazepines are mediated by the GABA(A) receptor alpha1 subtype. *Nat Neurosci* **3**, 587-92 (2000).

198. Low, K. et al. Molecular and neuronal substrate for the selective attenuation of anxiety. *Science* **290**, 131-4 (2000).

199. Morris, H.V., Dawson, G.R., Reynolds, D.S., Atack, J.R. & Stephens, D.N. Both alpha2 and alpha3 GABAA receptor subtypes mediate the anxiolytic properties of benzodiazepine site ligands in the conditioned emotional response paradigm. *Eur J Neurosci* **23**, 2495-504 (2006).

200. Knabl, J. et al. Reversal of pathological pain through specific spinal GABAA receptor subtypes. *Nature* **451**, 330-4 (2008).

201. van Rijnsoever, C. et al. Requirement of alpha5-GABAA receptors for the development of tolerance to the sedative action of diazepam in mice. *J Neurosci* **24**, 6785-90 (2004).

202. Rudolph, U. & Mohler, H. Analysis of GABAA receptor function and dissection of the pharmacology of benzodiazepines and general anesthetics through mouse genetics. *Annu Rev Pharmacol Toxicol* **44**, 475-98 (2004).

203. Atack, J.R. GABAA receptor alpha2/alpha3 subtype-selective modulators as potential nonsedating anxiolytics. *Curr Top Behav Neurosci* **2**, 331-60 (2010).

204. Atack, J.R. et al. TPA023 [7-(1,1-dimethylethyl)-6-(2-ethyl-2H-1,2,4-triazol-3-ylmethoxy)-3-(2-fluorophenyl)-1,2,4-triazolo[4,3-b]pyridazine], an agonist selective for alpha2- and alpha3-containing GABAA receptors, is a nonsedating anxiolytic in rodents and primates. *J Pharmacol Exp Ther* **316**, 410-22 (2006).

205. Bonetti, E.P. et al. Benzodiazepine antagonist Ro 15-1788: neurological and behavioral effects. *Psychopharmacology (Berl)* **78**, 8-18 (1982).

206. Conto, M.B., de Carvalho, J.G. & Benedito, M.A. Behavioral differences between subgroups of rats with high and low threshold to clonic convulsions induced by DMCM, a benzodiazepine inverse agonist. *Pharmacol Biochem Behav* **82**, 417-26 (2005).

207. Thompson, S.A., Whiting, P.J. & Wafford, K.A. Barbiturate interactions at the human GABAA receptor: dependence on receptor subunit combination. *Br J Pharmacol* **117**, 521-527 (1996).

208. Drafts, B.C. & Fisher, J.L. Identification of structures within GABAA receptor alpha subunits that regulate the agonist action of pentobarbital. *J Pharmacol Exp Ther* **318**, 1094-101 (2006).

209. Fisher, M.T. & Fisher, J.L. Activation of alpha6-containing GABAA receptors by pentobarbital occurs through a different mechanism than activation by GABA. *Neurosci Lett* **471**, 195-9 (2010).

210. Amin, J. A single hydrophobic residue confers barbiturate sensitivity to gamma-aminobutyric acid type C receptor. *Mol Pharmacol* **55**, 411-23 (1999).

211. Dalziel, J.E., Cox, G.B., Gage, P.W. & Birnir, B. Mutant human alpha(1)beta(1)(T262Q) GABA(A) receptors are directly activated but not modulated by pentobarbital. *Eur J Pharmacol* **385**, 283-6 (1999).

212. Rudolph, U. & Antkowiak, B. Molecular and neuronal substrates for general anaesthetics. *Nat Rev Neurosci* **5**, 709-20 (2004).

213. Belelli, D., Lambert, J.J., Peters, J.A., Wafford, K. & Whiting, P.J. The interaction of the general anesthetic etomidate with the gamma-aminobutyric acid type A receptor is influenced by a single amino acid. *Proc Natl Acad Sci U S A* **94**, 11031-6 (1997).

214. Hill-Venning, C., Belelli, D., Peters, J.A. & Lambert, J.J. Subunit-dependent interaction of the general anaesthetic etomidate with the gamma-aminobutyric acid type A receptor. *Br J Pharmacol* **120**, 749-56 (1997).

215. Reynolds, D.S. et al. Sedation and anesthesia mediated by distinct GABA(A) receptor isoforms. *J Neurosci* **23**, 8608-17 (2003).

216. Li, G.D. et al. Identification of a GABAA receptor anesthetic binding site at subunit interfaces by photolabeling with an etomidate analog. *J Neurosci* **26**, 11599-605 (2006).

217. Desai, R., Ruesch, D. & Forman, S.A. Gamma-amino butyric acid type A receptor mutations at beta2N265 alter etomidate efficacy while preserving basal and agonist-dependent activity. *Anesthesiology* **111**, 774-84 (2009).

218. Richardson, J.E. et al. A conserved tyrosine in the beta2 subunit M4 segment is a determinant of gamma-aminobutyric acid type A receptor sensitivity to propofol. *Anesthesiology* **107**, 412-8 (2007).

219. Stell, B.M., Brickley, S.G., Tang, C.Y., Farrant, M. & Mody, I. Neuroactive steroids reduce neuronal excitability by selectively enhancing tonic inhibition mediated by delta subunit-containing GABAA receptors. *Proc Natl Acad Sci U S A* **100**, 14439-44 (2003).

220. Hosie, A.M., Wilkins, M.E., da Silva, H.M. & Smart, T.G. Endogenous neurosteroids regulate GABAA receptors through two discrete transmembrane sites. *Nature* **444**, 486-9 (2006).

221. Ghare, S. et al. Ethanol inhibits lipid raft-mediated TCR signaling and IL-2 expression: potential mechanism of alcohol-induced immune suppression. *Alcohol Clin Exp Res* **35**, 1435-44 (2011).

222. Miyakawa, T. et al. Fyn-kinase as a determinant of ethanol sensitivity: relation to NMDA-receptor function. *Science* **278**, 698-701 (1997).

223. Ostrovskaya, O. et al. Ethanol is a fast channel inhibitor of P2X4 receptors. *J Pharmacol Exp Ther* **337**, 171-9 (2011).

224. Welsh, B.T., Kirson, D., Allen, H.M. & Mihic, S.J. Ethanol enhances taurine-activated glycine receptor function. *Alcohol Clin Exp Res* **34**, 1634-9 (2010).

225. Kumar, S. et al. The role of GABA(A) receptors in the acute and chronic effects of ethanol: a decade of progress. *Psychopharmacology (Berl)* **205**, 529-64 (2009).

226. Harris, R.A., Trudell, J.R. & Mihic, S.J. Ethanol's molecular targets. *Sci Signal* **1**, re7 (2008).

227. Lobo, I.A. & Harris, R.A. GABA(A) receptors and alcohol. *Pharmacol Biochem Behav* **90**, 90-4 (2008).

228. Weber, M. et al. Intravenous anaesthetics inhibit nicotinic acetylcholine receptor-mediated currents and Ca2+ transients in rat intracardiac ganglion neurons. *Br J Pharmacol* **144**, 98-107 (2005).

229. Pistis, M., Belelli, D., Peters, J.A. & Lambert, J.J. The interaction of general anaesthetics with recombinant GABAA and glycine receptors expressed in Xenopus laevis oocytes: a comparative study. *Br J Pharmacol* **122**, 1707-19 (1997).

230. Friederich, P. & Urban, B.W. Interaction of intravenous anesthetics with human neuronal potassium currents in relation to clinical concentrations. *Anesthesiology* **91**, 1853-60 (1999).

231. Lingamaneni, R., Birch, M.L. & Hemmings, H.C., Jr. Widespread inhibition of sodium channel-dependent glutamate release from isolated nerve terminals by isoflurane and propofol. *Anesthesiology* **95**, 1460-6 (2001).

232. Baulieu, E.-E., Robel, P. & Schumacher, M. Neurosteroids : a new regulatory function in the nervous system (Humana Press, Totowa, N.J., 1999).

233. Sur, C. et al. Loss of the major GABA(A) receptor subtype in the brain is not lethal in mice. *J Neurosci* **21**, 3409-18 (2001).

234. Kralic, J.E., Korpi, E.R., O'Buckley, T.K., Homanics, G.E. & Morrow, A.L. Molecular and pharmacological characterization of GABA(A) receptor alpha1 subunit knockout mice. *J Pharmacol Exp Ther* **302**, 1037-45 (2002).

235. Heinen, K. et al. Impaired dendritic spine maturation in GABAA receptor alpha1 subunit knock out mice. *Neuroscience* **122**, 699-705 (2003).

236. Kralic, J.E. et al. Genetic essential tremor in gamma-aminobutyric acidA receptor alpha1 subunit knockout mice. *J Clin Invest* **115**, 774-9 (2005).

237. Dixon, C.I., Rosahl, T.W. & Stephens, D.N. Targeted deletion of the GABRA2 gene encoding alpha2-subunits of GABA(A) receptors facilitates performance of a conditioned emotional response, and abolishes anxiolytic effects of benzodiazepines and barbiturates. *Pharmacol Biochem Behav* **90**, 1-8 (2008).

238. Vollenweider, I., Smith, K.S., Keist, R. & Rudolph, U. Antidepressant-like properties of alpha2-containing GABA(A) receptors. *Behav Brain Res* **217**, 77-80 (2011).

239. Winsky-Sommerer, R. et al. Normal sleep homeostasis and lack of epilepsy phenotype in GABA A receptor alpha3 subunit-knockout mice. *Neuroscience* **154**, 595-605 (2008).

240. Yee, B.K. et al. A schizophrenia-related sensorimotor deficit links alpha 3-containing GABAA receptors to a dopamine hyperfunction. *Proc Natl Acad Sci U S A* **102**, 17154-9 (2005).

241. Fiorelli, R., Rudolph, U., Straub, C.J., Feldon, J. & Yee, B.K. Affective and cognitive effects of global deletion of alpha3-containing gamma-aminobutyric acid-A receptors. *Behav Pharmacol* **19**, 582-96 (2008).

242. Schofield, C.M., Kleiman-Weiner, M., Rudolph, U. & Huguenard, J.R. A gain in GABAA receptor synaptic strength in thalamus reduces oscillatory activity and absence seizures. *Proc Natl Acad Sci U S A* **106**, 7630-5 (2009).

243. Chandra, D. et al. GABAA receptor alpha 4 subunits mediate extrasynaptic inhibition in thalamus and dentate gyrus and the action of gaboxadol. *Proc Natl Acad Sci U S A* **103**, 15230-5 (2006).

244. Sabaliauskas, N., Shen, H., Homanics, G.E., Smith, S.S. & Aoki, C. Knockout of the gamma-aminobutyric acid receptor subunit alpha4 reduces functional delta-containing extrasynaptic receptors in hippocampal pyramidal cells at the onset of puberty. *Brain Res* **1450**, 11-23 (2012).

245. Collinson, N. et al. Enhanced learning and memory and altered GABAergic synaptic transmission in mice lacking the alpha 5 subunit of the GABAA receptor. *J Neurosci* **22**, 5572-80 (2002).

246. Stephens, D.N., Pistovcakova, J., Worthing, L., Atack, J.R. & Dawson, G.R. Role of GABAA alpha5-containing receptors in ethanol reward: the effects of targeted gene deletion, and a selective inverse agonist. *Eur J Pharmacol* **526**, 240-50 (2005).

247. Glykys, J., Mann, E.O. & Mody, I. Which GABA(A) receptor subunits are necessary for tonic inhibition in the hippocampus? *J Neurosci* **28**, 1421-6 (2008).

248. Jones, A. et al. Ligand-gated ion channel subunit partnerships: GABAA receptor alpha6 subunit gene inactivation inhibits delta subunit expression. *J Neurosci* **17**, 1350-62 (1997).

249. Brickley, S.G., Revilla, V., Cull-Candy, S.G., Wisden, W. & Farrant, M. Adaptive regulation of neuronal excitability by a voltage-independent potassium conductance. *Nature* **409**, 88-92 (2001).

250. Korpi, E.R. et al. Cerebellar granule-cell-specific GABAA receptors attenuate benzodiazepine-induced ataxia: evidence from alpha 6-subunit-deficient mice. *Eur J Neurosci* **11**, 233-40 (1999).

251. Liljelund, P., Handforth, A., Homanics, G.E. & Olsen, R.W. GABAA receptor beta3 subunit gene-deficient heterozygous mice show parent-of-origin and gender-related differences in beta3 subunit levels, EEG, and behavior. *Brain Res Dev Brain Res* **157**, 150-61 (2005).

252. Homanics, G.E. et al. Mice devoid of gamma-aminobutyrate type A receptor beta3 subunit have epilepsy, cleft palate, and hypersensitive behavior. *Proc Natl Acad Sci U S A* **94**, 4143-8 (1997).

253. DeLorey, T.M. et al. Mice lacking the beta3 subunit of the GABAA receptor have the epilepsy phenotype and many of the behavioral characteristics of Angelman syndrome. *J Neurosci* **18**, 8505-14 (1998).

254. Ramadan, E. et al. GABA(A) receptor beta3 subunit deletion decreases alpha2/3 subunits and IPSC duration. *J Neurophysiol* **89**, 128-34 (2003).

255. Gunther, U. et al. Benzodiazepine-insensitive mice generated by targeted disruption of the gamma 2 subunit gene of gamma-aminobutyric acid type A receptors. *Proc Natl Acad Sci U S A* **92**, 7749-53 (1995).

256. Chandra, D., Korpi, E.R., Miralles, C.P., De Blas, A.L. & Homanics, G.E. GABAA receptor gamma 2 subunit knockdown mice have enhanced anxiety-like behavior but unaltered hypnotic response to benzodiazepines. *BMC Neurosci* **6**, 30 (2005).

257. Crestani, F. et al. Decreased GABAA-receptor clustering results in enhanced anxiety and a bias for threat cues. *Nat Neurosci* **2**, 833-9 (1999).

258. Lorez, M., Benke, D., Luscher, B., Mohler, H. & Benson, J.A. Single-channel properties of neuronal GABAA receptors from mice lacking the 2 subunit. *J Physiol* **527 Pt 1**, 11-31 (2000).

259. Peng, Z. et al. GABA(A) receptor changes in delta subunit-deficient mice: altered expression of alpha4 and gamma2 subunits in the forebrain. *J Comp Neurol* **446**, 179-97 (2002).

260. Spigelman, I. et al. Behavior and physiology of mice lacking the GABAA-receptor delta subunit. *Epilepsia* **43 Suppl 5**, 3-8 (2002).

261. Mihalek, R.M. et al. GABA(A)-receptor delta subunit knockout mice have multiple defects in behavioral responses to ethanol. *Alcohol Clin Exp Res* **25**, 1708-18 (2001).

262. Boehm, S.L., 2nd, Homanics, G.E., Blednov, Y.A. & Harris, R.A. delta-Subunit containing GABAA receptor knockout mice are less sensitive to the actions of 4,5,6,7-tetrahydroisoxazolo-[5,4-c]pyridin-3-ol. *Eur J Pharmacol* **541**, 158-62 (2006).

263. DeLorey, T.M. GABRB3 gene deficient mice: a potential model of autism spectrum disorder. *Int Rev Neurobiol* **71**, 359-82 (2005).

264. Earnheart, J.C. et al. GABAergic control of adult hippocampal neurogenesis in relation to behavior indicative of trait anxiety and depression states. *J Neurosci* **27**, 3845-54 (2007).

265. Simonian, S.X. et al. Role of the GABA(A) receptor gamma2 subunit in the development of gonadotropin-releasing hormone neurons in vivo. *Eur J Neurosci* **12**, 3488-96 (2000).

266. Leppa, E. et al. Removal of GABA(A) receptor gamma2 subunits from parvalbumin neurons causes wide-ranging behavioral alterations. *PLoS One* **6**, e24159 (2011).

267. Olsen, R.W. & Sieghart, W. International Union of Pharmacology. LXX. Subtypes of gamma-aminobutyric acid(A) receptors: classification on the basis of subunit composition, pharmacology, and function. Update. *Pharmacol Rev* **60**, 243-60 (2008).

268. Sur, C. et al. Preferential coassembly of alpha4 and delta subunits of the gamma-aminobutyric acidA receptor in rat thalamus. *Mol Pharmacol* **56**, 110-5 (1999).

269. Jia, F. et al. An extrasynaptic GABAA receptor mediates tonic inhibition in thalamic VB neurons. *J Neurophysiol* **94**, 4491-501 (2005).

270. Caraiscos, V.B. et al. Tonic inhibition in mouse hippocampal CA1 pyramidal neurons is mediated by alpha5 subunit-containing gamma-aminobutyric acid type A receptors. *Proc Natl Acad Sci U S A* **101**, 3662-7 (2004).

271. Jechlinger, M., Pelz, R., Tretter, V., Klausberger, T. & Sieghart, W. Subunit composition and quantitative importance of hetero-oligomeric receptors: GABAA receptors containing alpha6 subunits. *J Neurosci* **18**, 2449-57 (1998).

272. Nusser, Z., Sieghart, W. & Somogyi, P. Segregation of different GABAA receptors to synaptic and extrasynaptic membranes of cerebellar granule cells. *J Neurosci* **18**, 1693-703 (1998).

273. Poltl, A., Hauer, B., Fuchs, K., Tretter, V. & Sieghart, W. Subunit composition and quantitative importance of GABA(A) receptor subtypes in the cerebellum of mouse and rat. *J Neurochem* **87**, 1444-55 (2003).

274. Qian, H. & Dowling, J.E. GABAA and GABAC receptors on hybrid bass retinal bipolar cells. *J Neurophysiol* **74**, 1920-8 (1995).

275. Zhang, D., Pan, Z.H., Awobuluyi, M. & Lipton, S.A. Structure and function of GABA(C) receptors: a comparison of native versus recombinant receptors. *Trends Pharmacol Sci* **22**, 121-32 (2001).

276. Enz, R., Brandstatter, J.H., Wassle, H. & Bormann, J. Immunocytochemical localization of the GABAc receptor rho subunits in the mammalian retina. *J Neurosci* **16**, 4479-90 (1996).

277. Jurd, R. et al. General anesthetic actions in vivo strongly attenuated by a point mutation in the GABA(A) receptor beta3 subunit. *FASEB J* **17**, 250-2 (2003).

278. Glykys, J. et al. A new naturally occurring GABA(A) receptor subunit partnership with high sensitivity to ethanol. *Nat Neurosci* **10**, 40-8 (2007).

279. Sur, C., Quirk, K., Dewar, D., Atack, J. & McKernan, R. Rat and human hippocampal alpha5 subunit-containing gamma-aminobutyric AcidA receptors have alpha5 beta3 gamma2 pharmacological characteristics. *Mol Pharmacol* **54**, 928-33 (1998).

280. Li, M. & De Blas, A.L. Coexistence of two beta subunit isoforms in the same gamma-aminobutyric acid type A receptor. *J Biol Chem* **272**, 16564-9 (1997).

281. Mossier, B., Togel, M., Fuchs, K. & Sieghart, W. Immunoaffinity purification of gamma-aminobutyric acidA (GABAA) receptors containing gamma 1-subunits. Evidence for the presence of a single type of gamma-subunit in GABAA receptors. *J Biol Chem* **269**, 25777-82 (1994).

282. Mtchedlishvili, Z. & Kapur, J. High-affinity, slowly desensitizing GABAA receptors mediate tonic inhibition in hippocampal dentate granule cells. *Mol Pharmacol* **69**, 564-75 (2006).

283. Bencsits, E., Ebert, V., Tretter, V. & Sieghart, W. A significant part of native gamma-aminobutyric AcidA receptors containing alpha4 subunits do not contain gamma or delta subunits. *J Biol Chem* **274**, 19613-6 (1999).

284. Mortensen, M. & Smart, T.G. Extrasynaptic alphabeta subunit GABAA receptors on rat hippocampal pyramidal neurons. *J Physiol* **577**, 841-56 (2006).

285. Jia, F., Pignataro, L. & Harrison, N.L. GABAA receptors in the thalamus: alpha4 subunit expression and alcohol sensitivity. *Alcohol* **41**, 177-85 (2007).

286. Enz, R. & Cutting, G.R. GABAC receptor rho subunits are heterogeneously expressed in the human CNS and form homo- and heterooligomers with distinct physical properties. *Eur J Neurosci* **11**, 41-50 (1999).

287. Pan, Y., Ripps, H. & Qian, H. Random assembly of GABA rho1 and rho2 subunits in the formation of heteromeric GABA(C) receptors. *Cell Mol Neurobiol* **26**, 289-305 (2006).

288. Saxena, N.C. & Macdonald, R.L. Assembly of GABAA receptor subunits: role of the delta subunit. *J Neurosci* **14**, 7077-86 (1994).

289. Feng, H.J. & Macdonald, R.L. Multiple actions of propofol on alphabetagamma and alphabetadelta GABAA receptors. *Mol Pharmacol* **66**, 1517-24 (2004).

290. Fisher, J.L. A histidine residue in the extracellular N-terminal domain of the GABA(A) receptor alpha5 subunit regulates sensitivity to inhibition by zinc. *Neuropharmacology* **42**, 922-8 (2002).

291. Luddens, H. & Korpi, E.R. GABA antagonists differentiate between recombinant GABAA/benzodiazepine receptor subtypes. *J Neurosci* **15**, 6957-62 (1995).

292. Angelotti, T.P. & Macdonald, R.L. Assembly of GABAA receptor subunits: alpha 1 beta 1 and alpha 1 beta 1 gamma 2S subunits produce unique ion channels with dissimilar single-channel properties. *J Neurosci* **13**, 1429-40 (1993).

293. Cheng, V.Y. et al. Alpha5GABAA receptors mediate the amnestic but not sedative-hypnotic effects of the general anesthetic etomidate. *J Neurosci* **26**, 3713-20 (2006).

294. Wang, K.S., Liu, X.F. & Aragam, N. A genome-wide meta-analysis identifies novel loci associated with schizophrenia and bipolar disorder. *Schizophr Res* **124**, 192-9 (2010).

295. Feng, Y. et al. Association of the GABRD gene and childhood-onset mood disorders. *Genes Brain Behav* **9**, 668-72 (2010).

296. Green, E.K. et al. Variation at the GABAA receptor gene, Rho 1 (GABRR1) associated with susceptibility to bipolar schizoaffective disorder. *Am J Med Genet B Neuropsychiatr Genet* **153B**, 1347-9 (2010).

297. Craddock, N. et al. Strong genetic evidence for a selective influence of GABAA receptors on a component of the bipolar disorder phenotype. *Mol Psychiatry* **15**, 146-53 (2010).

298. Dean, B., Scarr, E. & McLeod, M. Changes in hippocampal GABAA receptor subunit composition in bipolar 1 disorder. *Brain Res Mol Brain Res* **138**, 145-55 (2005).

299. Otani, K. et al. The GABA type A receptor alpha5 subunit gene is associated with bipolar I disorder. *Neurosci Lett* **381**, 108-13 (2005).

300. Luscher, B., Shen, Q. & Sahir, N. The GABAergic deficit hypothesis of major depressive disorder. *Mol Psychiatry* **16**, 383-406 (2011).

301. Cherlyn, S.Y. et al. Genetic association studies of glutamate, GABA and related genes in schizophrenia and bipolar disorder: a decade of advance. *Neurosci Biobehav Rev* **34**, 958-77 (2010).

302. Blum, B.P. & Mann, J.J. The GABAergic system in schizophrenia. *Int J Neuropsychopharmacol* **5**, 159-79 (2002).

303. Dean, B. The neurobiology of bipolar disorder: findings using human postmortem central nervous system tissue. *Aust N Z J Psychiatry* **38**, 135-40 (2004).

304. Breuer, R. et al. Independent evidence for the selective influence of GABA(A) receptors on one component of the bipolar disorder phenotype. *Mol Psychiatry* **16**, 587-9 (2011).

305. Fatemi, S.H., Folsom, T.D., Kneeland, R.E. & Liesch, S.B. Metabotropic glutamate receptor 5 upregulation in children with autism is associated with underexpression of both Fragile X mental retardation protein and GABAA receptor beta 3 in adults with autism. *Anat Rec (Hoboken)* **294**, 1635-45 (2011).

306. Fatemi, S.H., Reutiman, T.J., Folsom, T.D. & Thuras, P.D. GABA(A) receptor downregulation in brains of subjects with autism. *J Autism Dev Disord* **39**, 223-30 (2009).

307. Delahanty, R.J. et al. Maternal transmission of a rare GABRB3 signal peptide variant is associated with autism. *Mol Psychiatry* **16**, 86-96 (2011).

308. McCauley, J.L. et al. A linkage disequilibrium map of the 1-Mb 15q12 GABA(A) receptor subunit cluster and association to autism. *Am J Med Genet B Neuropsychiatr Genet* **131B**, 51-9 (2004).

309. Oblak, A.L., Gibbs, T.T. & Blatt, G.J. Reduced GABAA receptors and benzodiazepine binding sites in the posterior cingulate cortex and fusiform gyrus in autism. *Brain Res* **1380**, 218-28 (2011).

310. Mendez, M.A. et al. The brain GABA-benzodiazepine receptor alpha-5 subtype in autism spectrum disorder: A pilot [(11)C]Ro15-4513 positron emission tomography study. *Neuropharmacology* (2012).

311. Schroer, R.J. et al. Autism and maternally derived aberrations of chromosome 15q. *Am J Med Genet* **76**, 327-36 (1998).

312. Menold, M.M. et al. Association analysis of chromosome 15 gabaa receptor subunit genes in autistic disorder. *J Neurogenet* **15**, 245-59 (2001).

313. Buxbaum, J.D. et al. Association between a GABRB3 polymorphism and autism. *Mol Psychiatry* **7**, 311-6 (2002).

314. Fatemi, S.H. et al. mRNA and protein levels for GABAAalpha4, alpha5, beta1 and GABABR1 receptors are altered in brains from subjects with autism. *J Autism Dev Disord* **40**, 743-50 (2010).

315. Hedges, D.J. et al. Evidence of novel fine-scale structural variation at autism spectrum disorder candidate loci. *Mol Autism* **3**, 2 (2012).

316. Cossette, P. et al. Mutation of GABRA1 in an autosomal dominant form of juvenile myoclonic epilepsy. *Nat Genet* **31**, 184-9 (2002).

317. Gallagher, M.J., Shen, W., Song, L. & Macdonald, R.L. Endoplasmic reticulum retention and associated degradation of a GABAA receptor epilepsy mutation that inserts an aspartate in the M3 transmembrane segment of the alpha1 subunit. *J Biol Chem* **280**, 37995-8004 (2005).

318. Gallagher, M.J., Ding, L., Maheshwari, A. & Macdonald, R.L. The GABAA receptor alpha1 subunit epilepsy mutation A322D inhibits transmembrane helix formation and causes proteasomal degradation. *Proc Natl Acad Sci U S A* **104**, 12999-3004 (2007).

319. Ding, L. et al. GABA(A) receptor alpha1 subunit mutation A322D associated with autosomal dominant juvenile myoclonic epilepsy reduces the expression and alters the composition of wild type GABA(A) receptors. *J Biol Chem* **285**, 26390-405 (2010).

320. Lachance-Touchette, P. et al. Novel alpha1 and gamma2 GABAA receptor subunit mutations in families with idiopathic generalized epilepsy. *Eur J Neurosci* **34**, 237-49 (2011).

321. Tanaka, M. et al. Hyperglycosylation and reduced GABA currents of mutated GABRB3 polypeptide in remitting childhood absence epilepsy. *Am J Hum Genet* **82**, 1249-61 (2008).

322. Maljevic, S. et al. A mutation in the GABA(A) receptor alpha(1)-subunit is associated with absence epilepsy. *Ann Neurol* **59**, 983-7 (2006).

323. Gurba, K.N., Hernandez, C.C., Hu, N. & Macdonald, R.L. GABRB3 Mutation, G32R, Associated with Childhood Absence Epilepsy Alters alpha1beta3gamma2L gamma-Aminobutyric Acid Type A (GABAA) Receptor Expression and Channel Gating. *J Biol Chem* **287**, 12083-97 (2012).

324. Hirose, S. A new paradigm of channelopathy in epilepsy syndromes: intracellular trafficking abnormality of channel molecules. *Epilepsy Res* **70 Suppl 1**, S206-17 (2006).

325. Bowser, D.N. et al. Altered kinetics and benzodiazepine sensitivity of a GABAA receptor subunit mutation [gamma 2(R43Q)] found in human epilepsy. *Proc Natl Acad Sci U S A* **99**, 15170-5 (2002).

326. Bianchi, M.T., Song, L., Zhang, H. & Macdonald, R.L. Two different mechanisms of disinhibition produced by GABAA receptor mutations linked to epilepsy in humans. *J Neurosci* **22**, 5321-7 (2002).

327. Frugier, G. et al. A gamma 2(R43Q) mutation, linked to epilepsy in humans, alters GABAA receptor assembly and modifies subunit composition on the cell surface. *J Biol Chem* **282**, 3819-28 (2007).

328. Goldschen-Ohm, M.P., Wagner, D.A., Petrou, S. & Jones, M.V. An epilepsy-related region in the GABA(A) receptor mediates long-distance effects on GABA and benzodiazepine binding sites. *Mol Pharmacol* **77**, 35-45 (2010).

329. Tan, H.O. et al. Reduced cortical inhibition in a mouse model of familial childhood absence epilepsy. *Proc Natl Acad Sci U S A* **104**, 17536-41 (2007).

330. Audenaert, D. et al. A novel GABRG2 mutation associated with febrile seizures. *Neurology* **67**, 687-90 (2006).

331. Kananura, C. et al. A splice-site mutation in GABRG2 associated with childhood absence epilepsy and febrile convulsions. *Arch Neurol* **59**, 1137-41 (2002).

332. Tian, M. & Macdonald, R.L. The Intronic GABRG2 Mutation, IVS6+2T->G, Associated with Childhood Absence Epilepsy Altered Subunit mRNA Intron Splicing, Activated Nonsense-Mediated Decay, and Produced a Stable Truncated gamma2 Subunit. *J Neurosci* **32**, 5937-52 (2012).

333. Baulac, S. et al. First genetic evidence of GABA(A) receptor dysfunction in epilepsy: a mutation in the gamma2-subunit gene. *Nat Genet* **28**, 46-8 (2001).

334. Harkin, L.A. et al. Truncation of the GABA(A)-receptor gamma2 subunit in a family with generalized epilepsy with febrile seizures plus. *Am J Hum Genet* **70**, 530-6 (2002).

335. Kang, J.Q., Shen, W. & Macdonald, R.L. The GABRG2 mutation, Q351X, associated with generalized epilepsy with febrile seizures plus, has both loss of function and dominant-negative suppression. *J Neurosci* **29**, 2845-56 (2009).

336. Sun, H. et al. SCN1A, SCN1B, and GABRG2 gene mutation analysis in Chinese families with generalized epilepsy with febrile seizures plus. *J Hum Genet* **53**, 769-74 (2008).

337. Dibbens, L.M. et al. GABRD encoding a protein for extra- or peri-synaptic GABAA receptors is a susceptibility locus for generalized epilepsies. *Hum Mol Genet* **13**, 1315-9 (2004).

338. Feng, H.J. et al. Delta subunit susceptibility variants E177A and R220H associated with complex epilepsy alter channel gating and surface expression of alpha4beta2delta GABAA receptors. *J Neurosci* **26**, 1499-506 (2006).

339. Wallace, R.H. et al. Mutant GABA(A) receptor gamma2-subunit in childhood absence epilepsy and febrile seizures. *Nat Genet* **28**, 49-52 (2001).

340. Klassen, T. et al. Exome sequencing of ion channel genes reveals complex profiles confounding personal risk assessment in epilepsy. *Cell* **145**, 1036-48 (2011).

341. Baumann, S.W., Baur, R. & Sigel, E. Subunit arrangement of gamma-aminobutyric acid type A receptors. *J Biol Chem* **276**, 36275-80 (2001).

342. Tretter, V., Ehya, N., Fuchs, K. & Sieghart, W. Stoichiometry and assembly of a recombinant GABAA receptor subtype. *J Neurosci* **17**, 2728-37 (1997).

343. Ericksen, S.S. & Boileau, A.J. Tandem couture: Cys-loop receptor concatamer insights and caveats. *Mol Neurobiol* **35**, 113-28 (2007).

344. Nelson, M.E., Kuryatov, A., Choi, C.H., Zhou, Y. & Lindstrom, J. Alternate stoichiometries of alpha4beta2 nicotinic acetylcholine receptors. *Mol Pharmacol* **63**, 332-41 (2003).

345. Buisson, B. & Bertrand, D. Chronic exposure to nicotine upregulates the human (alpha)4((beta)2 nicotinic acetylcholine receptor function. *J Neurosci* **21**, 1819-29 (2001).

346. Son, C.D., Moss, F.J., Cohen, B.N. & Lester, H.A. Nicotine normalizes intracellular subunit stoichiometry of nicotinic receptors carrying mutations linked to autosomal dominant nocturnal frontal lobe epilepsy. *Mol Pharmacol* **75**, 1137-48 (2009).

347. Farrar, S.J., Whiting, P.J., Bonnert, T.P. & McKernan, R.M. Stoichiometry of a ligand-gated ion channel determined by fluorescence energy transfer. *J Biol Chem* **274**, 10100-4 (1999).

348. Lo, W.Y. et al. Glycosylation of {beta}2 subunits regulates GABAA receptor biogenesis and channel gating. *J Biol Chem* **285**, 31348-61 (2010).

349. Selvin, P.R. The renaissance of fluorescence resonance energy transfer. *Nat Struct Biol* **7**, 730-4 (2000).

350. Boileau, A.J., Pearce, R.A. & Czajkowski, C. The short splice variant of the gamma 2 subunit acts as an external modulator of GABA(A) receptor function. *J Neurosci* **30**, 4895-903 (2010).

351. Farrant, M. & Nusser, Z. Variations on an inhibitory theme: phasic and tonic activation of GABA(A) receptors. *Nat Rev Neurosci* **6**, 215-29 (2005).

352. Mody, I. & Pearce, R.A. Diversity of inhibitory neurotransmission through GABA(A) receptors. *Trends Neurosci* **27**, 569-75 (2004).

353. Baumann, S.W., Baur, R. & Sigel, E. Forced subunit assembly in alpha1beta2gamma2 GABAA receptors. Insight into the absolute arrangement. *J Biol Chem* **277**, 46020-5 (2002).

354. Barrera, N.P. et al. Atomic force microscopy reveals the stoichiometry and subunit arrangement of the alpha4beta3delta GABA(A) receptor. *Mol Pharmacol* **73**, 960-7 (2008).

355. Akk, G., Li, P., Bracamontes, J. & Steinbach, J.H. Activation and modulation of concatemeric GABA-A receptors expressed in human embryonic kidney cells. *Mol Pharmacol* **75**, 1400-11 (2009).

356. Greenfield, L.J., Jr. et al. Expression of functional GABAA receptors in transfected L929 cells isolated by immunomagnetic bead separation. *Neuropharmacology* **36**, 63-73 (1997).

357. Connolly, C.N. et al. Subcellular localization and endocytosis of homomeric gamma2 subunit splice variants of gamma-aminobutyric acid type A receptors. *Mol Cell Neurosci* **13**, 259-71 (1999).

358. Boileau, A.J., Baur, R., Sharkey, L.M., Sigel, E. & Czajkowski, C. The relative amount of cRNA coding for gamma2 subunits affects stimulation by benzodiazepines in GABA(A) receptors expressed in Xenopus oocytes. *Neuropharmacology* **43**, 695-700 (2002).

359. Boileau, A.J., Li, T., Benkwitz, C., Czajkowski, C. & Pearce, R.A. Effects of gamma2S subunit incorporation on GABAA receptor macroscopic kinetics. *Neuropharmacology* **44**, 1003-12 (2003).

360. Nayeem, N., Green, T.P., Martin, I.L. & Barnard, E.A. Quaternary structure of the native GABAA receptor determined by electron microscopic image analysis. *J Neurochem* **62**, 815-8 (1994).

361. Baumann, S.W., Baur, R. & Sigel, E. Individual properties of the two functional agonist sites in GABA(A) receptors. *J Neurosci* **23**, 11158-66 (2003).

362. Hosie, A.M., Dunne, E.L., Harvey, R.J. & Smart, T.G. Zinc-mediated inhibition of GABA(A) receptors: discrete binding sites underlie subtype specificity. *Nat Neurosci* **6**, 362-9 (2003).

363. Jacob, T.C., Moss, S.J. & Jurd, R. GABA(A) receptor trafficking and its role in the dynamic modulation of neuronal inhibition. *Nat Rev Neurosci* **9**, 331-43 (2008).

364. Kaur, K.H., Baur, R. & Sigel, E. Unanticipated structural and functional properties of delta-subunit-containing GABAA receptors. *J Biol Chem* **284**, 7889-96 (2009).

365. Kozak, M. Point mutations define a sequence flanking the AUG initiator codon that modulates translation by eukaryotic ribosomes. *Cell* **44**, 283-92 (1986).

366. Kang, J.Q., Shen, W., Lee, M., Gallagher, M.J. & Macdonald, R.L. Slow degradation and aggregation in vitro of mutant GABAA receptor gamma2(Q351X) subunits associated with epilepsy. *J Neurosci* **30**, 13895-905 (2010).

367. Hackam, A.S., Wang, T.L., Guggino, W.B. & Cutting, G.R. A 100 amino acid region in the GABA rho 1 subunit confers robust homo-oligomeric expression. *Neuroreport* **8**, 1425-30 (1997).

368. Bracamontes, J.R. & Steinbach, J.H. Multiple modes for conferring surface expression of homomeric beta1 GABAA receptors. *J Biol Chem* **283**, 26128-36 (2008).

369. Storustovu, S.I. & Ebert, B. Pharmacological characterization of agonists at delta-containing GABAA receptors: Functional selectivity for extrasynaptic receptors is dependent on the absence of gamma2. *J Pharmacol Exp Ther* **316**, 1351-9 (2006).

370. Olsen, R.W., Hanchar, H.J., Meera, P. & Wallner, M. GABAA receptor subtypes: the "one glass of wine" receptors. *Alcohol* **41**, 201-9 (2007).

371. Sundstrom-Poromaa, I. et al. Hormonally regulated alpha(4)beta(2)delta GABA(A) receptors are a target for alcohol. *Nat Neurosci* **5**, 721-2 (2002).

372. Bianchi, M.T., Botzolakis, E.J., Haas, K.F., Fisher, J.L. & Macdonald, R.L. Microscopic kinetic determinants of macroscopic currents: insights from coupling and uncoupling of GABAA receptor desensitization and deactivation. *J Physiol* **584**, 769-87 (2007).

373. Bianchi, M.T., Haas, K.F. & Macdonald, R.L. Structural determinants of fast desensitization and desensitization-deactivation coupling in GABAa receptors. *J Neurosci* **21**, 1127-36 (2001).

374. Crunelli, V. & Leresche, N. Childhood absence epilepsy: genes, channels, neurons and networks. *Nat Rev Neurosci* **3**, 371-82 (2002).

375. Chen, Y. et al. Association between genetic variation of CACNA1H and childhood absence epilepsy. *Ann Neurol* **54**, 239-43 (2003).

376. Lu, J.J. et al. [T-type calcium channel gene-CACNA1H is a susceptibility gene to childhood absence epilepsy]. *Zhonghua Er Ke Za Zhi* **43**, 133-6 (2005).

377. Liang, J. et al. Common polymorphisms in the CACNA1H gene associated with childhood absence epilepsy in Chinese Han population. *Ann Hum Genet* **71**, 325-35 (2007).

378. Everett, K.V. et al. Linkage and association analysis of CACNG3 in childhood absence epilepsy. *Eur J Hum Genet* **15**, 463-72 (2007).

379. Everett, K. et al. Linkage and mutational analysis of CLCN2 in childhood absence epilepsy. *Epilepsy Res* **75**, 145-53 (2007).

380. Hernandez, C.C., Gurba, K.N., Hu, N. & Macdonald, R.L. The GABRA6 mutation, R46W, associated with childhood absence epilepsy, alters 6beta22 and 6beta2 GABAA receptor channel gating and expression. *J Physiol* **589**, 5857-78 (2011).

381. Helenius, A. & Aebi, M. Roles of N-linked glycans in the endoplasmic reticulum. *Annu Rev Biochem* **73**, 1019-49 (2004).

382. Bause, E. Structural requirements of N-glycosylation of proteins. Studies with proline peptides as conformational probes. *Biochem J* **209**, 331-6 (1983).

383. Imperiali, B. & Shannon, K.L. Differences between Asn-Xaa-Thr-containing peptides: a comparison of solution conformation and substrate behavior with oligosaccharyltransferase. *Biochemistry* **30**, 4374-80 (1991).

384. Kaplan, H.A., Welply, J.K. & Lennarz, W.J. Oligosaccharyl transferase: the central enzyme in the pathway of glycoprotein assembly. *Biochim Biophys Acta* **906**, 161-73 (1987).

385. Molinari, M. N-glycan structure dictates extension of protein folding or onset of disposal. *Nat Chem Biol* **3**, 313-20 (2007).

386. Glozman, R. et al. N-glycans are direct determinants of CFTR folding and stability in secretory and endocytic membrane traffic. *J Cell Biol* **184**, 847-62 (2009).

387. Antenos, M., Stemler, M., Boime, I. & Woodruff, T.K. N-linked oligosaccharides direct the differential assembly and secretion of inhibin alpha- and betaA-subunit dimers. *Mol Endocrinol* **21**, 1670-84 (2007).

388. Buller, A.L., Hastings, G.A., Kirkness, E.F. & Fraser, C.M. Site-directed mutagenesis of N-linked glycosylation sites on the gamma-aminobutyric acid type A receptor alpha 1 subunit. *Mol Pharmacol* **46**, 858-65 (1994).

389. Jaeken, J. Congenital disorders of glycosylation. *Ann N Y Acad Sci* **1214**, 190-8 (2010).

390. Fisher, J.L. & Macdonald, R.L. Single channel properties of recombinant GABAA receptors containing gamma 2 or delta subtypes expressed with alpha 1 and beta 3 subtypes in mouse L929 cells. *J Physiol* **505 (Pt 2)**, 283-97 (1997).

391. Twyman, R.E., Rogers, C.J. & Macdonald, R.L. Intraburst kinetic properties of the GABAA receptor main conductance state of mouse spinal cord neurones in culture. *J Physiol* **423**, 193-220 (1990).

392. Schwede, T., Kopp, J., Guex, N. & Peitsch, M.C. SWISS-MODEL: An automated protein homology-modeling server. *Nucleic Acids Res* **31**, 3381-5 (2003).

393. Bano-Polo, M., Baldin, F., Tamborero, S., Marti-Renom, M.A. & Mingarro, I. N-glycosylation efficiency is determined by the distance to the C-terminus and the amino acid preceding an Asn-Ser-Thr sequon. *Protein Sci* **20**, 179-86 (2011).

394. Sutachan, J.J. et al. Effects of Kv1.1 channel glycosylation on C-type inactivation and simulated action potentials. *Brain Res* **1058**, 30-43 (2005).

395. Kamei, N. et al. Definitive evidence that a single N-glycan among three glycans on inducible costimulator is required for proper protein trafficking and ligand binding. *Biochem Biophys Res Commun* **391**, 557-63 (2010).

396. Bocquet, N. et al. X-ray structure of a pentameric ligand-gated ion channel in an apparently open conformation. *Nature* **457**, 111-4 (2009).

397. Castillo, M. et al. Role of the N-terminal alpha-helix in biogenesis of alpha7 nicotinic receptors. *J Neurochem* **108**, 1399-409 (2009).

398. Smit, A.B., Brejc, K., Syed, N. & Sixma, T.K. Structure and function of AChBP, homologue of the ligand-binding domain of the nicotinic acetylcholine receptor. *Ann N Y Acad Sci* **998**, 81-92 (2003).

399. Hendsch, Z.S. & Tidor, B. Do salt bridges stabilize proteins? A continuum electrostatic analysis. *Protein Sci* **3**, 211-26 (1994).

400. Meeren, H., van Luijtelaar, G., Lopes da Silva, F. & Coenen, A. Evolving concepts on the pathophysiology of absence seizures: the cortical focus theory. *Arch Neurol* **62**, 371-6 (2005).

401. Cope, D.W. et al. Enhanced tonic GABAA inhibition in typical absence epilepsy. *Nat Med* **15**, 1392-8 (2009).

402. Miyazawa, A., Fujiyoshi, Y. & Unwin, N. Structure and gating mechanism of the acetylcholine receptor pore. *Nature* **423**, 949-55 (2003).

403. Macdonald, R.L. & Olsen, R.W. GABAA receptor channels. *Annu Rev Neurosci* **17**, 569-602 (1994).

404. Hirose, S., Mitsudome, A., Okada, M. & Kaneko, S. Genetics of idiopathic epilepsies. *Epilepsia* **46 Suppl 1**, 38-43 (2005).

405. Macdonald, R.L., Kang, J.Q. & Gallagher, M.J. Mutations in GABAA receptor subunits associated with genetic epilepsies. *J Physiol* **588**, 1861-9 (2010).

406. Dibbens, L.M. et al. The role of neuronal GABA(A) receptor subunit mutations in idiopathic generalized epilepsies. *Neurosci Lett* **453**, 162-5 (2009).

407. Marini, C. et al. Childhood absence epilepsy and febrile seizures: a family with a GABA(A) receptor mutation. *Brain* **126**, 230-40 (2003).

408. Kang, J.Q. & Macdonald, R.L. The GABAA receptor gamma2 subunit R43Q mutation linked to childhood absence epilepsy and febrile seizures causes retention of alpha1beta2gamma2S receptors in the endoplasmic reticulum. *J Neurosci* **24**, 8672-7 (2004).

409. Tang, X., Hernandez, C.C. & Macdonald, R.L. Modulation of spontaneous and GABA-evoked tonic alpha4beta3delta and alpha4beta3gamma2L GABAA receptor currents by protein kinase A. *J Neurophysiol* **103**, 1007-19 (2010).

410. Saxena, N.C. & Macdonald, R.L. Properties of putative cerebellar gamma-aminobutyric acid A receptor isoforms. *Mol Pharmacol* **49**, 567-79 (1996).

411. Bianchi, M.T., Haas, K.F. & Macdonald, R.L. Alpha1 and alpha6 subunits specify distinct desensitization, deactivation and neurosteroid modulation of GABA(A) receptors containing the delta subunit. *Neuropharmacology* **43**, 492-502 (2002).

412. Bianchi, M.T. & Macdonald, R.L. Slow phases of GABA(A) receptor desensitization: structural determinants and possible relevance for synaptic function. *J Physiol* **544**, 3-18 (2002).

413. Sancar, F. & Czajkowski, C. A GABAA receptor mutation linked to human epilepsy (gamma2R43Q) impairs cell surface expression of alphabetagamma receptors. *J Biol Chem* **279**, 47034-9 (2004).

414. Gallagher, M.J., Song, L., Arain, F. & Macdonald, R.L. The juvenile myoclonic epilepsy GABA(A) receptor alpha1 subunit mutation A322D produces asymmetrical, subunit position-dependent reduction of heterozygous receptor currents and alpha1 subunit protein expression. *J Neurosci* **24**, 5570-8 (2004).

415. Mukhtasimova, N., Free, C. & Sine, S.M. Initial coupling of binding to gating mediated by conserved residues in the muscle nicotinic receptor. *J Gen Physiol* **126**, 23-39 (2005).

416. Gay, E.A. & Yakel, J.L. Gating of nicotinic ACh receptors; new insights into structural transitions triggered by agonist binding that induce channel opening. *J Physiol* **584**, 727-33 (2007).

417. Sine, S.M. & Engel, A.G. Recent advances in Cys-loop receptor structure and function. *Nature* **440**, 448-55 (2006).

418. Cromer, B.A., Morton, C.J. & Parker, M.W. Anxiety over GABA(A) receptor structure relieved by AChBP. *Trends Biochem Sci* **27**, 280-7 (2002).

419. Ernst, M., Bruckner, S., Boresch, S. & Sieghart, W. Comparative models of GABAA receptor extracellular and transmembrane domains: important insights in pharmacology and function. *Molecular pharmacology* **68**, 1291-300 (2005).

420. Venkatachalan, S.P. & Czajkowski, C. A conserved salt bridge critical for GABA(A) receptor function and loop C dynamics. *Proc Natl Acad Sci U S A* **105**, 13604-9 (2008).

421. Jones, A. et al. Ligand-gated ion channel subunit partnerships: GABAA receptor alpha6 subunit gene inactivation inhibits delta subunit expression. *The Journal of neuroscience : the official journal of the Society for Neuroscience* **17**, 1350-62 (1997).

422. Homanics, G.E. et al. Gene knockout of the alpha6 subunit of the gamma-aminobutyric acid type A receptor: lack of effect on responses to ethanol, pentobarbital, and general anesthetics. *Molecular pharmacology* **51**, 588-96 (1997).

423. Korpi, E.R., Kleingoor, C., Kettenmann, H. & Seeburg, P.H. Benzodiazepine-induced motor impairment linked to point mutation in cerebellar GABAA receptor. *Nature* **361**, 356-9 (1993).

424. Korpi, E.R. & Seeburg, P.H. Natural mutation of GABAA receptor alpha 6 subunit alters benzodiazepine affinity but not allosteric GABA effects. *Eur J Pharmacol* **247**, 23-7 (1993).

425. Hanchar, H.J., Dodson, P.D., Olsen, R.W., Otis, T.S. & Wallner, M. Alcohol-induced motor impairment caused by increased extrasynaptic GABA(A) receptor activity. *Nature neuroscience* **8**, 339-45 (2005).

426. Heron, S.E., Scheffer, I.E., Berkovic, S.F., Dibbens, L.M. & Mulley, J.C. Channelopathies in idiopathic epilepsy. *Neurotherapeutics* **4**, 295-304 (2007).

427. Baram, T.Z., Eghbal-Ahmadi, M. & Bender, R.A. Is neuronal death required for seizure-induced epileptogenesis in the immature brain? *Prog Brain Res* **135**, 365-75 (2002).

428. Reid, A.Y., Galic, M.A., Teskey, G.C. & Pittman, Q.J. Febrile seizures: current views and investigations. *Can J Neurol Sci* **36**, 679-86 (2009).

429. Scheffer, I.E. & Berkovic, S.F. Generalized epilepsy with febrile seizures plus. A genetic disorder with heterogeneous clinical phenotypes. *Brain* **120 (Pt 3)**, 479-90 (1997).

430. Scantlebury, M.H. & Heida, J.G. Febrile seizures and temporal lobe epileptogenesis. *Epilepsy Res* **89**, 27-33 (2010).

431. Baulac, S. et al. Fever, genes, and epilepsy. *Lancet Neurol* **3**, 421-30 (2004).

432. Audenaert, D., Van Broeckhoven, C. & De Jonghe, P. Genes and loci involved in febrile seizures and related epilepsy syndromes. *Hum Mutat* **27**, 391-401 (2006).

433. Dube, C.M., Brewster, A.L., Richichi, C., Zha, Q. & Baram, T.Z. Fever, febrile seizures and epilepsy. *Trends Neurosci* **30**, 490-6 (2007).

434. Vihinen, M., Torkkila, E. & Riikonen, P. Accuracy of protein flexibility predictions. *Proteins* **19**, 141-9 (1994).

435. Miller, P.S. & Smart, T.G. Binding, activation and modulation of Cys-loop receptors. *Trends Pharmacol Sci* **31**, 161-74 (2010).

436. Hinkle, D.J., Bianchi, M.T. & Macdonald, R.L. Modifications of a commercial perfusion system for use in ultrafast solution exchange during patch clamp recording. *Biotechniques* **35**, 472-4, 476 (2003).

437. Gurba, K.N., Hernandez, C.C., Hu, N. & Macdonald, R.L. The GABRB3 mutation, G32R, associated with childhood absence epilepsy, alters alpha1beta3gamma2L GABAA receptor expression and channel gating. *J Biol Chem* (2012).

438. Tarentino, A.L. & Maley, F. Purification and properties of an endo-beta-N-acetylglucosaminidase from Streptomyces griseus. *J Biol Chem* **249**, 811-7 (1974).

439. Maley, F., Trimble, R.B., Tarentino, A.L. & Plummer, T.H., Jr. Characterization of glycoproteins and their associated oligosaccharides through the use of endoglycosidases. *Anal Biochem* **180**, 195-204 (1989).

440. Dick, L.R. et al. Mechanistic studies on the inactivation of the proteasome by lactacystin in cultured cells. *J Biol Chem* **272**, 182-8 (1997).

441. Ramirez-Alvarado, M., Kortemme, T., Blanco, F.J. & Serrano, L. Beta-hairpin and beta-sheet formation in designed linear peptides. *Bioorg Med Chem* **7**, 93-103 (1999).

442. Minor, D.L., Jr. & Kim, P.S. Measurement of the beta-sheet-forming propensities of amino acids. *Nature* **367**, 660-3 (1994).

443. Kumar, P., Henikoff, S. & Ng, P.C. Predicting the effects of coding non-synonymous variants on protein function using the SIFT algorithm. *Nat Protoc* **4**, 1073-81 (2009).

444. Adzhubei, I.A. et al. A method and server for predicting damaging missense mutations. *Nat Methods* **7**, 248-9 (2010).

445. Farzadfard, F., Gharaei, N., Pezeshk, H. & Marashi, S.A. Beta-sheet capping: signals that initiate and terminate beta-sheet formation. *J Struct Biol* **161**, 101-10 (2008).

446. Lagrange, A.H., Botzolakis, E.J. & Macdonald, R.L. Enhanced macroscopic desensitization shapes the response of alpha4 subtype-containing GABAA receptors to synaptic and extrasynaptic GABA. *J Physiol* **578**, 655-76 (2007).

447. Groot-Kormelink, P.J., Broadbent, S.D., Boorman, J.P. & Sivilotti, L.G. Incomplete incorporation of tandem subunits in recombinant neuronal nicotinic receptors. *J Gen Physiol* **123**, 697-708 (2004).

448. Khan, Z.U., Gutierrez, A. & De Blas, A.L. Short and long form gamma 2 subunits of the GABAA/benzodiazepine receptors. *J Neurochem* **63**, 1466-76 (1994).

449. Quirk, K., Gillard, N.P., Ragan, C.I., Whiting, P.J. & McKernan, R.M. gamma-Aminobutyric acid type A receptors in the rat brain can contain both gamma 2 and gamma 3 subunits, but gamma 1 does not exist in combination with another gamma subunit. *Mol Pharmacol* **45**, 1061-70 (1994).

450. Schuchmann, S. et al. Experimental febrile seizures are precipitated by a hyperthermia-induced respiratory alkalosis. *Nat Med* **12**, 817-23 (2006).

451. Feng, H.J. & Macdonald, R.L. Proton modulation of alpha 1 beta 3 delta GABAA receptor channel gating and desensitization. *J Neurophysiol* **92**, 1577-85 (2004).

452. Krishek, B.J., Moss, S.J. & Smart, T.G. Homomeric beta 1 gamma-aminobutyric acid A receptor-ion channels: evaluation of pharmacological and physiological properties. *Mol Pharmacol* **49**, 494-504 (1996).

453. Bollan, K.A., Baur, R., Hales, T.G., Sigel, E. & Connolly, C.N. The promiscuous role of the epsilon subunit in GABAA receptor biogenesis. *Mol Cell Neurosci* **37**, 610-21 (2008).

454. Neelands, T.R., Fisher, J.L., Bianchi, M. & Macdonald, R.L. Spontaneous and gamma-aminobutyric acid (GABA)-activated GABA(A) receptor channels formed by epsilon subunit-containing isoforms. *Mol Pharmacol* **55**, 168-78 (1999).

455. Cantor, R.M., Lange, K. & Sinsheimer, J.S. Prioritizing GWAS results: A review of statistical methods and recommendations for their application. *Am J Hum Genet* **86**, 6-22 (2010).

456. Petersen, T.N., Brunak, S., von Heijne, G. & Nielsen, H. SignalP 4.0: discriminating signal peptides from transmembrane regions. *Nat Methods* **8**, 785-6 (2011).

457. Chou, K.C. & Shen, H.B. Signal-CF: a subsite-coupled and window-fusing approach for predicting signal peptides. *Biochem Biophys Res Commun* **357**, 633-40 (2007).

458. Lachance-Touchette, P. et al. Screening of GABRB3 in French-Canadian families with idiopathic generalized epilepsy. *Epilepsia* **51**, 1894-7 (2010).